

SPECTROSCOPIC STUDIES OF TIN(IV) AND MIXED OXIDATION  
STATE TIN(II)TIN(IV) COMPOUNDS

By

© JAMES PATRICK JOHNSON, B.Sc.

A Thesis

Submitted to the Faculty of Graduate Studies

in Partial Fulfilment of the Requirements

for the Degree

Doctor of Philosophy

McMaster University

June 1983

SPECTROSCOPIC STUDIES OF TIN(IV) AND  
TIN(II)TIN(IV) COMPOUNDS

DOCTOR OF PHILOSOPHY (1983)  
(Chemistry)

McMaster University  
Hamilton, Ontario

TITLE: Spectroscopic Studies of Tin(IV) and Mixed Oxidation  
State Tin(II)Tin(IV) Compounds

AUTHOR: James Patrick Johnson, B.Sc. (McMaster University)

SUPERVISOR: Professor T. Birchall

NUMBER OF PAGES: xvi; 202

## ABSTRACT

Proton n.m.r. data are presented for the solvolysis of hexamethylditin and tetramethyltin with fluorosulfuric acid. The tetramethylditin dication  $[(CH_3)_4Sn_2^{2+}]$  is proposed as an intermediate in the suggested reaction sequence for the solvolysis of hexamethylditin with fluorosulfuric acid.

The reaction between hexamethylditin and a series of carboxylic acids has been investigated. Compounds of empirical formula  $(CH_3)_2Sn(O_2CR)$  were prepared and formulated as the tetramethylditin carboxylates,  $(CH_3)_4Sn_2(O_2CR)_2$ . Infrared, Raman,  $^1H$  and  $^{13}C$  n.m.r. and  $^{119}Sn$  Mössbauer data are presented for this series of compounds. The compounds have been shown to have a tetramethylditin moiety in which the carboxylate ligand bridges both tin atoms. The X-ray crystal structure of three of these compounds [ $R = CH_2Cl$ ,  $CCl_3$  and  $CF_3$ ] are presented and the spectroscopic data evaluated in light of the crystallographic data. The X-ray crystal structure of  $[(CH_3)_2Sn(O_2CCF_3)]_2O$  is also presented.

The solvolysis of hexaphenylditin by a series of carboxylic acids was investigated. Seven novel compounds of empirical formula  $Sn(O_2CR)_3$  were synthesized. Infrared, Raman and  $^{119}Sn$  Mössbauer spectra are reported for the series of  $Sn(O_2CR)_3$  compounds which are best formulated as  $[Sn(II)Sn(IV)O(O_2CR)_4(O_2OCR)_2]_2$ .  $^{119}Sn$  Mössbauer data for

$\text{Sn}(\text{O}_2\text{CR})_4$  are also presented. The X-ray crystal structure of  $[\text{Sn}(\text{II})\text{Sn}(\text{IV})\text{O}(\text{O}_2\text{CCF}_3)_4]_2\text{C}_6\text{H}_6$  has been determined and its relationship to other mixed oxidation state tin carboxylates examined.

The solvolysis of hexaphenylditin by inorganic acids has been investigated.  $^{119}\text{Sn}$  Mossbauer spectra are presented for the products and vibrational (infrared and/or Raman) data for the isolated solids. Compounds of empirical formula  $\text{SnF}_3$ ,  $\text{Sn}(\text{SO}_3\text{CF}_3)_3$  and  $\text{Sn}(\text{IV})\text{O}\cdot\text{SO}_4\text{Sn}(\text{II})(\text{SO}_3\text{F})_2$  are formulated as the polymers  $[\text{Sn}(\text{II})\text{Sn}(\text{IV})\text{F}_6]_x$ ,  $[\text{Sn}(\text{II})\text{Sn}(\text{IV})(\text{SO}_3\text{CF}_3)_6]_x$  and  $[\text{Sn}(\text{IV})\text{O}\cdot\text{SO}_4\text{Sn}(\text{II})(\text{SO}_3\text{F})_2]_x$ . The  $\text{Sn}(\text{SO}_3\text{R})_3$  compounds where  $\text{R} = \text{CH}_3$ ,  $\text{C}_2\text{H}_5$  and  $\text{OH}$  were not isolated free of excess acid.  $^{119}\text{Sn}$  Mossbauer spectroscopy also showed that these products contain tin(II) and tin(IV) and the formulation of  $[\text{Sn}(\text{II})\text{Sn}(\text{IV})(\text{SO}_3\text{R})_6]_x$  is suggested.

The interaction of  $\text{SnF}_2$  with  $\text{Sn}(\text{SO}_3\text{CF}_3)_3$  produced  $\text{Sn}_3\text{F}_2(\text{SO}_3\text{CF}_3)_6$ .  $^{119}\text{Sn}$  Mossbauer data together with infrared and Raman data have been interpreted in terms of a compound of formulation  $[(\text{Sn}(\text{II})\text{SO}_3\text{CF}_3)_2\text{Sn}(\text{IV})\text{F}_2(\text{SO}_3\text{CF}_3)_4]_x$ .

## ACKNOWLEDGEMENTS

The author wishes to thank his research director, Professor T. Birchall for his sincere interest, patience and guidance during the course of this work.

Special thanks are also due to Dr. I. D. Brown and Mr. R. Faggiani who provided the X-ray structural data for some of the compounds. Thanks are also due to the technical staff in the Department of Chemistry for their assistance and maintenance of the instruments. The author gratefully acknowledges Mrs. E. Denham, Word Processing Centre, Faculty of Science, for her swift typing of this thesis. The author wishes to thank Dr. J. G. Ballard for his assistance in the early stages of this work. The author also wishes to thank Dr. R. D. Myers and Mr. R. Batchelor for their friendship.

Financial assistance from McMaster University from 1974 to 1980 is gratefully acknowledged.

Finally the author wishes to thank his wife, Trudy, for her encouragement and support during the final stages of this work.

TO MY MOTHER AND FATHER

TABLE OF CONTENTS

	Page
CHAPTER ONE -- INTRODUCTION	1
A. <u>General</u>	1
B. <u><sup>119</sup>Sn Mössbauer Spectroscopy</u>	2
CHAPTER TWO -- EXPERIMENTAL	9
A. <u>General Experimental Techniques</u>	9
(i) Vacuum System	9
(ii) Dry Atmosphere System	9
(iii) Reaction Vessels	10
B. <u>Experimental Techniques and Apparatus</u>	12
(i) Mössbauer Spectrometer	12
(ii) Laser Raman Spectrometer	13
(iii) Infrared Spectrometer	14
(iv) X-ray Crystallography	14
(v) Nuclear Magnetic Resonance Spectroscopy	16
(vi) Chemical Analysis	16
C. <u>Purification and Preparation of Starting Materials</u>	17
I. <u>Reagents</u>	17
(i) Hexamethylditin	17
(ii) Hexphenylditin	18
(iii) Tetraphenyltin and Tetramethyltin	18
(iv) Acids and Anhydrides	18
II. <u>Solvents</u>	19
(i) Chloroform and Chloroform-d	19
(ii) Sulphur Dioxide	19
(iii) Benzene	19
(iv) Tetrahydrofuran	19
D. <u>Preparations</u>	20
(i) $C_4H_6F_3O_2Sn, (CH_3)_2Sn(O_2CCF_3)$	20
(ii) $C_4H_7F_2O_2Sn, (CH_3)_2Sn(O_2CCHF_2)$	20
(iii) $C_4H_6Cl_3O_2Sn, (CH_3)_2Sn(O_2CCCl_3)$	21
(iv) $C_4H_7Cl_2O_2Sn, (CH_3)_2Sn(O_2CCHCl_2)$	22
(v) $C_4H_8ClO_2Sn, (CH_3)_2Sn(O_2CCH_2Cl)$	22



(vi)	$\text{Sn}(\text{O}_2\text{CCF}_3)_3$	23
(vii)	$\text{Sn}(\text{O}_2\text{CC}_3\text{F}_7)_3$	23
(viii)	$\text{Sn}(\text{O}_2\text{CCCl}_3)_3$	24
(ix)	$\text{Sn}(\text{O}_2\text{CCHCl}_2)_3$	25
(x)	$\text{Sn}(\text{O}_2\text{CCH}_2\text{Cl})_3$	25
(xi)	$\text{Sn}(\text{O}_2\text{CCH}_3)_3$	26
(xii)	$\text{Sn}(\text{O}_2\text{CC}(\text{CH}_3)_3)_3$	26
(xiii)	$\text{Sn}(\text{O}_2\text{CCF}_3)_4$	27
(xiv)	$\text{Sn}(\text{O}_2\text{CCF}_2\text{CF}_2\text{CF}_3)_4$	27
(xv)	$\text{Sn}(\text{O}_2\text{CCCl}_3)_4$	28
(xvi)	$\text{Sn}(\text{O}_2\text{CCHCl}_2)_4$	28
(xvii)	$\text{Sn}(\text{O}_2\text{CCH}_2\text{Cl})_4$	28
(xviii)	$\text{SnF}_3$	29
(xix)	$\text{Sn}(\text{SO}_3\text{CF}_3)_3$	30
(xx)	$\text{Sn}(\text{SO}_3\text{OH})_3$	30
(xxi)	$\text{Sn}(\text{SO}_3\text{CH}_3)_3$	31
(xxii)	$\text{Sn}(\text{SO}_3\text{CH}_2\text{CH}_3)_3$	31
(xxiii)	Attempted Preparation of $\text{Sn}(\text{SO}_3\text{F})_3$	32
(xxiv)	$\text{Sn}(\text{SO}_3\text{CF}_3)_4$	32
(xxv)	$\text{Sn}_3\text{F}_2(\text{SO}_3\text{CF}_3)_6$	33

CHAPTER THREE -- ACID SOLVOLYSIS OF HEXAMETHYLDITIN AND TETRAPHENYLTIN	35
A. <u>General Introduction</u>	35
B. <u>Results and Discussion</u>	36
(i) Tetramethyltin and hexamethylditin in $\text{HSO}_3\text{F}$	36
C. <u>Bis(haloacetato)-bis[dimethyltin(IV)]: "Tetramethylditin Carboxylates"</u>	40
(i) Introduction	40
D. <u>Results and Discussion</u>	41
(i) Preparation and Chemical Properties	41
(ii) Vibrational Spectra	43
(iii) Tin-119 Mössbauer Spectra	50
(iv) Nuclear Magnetic Resonance Spectra	54
(v) Mechanism of the Formation of $(\text{CH}_3)_4\text{Sn}_2(\text{O}_2\text{CR})_2$	58

20

CHAPTER FOUR -- THE CRYSTAL STRUCTURES OF	
$(\text{CH}_3)_4\text{Sn}_2(\text{O}_2\text{CCH}_2\text{Cl})_2$ , $(\text{CH}_3)_4\text{Sn}_2(\text{O}_2\text{CCCl}_3)_2$ ,	
$\{[(\text{CH}_3)_2\text{Sn}(\text{O}_2\text{CCF}_3)]_2\text{O}\}_2$ and $\{[(\text{CH}_3)_2\text{Sn}(\text{O}_2\text{CCCl}_3)]_2\text{O}\}_2$	
A. <u>Introduction</u>	61
B. <u>Experimental</u>	64
(i) The Crystal Structure Data for Bis( $\mu$ -trichloroacetato-0,0')- bis[dimethyltin(IV)]	64
(ii) The Crystal Structure Data for Bis( $\mu$ -trifluoroacetato-0,0')- bis[dimethyltin(IV)] and ( $\mu$ -monochloro- acetato-0,0')-bis[dimethyltin(IV)]	70
C. <u>Discussion</u>	73
D. <u>Crystal Structure of <math>\{[(\text{CH}_3)_2\text{Sn}(\text{O}_2\text{CCF}_3)]_2\text{O}\}</math> and <math>\{[(\text{CH}_3)_2\text{Sn}(\text{O}_2\text{CCCl}_3)]_2\text{O}\}</math></u>	82
(i) Introduction	82
(ii) Crystal Structure Data for Di- $\mu_3$ -oxo- bis( $\mu$ -trifluoroacetato-0,0')- bis(trifluoroacetato)tetrakis- [dimethyltin(IV)] and Di- $\mu_3$ -oxo-bis( $\mu$ - trifluoroacetato-0,0')-bis(trichloro- acetato)tetrakis[dimethyltin(IV)]	83
(iii) Preparation and Chemical Properties	88
(iv) Discussion of the Crystal and Molecular Structure of $\{[(\text{CH}_3)_2\text{Sn}(\text{O}_2\text{CCF}_3)]_2\text{O}\}_2$	89
 CHAPTER FIVE -- ACID SOLVOLYSIS OF HEXAPHENYLDITIN AND TETRAPHENYLTIN	93
A. <u>Introduction</u>	93
B. <u>Results and Discussion</u>	96
(i) Preparation and Chemical Properties	96
(ii) Tin-119 Mössbauer Data	101
(iii) Tin(II) Mössbauer Region	105
(iv) Tin(IV) Mössbauer Region	116
(v) Temperature Dependent Mössbauer Effect	122
(vi) Vibrational Data	126
(vii) Mechanism of Formation of $[\text{Sn(II)Sn(IV)O}(\text{O}_2\text{CR})_4\text{O}(\text{OCR})_2]_2$	134

CHAPTER SIX	-- CRYSTAL STRUCTURE OF	
	$[\text{Sn(II)Sn(IV)O}(\text{O}_2\text{CCF}_3)_4]_2\text{C}_6\text{H}_6$	137
	A. <u>Introduction</u>	137
	B. <u>Experimental for the Crystal Structure of</u>	
	<u>Di-<math>\mu_3</math>-oxo-octakis-<math>\mu</math>-(trifluoroacetato)-</u>	
	<u>ditin(II)ditin(IV)-Benzene (1/1)</u>	138
	C. <u>Results and Discussion</u>	143
	(i) Crystal Structure of	
	$[\text{Sn(II)Sn(IV)O}(\text{O}_2\text{CCF}_3)_4]_2\text{C}_6\text{H}_6$	143
	(ii) Mechanism of Formation of	
	$[\text{Sn(II)Sn(IV)O}(\text{O}_2\text{CCF}_3)_4]_2\text{C}_6\text{H}_6$	157
CHAPTER SEVEN	-- MIXED OXIDATION STATE TIN COMPOUNDS DERIVED FROM	
	THE REACTION OF HEXAPHENYLDITIN WITH INORGANIC	
	ACIDS	160
	A. <u>Introduction</u>	160
	B. <u>Results and Discussion</u>	165
	(i) Preparations	165
	(ii) $^{119}\text{Sn}$ Mössbauer Data	166
	(iii) Vibrational Data	178
CHAPTER EIGHT	-- CONCLUSIONS	186
	A. <u>Summary</u>	186
	B. <u>Suggested Topics for Future Research</u>	188

REFERENCES

STRUCTURE FACTOR TABLES BOUND SEPARATELY  
 McMaster Thesis Table #1

LIST OF TABLES

	Page
Table 2.1 Analytical Data for Preparations	34
Table 3.1 $^1\text{H}$ N.M.R. Data for Solvolysis of $(\text{CH}_3)_4\text{Sn}$ in Excess $\text{HSO}_3\text{F}$	37
Table 3.2 Infrared and Raman Data for $(\text{CH}_3)_4\text{Sn}_2(\text{O}_2\text{CR})_2$	45
Table 3.3 Symmetric and Asymmetric Stretches (IR) of the $-\text{CO}_2$ Group for $(\text{CH}_3)_4\text{Sn}_2(\text{O}_2\text{CR})_2$ , $(\text{C}_6\text{H}_5)_4\text{Sn}_2(\text{O}_2\text{CR})_2$ and $(\text{CH}_3)_3\text{Sn}(\text{O}_2\text{CR})$	48
Table 3.4 Comparison of the $-\text{CO}_2$ Group and Tin-Carbon Stretches (IR) for $(\text{CH}_3)_4\text{Sn}_2(\text{O}_2\text{CR})_2$	49
Table 3.5 $^{119}\text{Sn}$ Mössbauer Data for $(\text{CH}_3)_4\text{Sn}_2(\text{O}_2\text{CR})_2$ at $77^\circ\text{K}$	51
Table 3.6 N.M.R. Data for $(\text{CH}_3)_4\text{Sn}_2(\text{O}_2\text{CR})_2$ Compounds in $\text{CDCl}_3$ at $37^\circ\text{C}$	55
Table 4.1 Atomic Coordinates for $(\text{CH}_3)_4\text{Sn}_2(\text{O}_2\text{CCCl}_3)_2$	67
Table 4.2 Thermal Parameters for $(\text{CH}_3)_4\text{Sn}_2(\text{O}_2\text{CCCl}_3)_2$	68
Table 4.3 Bond Lengths and Bond Angles for $(\text{CH}_3)_4\text{Sn}_2(\text{O}_2\text{CCCl}_3)_2$	69
Table 4.4 Interatomic Distances and Angles for $(\text{CH}_3)_4\text{Sn}_2(\text{O}_2\text{CCH}_2\text{Cl})_2$	71
Table 4.5 Interatomic Distances and Angles for $(\text{CH}_3)_4\text{Sn}_2(\text{O}_2\text{CCF}_3)_2$	72
Table 4.6 A Summary of Bond Lengths and Bond Angles for $(\text{CH}_3)_4\text{Sn}_2(\text{O}_2\text{CR})_2$	74
Table 4.7 Interatomic Distances and Angles for $\{[(\text{CH}_3)_2\text{Sn}(\text{O}_2\text{CCF}_3)]_2\text{O}\}_2$	84

Table 5.1	$^{13}\text{C}$ N.M.R. Data for $\text{Sn}(\text{O}_2\text{CR})_3$ in a Solution of $(\text{RCO})_2\text{O}$ and $\text{C}_6\text{D}_6$	99
Table 5.2	$^{119}\text{Sn}$ Mössbauer Data for $\text{Sn}(\text{O}_2\text{CR})_3$ , $\text{Sn}(\text{O}_2\text{CR})_4$ and Related Tin Compounds	102
Table 5.3	Infrared and Raman Data for $\text{Sn}(\text{O}_2\text{CCF}_3)_4$ and the Tin Carboxylates, $\text{Sn}(\text{O}_2\text{CR})_3$	127
Table 6.1	Atomic Coordinates for $[\text{Sn}(\text{II})\text{Sn}(\text{IV})\text{O}(\text{O}_2\text{CCF}_3)_4]_2\text{C}_6\text{H}_6$	140
Table 6.2	Thermal Parameters for $[\text{Sn}(\text{II})\text{Sn}(\text{IV})\text{O}(\text{O}_2\text{CCF}_3)_4]_2\text{C}_6\text{H}_6$	141
Table 6.3	Bond Lengths and Bond Angles for $[\text{Sn}(\text{II})\text{Sn}(\text{IV})\text{O}(\text{O}_2\text{CCF}_3)_4]_2\text{C}_6\text{H}_6$	144
Table 6.4	Deviations in Å, of Atoms from a Least Squares Plane	146
Table 6.5	Estimation of Hydrogen Bonding Interactions	156
Table 7.1	$^{119}\text{Sn}$ Mössbauer Data for $\text{Sn}(\text{SO}_3\text{R})_3$ , $\text{Sn}_3\text{F}_2(\text{SO}_3\text{CF}_3)_6$ , $\text{Sn}(\text{IV})\text{O}\cdot\text{SO}_4$ , $\text{Sn}(\text{II})(\text{SO}_3\text{F})_2$ , $\text{SnF}_3$ and Related Tin Compounds	167
Table 7.2	Vibrational Data for $\text{Sn}(\text{SO}_3\text{R})_3$ , $\text{Sn}_3\text{F}_2(\text{SO}_3\text{CF}_3)_6$ , $\text{Sn}(\text{IV})\text{O}\cdot\text{SO}_4$ , $\text{Sn}(\text{II})(\text{SO}_3\text{F})_2$ and Related Compounds	179
Table 7.3	Vibrational Data for $\text{SnF}_3$ and Related Compounds	183

LIST OF FIGURES

		Page
Figure 2.1	Apparatus for the preparation of compounds in the absence of air	11
Figure 3.1	Possible structures for $(\text{CH}_3)_4\text{Sn}_2(\text{O}_2\text{CR})_2$	42
Figure 3.2	$^{119}\text{Sn}$ Mössbauer spectrum of $(\text{CH}_3)_4\text{Sn}_2(\text{O}_2\text{CCF}_3)_2$	52
Figure 3.3	100 MHz $^1\text{H}$ N.M.R. spectrum of $(\text{CH}_3)_4\text{Sn}_2(\text{O}_2\text{CCF}_3)_2$	57
Figure 4.1	A view of $(\text{CH}_3)_4\text{Sn}_2(\text{O}_2\text{CCCl}_3)_2$	75
Figure 4.2	$(\text{CH}_3)_4\text{Sn}_2(\text{O}_2\text{CCH}_2\text{Cl})_2$ viewed down the two-fold axis	76
Figure 4.3	A view of $(\text{CH}_3)_4\text{Sn}_2(\text{O}_2\text{CCF}_3)_2$	77
Figure 4.4	A view of $\{[(\text{CH}_3)_2\text{Sn}(\text{O}_2\text{CCF}_3)]_2\text{O}\}_2$	87
Figure 4.5	Molecular packing of $\{[(\text{CH}_3)_2\text{Sn}(\text{O}_2\text{CCF}_3)]_2\text{O}\}_2$	91
Figure 5.1	$^{119}\text{Sn}$ Mössbauer spectrum of $\text{Sn}(\text{O}_2\text{CCH}_3)_3$ at 77°K	103
Figure 5.2	$^{119}\text{Sn}$ Mössbauer spectrum of $\text{Sn}(\text{O}_2\text{CCF}_3)_3$ at 77° K	104
Figure 5.3	A plot of the isomer shift of the tin(II) site versus the quadrupole splitting of this site for the series $\text{Sn}(\text{O}_2\text{CR})_3$	107
Figure 5.4	A plot of the isomer shift of the tin(II) site against the pKa of the acid for the series $\text{Sn}(\text{O}_2\text{CR})_3$	108
Figure 5.5	A plot of the isomer shift of the tin(II) site against the Taft inductive factor $\sigma^*$ , of the R groups for the series $\text{Sn}(\text{O}_2\text{CR})_3$	109

Figure 5.6	A diagram of the tetranuclear skeleton of [Sn(II)Sn(IV)O(O <sub>2</sub> CC <sub>6</sub> H <sub>4</sub> NO <sub>2</sub> -o) <sub>4</sub> THF] <sub>2</sub>	112
Figure 5.7	<sup>119</sup> Sn Mössbauer spectrum of Sn(O <sub>2</sub> CCF <sub>3</sub> ) <sub>4</sub> at 77° K	120
Figure 5.8	<sup>119</sup> Sn Mössbauer spectrum of Sn(O <sub>2</sub> CCH <sub>3</sub> ) <sub>3</sub> at 4° K	124
Figure 5.9	<sup>119</sup> Sn Mössbauer spectrum of Sn(O <sub>2</sub> CCF <sub>3</sub> ) <sub>3</sub> at 4° K	125
Figure 6.1	The molecular structure of [Sn(II)Sn(IV)O(O <sub>2</sub> CCF <sub>3</sub> ) <sub>4</sub> ] <sub>2</sub>	147
Figure 6.2	A stereoscopic view of the molecular packing of benzene rings and Sn <sub>4</sub> O <sub>2</sub> units	154
Figure 7.1	<sup>119</sup> Sn Mössbauer spectrum of Sn(SO <sub>3</sub> CF <sub>3</sub> ) <sub>3</sub> at 77° K	170
Figure 7.2	<sup>119</sup> Sn Mössbauer spectrum of Sn <sub>3</sub> F <sub>2</sub> (SO <sub>3</sub> CF <sub>3</sub> ) <sub>6</sub> at 77° K	175

DEFINITIONS FOR TABLES

I. Vibrational spectra

Definition	Symbol or Abbreviation	Subscript
Wave number shift of Raman line, $\text{cm}^{-1}$	Raman	
Wave number of infrared absorption band, $\text{cm}^{-1}$	IR	
Weak	w	
Medium	m	
Strong	s	
Very strong	vs	
Stretching	v	
Bending	$\delta$	
Rocking	$\rho$	
Asymmetrical		as
Symmetrical		s
Shoulder	sh	
Broad	b	
Relative intensities of Raman lines are given in parentheses		



## II. Mössbauer Data

Definition	Symbol	Units
Isomer shift	$\delta$	$\text{mm s}^{-1}$
Quadrupole splitting	$\Delta$	$\text{mm s}^{-1}$
Line-width at half-height	$\Gamma$	$\text{mm s}^{-1}$
Chi square	$\chi^2$	

## III. N.M.R. Spectra Data

Definition	Symbol	Units
Chemical shift	$\delta$	ppm
Coupling constant	J	Hz

## IV. Crystal Structural Data

### Definition

All values are reported with estimated standard deviations in parentheses

## CHAPTER ONE

### INTRODUCTION

#### A. General

Historically, the first known hexa-organoditin, hexaethyliditin, was prepared by Lowig in 1852 by the interaction of ethyl iodide with tin-sodium alloy.<sup>1</sup> By 1972, 38  $R_3Sn-SnR_3$  compounds were listed in a review of organotin compounds.<sup>2</sup> It has been noted by Gilman<sup>3</sup> that most of the chemistry of organopolytins involves cleavage of the tin-tin bond, either by homolytic cleavage or in some cases disproportionation.<sup>2</sup> The acid solvolysis of hexa-organoditin compounds has received little attention in the past. This may be in part due to the fact that when an organoditin compound reacts with an acid, cleavage of the tin-tin bond usually occurs with formation of organotin compounds which may be prepared more conveniently by alternate methods. This general reactivity of hexa-organoditin compounds may be associated with a relatively thermodynamically weak or kinetically reactive tin-tin bond. A brief introduction, reviewing the previously established or proposed reactions of hexa-organoditin compounds in acid medium and related studies, will be presented in the appropriate chapter of this thesis. The purpose of the work presented in this thesis was to extend the knowledge of the structure and chemistry of tin compounds and to synthesize tin compounds which had not been previously prepared or which were poorly characterized. The spectroscopic studies of the reaction products from

the acid solvolysis of hexamethylditin, hexaphenylditin, tetramethyltin and tetraphenyltin form the basis of this thesis.

A powerful array of physical techniques is now available for the investigation of tin compounds. The most important of these are  $^{119}\text{Sn}$  Mössbauer spectroscopy, nuclear magnetic resonance spectroscopy, X-ray crystallography and infrared and Raman spectroscopy. These techniques are no longer in their infancy, and are powerful, sensitive, probes for the examination of the chemical and physical properties of tin compounds. A number of comprehensive reviews, monographs and introductions to the theory and application of  $^{119}\text{Sn}$  Mössbauer spectroscopy,<sup>4-9</sup> n.m.r.,<sup>10-13</sup> and X-ray crystallography,<sup>14-16</sup> to the study of tin compounds may be found elsewhere. One of the most convenient techniques for the study of compounds of tin in the solid state which provides information not readily accessible from other techniques is  $^{119}\text{Sn}$  Mössbauer spectroscopy. The application of this technique to the study of tin compounds forms an important part of this thesis.

#### B. $^{119}\text{Sn}$ Mössbauer Spectroscopy

The recoilless emission and resonant reabsorption of  $\gamma$ -rays without thermal broadening is known as the Mössbauer effect. The process of decay of  $^{119\text{m}}\text{Sn}$  to the first excited state of  $^{119}\text{Sn}$  followed by relaxation of the nucleus to the ground state produces the " $^{119}\text{Sn}$  Mössbauer"  $\gamma$ -radiation of 23.875 Kev. The recoilless emission of  $\gamma$ -rays is achieved using  $\text{Ca}^{119\text{m}}\text{SnO}_3$  as a source where the tin is held in a

strong ionic lattice. Since organotin compounds have a low Debye temperature the majority of these compounds require cooling to 77°K.

The nuclear energy levels responsible for the transitions giving rise to the  $\gamma$ -ray emission ( $I = 3/2$  to  $I = 1/2$ ) and reabsorption ( $I = 1/2$  to  $3/2$ ) will be perturbed to a slight extent by the presence of  $s$ , electron density at the nucleus. When the absorber is in a different chemical environment from the emitter then the nuclear energy level separation will be different and the emitted  $\gamma$ -ray will not be resonantly absorbed by the absorber. Resonance can be achieved by modulating the emitted  $\gamma$ -ray by means of the Doppler effect, that is by moving the source relative to the absorber. If the emitter is moved towards the absorber the photons will have a higher energy than when these relative velocities are zero. Resonance occurs when the  $\gamma$ -ray energy plus the Doppler energy exactly matches that in the absorber. The Doppler velocity, measured in  $\text{mm s}^{-1}$  relative to the source is called the isomer shift,  $\delta$ , and is a measure of the difference in  $s$  electron density of the two nuclei in their environments. The line shape of the absorption is derived simply from the Heisenberg uncertainty in energy and is determined by the life-time of the excited state. The distribution of the absorption is ideally a Lorentzian shape with a width at half-peak height of twice the natural line width, which is  $0.626 \text{ mm s}^{-1}$  for  $^{119}\text{Sn}$  Mössbauer spectroscopy. Only the tin  $s$  orbitals have a finite electron density at the nucleus and only  $s$  electrons can electrostatically interact with the charge distribution of the nucleus. Only  $s$  electrons can directly perturb the nucleus and the isomer shift is a relative

measure of the core s and valence s electron density. The isomer shift is given by (1.1).<sup>4</sup>

$$\delta = \frac{4\pi}{5} Ze^2 R \left(\frac{\delta R}{R}\right) [|\psi_s(o)|_{\text{absorber}}^2 - |\psi_s(o)|_{\text{source}}^2] \quad (1.1)$$

R is the radius of the nucleus and  $\delta R$  is the change in nuclear radius during emission. The value of  $\delta R/R$  is positive for  $^{119}\text{Sn}$ . Because  $\delta R/R$  is positive, an increase in isomer shift means an increase in s electron density at the tin nucleus. The term  $|\psi_s(o)|^2$  represents the total s electron density at the tin atom in this thesis.

Only the uncertainty in the absolute value of  $\delta R/R$  prevents the direct calculation of the chemical term  $[|\psi_s(o)_{\text{absorber}}|^2 - |\psi_s(o)_{\text{source}}|^2]$  from the measured isomer shift, and hence the direct study of changes in s electron density. Mossbauer spectroscopy provides the only direct measurement of the relative s electron density at the nucleus which can provide a stringent test for theoretical models of the structure and bonding in compounds. Provided the effects of hybridization can be clearly defined, it is possible to correlate isomer shifts of tin compounds with electronegativity effects.<sup>6,7</sup>

The observed range of isomer shifts of tin compounds,  $-0.5$  to  $4.4 \text{ mm s}^{-1}$ , is relatively large in comparison to the experimental line width,  $\sim 1 \text{ mm s}^{-1}$ . This makes highly precise measurements of isomer shifts possible. Reasonable agreement, when there exists more than one independent determination of an isomer shift, is within three sigma ( $3\sigma$ ), where the  $\sigma$  error (standard deviation of the measurement) is  $0.03$  to  $0.04 \text{ mm s}^{-1}$ .<sup>17</sup> The observed range of isomer shifts for various

classes of tin compounds are in approximate accord with predictions based on the model of Lees and Flinn.<sup>18</sup> Isomer shifts for tin(II) are predicted to be in the range 2.26 to 4.84 mm s<sup>-1</sup> and for compounds of tin(IV) from -0.38 to 1.92 mm s<sup>-1</sup>. The Lees and Flinn approach is limited in validity and ignores effects of 5d electrons and deviations of tin from sp<sup>3</sup> geometry. However, it does demonstrate the effects of 5s and 5p electrons on the magnitude of the isomer shift.

The correlation of isomer shifts with electronegativity of the ligands for tin(IV) compounds of a given structural type has been quite successful.<sup>6,7</sup> Isomer shifts for new tin(IV) compounds may be at least qualitatively predicted from an additive model<sup>6</sup> based on an assignment of partial isomer shifts for various ligands from measured isomer shifts of compounds having well established structures. The isomer shift predicted for the new compound is the sum of ligand isomer shifts derived from compounds of the same structural type. Such predictions are not reliable for tin(II) compounds and this aspect will be discussed in Chapter 5.

When the tin nucleus is in a non-cubic environment the degeneracy of the excited nuclear state ( $I = 3/2$ ) is partially lifted and two components,  $m_I = \pm 1/2$  and  $m_I = \pm 3/2$ , result and two lines are observed in the spectrum. The energy of these two lines is expressed by (1.2).

$$E_q = \frac{e^2 q_0}{4I(2I-1)} [3m_I^2 - I(I+1)] (1+n^2/3)^{1/2} \quad (1.2)$$

For  $^{119}\text{Sn}$  the quadrupole splitting,  $\Delta, \text{mm s}^{-1}$ , is the separation of the  $\pm 1/2$  and  $\pm 3/2$  levels and is given by (1.3).

$$\Delta = 1/2e \cdot Q \cdot V_{zz} (1+n^2/3)^{1/2} \quad (1.3)$$

$Q$  is the nuclear quadrupole moment,  $V_{zz}$  the electric field gradient tensor  $\partial^2 V / \partial z^2$ , and  $n$  the asymmetry parameter defined by  $n = (V_{xx} - V_{yy}) / V_{zz}$ . The sign of the quadrupole interaction in compounds determines the shape of the charge distribution about the tin nucleus. When the principal component of the electric field gradient tensor,  $V_{zz}$ , is negative then the  $\pm 3/2$  nuclear spin state lies above the  $\pm 1/2$  state in energy. There is a greater electron density along the  $z$  axis than in the  $x$ - $y$  plane, that is the charge distribution about tin is prolate.

It has been deduced from  $^{119}\text{Sn}$  Mossbauer quadrupole splitting data on organotin(IV) compounds that the electric field gradient at the tin nucleus is given, to the first approximation, by the sum of independent contributions, one for each ligand bonded to the tin atom.<sup>19</sup> These contributions are considered to arise mainly from an asymmetric distribution of valence shell electrons in the tin-ligand  $\sigma$  bonds. This theory was originally developed as a "point charge model"<sup>20</sup> in which effective charges are assigned to each ligand. A closely related molecular orbital model<sup>21</sup> using localized orbitals provides the natural framework for a discussion of additive electric field gradients. Relative partial field gradient parameters are assigned on the basis of these models from observed quadrupole splitting data for established structure types. Quadrupole splittings for other molecules can be

predicted to within  $0.4 \text{ mm s}^{-1}$ , or better, depending on the data base. Disagreement between measured and calculated quadrupole splittings can be used as evidence of large distortions or an incorrect assignment of structures. The model is an approximation in which d orbital contributions to the partial field gradient parameter are assumed to be negligible compared to p orbital contributions and non-additivity, or distortions from ideal geometry, contribute no more than 10-20% of the total field gradient.<sup>21</sup> The molecular model gives a consistent description of the relationship between quadrupole splitting data and stereochemistry in organotin(IV) complexes. Combined with chemical judgement and a reliable data base this method gives a good guide to the likelihood of an assigned structure being correct. The method is well established for a large variety of structures of organotin(IV) compounds. Exact expressions for the calculation of quadrupole splittings for compounds having tetrahedral  $R_3\text{SnL}$ , trigonal bipyramidal  $R_3\text{SnL}$  and  $R_2R'\text{SnL}$  geometries are given by (1.4),<sup>21</sup> (1.5)<sup>21</sup> and (1.6)<sup>22</sup> respectively.

$$|\Delta| = 2R^{\text{tet}} - 2L^{\text{tet}} \quad (1.4)$$

$$|\Delta| = 3R - 4L \quad (1.5)$$

$$|\Delta| = [7R^2 - 2RR' + 4R'^2 - 16RL - 8R'L + 16L^2]^{1/2} \quad (1.6)$$

These expressions allow for the calculation of the magnitude of the quadrupole splitting provided a significant data base for the evaluation of the various partial field gradient parameters for the ligands  $R^{\text{tet}}$ ,  $R$ ,  $R'$  and  $L$  of the structure type of interest is available.



The absence of a quadrupole splitting indicates an undistorted ligand field of cubic symmetry. Small but unresolved quadrupole splittings may result in large apparent line width values,  $\Gamma$  mm s<sup>-1</sup>. The limit of resolution of quadrupole splitting is commonly assigned as being about 0.5 mm s<sup>-1</sup>.

The two lines of a quadrupole doublet should be of equal intensity but sometimes the spectrum is in fact not symmetric. There are a number of sources of this asymmetry.<sup>23</sup> When partial orientation of absorber crystallites occurs the two transitions then have different dependence of intensity on the angle  $\theta$  made by the direction of the  $\gamma$ -ray with the axis of the electric field gradient tensor in the molecule. To reduce orientation effects samples for the Mössbauer experiment are ground with a grease or a powdered dilutant, such as boron nitride, to abrade the crystallites. When the tin atom is not in a site of cubic symmetry, asymmetry may also arise from the anisotropy of the recoil-free fraction and is known as the Goldanskii-Karyagin effect.<sup>23</sup> This asymmetry increases as the temperature is raised.

## CHAPTER TWO

### EXPERIMENTAL

#### A. General Experimental Techniques

##### (i) Vacuum System

In most instances the preparative work presented here was performed using a pyrex vacuum system. The vacuum line was divided into a high-vacuum, all pyrex section and a greaseless pyrex section with teflon stopcocks for more corrosive materials. Both sections were accessible from a pyrex manifold which was connected to a liquid nitrogen trap, a two-stage mercury diffusion pump and a rotary pump. Connections were made to the high-vacuum section by 9 mm i.d. ball joints and connections were made to the teflon stopcocks by 1/4" o.d. pyrex fitted by a straight swagelock union or a teflon valve with swagelock fittings. A simple manometer with an evacuable mercury bulb source at its base was used to measure gas pressure in the system. The vacuum was monitored with a Vacustat Gauge (Edwards High Vacuum Ltd.), which was accurate to  $1 \times 10^{-3}$  mm Hg. The system was designed so that each section could be dismantled using 9 mm i.d. ball joints, for easy maintenance.

##### (ii) Dry Atmosphere System

All of the samples or reagents which reacted in air were handled in a dry nitrogen filled Labcono glove box fitted with an external constant circulation drying system using liquid nitrogen cooled traps.

The glove box was filled with "extra-dry nitrogen", supplied by Specialty Gases, and four trays of  $P_4O_{10}$  were maintained in the glove box to ensure a dry atmosphere. An evacuable port provided access to the glove box. All air sensitive reaction products, not stored in sealed glass tubes, were stored in closed glass containers in the glove box.

### (iii) Reaction Vessels

When it was necessary for samples to be prepared in the absence of air, a reaction vessel<sup>24</sup> of the type shown in Figure 2.1 was used. The vessels were carefully dried by repeated flaming under vacuum before use. All transfers of reagents or solvents into vessels were done on a vacuum line or in a dry glove box. The vessel, unless otherwise specified, consisted of two reaction bulbs separated by a medium glass frit. The stopcocks used were teflon or rotoflow, TF2/13, quickfit (Jobling Laboratory Division). When addition of reagents and solvents was complete, the vessel was degassed on the vacuum line. Teflon stopcocks or 1/4" i.d. teflon swagelock unions were removed from the vessel by sealing off the glass tube at a convenient point (a or b, Figure 2.1) on the reaction vessel. The contents of the vessel were frozen in liquid nitrogen prior to the sealing of all glass connections. Preparations were designed such that the desired solid product was in side A of the reaction vessel and the bulk of the solvent, excess reagents and undesired products were in side B of the vessel. When vessels were heated for long periods of time, the rotoflow valves were kept cool by wrapping them with tygon tubing through which cold water flowed.

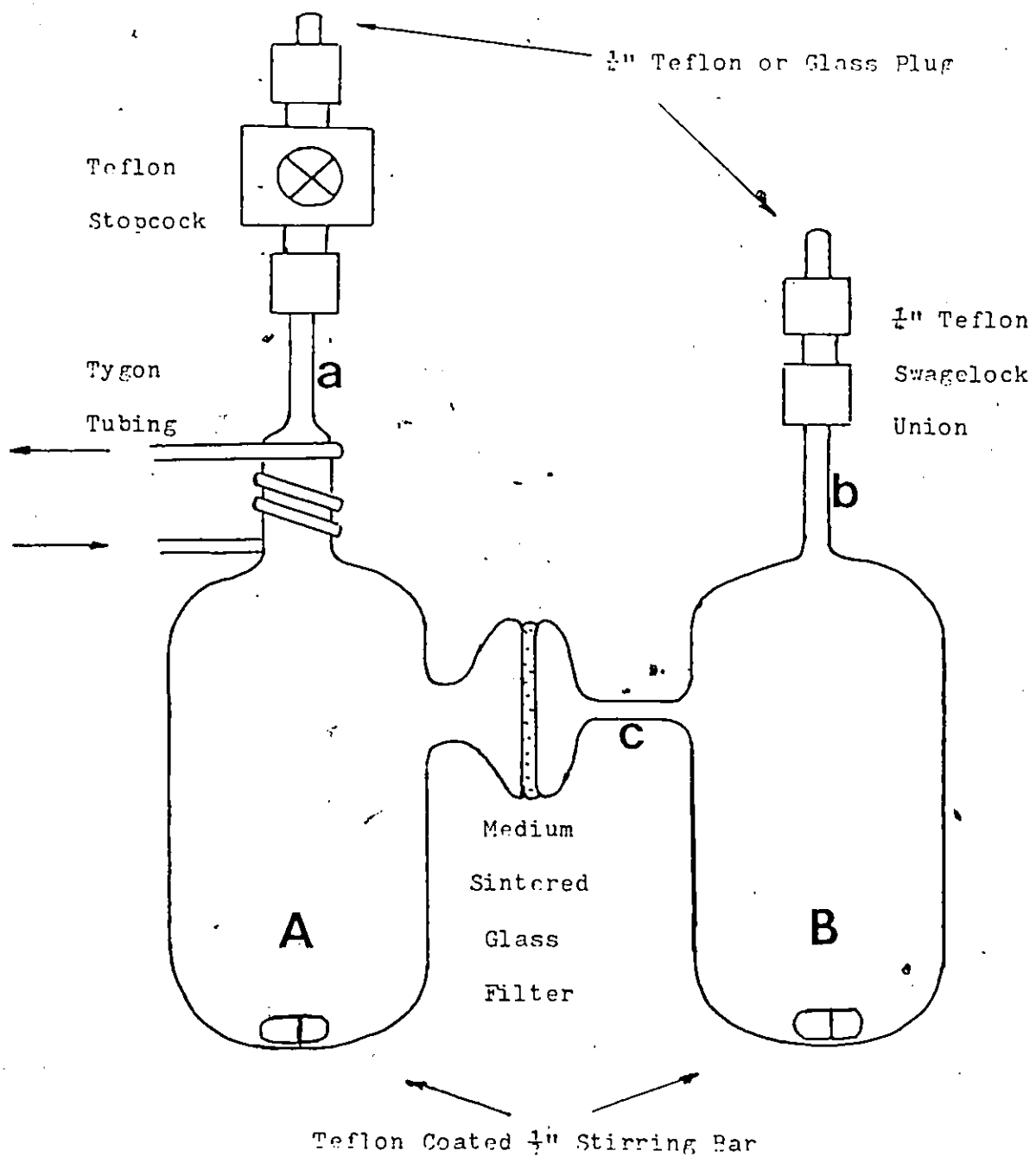


Figure 2.1. Apparatus for the preparation of compounds in the absence of air.

B. Experimental Techniques and Apparatus

(i) Mössbauer Spectrometer

Mössbauer spectra ( $^{119}\text{Sn}$ ) were recorded using an Elscint AME 40 drive system which was operated in the constant acceleration mode with automatic folding of the triangular waveform. The transmitted radiation, through a Pd filter, was detected by a Kr-CO<sub>2</sub> (1 atm) proportional counter and fed to a Tracor-Northern multi-channel analyzer which was operated in the up-down multi-scaling mode. The data were transferred onto a teletypewriter, TTY33, which included a typewriter and a paper tape punch. The data were then transferred to computer cards for processing. Spectra were computer fitted using a program written by Dr. A. J. Stone<sup>25</sup> and modified by Dr. D. G. Grundy of the Department of Geology, McMaster University.

This program fitted a sum of Lorentzian lines to a given Mössbauer spectrum using the Gauss non-linear regression procedure. The program was taken to converge when the computational error in each parameter was at least 1000 times less than the estimated error. The program provided the goodness of fit criterion,  $\chi^2$ . The 5, 1 and 0.1 percent confidence points for the maximum value of the ratio  $\chi^2/\text{degree of freedom}$  are 1.15, 1.22 and 1.30 respectively. A value of less than 1.22 for this ratio was acceptable, while a value greater than 1.30 indicated an unreasonable fit. One spurious count can lead to a very poor value for this ratio.

Samples contained approximately 10 mg natural tin cm<sup>-2</sup>, and were rigidly held in a liquid Transfer Cryotip system manufactured by Air Products and Chemicals Inc. The source was Ca<sup>119</sup>/SnO<sub>3</sub>, obtained from

Amersham-Searle, and was maintained at room temperature. Temperature was monitored by means of a calibrated iron-doped gold chromel thermocouple and a Hewlett-Packard 419A DC null voltage detector. The velocity range was calibrated using a  $^{57}\text{Co}/\text{Rh}$  source and a standard iron foil at ambient temperature. All isomer shifts were measured relative to  $\text{SnO}_2$  as zero at ambient temperature.

Solid samples were finely ground powders, intimately mixed with Apiezon N Grease and sandwiched in a copper holder with a window of cross section  $2.5 \text{ cm}^2$  between thin aluminum foils. Any sample which reacted with Apiezon grease was finely powdered and compressed between two teflon discs in a copper holder between thin aluminum foils. Liquid samples were syringed into a teflon holder, which is described elsewhere,<sup>26</sup> and mounted on a copper block which was cooled in a liquid nitrogen bath.

The estimated error in the parameters presented in the  $^{119}\text{Sn}$  Mossbauer Tables in standard deviation units is 0.03 to 0.04. These values are based on the statistics derived for the computer fitted spectra.

#### (ii) Laser Raman Spectrometer

Raman spectra were recorded with a Spectra-Physics He/Ne (6328 Å), or an Ar ion (5145 Å) laser using a Spex 1400 spectrophotometer system. The instrument has been described previously.<sup>27</sup> Non-hygroscopic samples were prepared in either a 5 mm o.d. thin walled polished n.m.r. tube, or in a melting point tube. Hygroscopic solids were handled in a glove box, with samples in pre-dried melting point tubes or 1/4" Pyrex tubes which were sealed before recording spectra.

(iii) Infrared Spectrometer

Infrared spectra were recorded on a Perkin Elmer 283, or a Nicolet 7000 F.T.I.R., the sample compartments of which were constantly flushed with dry nitrogen. Infrared spectra were recorded for finely powdered samples, nujol mulls, halocarbon mulls, or  $\text{CHCl}_3$  solutions with NaCl, KBr, AgCl windows or polyethylene plates.

(iv) X-Ray Crystallography

Crystals chosen were small blocks or fibers, and were mounted with the longest crystal dimension approximately parallel to the tubes. The crystal dimensions were obtained using a microscope.

The crystal symmetry and preliminary cell dimensions were determined from precession photographs when possible. Zero layer and first layer precession photographs gave systematic absences, from which the space group was determined. The crystal was placed on the Syntex P2<sub>1</sub> diffractometer and an orientation matrix was obtained using Polaroid film. Ten strong, low angle reflections obtained from the film were accurately centered, and a unit cell was chosen based on these centered reflections. These reflections were indexed, and data in the range  $10^\circ < 2\theta < 30^\circ$  were collected. The final unit cell parameters were obtained by least squares refinement of fifteen accurately centered reflections within this range. The intensity data collected for refinement were collected on the basis of this accurate unit cell.

X-ray intensity measurement and structure determination and refinement have been described previously.<sup>15</sup> Treatment of data here was as follows.

Intensity data from the diffractometer were stored on magnetic tape and then transferred to computer cards using the computer program Syntex (written by Syntex Analytical Instruments, Cupertino, California, U.S.A.). The information consisted of Miller indices, peak height, background heights and scan rate. DATCO3 (part of XRAY 71 package of crystallography programs, McMaster University), was then used to sort data and to calculate intensities,  $I$ , from peak heights, background intensities and scan rates, along with  $\sigma(I)$ , the standard deviation of the intensities of the reflections. The unscaled structure factors,  $F$ , were calculated by DATRDN (part of XRAY 71 package), and a spherical correction may be applied using this program. The intensities were corrected for both Lorentz and polarization effects. Output consisted of computer cards with structure factors and  $\sigma(F)$  calculated along with Miller indices. The Fourier synthesis program (part of XRAY 71 package), was used to generate Patterson function maps from which the positions of the heavy atoms were located. Location of heavy atom positions was followed by full matrix least squares refinement of these positions using CUDLS (written by J. S. Stephens, McMaster University). CUDLS was followed by SYMFOU (the Fourier synthesis program, written by J. K. Brandon and J. S. Rutherford), for generation of a difference electron density map for location of other atoms in the unit cell. Positional, thermal and scale factor parameters were refined using CUDLS. Atomic scattering factors corrected for anomalous dispersion were used in CUDLS. Near the end of the refinement a weighting scheme was applied using SIGMA (written by I. D. Brown, McMaster University). A secondary



extinction correction was calculated using SEC (part of XRAY 71 package), and refined using CUDLS. Plots of atoms with thermal ellipsoids were generated using ORTEP (part of XRAY 71 package). Least squares planes of atoms were calculated using PALS (part of XRAY 71 package). Bond geometry was calculated for final refinement using CUDLS. Structure factors from final refinement were tabulated using MODPRIN (part of XRAY 71 package).

Hydrogen atom positions of benzene molecules were selected such that these atoms were in the least squares plane of the carbon atoms with C-H bond lengths of 1Å and H-C-C angles of 120°. All interatomic distances, Å, and angles, (°), involving hydrogen atoms were calculated using ORTEP.

(v) Nuclear Magnetic Resonance Spectroscopy

Proton m.r. spectra were obtained using a Varian H.A. 100, or E.M. 390, or a Bruker W.H. 90. The latter instrument was also used to obtain <sup>13</sup>C m.r. spectra. Fluorine m.r. were obtained on a Varian D.P. 60. Samples were prepared as saturated solutions in the appropriate solvents. Air sensitive compounds were sealed in n.m.r. tubes.

(vi) Chemical Analysis

All hygroscopic samples were transferred into weighing bottles in a dry atmosphere glove box. The weight of sample used was determined by the difference method after the compound had been transferred to an

analysis vessel. The tin was determined as  $\text{SnO}_2$ .<sup>28</sup> Approximately 200-300 mg of sample were transferred to a platinum crucible, and 20-30 drops of fuming sulfuric acid were added. Samples were heated to dryness before ignition to  $\text{SnO}_2$ . Tin(II) was determined by the method of Donaldson.<sup>29</sup>

The percentage of acid ligand was determined,<sup>30</sup> using 200-500 mg of sample dissolved in distilled water, by titration with 10-20  $\text{cm}^3$  of standard 0.1 N sodium hydroxide solution, using phenolphthalein as an indicator. Water insoluble tin acetates were dissolved in 25  $\text{cm}^3$  of tetrahydrofuran, titrated to 80% completion, and 50 ml of distilled water were added before titration to the end point.

Carbon, hydrogen and halogen analyses were done by Chemalytics, Inc., Arizona, and/or Schwarzkopf Microanalytical Laboratory, New York.

## C. Purification and Preparation of Starting Materials

### I. Reagents

#### (i) Hexamethylditin

Hexamethylditin (Alfa Products), was normally used without further purification. When purification was necessary, the reagent was vacuum condensed and/or distilled under reduced pressure (139 mm Hg,  $124 \pm 2^\circ\text{C}$ ). Hexamethylditin was stored in an inert atmosphere or under vacuum.

(ii) Hexaphenylditin

Hexaphenylditin (Alfa Products), 99+%, was recrystallized three times by dissolution in dry chloroform and precipitation with absolute ethanol. The compound was pumped dry under vacuum, and stored under vacuum and/or inert atmosphere prior to use.

(iii) Tetraphenyltin and Tetramethyltin

Tetraphenyltin and tetramethyltin (Alfa Products), were used without further purification. Tetraphenyltin was also prepared from triphenyltin chloride (Alfa Products), with an excess of phenyl lithium (Alfa Products). The product isolated was recrystallized from benzene.

(iv) Acids and Anhydrides

The following reagents were used directly without further purification unless otherwise stated in the preparation of the compounds.

Iodoacetic acid (97%), tribromoacetic acid (99%), trifluoroacetic anhydride (99+%), trimethylacetic acid (99+%), heptafluorobutyric acid (99%), ethanesulfonic acid and trifluoromethanesulfonic acid were obtained from Aldrich Chemical Company Inc. Acetic anhydride (certified A.C.S.), and chloroacetic acid (certified), were obtained from Fisher Scientific Co. Dichloroacetic acid and trifluoroacetic acid were obtained from J. T. Baker Company. Trichloroacetic acid (99%, B.D.H. Chemical Ltd.), acetic acid (C-I-L, C.P. Reagent), methanesulfonic acid (98%, anhydrous, Matheson, Coleman and Bell Manufacturing Chemist) were also used.

Anhydrous hydrofluoric acid and doubly distilled fluorosulfonic acid were obtained from Dr. R. J. Gillespie's laboratory, McMaster University.

## II. Solvents

### (i) Chloroform and Chloroform-d

Dry chloroform (Fisher Scientific Co.), was used without further purification. Chloroform-d (Merck, Sharp and Dohme, Canada, Ltd.), was dried over molecular sieves.

### (ii) Sulfur Dioxide

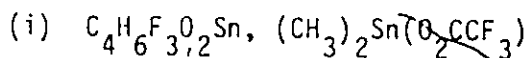
Sulfur dioxide (Matheson Co.), was dried and stored over  $P_4O_{10}$  before use. When required, it was vacuum condensed into the reaction vessel.

### (iii) Benzene

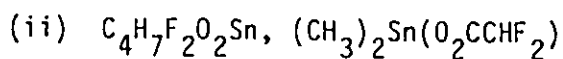
Benzene (J. T. Baker Chemical Co.), when used in reaction bulb vessels, was dried and stored over lithium aluminum hydride. When required, it was directly condensed into the reaction vessel.

### (iv) Tetrahydrofuran

Tetrahydrofuran (certified, Fisher Scientific Co.), was dried and stored over lithium aluminum hydride. When required, it was condensed into the reaction vessel.

D. Preparations

This product was prepared by the reaction of freshly condensed  $(CH_3)_6Sn_2$  ( $7.0\text{ cm}^3$ , 34 moles), with  $CF_3COOH$  ( $40\text{ cm}^3$ , 540 mmoles), in a two bulb reaction vessel. The acid was condensed onto the  $(CH_3)_6Sn_2$  and the mixture was stirred at  $-7$  to  $0^\circ C$  until gas evolution had ceased (6 hours). The dark orange mixture was filtered and yielded 17.1 g of an orange solid which was pumped dry on a vacuum line. Part of the crude product ( $3.24\text{ g}$ ), was purified by being washed twice with  $CF_3COOH$  ( $10\text{ cm}^3$ ), in a two bulb reaction vessel at  $0^\circ C$ , and yielded  $2.25\text{ g}$  of the desired product as a white crystalline solid. (Analytical data, Table 2.1). In subsequent preparations of (i), the desired product was purified by quenching the reaction with distilled water and filtering.



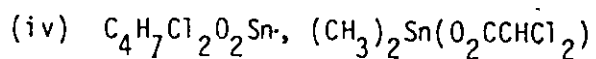
This product was prepared from the reaction of  $(CH_3)_6Sn_2$  ( $5\text{ cm}^3$ , 24 mmoles) and  $CHF_2COOH$  ( $10\text{ g}$ , 104 mmoles), in the presence of dry  $CHCl_3$  ( $4\text{ cm}^3$ ), under nitrogen at ice-acetone temperature. The reaction mixture was stirred for 12 hours, during which time mild gas evolution occurred and the mixture turned light orange. The mixture was washed with  $110\text{ cm}^3$  of distilled water, filtered, and gave a pale orange solid. The product was then washed with three  $20\text{ cm}^3$  portions of distilled water followed by  $50\text{ cm}^3$  of warm distilled water. The yield was  $1.39\text{ g}$  (12%), of a bright yellow solid. The colored impurity was extracted with dry  $CHCl_3$  ( $25\text{ cm}^3$ ), and the resulting white solid pumped dry on a vacuum line.

The procedure was repeated with 3 cm<sup>3</sup> (14 mmoles) of (CH<sub>3</sub>)<sub>6</sub>Sn<sub>2</sub> and 10 g (104 mmoles) of CHF<sub>2</sub>COOH. After two days gas evolution had not ceased. The mixture was then purified to yield 0.49 g (7.0%) of white solid.

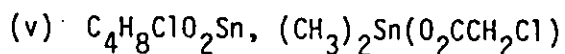
Both crude products from the above procedures were combined and added to dry CHCl<sub>3</sub> (50 cm<sup>3</sup>), concentrated to 6 cm<sup>3</sup>, and filtered. The white solid (1.0 g), was further dried on a vacuum line. (Analytical data, Table 2.1).

(iii) C<sub>4</sub>H<sub>6</sub>Cl<sub>3</sub>O<sub>2</sub>Sn, (CH<sub>3</sub>)<sub>2</sub>Sn(O<sub>2</sub>CCCl<sub>3</sub>)

Trichloroacetic acid (46.2 g, 283 mmoles), and dry CHCl<sub>3</sub> (10 cm<sup>3</sup>, 125 mmoles) were introduced under dry nitrogen into a 100 cm<sup>3</sup> flask containing a 1/2" magnetic stirring bar. The flask was cooled in an acetone-ice bath. Hexamethylditin (5.0 cm<sup>3</sup>, 24 mmoles) was added via a 10 cm<sup>3</sup> syringe through a rubber septum cap onto the stirred, cold, acid-chloroform mixture. An immediate and steady evolution of gas occurred. After approximately 23 hours at 0 to -10°C, the gas evolution had ceased and 90 cm<sup>3</sup> of distilled water were added to the pale orange mixture which was allowed to warm to room temperature. The color was discharged and the mixture was filtered through a fine glass frit under suction. The white solid was washed with 140 cm<sup>3</sup> of distilled water and gave 12.96 g of product. Continued work-up of the filtrate produced a further 1.173 g, for a total yield of vacuum dried product of 14.13 g. (Analytical data, Table 2.1).



To a two neck round bottom flask, attached by a cold-finger to a vacuum line,  $6.53 \text{ cm}^3$  (31.3 mmol) of freshly vacuum condensed  $(CH_3)_6Sn_2$  were added. It was subsequently degassed and frozen in liquid nitrogen. Freshly vacuum condensed  $CHCl_2COOH$  ( $7.6 \text{ cm}^3$ , 86 mmol), was introduced into the vessel. The reaction mixture was stirred at  $0^\circ\text{C}$  for 20 hours with continuous removal under vacuum of any gas formed. During this time the mixture turned yellow in colour. The acid was sublimed from the yellow mixture to leave a red solid which was washed with  $30 \text{ cm}^3$  of diethyl ether. Solid grey impurities in the now white solid were removed by extraction with  $30 \text{ cm}^3$  of  $CHCl_3$  and subsequent filtration. The  $CHCl_3$  was evaporated and the white solid pumped dry on a vacuum line. Part of the crude sample of white solid material was purified by vacuum sublimation at  $90^\circ\text{C}$  to remove volatile impurities to yield 3.2 g of white solid product. (Analytical data, Table 2.1).



This product was prepared by refluxing a mixture of  $(CH_3)_6Sn_2$  ( $3.2 \text{ cm}^3$ , 15 mmol) and  $CH_2ClCOOH$  (25 g, 270 mmol) in anhydrous  $CHCl_3$  at  $35^\circ\text{C}$  under nitrogen for three days. The amount of  $CHCl_3$  was such that solid acid was present. Mild gas evolution had ceased after three days and the product was washed with  $100 \text{ cm}^3$  of distilled water and filtered. A total of 4.53 g of white crystalline product was obtained. (Analytical data, Table 2.1).

(vi)  $\text{Sn}(\text{O}_2\text{CCF}_3)_3$ 

Hexaphenylditin (6.785 g, 9.692 mmoles) was added to one side of a two bulb reaction vessel and pumped on a vacuum line overnight. A mixture of 30 cm<sup>3</sup> (46 mmoles) of trifluoroacetic acid and 5 cm<sup>3</sup> of trifluoroacetic anhydride, which had been vacuum condensed into a storage vessel and stirred at ambient temperature for one day, was condensed into the other side of the vessel. When the mixture was condensed onto the hexaphenylditin and the reactants then mixed there was no apparent reaction and the white suspension was stirred at ambient temperature for two days, during which time the solvent turned pale yellow. A white, talc-like powder was removed from the yellow solvent by filtration. The solvent was recondensed onto the solid and the process was repeated until no yellow impurities remained. The solvent side of the vessel was sealed and the white solid was pumped dry overnight. A total of 8.879 g of product was obtained. (Analytical data, Table 2.1).

This compound was very insoluble in the parent acid. Sublimation of the compound at 100°C produced a hard, white solid which contained 27.38% Sn and a <sup>119</sup>Sn Mössbauer spectrum identical to the unsublimed material.

(vii)  $\text{Sn}(\text{O}_2\text{CC}_3\text{F}_7)_3$ 

Hexaphenylditin (2.560 g, 3.658 mmoles) was added to one side of a two bulb vessel which did not contain a glass frit. Excess  $\text{CF}_3(\text{CF}_2)_2\text{COOH}$  (20 cm<sup>3</sup>, 140 mmoles) was added to the other bulb, degassed on a vacuum line, then poured onto the solid. All of the solid had



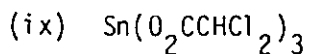
dissolved to give a clear liquid after 48 hours of stirring the mixture. The excess acid solvent was then condensed under vacuum to the opposite bulb which was cooled in a liquid nitrogen bath. The glass connection between the two bulbs was sealed and the white solid was pumped dry overnight. The isolated product (3.88 g) was a white fibrous solid. (Analytical data, Table 2.1.)

Attempts to remove the acid at its boiling point under vacuum produced a white oil.

(viii)  $\text{Sn}(\text{O}_2\text{CCCl}_3)_3$

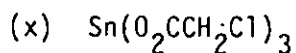
Hexaphenylditin (4.342 g, 6.203 mmoles), was added to one side of a two bulb reaction vessel and degassed. Trichloroacetic acid (19.48 g, 19.2 mmoles) which had been dried over  $\text{P}_4\text{O}_{10}$  for six hours, was added to the opposite side of the vessel and the vessel was degassed. Dry benzene (14.28 g), was condensed onto the acid and degassed. The acid-benzene mixture was filtered into the hexaphenylditin and the suspension was stirred for three days, during which time no apparent reaction occurred. The solvent was removed by filtration and condensed back onto the white solid. An amount of dry  $\text{SO}_2$ , 1-2  $\text{cm}^3$ , was then added to aid filtration. After repeated filtrations, the solvent side of the vessel was sealed and the white solid was pumped dry on a vacuum line. A total of 7.183 g of product was obtained. (Analytical data, Table 2.1.)

The reaction was repeated in the presence and absence of dry  $\text{SO}_2$  and yielded the same product.



Hexaphenylditin (1.745 g, 2.493 mmoles) was added to a reaction bulb attached to a U-trap. Excess  $\text{CHCl}_2\text{COOH}$  ( $10 \text{ cm}^3$ , 121 mmoles) was added to the trap, degassed on a vacuum line and decanted onto the solid. The mixture was stirred for five days, during which time all of the solid dissolved.

The benzene produced was pumped off under vacuum and the excess acid was condensed into the U-trap which was cooled in liquid nitrogen. The connection between the bulb and the U-trap was sealed and the product was further dried on a vacuum line. The isolated product, 1.50 g. was a white solid. (Analytical data, Table 2.1.)



Hexaphenylditin (~~2.465~~ g, 3.521 mmoles) was reacted with an excess of  $\text{CH}_2\text{ClCOOH}$  (8.97 g, 94.9 mmoles) at  $80^\circ\text{C}$  in a sealed Pyrex two-bulb reaction vessel. After the reagents were added, degassed, and the vessel sealed, the vessel was warmed to  $80^\circ\text{C}$ . The acid was decanted onto the solid, which dissolved after one hour. After stirring the mixture at  $80^\circ\text{C}$  for 48 hours, the benzene produced was condensed into the other bulb, cooled in liquid nitrogen, and the connection between the two bulbs sealed. The excess acid was removed from the white solid by high vacuum sublimation at  $40^\circ\text{C}$  using a dry ice-acetone cold-finger. The yield was not recorded but was sufficient to completely characterize the compound. (Analytical data, Table 2.1.) Prolonged heating of the mixture at  $80^\circ\text{C}$  was undesirable since this produced a light tan coloured solid.

(xi)  $\text{Sn}(\text{O}_2\text{CCH}_3)_3$ 

This product was prepared by the reaction of hexaphenylditin (6.754 g, 9.648 mmoles) with acetic acid ( $25 \text{ cm}^3$ , 3.60 mmoles) in the presence of acetic anhydride ( $5 \text{ cm}^3$ ). The acid/anhydride was pretreated by heating a degassed mixture in a closed vessel under vacuum at  $100^\circ\text{C}$  overnight. This mixture was vacuum condensed into one side of a two-bulb reaction vessel which contained hexaphenylditin. The mixture was degassed and poured onto the hexaphenylditin. Since no reaction occurred at room temperature, the mixture was heated at  $100^\circ\text{C}$  for 40 hours, during which time all the solid dissolved. When cooled to room temperature, a wet, sponge-like material was produced. The solvent was removed under vacuum to give 5.710 g of a white, fibrous solid. (Analytical data, Table 2.1.)

(xii)  $\text{Sn}(\text{O}_2\text{C}(\text{CH}_3)_3)_3$ 

Hexaphenylditin (3.264 g, 4.663 mmoles) and excess  $(\text{CH}_3)_3\text{CCOOH}$  ( $20 \text{ cm}^3$ , 180 mmoles), were added to opposite sides of a two-bulb reaction vessel which did not contain a glass frit. The reagents were degassed under vacuum, and the vessel was sealed. The vessel was warmed and the acid was poured onto the solid. After reaction at  $100^\circ\text{C}$  for 8 hours all of the solid had dissolved and the mixture was maintained at this temperature overnight. The bulk of the solvent was condensed into the opposite bulb, which was then sealed. The residual acid was removed under high vacuum, and 3.20 g of a white, flakey solid remained. (Analytical data, Table 2.1.)

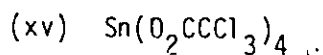
Excess acid may not be removed by washing the product with dry  $\text{SO}_2$  since this caused the product to turn brown.

(xiii)  $\text{Sn}(\text{O}_2\text{CCF}_3)_4$

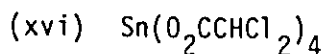
To the opposite side of a two-bulb reaction vessel which contained tetraphenyltin (1.775 g, 4.153 mmoles), were added  $\text{CF}_3\text{COOH}$  (20 g, 175 mmoles) and  $(\text{CF}_3\text{CO})_2\text{O}$  ( $1 \text{ cm}^3$ ), which were then degassed. The liquid mixture was poured onto the tetraphenyltin and stirred for 10 hours, during which time almost all of the solid had dissolved and the solution became a straw yellow colour. The solvent was removed under vacuum and 2.303 g of a white solid, which contained a yellow impurity, remained. Dry  $\text{SO}_2$  was condensed into the vessel. The slurry was stirred and concentrated to  $5 \text{ cm}^3$  and filtered. This process was repeated three times. A total of 1.810 g of white solid was obtained. (Analytical data, Table 2.1.)

(xiv)  $\text{Sn}(\text{O}_2\text{CCF}_2\text{CF}_2\text{CF}_3)_4$

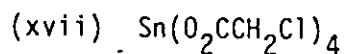
Tetraphenyltin (1.882 g, 4.405 mmoles), and an excess of  $\text{CF}_3(\text{CF}_2)_2\text{COOH}$  ( $15 \text{ cm}^3$ ), were added to a one-bulb reaction vessel and degassed under high vacuum. After the mixture was stirred at room temperature for 7 hours all of the solid dissolved to give an orange-brown coloured solution. The excess acid was removed under vacuum, leaving a solid which ranged in colour from white to dark brown. The apparently impure product was dried under vacuum and was not analysed.



Dry benzene (9.90 g, 127 mmoles), was condensed onto  $\text{CCl}_3\text{COOH}$  (3.340 g, 20.44 mmoles), which was contained in a two-bulb reaction vessel under vacuum. The mixture was poured onto tetraphenyltin (1.941 g, 4.545 mmoles). After 2.5 hours of stirring the mixture, all the solid had dissolved to yield a bright, yellow-coloured solution. The benzene was pumped off leaving a deep red oil (3.80 g) which was soluble in dry  $\text{SO}_2$ . A 100% yield would have been 3.49 g of  $\text{Sn}(\text{O}_2\text{CCCl}_3)_4$ . Attempts to remove excess acid by repeated vacuum sublimation resulted in decomposition of the product. (% acid ligand: calculated 85.08; found 102.2.)



Tetraphenyltin (2.035 g, 4.764 mmoles) and a slight excess of  $\text{CHCl}_2\text{COOH}$  (2.646 g, 20.52 mmoles) were introduced into a one-bulb reaction vessel and degassed on a vacuum line. The acid immediately turned pale brown upon contact of the two reagents, and the mixture was stirred overnight at room temperature. Benzene (1.44 g, 1.64  $\text{cm}^3$ ) was condensed into the vessel and the mixture was stirred for an additional two days. The benzene and excess acid were pumped off under high vacuum to produce a tan coloured viscous liquid.



Tetraphenyltin (2.020 g, 4.729 mmoles), and a slight excess of  $\text{CH}_2\text{ClCOOH}$  (1.854 g, 19.62 mmoles), were added to a one-bulb reaction vessel, degassed under vacuum and allowed to react at 80°C for several

hours. Most of the solid dissolved and further reaction overnight produced a white, solid mass. Dry benzene (0.98 g, 1.1 cm<sup>3</sup>), was condensed into the vessel, and the mixture was stirred at 80°C overnight to ensure complete reaction. The benzene was removed under vacuum and the light tan coloured solid was dried under high vacuum.

Attempts to remove the excess acid from the light tan coloured solid by high vacuum sublimation at 40°C using a dry ice-acetone cold finger were unsuccessful. (% Acid ligand: calculated, 72.21; found, 77.96.)

(xviii) SnF<sub>3</sub>

The reaction was carried out in a Kel-F reaction tube which had been pretreated with anhydrous HF. Anhydrous HF was condensed into the tube which contained hexaphenylditin (1.455 g, 2.079 mmoles). The tube was warmed from liquid nitrogen to ambient temperature using dry ice-acetone, pentane, and then an ice bath. No apparent reaction occurred. The tube was agitated for 20 hours, during which time the solvent turned bright yellow, and the volume of solid was one-third of the original amount. A liquid (benzene) was present on top of the bulk HF solvent. The solvent was removed under vacuum to give 0.741 g of a pale yellow solid. A 100% yield would have been 0.730 g of SnF<sub>3</sub>. The crude solid was insoluble in benzene, HF or SO<sub>2</sub>, at room temperature. The crude SnF<sub>3</sub> was placed in a two-bulb Pyrex reaction vessel which contained a medium glass frit. Several washings of the solid with dry SO<sub>2</sub> (5 cm<sup>3</sup> portions), resulted in a white solid. (Analytical data, Table 2.1.)

(xix)  $\text{Sn}(\text{SO}_3\text{CF}_3)_3$

Hexaphenylditin (3.118 g, 4.455 mmoles), was added to one side of a two-bulb reaction vessel. Excess trifluoromethanesulfonic acid (25 g, 167 mmoles), was added to the opposite bulb, and degassed on a vacuum line. The acid was slowly condensed under vacuum onto the solid which was cooled in a liquid nitrogen bath. As the reaction vessel was warmed to room temperature, volatile reaction products were pumped off. The solid did not appear to dissolve, nor was the generation of heat apparent. After 20 minutes, the solvent had turned pale yellow, and 25 minutes later, no more volatile reaction products were generated. Dry  $\text{SO}_2$  was added and the mixture was stirred overnight. After repeated filtrations with  $\text{SO}_2$ , the solvent side of the vessel was sealed and a white solid was obtained. A total of 4.574 g of a white solid was then transferred to a storage vessel. (Analytical data, Table 2.1.)

(xx)  $\text{Sn}(\text{SO}_3\text{OH})_3$

Hexaphenylditin (1.992 g, 3.768 mmoles), was added to one side of a two-bulb reaction vessel. Excess 100%  $\text{H}_2\text{SO}_4$  (6.481 g, 66.08 mmoles), was added to the opposite bulb, degassed, and dry  $\text{SO}_2$  (10  $\text{cm}^3$ ), was condensed onto the acid, which was cooled in a dry ice-acetone bath. The cold acid mixture which was poured onto the solid turned olive green, but the colour disappeared at room temperature. After one day, the mixture had turned a pale yellow colour. The mixture was stirred for two weeks, during which time none of the solid appeared to dissolve. The white solid was removed by filtration. The  $\text{SO}_2$  was condensed back onto the solid, stirred, and filtered off. After repeated filtrations, the

connecting glass tube between the two bulbs was sealed. A total of 5.525 g of a wax-like white solid was isolated which apparently contained excess acid ( $\text{Sn}_2(\text{SO}_4)_3$  1.992 calculated;  $\text{Sn}_2(\text{SO}_4\text{H})_6$  3.089 calculated). Direct reaction of  $\text{H}_2\text{SO}_4$  with hexaphenylditin was extremely vigorous, with extensive heat generation and darkening of the reaction mixture.

(xxi)  $\text{Sn}(\text{SO}_3\text{CH}_3)_3$

Anhydrous methanesulfonic acid ( $11 \text{ cm}^3$ ), was syringed onto hexaphenylditin (1.765 g, 2.522 mmoles), contained in a two-bulb reaction vessel. Immediate heat generation occurred.

All volatile products were removed under vacuum. Dry  $\text{SO}_2$  was condensed into the vessel. No dissolution of solid was apparent. However, after the mixture was stirred for one day, all the solid had dissolved. The  $\text{SO}_2$  was removed under vacuum, leaving an insoluble white solid. The solvent was decanted off and a "wet" solid was isolated.

(xxii)  $\text{Sn}(\text{SO}_3\text{CH}_2\text{CH}_3)_3$

Ethanesulfonic acid ( $8 \text{ cm}^3$ ), was syringed onto hexaphenylditin (1.318 g, 1.882 mmoles), contained in a two-bulb reaction vessel. Immediate heat generation was apparent and the solution turned slightly grey. After all volatile products had been removed under vacuum, dry  $\text{SO}_2$  was condensed into the vessel and all of the solid dissolved. The mixture was stirred for one week, during which time no solid was precipitated. When the  $\text{SO}_2$  was removed under vacuum no precipitation of solid occurred. Attempts to remove excess acid at  $120^\circ\text{C}$ , under a vacuum resulted in formation of a dark oil.



(xxiii) Attempted Preparation of  $\text{Sn}(\text{SO}_3\text{F})_3$ 

Hexaphenylditin (3.223 g, 4.605 mmoles), and  $\text{HSO}_3\text{F}$  (6 cm<sup>3</sup>), were added to opposite sides of a two-bulb reaction vessel. Because direct reaction of acid and solid was vigorous with a large amount of heat being generated, dry  $\text{SO}_2$  was condensed onto the degassed acid, which was cooled in a dry ice-acetone bath. The now cold mixture was slowly poured onto the hexaphenylditin. The mixture immediately turned pale yellow. At room temperature almost all of the solid had dissolved, and the solvent was a deep green colour. The mixture was stirred for 10 days, during which time a white solid formed and the colour of the solvent faded. The white solid was purified by repeated filtration with  $\text{SO}_2$ . The very hygroscopic white solid (1.82 g) isolated had the following analysis:

	Found	Calculated
% Sn:	46.33	28.54.
% Sn(II):	21.6,	14.27
	26.3	

(xxiv)  $\text{Sn}(\text{SO}_3\text{CF}_3)_4$ 

Tetraphenyltin (3.606 g, 8.442 mmoles), was added to one side of a two-bulb reaction vessel. Trifluoromethanesulfonic acid (11.079 g, 73.828 mmoles), was added to the opposite bulb, degassed, and poured onto the solid, which was cooled in a dry ice-acetone bath. After one hour, none of the compound had appeared to dissolve but the solvent had turned pale brown. Dry  $\text{SO}_2$  was condensed into the vessel and most of the solid dissolved after five hours. After four days, a white solid had started to precipitate and the solvent was red-brown in colour. When after

two more days no further solid appeared to have formed, the mixture was filtered. The  $\text{SO}_2$  was condensed back onto the solid, stirred and filtered. This process was repeated until a very light tan coloured solid was obtained. The solvent side of the vessel was frozen in a liquid nitrogen bath, and the glass connection between the two bulbs sealed. A total of 2.992 g of product was obtained. (Analytical data, Table 2.1.)

(xxv)  $\text{Sn}_3\text{F}_2(\text{SO}_3\text{CF}_3)_6$

A 1:2 molar mixture of  $\text{SnF}_2$  (0.143 g, 0.915 mmol), and  $\text{Sn}(\text{SO}_3\text{CF}_3)_3$  (1.038 g, 1.834 mmol), was introduced into a reaction ampoule. Dry  $\text{SO}_2$  was condensed onto the mixture and the slurry was stirred at room temperature for several days. No reaction was apparent, nor was there apparent dissolution of the solids. The  $\text{SO}_2$  was removed under vacuum and the solid was dried on a vacuum line. (Analytical data, Table 2.1.)

Table 2.1

## Analytical Data for Preparations

Preparation	Empirical Formula or -Composition		% Sn	% C	% H	% Halogen	% Acid Ligand	Melting Point <sup>a</sup> , °C	% Yield <sup>b</sup>
(i)	$C_4H_6F_3O_2Sn$	Calc.	45.34	18.35	2.31			147(d)	13 90 <sup>c</sup>
		Found	44.61	18.29	2.23				
			44.87	18.45	2.30				
(ii)	$C_4H_7F_2O_2Sn$	Calc.	48.69	19.71	2.89			131(d)	5
		Found	47.50	19.51	2.32				
				19.50	2.53				
(iii)	$C_4H_6Cl_3O_2Sn$	Calc.	38.14	15.44	1.94			150(d)	95
		Found	37.99	14.88	1.64				
				14.92	1.71				
(iv)	$C_4H_7Cl_2O_2Sn$	Calc.	42.90	17.36	2.55			125(d)	21 80 <sup>c</sup>
		Found	42.89	17.62	2.39				
			42.55	17.47	2.39				
(v)	$C_4H_8ClO_2Sn$	Calc.	48.99	19.83	3.33			158(d)	61
		Found	48.83	20.00	3.05				
				20.13	3.14				
(vi)	$Sn(O_2CCF_3)_3$	Calc.	25.93	15.74	0.0	37.34	74.07	184-186.5	100
		Found	26.45	15.75	0.09	37.49	73.84		
			26.35	15.80	0.06	37.44			
(vii)	$Sn(O_2CCF_7)_3$	Calc.	15.66	19.02	0.0	52.66	84.34	118(d)	70.0
		Found	15.50	18.97	0.15	49.12	83.78		
						83.41			
(viii)	$Sn(O_2CCCl_3)_3$	Calc.	19.59	19.02	0.0	52.66	80.41	155-156	95.6
		Found	19.13	18.97	0.19	48.37	79.78		
			19.09				80.71		
(ix)	$Sn(O_2CCHCl_2)_3$	Calc.	23.62	14.34	0.60		76.38	117(d)	59.8
		Found	25.10	13.64	0.69		76.51		
(x)	$Sn(O_2CCH_2Cl)_3$	Calc.	29.74	18.05	1.52		70.27	135(d)	
		Found	30.11	17.52	1.64		74.56		
(xi)	$Sn(O_2CCH_3)_3$	Calc.	40.12	24.36	3.06		59.88	310(d)	100
		Found	39.52	24.44	3.30		58.61		
				24.39	3.13				
(xii)	$Sn(O_2CC(CH_3)_3)_3$	Calc.	28.12	42.68	6.45		71.88	184(d)	81.3
		Found	28.50	43.03	6.51		72.89		
(xiii)	$Sn(O_2CCF_3)_4$	Calc.	20.80				79.20	115-116	76.3
		Found	20.50				79.77		
(xviii)	$SnF_3$	Calc.	67.6				32.4		
		Found	63.7				29.0		
(xix)	$Sn(SO_3CF_3)_3$	Calc.	20.97	6.37	0.0	30.22	79.03	90.7	
		Found	20.43	5.14	0.10	29.27	79.43		
(xxiv)	$Sn(SO_3CF_3)_4$	Calc.	11.45				83.40		
		Found	16.60				86.81		
(xxv)	$Sn_3F_2(SO_3CF_3)_6$	Calc.	27.63				37.15		
		Found	27.40				35.95		

<sup>a</sup> The letter d in parenthesis denotes decomposition with melting of solid.

<sup>b</sup> Percentage yield based on organotin compound used in the preparation unless otherwise indicated.

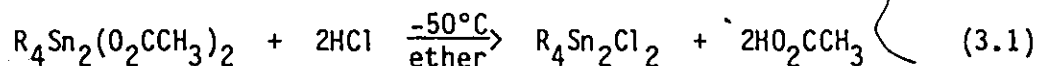
<sup>c</sup> Percentage yield based on <sup>1</sup>H n.m.r. analysis of reaction mixture.

## CHAPTER THREE

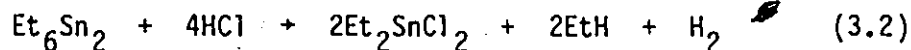
### ACID SOLVOLYSIS OF HEXAMETHYLDITIN AND TETRAMETHYLTIN

#### A. General Introduction

The acid solvolysis of hexa-alkylditin compounds was investigated as a synthetic route to substituted organoditin compounds. Previous workers had established that hexa-alkylditin compounds reacted by cleavage of the thermodynamically weaker tin-tin bond, rather than substitution of the tin-carbon bond.<sup>31-34</sup> However, bis(acetato)-bis[di-alkyltin(IV)] compounds, (iso-C<sub>4</sub>H<sub>9</sub>)<sub>4</sub>Sn<sub>2</sub>(O<sub>2</sub>CCH<sub>3</sub>)<sub>2</sub><sup>35,36</sup> and (n-C<sub>4</sub>H<sub>9</sub>)<sub>4</sub>Sn<sub>2</sub>(O<sub>2</sub>CCH<sub>3</sub>)<sub>2</sub><sup>37,38</sup> retained the tin-tin bond in mildly acidic media.<sup>36-38</sup>



Most of the chemistry of organoditin compounds involves scission of the tin-tin bond.<sup>3</sup> As early as 1870, the reaction of hexaethyl-ditin with HCl was studied<sup>31</sup> and found to react according to:

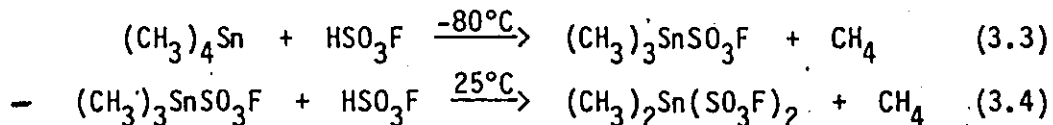


At 135°C hexaethyl-ditin in acetic acid<sup>32</sup> produced mostly trimethyltin acetate, hydrogen and ethane and a small amount of

diethyltin acetate. Hexamethylditin reacted with  $\text{HBr}^{33}$  and  $\text{HCl}^{34}$  with the formation of trimethyltin halides. It was apparent that the formation of hydrogen as a reaction product was associated with the cleavage of the tin-tin bond.

As in the case of organotin compounds which did not contain a tin-tin bond,<sup>39-47</sup> the extent of cleavage of the number of carbon bonds attached to each tin atom was dependent upon the nature of the group, the type of acid used and the reaction conditions.

It has been shown that excess  $(\text{CH}_3)_4\text{Sn}$  reacts with  $\text{HSO}_3\text{F}$  at  $-80^\circ\text{C}$  with the formation of  $\text{CH}_4$  and  $(\text{CH}_3)_3\text{SnSO}_3\text{F}$ .<sup>41,47</sup> In excess  $\text{HSO}_3\text{F}$  at  $25^\circ\text{C}$  the products formed are  $\text{CH}_4$  and  $(\text{CH}_3)_2\text{Sn}(\text{SO}_3\text{F})_2$ .<sup>41</sup>



Both compounds have been well characterized<sup>41,46-48</sup> and are likely to be strongly solvated in fluorosulfuric acid solutions.<sup>45</sup> While much is known about the compounds isolated from these reactions little is known about the nature of the species present in the  $\text{Me}_4\text{Sn}-\text{HSO}_3\text{F}$  system prior to crystallization.

## B. Results and Discussion

### (i) Tetramethyltin and hexamethylditin in $\text{HSO}_3\text{F}$

The reaction of  $(\text{CH}_3)_4\text{Sn}$  with excess  $\text{HSO}_3\text{F}$  in a sealed  $^1\text{H}$  n.m.r. tube was studied as a function of both temperature and time of reaction.

Table 3.1

<sup>1</sup>H N.M.R. Data for Solvolysis of (CH<sub>3</sub>)<sub>4</sub>Sn in Excess HSO<sub>3</sub>F

Relative Integrated Peak Intensities		Time (min.)	Temp. (°C)
[(CH <sub>3</sub> ) <sub>3</sub> Sn <sup>+</sup> ]	[(CH <sub>3</sub> ) <sub>2</sub> Sn <sup>+2</sup> ]		
90	10	15-60	-78.5
80	20	120	-50
50	50	150	-10
50	50	43200	-78.5

Species	Chemical Shift (ppm) <sup>1</sup> H (T.M.S. = 0)	Coupling Constant (Hz)		Temp. (°C)
		J <sub>119</sub> Sn-C- <sup>1</sup> H	J <sub>117</sub> Sn-C- <sup>1</sup> H	
[(CH <sub>3</sub> ) <sub>3</sub> Sn <sup>+</sup> ]	0.75	63.0	60.0	-35
[(CH <sub>3</sub> ) <sub>2</sub> Sn <sup>+2</sup> ]	1.68	84.0	80.0	-10
Unknown*	3.21			
CH <sub>4</sub>	0.00			

\* Presence of this species established only after reaction of (CH<sub>3</sub>)<sub>4</sub>Sn in HSO<sub>3</sub>F for one month at -78.5°C.

The results shown in Table 3.1 are consistent with a two-step process in which initially  $[(\text{CH}_3)_3\text{Sn}^+]$  is formed by reaction (3.3) above, at  $-78.6^\circ\text{C}$ . As the temperature of the reaction tube is raised to  $-50^\circ\text{C}$   $[(\text{CH}_3)_2\text{Sn}^{+2}]$  is formed by cleavage of a second carbon-tin bond, with the evolution of more methane (reaction 3.4). No further cleavage of carbon-tin bonds occurs, even at room temperature. The  $^1\text{H}$  n.m.r. data presented are consistent with data previously mentioned and are similar to data reported for  $[(\text{CH}_3)_2\text{Sn}^{+2}]$  in  $\text{H}_2\text{SO}_4$ .<sup>45</sup> Unfortunately, no signals other than  $\text{HSO}_3\text{F}$  were observed in the  $^{19}\text{F}$  n.m.r. spectrum of  $(\text{CH}_3)_4\text{Sn}$  in  $\text{HSO}_3\text{F}$ , so that further study was not possible. These results are consistent with the formation of a stable  $[(\text{CH}_3)_3\text{Sn}^+]$  cation at  $-78.5^\circ\text{C}$ . The small amount of  $[(\text{CH}_3)_2\text{Sn}^{+2}]$  initially formed is attributed to the vigorous nature of the reaction.

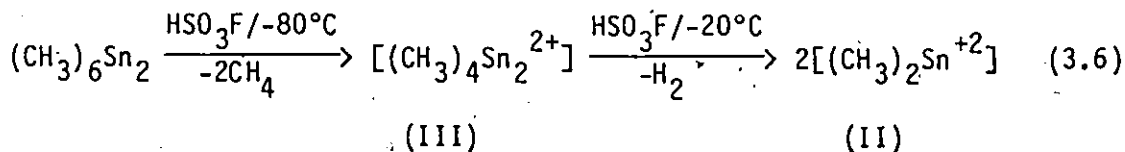
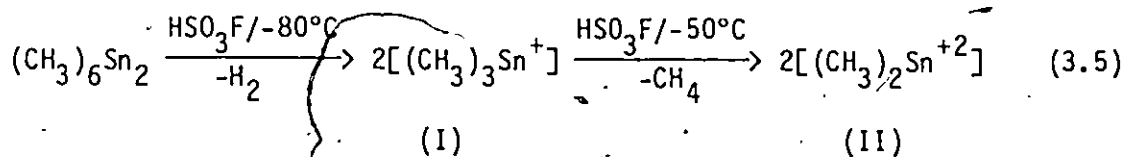
The stabilization of  $[(\text{CH}_3)_3\text{Sn}^+]$  at low temperature in  $\text{HSO}_3\text{F}$  increased the possibility that cations containing tin-tin bonds may be detected at low temperatures. At  $-80^\circ\text{C}$  hexamethylditin,  $(\text{CH}_3)_6\text{Sn}_2$ , reacts with excess  $\text{HSO}_3\text{F}$  in a sealed n.m.r. tube with the formation of two methyl-tin cations in approximately equal amounts, with minor amounts of  $[(\text{CH}_3)_2\text{Sn}^{+2}]$ , and  $\text{CH}_4$  also present. One tin species is readily identified as  $[(\text{CH}_3)_3\text{Sn}^+]$  on the basis of its  $^1\text{H}$  n.m.r. parameters. The other major component has a proton shift between  $[(\text{CH}_3)_3\text{Sn}^+]$  and  $[(\text{CH}_3)_2\text{Sn}^{+2}]$ , ( $\delta = 1.05$  ppm, TMS). This species has two sets of proton-tin coupling constants which establish the presence of a tin-tin bond ( $J_{119/117\text{Sn-C-}^1\text{H}} = 56$  Hz,  $J_{119/117\text{Sn-Sn-C-}^1\text{H}} = 12$  Hz); these

are similar to those reported for  $\text{Me}_6\text{Sn}_2$  (48.4 Hz, 16.9 Hz).<sup>49</sup> These  $^1\text{H}$  n.m.r. data are consistent with the formation of a methyl-ditin cation. The presence of only one methyl signal with a chemical shift between that of  $[(\text{CH}_3)_3\text{Sn}^+]$  and  $[(\text{CH}_3)_2\text{Sn}^{+2}]$  is consistent with the formation of the symmetrical dication  $[(\text{CH}_3)_4\text{Sn}_2^{2+}]$ . A Mössbauer spectrum of a frozen solution of an approximately equal molar mixture of  $[(\text{CH}_3)_3\text{Sn}^+]$  and  $[(\text{CH}_3)_2\text{Sn}^{+2}]$  indicates that the Mössbauer parameters of  $[(\text{CH}_3)_2\text{Sn}^{+2}]_2$  are not significantly different from those of  $[(\text{CH}_3)_3\text{Sn}^+]$ . This implies that the structure of this ditin species is therefore very similar to the five coordinate structure proposed for  $(\text{CH}_3)_3\text{SnSO}_3\text{F}$ .<sup>47</sup>

The tetramethylditin dication does not react with  $\text{HSO}_3\text{F}$  below  $-20^\circ\text{C}$ , whereas the trimethyltin cation rapidly loses methane at this temperature. As the temperature is increased above  $-20^\circ\text{C}$ ,  $[(\text{CH}_3)_4\text{Sn}_2^{2+}]$ , the tin-tin bond is cleaved, gas evolution occurs and  $[(\text{CH}_3)_2\text{Sn}^{+2}]$  is produced.

The reaction of  $(\text{CH}_3)_6\text{Sn}_2$  with  $\text{HSO}_3\text{F}$  occurs with gas evolution according to either sequence of reactions (3.5) or (3.6). Both pathways, if allowed to proceed under the most vigorous conditions ultimately produce species (II).





Cleavage of the tin-tin bond by either pathway results in the same overall stoichiometry, and is consistent with previous studies of hexa-alkylditin compounds in acid media.<sup>31-34</sup>

C. Bis(haloacetato)-bis[dimethyltin(IV)]: "Tetramethylditin Carboxylates"

(i) Introduction

The stability of  $[(\text{CH}_3)_4\text{Sn}_2^{2+}]$  in  $\text{HSO}_3\text{F}$  at low temperature suggested the possibility that low temperature acid solvolysis may be used as a synthetic route to bis(haloacetato)-bis[dimethyltin(IV)] compounds. Compounds of this kind<sup>4</sup> have been prepared before by the reaction of  $\text{R}_2\text{SnH}_2$  ( $\text{R} = \text{C}_6\text{H}_5, \text{nBu}$ ), with carboxylic acids,<sup>50</sup> or by mixing  $\text{R}_2\text{SnH}_2$  with equimolar amounts of diorganotin carboxylates,  $\text{R}_2\text{Sn}(\text{O}_2\text{CR})_2$ .<sup>51</sup>

Several spectroscopic studies have been carried out to establish the geometry at tin for triorganotin carboxylates.<sup>52-62</sup> Pentacoordinate tin atoms and bridging carboxylates have been established by X-ray crystallography for tribenzyltin acetate,<sup>59</sup> trimethyltin acetate<sup>61</sup> and

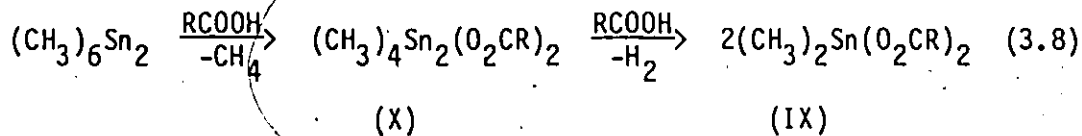
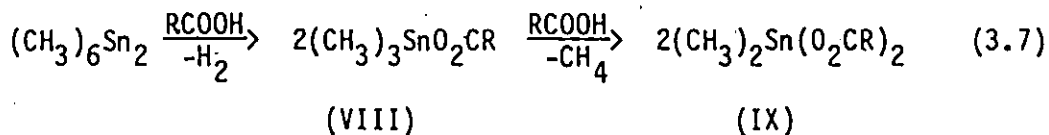
trimethyltin trifluoroacetate.<sup>61</sup> Several spectroscopic studies have been reported for bis( $\mu$ -carboxylate)-bis[diphenyltin(IV)] compounds to establish the nature of the structure of  $(C_6H_5)_4Sn_2(O_2CR)_2$  compounds in both the solid state,<sup>63-65</sup> and solutions.<sup>64</sup>

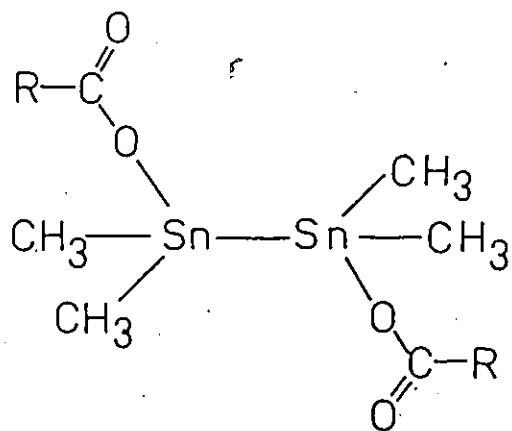
The structure of  $(CH_3)_4Sn_2(O_2CR)_2$  compounds was of interest since a number of structures were possible, Figure 3.1. The tin atoms could be four-coordinate, with monodentate carboxylates, as in (IV); or five-coordinate, as in (V-VII). In (V) the carboxylate group bridges the  $(CH_3)_2Sn-Sn(CH_3)_2$  units intermolecularly to give a polymeric structure. On the other hand, intramolecular bridging carboxylates could bond in a symmetric fashion, as indicated in (VI), or asymmetrically, to give two C-O and two Sn-O distances, as in (VII).

#### D. Results and Discussion

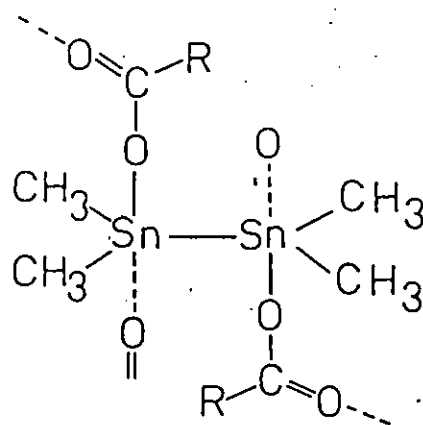
##### (i) Preparation and Chemical Properties

Hexamethylditin can react with substituted acetic acids, with gas evolution, according to either (3.7) and/or (3.8).

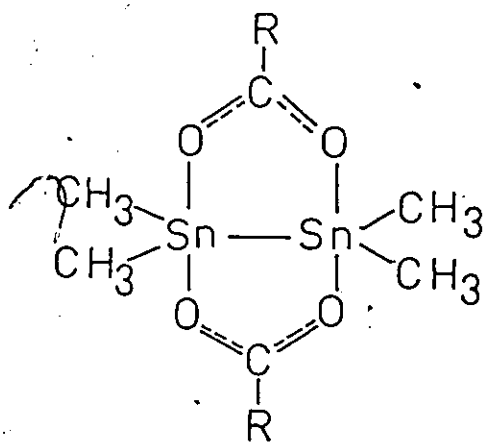




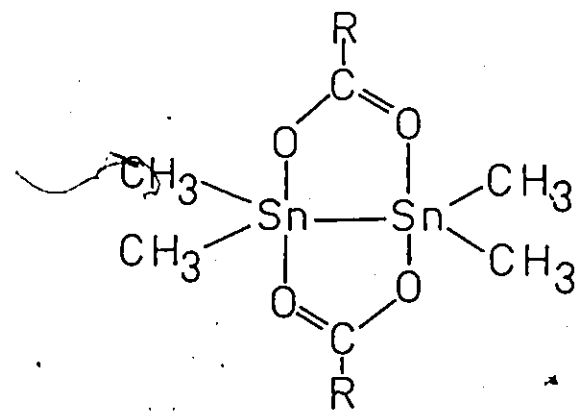
IV



V



VI



VII

Figure 3.1. Possible structures for  $(\text{CH}_3)_4\text{Sn}_2(\text{O}_2\text{CR})_2$ .

Both pathways, if carried out under the most vigorous conditions (cf, R =  $\text{CHCl}_2$ ,  $90^\circ\text{C}$ ), ultimately result in species (IX) discussed earlier. These reactions can be monitored very conveniently by  $^1\text{H}$  n.m.r. and such a study allows one to choose the correct conditions so that the yield of (X) can be optimized.

With trichloro-, trifluoro- and dichloroacetic acid all of the hexamethylditin was found to react with excess acid ( $-5$  to  $0^\circ\text{C}$ ), with yields in excess of 80% of (X). This indicated that a substitution reaction predominated over cleavage of the tin-tin bond. Compound (X) was also the major tin product for difluoroacetic acid ( $0^\circ\text{C}$ ), and monochloroacetic acid ( $35^\circ\text{C}$ ), although the majority of the starting material did not undergo reaction.

#### (ii) Vibrational Spectra

The application of vibrational spectroscopy to structure elucidation is often fraught with difficulty, particularly when the molecule contains as many atoms as those discussed here. However, judicious use of infrared and Raman spectroscopy, and simple group theoretical treatments, can provide valuable structural information. The vibrational spectra of molecules containing a heavy atom generally appear more "simple" than light atom analogs as a result of the large mass of the heavy atom preventing coupling of internal vibrations of two or more organic groups attached to it.<sup>66,67</sup>

Considerable piling-up of fundamental frequencies occurs which allows characteristic group frequencies to be readily identified. The assignment of vibrational solid state spectra of these compounds,

Table 3.2, is simplified by considering the methyl and carboxylate groups separately from the  $\text{Sn}_2\text{C}_4$  moiety.

The effect of tin on the methyl group is apparent, for only four fundamental frequencies may be assigned which are essentially unchanged from other methyl-tin compounds.<sup>66-68</sup> The four methyl group fundamentals consist of a symmetric bending mode ( $\sim 1200 \text{ cm}^{-1}$ , sharp), an asymmetric bending mode ( $\sim 1400 \text{ cm}^{-1}$ ), a symmetric stretching mode ( $\sim 2930 \text{ cm}^{-1}$ , broad), and an asymmetric stretching mode ( $\sim 3010 \text{ cm}^{-1}$ , broad). The broad band at  $\sim 780 \text{ cm}^{-1}$  is also characteristic of methyl-tin compounds<sup>66-68</sup> and is assigned to a Sn-CH<sub>3</sub> rocking mode.

The skeletal vibrations involving atoms attached directly to tin are sensitive to the environment about the tin atoms. Twelve normal modes are expected from the  $\text{Sn}_2\text{C}_4$  moiety. How these vibrational modes will be distributed between the infrared and Raman active modes will be determined by the overall symmetry of the molecule. Previous workers<sup>55,56</sup> have established that carbon-tin symmetric stretches occur in the  $520\text{-}550 \text{ cm}^{-1}$  region of the spectrum. Two bands are present in this region in both the infrared and the Raman spectra of the molecules reported here. The lower frequency band may be assigned to the symmetric stretch of the  $\text{Sn}_2\text{C}_4$  group, and the higher frequency band to the asymmetric stretch of this group. These stretches in the infrared are not identical to those in the Raman, as close examination of Table 3.2 reveals. In all cases the symmetric stretch is at a lower frequency in the infrared than in the Raman, while the reverse is true for the asymmetric stretch. In general, all symmetry allowed vibrations due to tin-carbon stretches, are normally observed. Four carbon-tin

Table 3.2 Infrared\* and Raman Data for  $(\text{CH}_3)_4\text{Sn}_2(\text{O}_2\text{CR})_2$ 

R*	$\text{CF}_3$		$\text{CHF}_2$		$\text{CCl}_3$		$\text{CHCl}_2$		$\text{CH}_2\text{Cl}$		Assignment
	IR	Raman	IR	Raman	IR	Raman	IR	Raman	IR	Raman	
150(m,b)	100(25) 137(81)	149(30) 171(18)	140(w) 167(w)	98(29) 146(47)	140(m)	104(15) 145(52)	143(m)	41(33) 101(19) 142(47)	166(15) 200(6)		LATTICE MODE $\nu_{\text{C}}\text{C}_2\text{O}_2$
265(w) 310(w)	204(64) 267(11) 307(1)	211(32) 275(w) 303(3) 343(10)	212(w) 275(w) 355(w)	207(35) 225(8) 283(7) 347(11)	210(w) 262(m) 350(m)	182(12) 204(32) 279(14) 347(11)	205(m) 292(m) 360(w)	214(31) 303(2)			$\nu_{\text{S}}\text{Sn-Sn}$ $\nu_{\text{S}}\text{Sn-O}$
440(m)	506(2)	380(w,b) 490(m,b)	450(m)	434(2) 453(8) 475(3)	456(m)	453(5)	490(m)	479(2)			$\nu_{\text{S}}\text{Sn-O}$
523(m)	528(100) 546(40)	527(m) 531(100) 548(44)	523(m)	530(100) 548(50)	530(m)	535(100) 546(47)	535(m)	538(100) 544(52)			$\nu_{\text{S}}\text{SnO}_2$ $\nu_{\text{S}}\text{SnO}_2$ $\nu_{\text{S}}\text{SnO}_2$ $\nu_{\text{S}}\text{SnO}_2$
552(m)	599(1)	555(m)	553(m)	552(m)	552(m)	552(m)	550(m)				
727(s)	726(1)	615(m,b)	686(s)	685(4)	680(s)	630(m) 680(s)	575(w) 680(m)				$\nu_{\text{C}}\text{O}_2$
770(m,b) 793(m)		785(m,b)	750(s)	750(11)	705(s,b)	705(1) 708(1)	770(m,b) 785(m,b)	782(7)			$\nu_{\text{C}}\text{-Cl}$ $\nu_{\text{C}}\text{H}_3$
845(s)	844(9)	870(s) 950(m)	840(s) 848(s) 900(w)	835(5)	832(s)	827(4)	935(m)	933(5)			$\nu_{\text{C}}\text{O}_2$ $\nu_{\text{C}}\text{-C}$
1142(s,b)	1160(1)	1090(s,b) 1110(s,b)	932(c)	961(6)	950(m)	947(7)					$\nu_{\text{S}}\text{CF}_3$ $\nu_{\text{C}}\text{F}_2$
1200(s,b)	1190(14)	1192(30)	1190(w)	1192(25)	1192(w)	1190(26)	1180(w)	1177(6) 1187(23)			$\nu_{\text{S}}\text{CF}_3$ $\nu_{\text{C}}\text{H}_3$
	1207(8)	1200(20)	1200(w)	1200(37)	1200(w)	1197(36)	1195(w)	1200(47)			$\nu_{\text{S}}\text{CH}_3$
		1211(6)	1350(s,b)	1335(3) 1379(6)	1235(s)	1223(1) 1240(1)	1250(s)	1214(2)			$\nu_{\text{C}}\text{H}_3$ $\nu_{\text{C}}\text{-H of R group}$
1443(m)	1443(6)	1330(s) 1340(m)	1443(2)	1407(9)	1385(s)	1378(3)	1390(s,b)	1309(2)			$\nu_{\text{S}}\text{CO}_2$
1650(s,b)	1619(1)	1605(s,b)	1615(s,b)	1601(2)	1608(s)	1401(1) 1543(1)	1409(2) 1583(s,b)				$\nu_{\text{S}}\text{CH}_3$ $\nu_{\text{S}}\text{CO}_2$
	2370(1) 2782(1)	2927(23)	2380(w) 2440(w) 2480(w) 2780(w)	2367(1) 2779(1)	2920(w)	2920(16)	2926(10)				$\nu_{\text{C}}\text{H}_3$
	2939(13)	2982(10) 3009(12)	3009(12)	3009(12)	3020(s)	3009(32) 3001(11)	2955(13) 3002(11)				$\nu_{\text{C}}\text{-H of R group}$ $\nu_{\text{S}}\text{CH}_3$
	3017(5)										

\*Infrared were recorded from 4000 to 20  $\text{cm}^{-1}$ .

stretching vibrations are required for the  $\text{Sn}_2\text{C}_4$  unit. Since only two are found in the infrared and two in the Raman, these vibrations cannot be identical. There is then mutual exclusion of bands in the infrared and Raman, indicating the presence of an inversion centre in the molecule as a whole, and the point group symmetry  $C_i$ ,  $C_{2h}$  and/or  $D_{2h}$  which may be assigned. The latter is only possible in solution. These assignments of tin-carbon stretching modes are consistent since the symmetric stretch is more intense than the asymmetric stretch in the Raman spectra, while the reverse is true in the infrared.

The solid state Raman spectra of these compounds (Table 3.2) show the presence of a strong vibration at  $\sim 210 \text{ cm}^{-1}$  which is absent or weak in intensity in the infrared spectra and is therefore assigned to the symmetric tin-tin stretch. There is also a strong band at  $\sim 145 \text{ cm}^{-1}$  in the Raman and because of the low frequency of this band it is therefore assigned to a  $\text{Sn}_2\text{C}_4$  bending mode. The Raman bands at  $\sim 210 \text{ cm}^{-1}$  and  $\sim 145 \text{ cm}^{-1}$  for the tin-tin stretching and  $\text{Sn}_2\text{C}_4$  bending mode agree well with those reported for  $(\text{CH}_3)_6\text{Sn}_2$ ,<sup>67</sup> where the corresponding bands are found at  $192 \text{ cm}^{-1}$  and  $135 \text{ cm}^{-1}$ .

The Raman spectrum of  $(\text{CH}_3)_4\text{Sn}_2(\text{O}_2\text{CCl}_3)_2$  in  $\text{CHCl}_3$  was recorded. Polarization measurements were made and the following bands,  $\text{cm}^{-1}$ , with their polarization factor in parentheses were 147 (0.65), 206 (0.08), 530 (0.08), 544 (0.72), 1182 (0.64), 1212 (0.29) and 2917 (0.05). According to Raman theory the depolarization factor approaches the value of zero for highly symmetrical types of vibrations. The assignment of the symmetric modes  $\nu_s \text{ Sn-Sn}$  ( $\sim 210 \text{ cm}^{-1}$ ),  $\nu_s \text{ Sn}_2\text{C}_4$  ( $\sim 530 \text{ cm}^{-1}$ ),  $\delta_s \text{ CH}_3$  ( $\sim 1200 \text{ cm}^{-1}$ ) and  $\nu_s \text{ CH}_3$  ( $\sim 2930 \text{ cm}^{-1}$ ) for the solid state Raman spectra

of these compounds is based on the fact that for the  $\text{CHCl}_3$  solution of the  $-\text{CCl}_3$  derivative these bands are polarized.

Comparison of these spectra in the carboxylate region with  $(\text{C}_6\text{H}_5)_4\text{Sn}_2(\text{O}_2\text{CR})_2$ <sup>64</sup> and  $(\text{CH}_3)_3\text{Sn}(\text{O}_2\text{CR})$ <sup>53</sup> allows identification of the  $\nu_s \text{CO}_2$  and  $\nu_{as} \text{CO}_2$  modes. The relevant bands are compared in Table 3.3. Agreement between the series of compounds is good for the solid state spectra, suggesting that the carboxylate ligands are similarly bonded in all three types of molecules. In solution  $(\text{CH}_3)_3\text{Sn}(\text{O}_2\text{CR})$  has been shown to be largely monomeric<sup>55,56</sup> but with some degree of association, while X-ray crystallography has shown that  $(\text{C}_6\text{H}_5)_4\text{Sn}_2(\text{O}_2\text{CCH}_3)_2$ <sup>69</sup> and  $(\text{CH}_3)_3\text{Sn}(\text{O}_2\text{CR})$ <sup>61</sup> have bridging carboxylate groups which complete the five coordinate arrangement about the tin atoms. The vibrational spectra of the ditin compounds strongly suggest that the carboxylate groups bridge the two tin atoms intramolecularly in these methyl derivatives, as has been established for the phenyl compound.<sup>69</sup> The fact that for the methyl and phenyl<sup>64</sup> ditin compounds, neither  $\nu_s \text{CO}_2$  nor  $\nu_{as} \text{CO}_2$  changes on going from solid state to solution, suggests that their structures are the same in both phases. A significant increase in  $\nu_{as} \text{CO}_2$  and decrease in  $\nu_s \text{CO}_2$  accompanies a change from bidentate acetate to monodentate acetate, as has been observed for  $(\text{CH}_3)_3\text{Sn}(\text{O}_2\text{CR})$  on going from the solid state to solution.<sup>53</sup>

An increase in frequency of  $\nu_{as} \text{CO}_2$  is normally regarded as a reflection of an increase in double bond character of a carboxylate group. Such an increase is observed with successive substitutions by



Table 3.3

Symmetric and Asymmetric Stretches (IR) of the  $-CO_2$  Group for

$(CH_3)_4Sn_2(O_2CR)_2$ ,  $(C_6H_5)_4Sn_2(O_2CR)_2$  and  $(CH_3)_3Sn(O_2CR)$

R	Solid <sup>a</sup>		Solid <sup>b</sup>		Solid		Solution	
	$\nu_{as} CO_2$	$\nu_s CO_2$	$\nu_{as} CO_2$	$\nu_s CO_2$	$\nu_{as} CO_2$	$\nu_s CO_2$	$\nu_{as} CO_2$	$\nu_s CO_2$
$(CH_3)_4Sn_2(O_2CR)_2$	1650	1443	1625	-	1680	1435	1720	1400
$(C_6H_5)_4Sn_2(O_2CR)_2$	1615	1350	1610	1350	1655	1342	1702	1290
$(CH_3)_3Sn(O_2CR)$	1605	1330	-	-	1630	1460	-	-
$CHCl_2$	1605	1380	1585	1385	1615	1375	1700	1324
$CH_2Cl$	1585	1390	1560	1395	1610	1380	1690	1335
$CH_3$	-	-	-	-	-	-	-	-

<sup>a</sup>  $\nu_{as} CO_2$  and  $\nu_s CO_2$  have the same values in  $CHCl_3$ , see Table 3.5.

<sup>b</sup>  $\nu_{as} CO_2$  and  $\nu_s CO_2$  have the same values in  $CHCl_3$ , see reference 64.

Table 3.4  
 Comparison of the  $-CO_2$  Group and Tin-Carbon Stretches (IR)  
 for  $(CH_3)_4Sn_2(O_2CR)_2$

R	$\nu_{as}CO_2$		$\nu_sCO_2$		$\nu_{as}Sn_2C_4$		$\nu_sSn_2C_4$	
	solid	soln.*	solid	soln.*	solid	soln.*	solid	soln.*
CF <sub>3</sub>	1650	1635	1443	-	552	550	523	522
CCl <sub>3</sub>	1615	1625	1350	1345	553	550	523	520
CHF <sub>2</sub>	1605	1615	1330	1320	555	549	527	521
CHCl <sub>2</sub>	1605	1602	1385	1380	552	549	530	521
CH <sub>2</sub> Cl	1585	1590	1390	1395	550	547	535	520

\* Infrared data for  $(CH_3)_4Sn_2(O_2CR)_2$  in a solution of CHCl<sub>3</sub>.

chlorine or fluorine for the tetramethylditin carboxylates (Table 3.1).

The increase in double bond character of the carboxylato group would imply a decrease in Lewis base strength of this group and one would expect the average tin-oxygen distance to increase with increasing electronegativity of the R group.

As is the case for the stretching  $\text{-CO}_2$  vibrations, the tin-carbon stretching frequencies do not change on going from the solid state to solution (Table 3.4). The number of  $\text{Sn}_2\text{C}_4$  modes in the infrared spectrum does not change on going from the solid state to solution for the tetramethylditin carboxylates. This also suggests that the structures are the same in both the solid state and the solution.

### (iii) Tin-119 Mössbauer Spectra

Tin-119 Mössbauer spectroscopy has proven to be extremely valuable in structural studies of organo-tin systems.<sup>4</sup> Mössbauer data for the  $(\text{CH}_3)_4\text{Sn}_2(\text{O}_2\text{CR})_2$  compounds are presented in Table 3.5. No significant room temperature absorptions were observed for these compounds. All spectra appear as simple doublets (Fig. 3.2), having line widths of about  $1 \text{ mm s}^{-1}$ . The isomer shift, quadrupole splitting and line widths are consistent with only one type of tin site per molecule. The isomer shifts are slightly greater than those found for  $(\text{CH}_3)_3\text{Sn}(\text{O}_2\text{CR})$  systems,<sup>55,57</sup> but are very similar to shifts for the  $(\text{C}_6\text{H}_5)_4\text{Sn}_2(\text{O}_2\text{CR})_2$  series.<sup>65</sup> However, while earlier workers<sup>57</sup> report changes in isomer shifts with different R groups for the  $(\text{CH}_3)_3\text{Sn}(\text{O}_2\text{CR})$

Table 3.5

 $^{119}\text{Sn}$  Mössbauer Data for  $(\text{CH}_3)_4\text{Sn}_2(\text{O}_2\text{CR})_2$  at 77°K

R	Isomer Shift $\delta$	Quadrupole Splitting		Line Width		$\chi^2/\text{degree}$ of freedom
		$\Delta_{\text{measured}}$	$\Delta_{\text{calculated}}$	$\Gamma_1$	$\Gamma_2$	
$\text{CF}_3$	1.63	3.99	3.95	0.83	0.85	1.03
$\text{CHF}_2$	1.53	3.81	3.81	0.92	0.92	1.45
$\text{CCl}_3$	1.61	3.87	3.87	0.89	0.94	1.16
$\text{CHCl}_2$	1.59	3.84	3.81	0.84	0.84	0.84
$\text{CH}_2\text{Cl}$	1.63	3.63	a	1.03	1.10	1.76

<sup>a</sup>This compound was used to derive a partial quadrupole splitting of  $-0.807$   $\text{mm s}^{-1}$  for the  $(\text{CH}_3)_2\text{Sn}(\text{O}_2\text{CR})_2$  fragment.

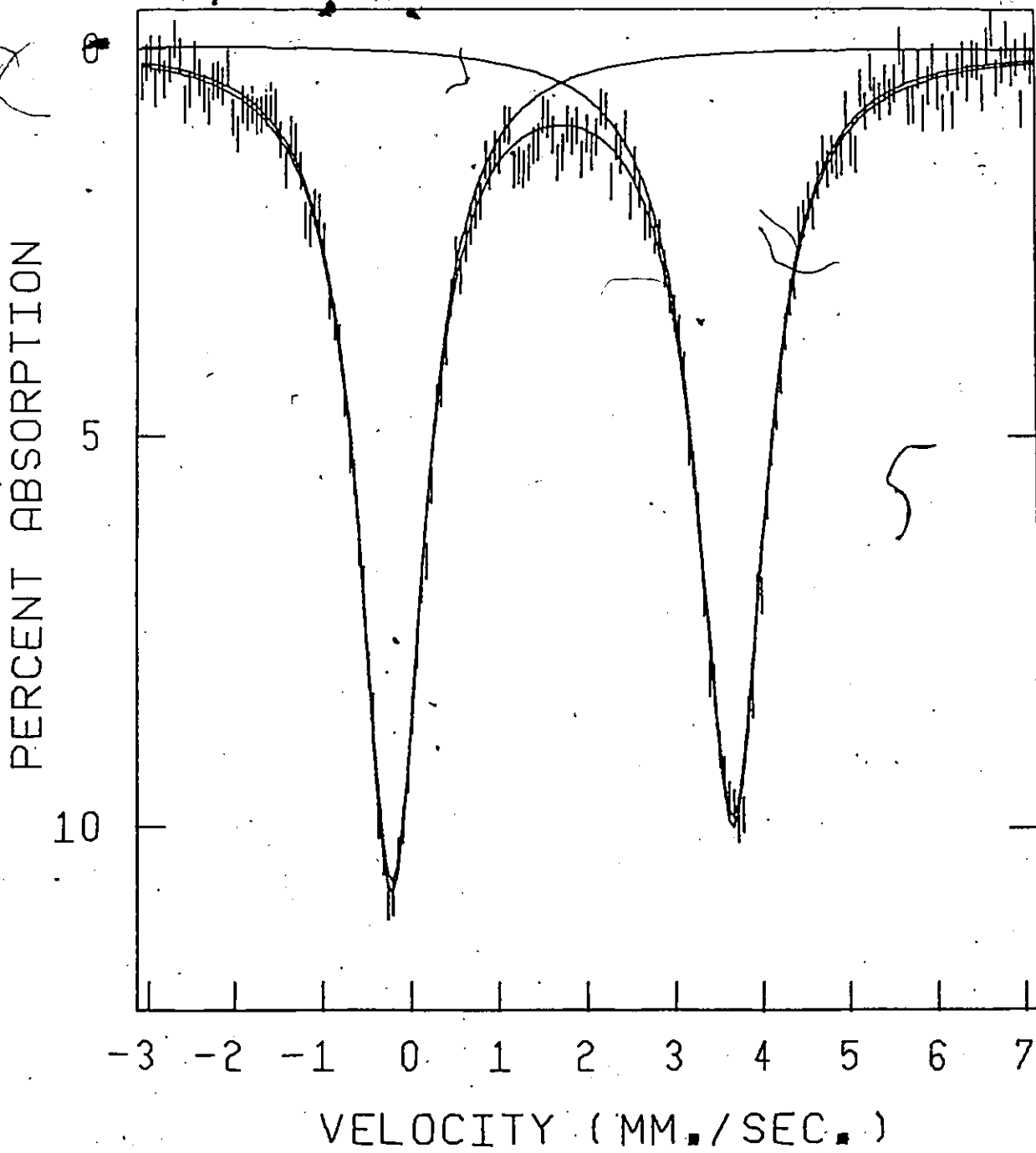


Figure 3.2.  $^{119}\text{Sn}$  Mössbauer spectrum of  $(\text{CH}_3)_4\text{Sn}_2(\text{O}_2\text{CCF}_3)_2$ .

series, this study found no such variation for the  $(\text{CH}_3)_4\text{Sn}_2(\text{O}_2\text{CR})_2$  derivatives. This indicates that the s electron density at the tin nucleus undergoes no observable change through this series of compounds.

Changes in quadrupole splitting values do occur, and although these changes are small, the trend is toward decreasing values as R becomes less electron withdrawing. The quadrupole splitting values are large, 3.6-4.0  $\text{mm s}^{-1}$ , and only slightly smaller than the corresponding values for the analogous  $(\text{C}_6\text{H}_5)_4\text{Sn}_2(\text{O}_2\text{CR})_2$  compounds.<sup>65</sup> Such values are those that one would predict by the point charge model for a five coordinate tin atom.<sup>70</sup> The sign, which was not determined here, should be negative. If this is so, this means that there is greater electron density in the xy plane than there is along the z axis, which presumably contains the O-Sn-O atoms. Herber's criterion that  $\Delta/\delta > 2.1$  for five-coordination,<sup>71</sup> is also satisfied for these compounds. Calculation of the quadrupole splittings for these compounds using the approach of Bancroft et al.<sup>19</sup> gives excellent agreement with experimental findings, if five-coordination is assumed. Finally, since  $(\text{C}_6\text{H}_5)_4\text{Sn}_2(\text{O}_2\text{CCH}_3)_2$  has been shown to be monomeric and have five-coordinate tin atoms, the tetramethylditin derivatives reported here likely have the same structure.

It has been found that there is an increase in the quadrupole splittings of 0.54  $\text{mm s}^{-1}$  on going from  $(\text{CH}_3)_3\text{Sn}(\text{O}_2\text{CCH}_3)$  to  $(\text{CH}_3)_3\text{Sn}(\text{O}_2\text{CCF}_3)$ ,<sup>55</sup> and that the Sn-O distances are 2.205(3) and 2.391(4) in the former, and 2.18(1) and 2.46(2) Å in the latter compound.<sup>61</sup> The trifluoroacetate has somewhat more asymmetric bonds to the tin, and there

is a slight increase in the average Sn-O distance, 2.32(2) Å for the  $-\text{CF}_3$  compound compared to 2.298(5) Å for the  $-\text{CH}_3$  compound. Although the differences in average Sn-O distances in these two compounds do not fulfill the criteria of a  $3\sigma$  difference, they are paralleled by the trends in quadrupole splittings. On the basis of the trends observed in the quadrupole splitting for the  $(\text{CH}_3)_4\text{Sn}_2(\text{O}_2\text{CR})_2$  series, a similar increase in average Sn-O distance from the monochloroacetate to the trifluoroacetate is expected. The small changes in bonding are apparently not large enough to cause any observable change in isomer shift.

#### (iv) Nuclear Magnetic Resonance Spectra

N.m.r. spectra ( $^1\text{H}$  and  $^{13}\text{C}$ ) have been recorded and the data are summarized in Table 3.6. The chemical shifts of the  $^1\text{H}$  and  $^{13}\text{C}$  nuclei are similar to those reported for  $^1\text{H}$  10, 52, 53, 57, 72, 73 and  $^{13}\text{C}$  10, 11, 58, 73 nuclei for methyl tin compounds. The  $^1\text{H}$  and  $^{13}\text{C}$  coupled and decoupled spectra provide confirmation of only one type of methyl and carboxylate group being present in these molecules. The integrated  $^1\text{H}$  n.m.r. peak intensities provide the relative number of methyl to R group protons ( $\text{R} = \text{CHF}_2$ , 6:1;  $\text{R} = \text{CHCl}_2$ , 6:1,  $\text{R} = \text{CH}_2\text{Cl}$ , 3:2) consistent with two methyl groups per carboxylate ligand. The relatively weak peak intensities of non-hydrogen bearing carbon atoms in  $^{13}\text{C}$  n.m.r. spectra together with  $^{13}\text{C}$  decoupled spectra provide confirmation of the  $\text{RCO}_2$  group. The  $^1\text{H}$ ,  $^{13}\text{C}$  and  $^{19}\text{F}$  chemical shifts and coupling constants for the  $\text{RCO}_2$  group confirm the presence of a carboxylate group in these compounds.

Table 3.6 N.M.R. Data for  $(\text{CH}_3)_4\text{Sn}_2(\text{O}_2\text{CR})_2$  Compounds in  $\text{CDCl}_3$  at  $37^\circ\text{C}$ .

	R = $\text{CF}_3$	$\text{CHF}_2^a$	$\text{CCl}_3$	$\text{CHCl}_2$	$\text{CH}_2\text{Cl}$
<u>Chemical Shift (p.p.m.)</u>					
$^1\text{H}$ (T.M.S. = 0)					
$\delta_{\text{CH}_3}$	0.82	0.75	0.82	0.73	0.70
$\delta_{\text{R}}$	-	5.65	-	5.75	3.88
$^{13}\text{C}$ (T.M.S. = 0)					
$\delta_{\text{CH}_3}$	-1.2	-	-0.9	-1.4	-1.7
$\delta_{\text{CO}}$	166.7	-	171.2	174.8	178.2
$\delta_{\text{R}}$	113.5	-	90.7	65.4	42.0
$^{19}\text{F}$ ( $\text{CFCl}_3 = 0$ )					
$\delta_{\text{CF}_3}$	-76.76				
<u>Coupling Constants (Hz)</u>					
$J_{^{117}\text{Sn}-^1\text{H}}$	57.5	58.5	59.0	58.4	57.9
$J_{^{119}\text{Sn}-^1\text{H}}$	60.2	61.0	61.7	60.8	60.5
$J_{^{117/119}\text{Sn}-\text{Sn}-^1\text{H}}$	13.2	13.5	13.9	13.5	13.2
$J_{^{13}\text{C}-^1\text{H}}$	133.8	-	133.8	133.4	132.9
$J_{^{117}\text{Sn}-^{13}\text{C}}$	331.5	-	328.7	333.9	340.5 <sup>b</sup>
$J_{^{119}\text{Sn}-^{13}\text{C}}$	347.6	-	344.2	349.3	-
$J_{^{117/119}\text{Sn}-\text{Sn}-^{13}\text{C}}$	75.5	-	78.7	79.4	77.2
$J_{^{19}\text{F}-^{13}\text{C}}$	284.5	-	-	-	-
$J_{^{19}\text{F}-^1\text{H}}$	-	55.5	-	-	-
$J_{^{19}\text{F}-\text{C}-^{13}\text{C}}$	37.7	-	-	-	-
$J_{^{13}\text{C}-^1\text{H}(\text{R})}$	-	-	-	180.2	150.0

<sup>a</sup>Not sufficiently soluble for  $^{13}\text{C}$  spectra to be recorded.

<sup>b</sup>Satellite doublets not resolved.



All compounds show  $^{117,119}\text{Sn}$  satellite peaks associated with the methyl groups, proving that the methyl groups are bonded to tin. Furthermore, these satellites occur in two groups: those arising from  $J_{^{117,119}\text{Sn-C-}^1\text{H}}$ , and those from  $J_{^{117,119}\text{Sn-Sn-C-}^1\text{H}}$ . The  $^{13}\text{C}$  spectra also show the same pattern. The coupling to the far tin indicates that the tin-tin bond is intact in solution. The two far Sn satellite peaks were resolvable only in the  $^1\text{H}$  n.m.r. spectra of the  $-\text{CF}_3$  derivative, shown in Figure 3.1, where both  $J_{^{117}\text{Sn-Sn-C-}^1\text{H}}$  and  $J_{^{119}\text{Sn-Sn-C-}^1\text{H}}$  (13.10 and 13.70 Hz) are measurable. The magnitude of  $J_{^{117,119}\text{Sn-C-}^1\text{H}}$  has been used to infer the coordination of the tin in  $(\text{CH}_3)_3\text{Sn}(\text{O}_2\text{CR})$ .<sup>52,53,57</sup> Coupling constants in the range 55-60 Hz have been taken as an indication that the trimethyltin acetate is monomeric and hence that the tin is four-coordinate in solution.<sup>52,53,57</sup> However, other molecules containing the  $(\text{CH}_3)_3\text{Sn}$  moiety in which the tin must be four-coordinate, e.g.,  $(\text{CH}_3)_3\text{MSn}(\text{CH}_3)_3$  ( $\text{M} = \text{C}, \text{Si}, \text{Ge}, \text{Sn}$ ), have  $J_{^{117,119}\text{Sn-C-}^1\text{H}}$  ranging from 47-49 Hz.<sup>72</sup> Also n.m.r. data for  $(\text{CH}_3)_4\text{Sn}_2\text{X}_2$  ( $\text{X} = \text{Cl}, \text{Br}, \text{I}, \text{H}$ ), having four-coordinate tin atoms, show two-bond tin-hydrogen coupling constants ranging from 52.2-53.5 Hz,<sup>73,74</sup> considerably lower than the coupling constants for the supposedly four-coordinate tin in  $(\text{CH}_3)_3\text{Sn}(\text{O}_2\text{CR})$ . It should be noted also that  $J_{^{119}\text{Sn-}^{13}\text{C}}$  for  $(\text{CH}_3)_4\text{Sn}_2\text{X}_2$ <sup>73</sup> range from 257 to 281 Hz and are much lower than the corresponding values (344 to 349 Hz), for the carboxylate compounds (Table 3.6). It would seem preferable to infer the geometry about the tin in the carboxylate compounds by comparing their n.m.r. data with the ditin compounds,  $(\text{CH}_3)_4\text{Sn}_2\text{X}_2$ , ( $\text{X} = \text{Cl}, \text{Br}, \text{I}, \text{H}$ ).<sup>73,74</sup> Because the coupling constants for

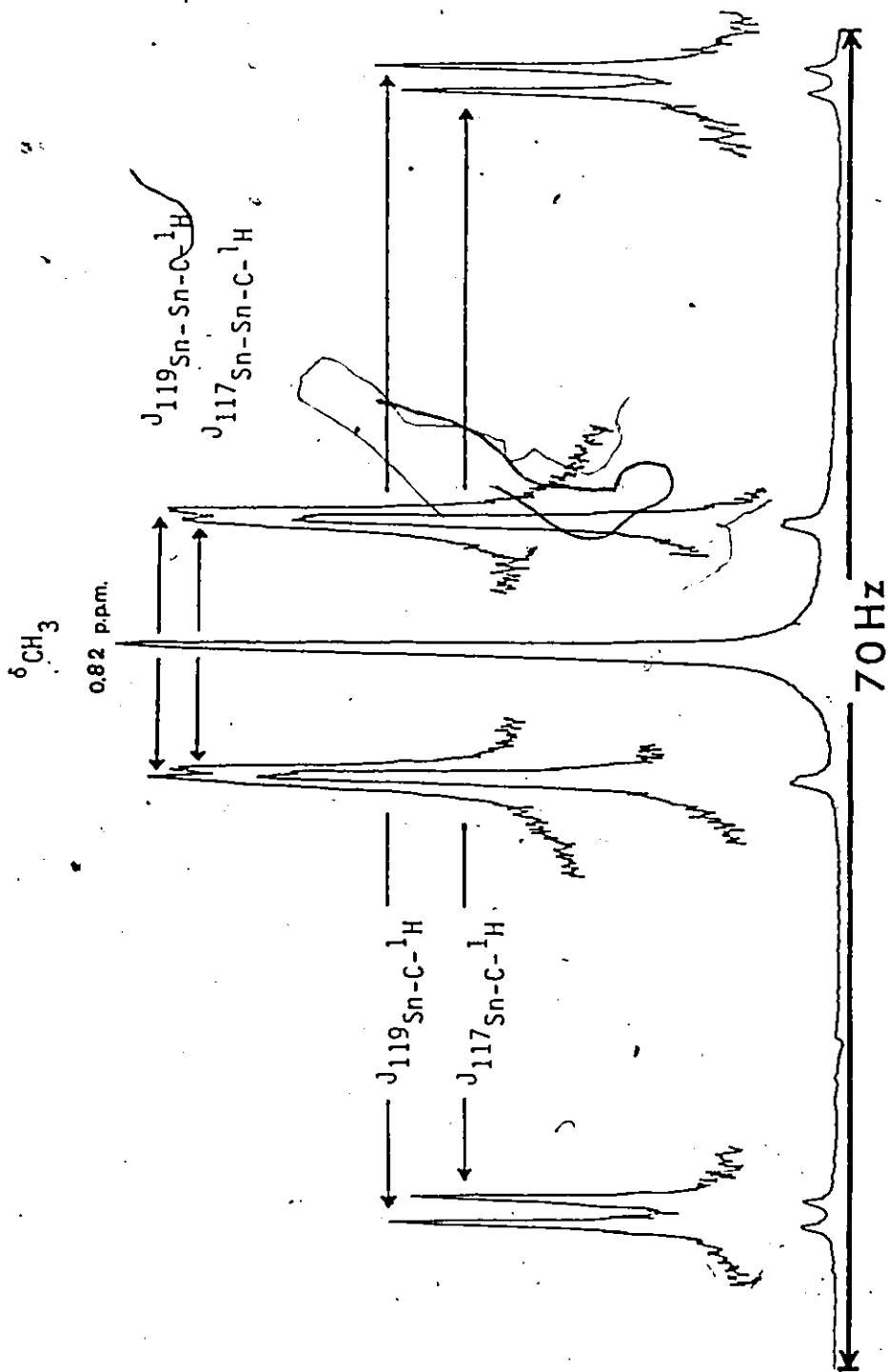
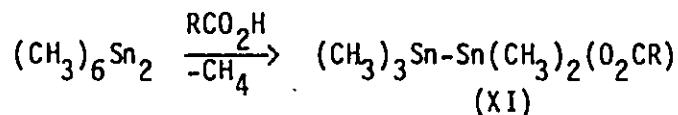


Figure 3.3. 100 MHz  ${}^1\text{H}$  N.M.R. spectrum of  $(\text{CH}_3)_4\text{Sn}_2(\text{O}_2\text{CCF}_3)_2$  in  $\text{CDCl}_3$ .

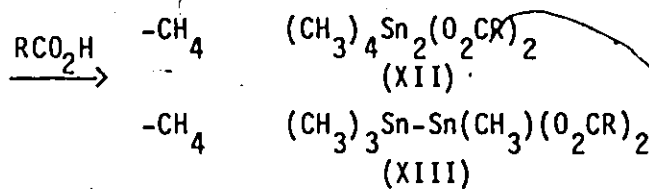
$(\text{CH}_3)_4\text{Sn}(\text{O}_2\text{CR})_2$  are considerably larger than those for  $(\text{CH}_3)_4\text{Sn}_2\text{X}_2$ , one may conclude that the five-coordination established in the solid state for the carboxylate compounds is maintained in solution. Also, it has been shown that the addition of excess pyridine to solutions of  $(\text{CH}_3)_3\text{Sn}(\text{O}_2\text{CR})_2$  results in  $J_{119\text{Sn-C-}^1\text{H}}$  shifting from  $\sim 59$  to  $68$  Hz while for  $(\text{CH}_3)_4\text{Sn}_2\text{X}_2$  it changes from  $52.2-53.5$  to  $59.6-60.4$  Hz. This may be taken as an indication of a change from four- to five-coordination about the tin. Addition of excess pyridine to a  $\text{CHCl}_3$  solution of the  $-\text{CF}_3$  derivative produces no significant change in  $J_{117\text{Sn-C-}^1\text{H}}$  or  $J_{119\text{Sn-C-}^1\text{H}}$  ( $58.0$  and  $60.0$  Hz). This may be taken as further confirmation for the five-coordinate tin environment in solution of these compounds.

(v) Mechanism of the Formation of  $(\text{CH}_3)_4\text{Sn}_2(\text{O}_2\text{CR})_2$

No mechanistic studies have been reported on the acid solvolysis of hexa-alkylditin compounds. Two mechanistic pathways are feasible for the formation of tetramethylditin carboxylates from hexamethylditin in carboxylic acids. Simple stepwise acid cleavage of the methyl groups could yield two distinct types of disubstituted tetramethylditin carboxylates (XII, XIII).

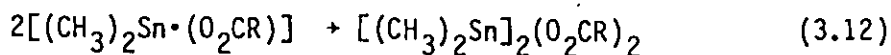
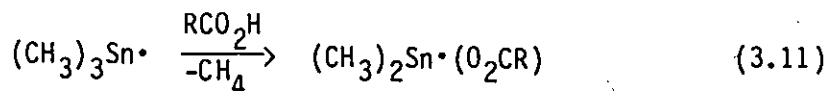
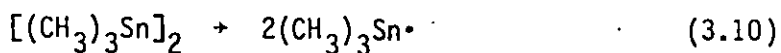


(3.9)



However, only the symmetrical disubstituted tetramethylditin carboxylate XII, is isolated. Neither the intermediate XI, nor the asymmetrically disubstituted tetramethylditin carboxylate XIII, were detected in the  $^1\text{H}$  n.m.r. spectra of the reaction mixtures. Such selectivity is indeed surprising since these and other products should be stable. However, the demethylation of  $(\text{CH}_3)_6\text{M}_2$  ( $\text{M} = \text{Si}, \text{Ge}$ ) with concentrated sulfuric acid and ammonium chloride is a convenient route to  $(\text{CH}_3)_5\text{Si}_2\text{Cl}$ <sup>76</sup> or  $\text{Cl}(\text{CH}_3)_2\text{GeGe}(\text{CH}_3)_2\text{Cl}$ .<sup>77</sup>

The free radical mechanism proposed below is another possible pathway for the formation of XII.



Although organotin radicals have been well established,<sup>2</sup> considerable controversy and conflicting evidence exist as to whether or not hexamethylditin dissociates into free radicals. There is no good evidence to support substantial formation of stable organotin free radicals by facile homolytic dissociation of hexamethylditin.<sup>2</sup> However, the highly coloured nature of the reaction medium, which dissipates upon addition of water in the acid solvolysis of hexamethylditin suggests the formation of free radicals in the reaction medium. However, the

symmetrically disubstituted tetrabutyliditin  $(n\text{Bu})_4\text{Sn}_2\text{Cl}_2$ , readily undergoes thermal disproportionation at  $\sim 120^\circ\text{C}$  qualitatively into  $(n\text{Bu})_2\text{SnCl}_2$  and an inhomogeneous red  $\text{Bu}_2\text{Sn}$  polymer.<sup>78</sup> The red-orange colour of the reaction medium may be associated with the decomposition of some  $(\text{CH}_3)_4\text{Sn}_2(\text{O}_2\text{CR})_2$  in solution since the reaction of hexamethylditin with carboxylic acids of higher acidity were vigorous and exothermic. Further work is necessary in order to establish the mechanistic pathway of the formation of tetramethylditin carboxylates from hexamethylditin in carboxylic acid solutions.

## CHAPTER FOUR

THE CRYSTAL STRUCTURES OF  $(\text{CH}_3)_4\text{Sn}_2(\text{O}_2\text{CCCl}_3)_2$ ,  
 $(\text{CH}_3)_4\text{Sn}_2(\text{O}_2\text{CCF}_3)_2$ ,  $(\text{CH}_3)_4\text{Sn}_2(\text{O}_2\text{CCH}_2\text{Cl})_2$ ,  
 $\{[(\text{CH}_3)_2\text{Sn}(\text{O}_2\text{CCF}_3)]\text{O}\}_2$  and  $\{[(\text{CH}_3)_2\text{Sn}(\text{O}_2\text{CCCl}_3)]\text{O}\}_2$

### A. Introduction

In order to determine accurate tin-oxygen distances for the three derivatives of  $(\text{CH}_3)_4\text{Sn}_2(\text{O}_2\text{CR})_2$  ( $\text{R} = \text{CF}_3, \text{CCl}_3, \text{CH}_2\text{Cl}$ ), it was necessary to carry out X-ray crystallographic analyses of these compounds. The spectroscopic results had suggested that these molecules were centrosymmetric with five-coordinate tin atoms. The carboxylato group was believed to bridge the tin-tin bond of a planar tetramethylditin moiety, and be isostructural with  $(\text{C}_6\text{H}_5)_4\text{Sn}_2(\text{O}_2\text{CCH}_3)_2$ .<sup>69</sup> Accurate X-ray crystallographic structure determinations for these compounds are necessary in order to determine if there are two distinct tin-oxygen distances, and if so, to try to ascertain the cause of such asymmetry. It was earlier suggested (Chapter 3) that the average tin-oxygen distance was believed to increase in the same fashion as the <sup>119</sup>Sn Mossbauer quadrupole splitting values, which follow the electronegativities of the R substituent of the carboxylato group. The crystal structure of  $(\text{C}_6\text{H}_5)_4\text{Sn}_2(\text{O}_2\text{CCH}_3)_2$ ,<sup>69</sup> was also not of sufficient accuracy to establish an asymmetry in the tin-oxygen linkage (Sn-O; 2.25(2), 2.25(2)Å). Before any conclusions can be made more accurate data for this compound are required.

The structurally related trimethyltin-carboxylates, which have an almost planar trimethyltin unit bridged intermolecularly by carboxylato groups are known to have two distinct tin-oxygen distances,<sup>61</sup> and their <sup>119</sup>Sn Mössbauer quadrupole splitting values<sup>55</sup> follow the same trend as the  $(\text{CH}_3)_4\text{Sn}_2(\text{O}_2\text{CR})_2$  series reported in this thesis. Since the average tin-oxygen distance for trimethyltin acetate of 2.298(2) Å [2.205(3), 2.391(4) Å] was not significantly different from that of trimethyltin trifluoroacetate, 2.37(2) Å [2.18(1), 2.46(2) Å], the changes in <sup>119</sup>Sn Mössbauer quadrupole splitting data were interpreted to be a reflection of the increase in asymmetry of the tin-oxygen distances from the acetate (0.186(5) Å), to the trifluoroacetate (0.281(21) Å).<sup>61</sup> This asymmetry was believed to be caused by a change in distribution of electron density in the two C-O bonds of the carboxylato group.<sup>55,61</sup> It was suggested that an increase in electronegativity of the R group of the carboxylato group increased the difference in these tin-oxygen distances,<sup>55,61</sup> and this was reflected in a larger quadrupole splitting value.<sup>55,61</sup> The average tin-oxygen distance was believed to be constant since there was no overall change in electron density at the tin nucleus as the isomer shifts were constant.<sup>55</sup> However, the point charge model for quadrupole splittings is independent of the asymmetry of tin-oxygen distances since these are along the same axis, and qualitatively predicts the observed quadrupole splitting values for organotin carboxylates.<sup>22</sup> This model, however, is sensitive to the average tin-oxygen distance. The change in the average tin-oxygen distance between trimethyltin acetate and trimethyltin trifluoroacetate is small (0.05 Å).

However, although the data reported for the tin-oxygen distances of trimethyltin acetate (2.205(3), 2.391(4)Å),<sup>61</sup> are quite accurate those for trimethyltin trifluoroacetate (2.18(1), 2.46(2)Å)<sup>61</sup> are not, which makes it difficult to discuss the variation in average Sn-O distances for the two compounds. Chin and Penfold have suggested that the argument<sup>55,61</sup> used to justify the increase in the difference in the tin-oxygen distance from the trimethyltin acetate to trimethyltin trifluoroacetate must be restricted to triorganotin carboxylates where the organotin substituent is similar.<sup>61</sup> In tribenzyltin acetate the tin-oxygen bond length difference is 0.51(3)Å [2.14(2), 2.65(2)Å]<sup>59</sup> and is greater than in either of the trimethyltin carboxylates.<sup>61</sup> The large Sn-O bond length difference for tribenzyltin acetate has been attributed to the difference in the tin-alkyl substituent.<sup>61,79</sup> In tricyclohexyltin acetate, the Sn-O bond length distance is 2.12(3)Å<sup>60</sup> and this compound is regarded as a monomeric four-coordinate tin compound.<sup>61,79,80</sup> Recently Peruzzo and coworkers have reported X-ray structural data for trivinyltin trichloroacetate<sup>79</sup> and compared these data with those previously reported for trimethyltin acetate,<sup>61</sup> trimethyltin trifluoroacetate,<sup>61</sup> tribenzyltin acetate<sup>59</sup> and tricyclohexyltin acetate.<sup>60</sup> A difference in the Sn-O distances, 0.32(2)Å [2.17(2), 2.49(1)Å], was established for trivinyltin trichloroacetate.<sup>79</sup> This five-coordinate tin carboxylate possesses a trigonal bipyramidal geometry distorted to different degrees than in other five-coordinate tin carboxylates.<sup>79</sup>



The argument originally proposed by Sams and Poder to account for the  $^{119}\text{Sn}$  Mössbauer data of the trimethyltin carboxylates was used to account for the similar  $^{119}\text{Sn}$  Mössbauer data for trivinyltin carboxylates.<sup>79</sup> Recently Peruzzo and coworkers have established the structure of tricyclohexyltin trifluoroacetate by X-ray analysis.<sup>80</sup> The  $^{119}\text{Sn}$  Mössbauer data on a series of tricyclohexyltin carboxylates were interpreted in terms of a distorted tetrahedral geometry for the four-coordinate tin atoms.<sup>80</sup>

#### B. Experimental

##### (i) The Crystal Structure Data for Bis( $\mu$ -trichloroacetato-0,0')-bis[dimethyltin(IV)].

Good quality single crystals of  $(\text{CH}_3)_4\text{Sn}_2(\text{O}_2\text{CCCl}_3)_2$  were obtained from the reaction of hexamethylditin with trichloroacetic acid in chloroform at 0°C under vacuum, as reported in the experimental section of this thesis. The majority of crystals were thin, clear, crystalline hexagonal plates.

The unit cell parameters for  $(\text{CH}_3)_4\text{Sn}_2(\text{O}_2\text{CCCl}_3)_2$  initially determined from precession photographs were:  $a = 10.15(5)$ ,  $b = 7.54(3)$ ,  $c = 12.59(5)\text{Å}$ ,  $\beta = 97.5(5)$ . Zero and the first layer precession photographs showed the systematic absences of  $0k0$ ,  $k$  (odd), and  $h0l$ ,  $l$  (odd), consistent with the monoclinic space group  $P2_1/C$  (#14). A crystal suitable for intensity measurements was then selected. An almost spherical crystal of radius 0.15 mm was sealed in a quartz capillary and then mounted on a Syntex  $P2_1$ . The following crystal data were obtained.

$C_8H_{16}Cl_6O_4Sn_2$ ,  $M = 622.27$ , monoclinic,  $a = 10.223(3) \text{ \AA}$ ,  $b = 7.539(2) \text{ \AA}$ ,  
 $c = 12.71(4) \text{ \AA}$ ,  $\beta = 97.76(2)^\circ$ ,  $U = 970.7(5) \text{ \AA}^3$ ,  $Z = 2$ ,  $D_c = 2.13 \text{ g cm}^{-3}$ ,  
 $D_m = 2.06(2) \text{ g cm}^{-3}$ ,  $F(000) = 588$ ,  $\lambda(\text{Mo-K}\alpha) = 0.71069 \text{ \AA}$  and  $\mu(\text{Mo-K}\alpha) =$   
 $34 \text{ cm}^{-1}$ .

The unit cell parameters were obtained from a least squares refinement of 15 well centered reflections with  $17.96^\circ < 2\theta < 29.71^\circ$ . The diffractometer data were also consistent with the space group  $P2_1/C$  (#14) and the structure was successfully refined in this space group. The equivalent positions for  $P2_1/C$  (#14) are  $x, y, z$  and  $\bar{x}, \frac{1}{2} + y, \frac{1}{2} - z$ .

Intensities were measured with graphite monochromated radiation, using a  $\theta$ - $2\theta$  scan, for a total of 2560 reflections with  $0 < h < 13$ ,  $-1 < k < 9$ ,  $-16 < l < 16$  and  $3.23 < 2\theta < 55.13^\circ$ .

A total of 242 reflections were averaged. The 181 reflections that were systematically absent, along with 207 reflections that had zero intensity were removed from the data set. A total of 2051 reflections remained, of which 755 had intensities less than the standard error based on the counting statistics. Two standard reflections (2,3,-1 and 2,1,-4), were measured every 50 reflections, and these showed a small but significant reduction in intensity during data collection. Such a variation is consistent with there being increasing surface decomposition of the crystal. A slight surface dullness or coating was noted on the crystal surface after intensity collection was complete. The data were divided into three batches for refinement, each set with a different.

scale factor. A spherical absorption correction was applied to each batch. This was necessary since  $\mu(\text{Mo-K}\alpha)\text{R} = 0.5$ .

The solution and refinement of the structure of  $(\text{CH}_3)_4\text{Sn}_2(\text{O}_2\text{CCCl}_3)_2$  was as follows. The positional parameters of the tin atom in the asymmetric unit were obtained from a three-dimensional Patterson synthesis, and were used to phase the initial structure-factor calculations. Two cycles of least squares refinement of this tin position, along with its isotropic temperature factor, were carried out using the locally written program CUDLS, to yield an R index of 0.39. The positions of nine light atoms were located from a difference Fourier synthesis. Least squares refinement proved satisfactory for eight of these positions, yielding an R index of 0.19. Refinement of the anisotropic temperature factors of the tin and then the chlorine atoms yielded an R index of 0.14 and 0.08, respectively. The remaining carbon atom, C(1), was then successfully refined.

When the refinement of the positional parameters and anisotropic temperature factors yielded the R index 0.073, a weighting scheme, followed by a secondary extinction given by  $F^* = F[1 + 0.542 \times 10^{-6} \times \sin^2(2\theta) F^2]^{1/2}$ ,<sup>81</sup> were applied. Refinement converged at  $R = 0.0527$ , and  $R_w = \{[\sum \omega(|F_o| - |F_c|)^2 / \sum \omega |F_o|^2]^{1/2}\}$  equal to 0.0518, where  $\omega = [\sigma^2 + (0.027 F_o)^2]^{-1}$ ,  $\sigma$  being the standard error in  $F_o$  derived from the counting statistics. The value of  $k$ , 0.027, was chosen to make  $\langle \omega |\Delta F|^2 \rangle$  independent of  $|F_o|$ . The maximum value of the shift over error was 0.0041 for the x coordinate of the tin atom, while the average shift over error for all variables (A.S.E.) was 0.0009. The final value of

Table 4.1  
 Atomic Coordinates ( $\times 10^4$ ) for  $(\text{CH}_3)_4\text{Sn}_2(\text{O}_2\text{CCCl}_3)_2$

	x/a	y/b	z/c
Sn	4489(1)	1610(1)	187(1)
C1(1)	8115(3)	384(3)	3300(3)
C1(2)	9442(2)	2440(5)	5017(2)
C1(3)	9100(3)	3845(4)	2902(2)
O(1)	2963(5)	41(7)	964(5)
O(2)	6255(5)	2341(7)	4379(4)
C(1)	8399(7)	2547(12)	3821(7)
C(2)	7078(7)	3407(12)	4088(6)
C(3)	2984(8)	2187(14)	4094(7)
C(4)	5157(9)	1986(12)	6609(7)

Table 4.2.

Thermal Parameters<sup>a</sup> for  $(\text{CH}_3)_4\text{Sn}_2(\text{O}_2\text{CCCl}_3)_2$ 

	$U_{11}$	$U_{22}$	$U_{33}$	$U_{12}$	$U_{13}$	$U_{23}$
Sn	416(5)	316(4)	494(4)	1(3)	147(2)	-3(3)
Cl(1)	693(16)	639(16)	1203(23)	127(13)	360(15)	-342(16)
Cl(2)	589(15)	1132(23)	820(20)	192(16)	-81(14)	90(17)
Cl(3)	735(16)	904(20)	887(19)	157(14)	524(14)	191(15)
O(1)	552(32)	343(32)	747(40)	-58(27)	342(29)	-24(28)
O(2)	452(30)	320(27)	610(34)	44(25)	279(27)	-53(26)
C(1)	395(42)	468(47)	593(52)	90(38)	130(38)	-80(42)
C(2)	369(37)	456(43)	409(39)	95(40)	103(32)	-58(40)
C(3)	423(45)	700(63)	654(59)	-70(43)	-28(41)	-155(49)
C(4)	762(60)	547(59)	483(50)	133(45)	62(44)	150(42)

<sup>a</sup>Temperature factors ( $\times 10^4$ ) in the form  $\exp(-2\pi^2 \sum_{ij} U_{ij} H_i H_j a_i^* a_j^*)$ .

Table 4.3

Bond Lengths (Å) and Bond Angles (°) for  $(\text{CH}_3)_4\text{Sn}_2(\text{O}_2\text{CCCl}_3)_2$ 

(a) Bond Lengths (Å)		(b) Bond Angles (°)	
Sn-O(1)	2.285(6)	Sn'-Sn-O(1)	85.07(14)
Sn-O(2)	2.332(5)	Sn'-Sn-O(2)	83.49(13)
Sn-Sn'	2.711(1)	Sn'-Sn-C(3)	121.9(3)
Sn-C(3)	2.131(9)	Sn'-Sn-C(4)	120.5(2)
Sn-C(4)	2.126(9)	C(3)-Sn-C(4)	117.6(4)
C(1)-O(1)	1.234(10)	C(3)-Sn-O(1)	91.6(3)
C(1)-O(2)	1.255(9)	C(3)-Sn-O(2)	95.9(3)
C(1)-C(2)	1.576(11)	C(4)-Sn-O(1)	92.9(3)
C(2)-Cl(1)	1.769(9)	C(4)-Sn-O(2)	91.5(3)
C(2)-Cl(2)	1.736(8)	Sn-O(1)-C(1)	120.9(5)
C(2)-Cl(3)	1.751(9)	Sn-O(2)-C(1)	120.2(5)
		O(1)-C(1)-O(2)	119.5(7)
		O(1)-C(1)-C(2)	114.0(7)
		O(2)-C(1)-C(2)	115.4(7)
		C(1)-C(2)-Cl(1)	111.0(5)
		C(1)-C(2)-Cl(2)	105.9(5)
		C(1)-C(2)-Cl(3)	110.7(6)
		Cl(1)-C(2)-Cl(2)	109.6(5)
		Cl(1)-C(2)-Cl(3)	109.0(5)
		Cl(2)-C(2)-Cl(3)	110.6(4)

Prime denotes symmetry-related atoms.

$[\sum w(|F_o| - |F_c|)^2 / (N_F - N_P)]^{1/2} = 1.08$ , where  $N_F$  = number of reflections and  $N_P$  = number of refined parameters (94). This indicates that the model accounts for all structurally significant information in the observed structure factors. A final electron difference map did not indicate the positions of the hydrogen atoms of the methyl groups. The largest features were peaks of  $1 \text{ e } \text{Å}^{-3}$  within  $1 \text{ Å}$  of the tin atoms along the Sn-Sn axis, with a minimum of  $-1 \text{ e } \text{Å}^{-3}$  at the centre of symmetry of the molecule. All other features were  $\pm 0.5 \text{ e } \text{Å}^{-3}$ , with random distribution throughout the cell. Atomic scattering factors corrected for anomalous dispersion were taken from reference 82.

The final positional coordinates of the atoms in the asymmetric unit are given in Table 4.1. Table 4.2 contains the temperature factors. Structure factors are presented in Table 1, J. P. Johnson, McMaster University Thesis Tables #1, June 1983, and are available from Thode Library, McMaster University. The bond lengths and bond angles of  $(\text{CH}_3)_4\text{Sn}_2(\text{O}_2\text{CCl}_3)_2$  are given in Table 4.3.

(ii) The Crystal Structure Data for Bis( $\mu$ -trifluoroacetafo-0,0')-bis[ $\mu$ -dimethyltin(IV)] and Bis( $\mu$ -monochloroacetato-0,0')-bis[ $\mu$ -dimethyltin(IV)]

The preparation of these compounds is described in the experimental section of this thesis. Crystals of  $(\text{CH}_3)_4\text{Sn}_2(\text{O}_2\text{CCF}_3)_2$  suitable for X-ray study were obtained from the reaction product. Those obtained from the  $(\text{CH}_3)_4\text{Sn}_2(\text{O}_2\text{CCH}_2\text{Cl})_2$  reaction product however, were twinned and required recrystallization from  $\text{CHCl}_3$ .

Table 4.4

Interatomic Distances (Å) and Angles (°) for  $(\text{CH}_3)_4\text{Sn}_2(\text{O}_2\text{CCH}_2\text{Cl})_2$ 

## (a) Bond Lengths (Å)

Sn-O(1)	2.241(7)
Sn-O(2)	2.349(7)
Sn-Sn	2.691(2)
Sn-C(3)	2.112(14)x2
C(1)-O(1)	1.27(2)
C(1)-O(2)	1.25(2)
C(1)-C(2)	1.51(2)
C(2)-Cl	1.76(2)

## (b) Bond Angles (°)

Sn-Sn-C(3)	122.3(4)
Sn-Sn-O(1)	86.3(3)
Sn-Sn-O(2)	82.4(3)
C(3)-Sn-C(3)'	115.1(5)
Sn-O(1)-C(1)	123.0(8)
Sn-O(2)-C(1)	122.8(9)
O(1)-C(1)-O(2)	125.5(10)
O(1)-C(1)-C(2)	112.5(13)
O(2)-C(1)-C(2)	122.0(14)
C(1)-C(2)-Cl	114.3(12)

## (c) Intermolecular Interactions (Å)

O(2)---H	3.06x2
----------	--------

Prime denotes symmetry-related atoms.



Table 4.5. Interatomic Distances (Å) and Angles (°) for  $(\text{CH}_3)_4\text{Sn}_2(\text{O}_2\text{CCF}_3)_2$ .

(a) Bond Lengths (Å)		(b) Bond Angles (°)	
Sn-Sn'	2.707(1)	C(3)-Sn-C(3)	117.8(4)
Sn-O(1)	2.319(4)	C(3)-Sn-Sn'	121.1(3)x2
Sn-O(2)	2.345(4)	C(3)-Sn-O(1)	92.8(2)x2
Sn-C(3)	2.100(10)x2	C(3)-Sn-O(2)	93.2(2)x2
C(1)-O(1)	1.218(12)	Sn'-Sn-O(1)	84.6(2)
C(1)-O(2)	1.251(12)	Sn'-Sn-O(2)	83.8(2)
C(1)-C(2)	1.536(9)	Sn-O(1)-C(1)	121.4(5)
C(2)-F(1)	1.258(9)x2	Sn-O(2)-C(1)	120.3(5)
C(2)-F(2)	1.274(13)x2	O(1)-C(1)-O(2)	129.9(6)
C(2)-F(3)	1.337(18)	O(1)-C(1)-C(2)	115.9(8)
C(2)-F(4)	1.318(19)	O(2)-C(1)-C(2)	114.2(8)
C(3)-H(1)	0.97(7)	C(1)-C(2)-F(1)	112.9(5)x2
C(3)-H(2)	0.90(8)	C(1)-C(2)-F(2)	111.4(7)x2
C(3)-H(3)	0.59(13)	C(1)-C(2)-F(3)	112.4(9)
		C(1)-C(2)-F(4)	113.8(9)
(c) Intermolecular Interactions (Å)		F(1)-C(2)-F(1)'	110.2(9)
H(1)---F(2)	2.60(8)	F(1)-C(2)-F(3)	103.9(7)x2
H(1)---F(3)	2.76(8)	F(2)-C(2)-F(2)'	108.5(10)
H(2)---F(1)	2.87(9)	F(2)-C(2)-F(4)	105.7(9)
H(2)---F(4)	2.92(8)	Sn-C(3)-H(1)	112(6)
H(3)---F(4)	3.13(12)	Sn-C(3)-H(2)	115(6)
H(3)---O(2)	3.20(12)	Sn-C(3)-H(3)	105(10)
		H(1)-C(3)-H(2)	96(7)
		H(1)-C(3)-H(3)	102(10)
		H(2)-C(3)-H(3)	124(11)

Prime denotes symmetry-related atoms.

Fluorine has an occupancy of half an atom.

The crystallographic work on the  $-CF_3$  and  $-CH_2Cl$  derivatives were performed by R. Faggiani and Dr. I. D. Brown, of the Institute of Materials Research at this University. Information on the X-ray intensity measurements and information on the solution and refinement of these two structures have been published elsewhere.<sup>83,84</sup> The interatomic distances and angles for  $(CH_3)_4Sn_2(O_2CCH_2Cl)_2$  and  $(CH_3)_4Sn_2(O_2CCF_3)_2$  are given in Table 4.4 and Table 4.5 respectively.

### C. Discussion

Views of the molecular structures of the  $(CH_3)_4Sn_2(O_2CR)_2$  complexes are shown in Figures 4.1-4.3. Some of the more important bond lengths and bond angles are summarized in Table 4.6.

The molecular structures of the three tetramethylditin carboxylates are similar. All three compounds contain five coordinate tin atoms with a slightly distorted trigonal-bipyramidal geometry, with two carbon and one tin atom occupying the equatorial positions and with oxygen atoms in the axial positions. Each molecule has an inversion centre half-way between the chemically bonded tin atoms. These tin atoms are held in place by two equivalent bidentate bridging carboxylato ligands and a short tin-tin bond.

The  $C_4Sn_2$  moiety is a planar unit, normal to the plane of the carboxylato bridge. The carbon-tin bond lengths appear to be independent of the type of carboxylate group and are similar to the values reported for other methyl-tin compounds (2.10Å).<sup>61</sup> However, the tin-tin bond length is appreciably shorter than the sum of the covalent radii (2.80Å,

Table 4.6. A Summary of Bond Lengths and Bond Angles

for  $(\text{CH}_3)_4\text{Sn}_2(\text{O}_2\text{CR})_2$ .

R	$\text{CH}_2\text{Cl}$	$\text{CCl}_3$	$\text{CF}_3$
Sn-Sn	2.691(2) Å	2.711(1) Å	2.707(1) Å
Sn-O(1)	2.241(7)	2.285(6)	2.319(4)
Sn-O(2)	2.349(7)	2.332(5)	2.345(4)
Sn-C*	2.112(14)	2.131(9) 2.126(9)	2.100(10)
C(1)-O(1)	1.27(2)	1.255(9)	1.218(12)
C(1)-O(2)	1.25(2)	1.234(10)	1.251(12)
C(1)-C(2)	1.51(2)	1.576(11)	1.536(9)
Sn-Sn-O(1)	86.3(3)°	85.07(14)°	84.6(2)°
Sn-Sn-O(2)	82.4(3)°	83.49(13)°	83.8(2)°
Sn-Sn-C*	122.3(4)°	121.9(3)° 120.5(2)°	121.1(3)°
C*-Sn-C*	115.1(5)°	117.6(4)°	117.8(4)°
Sn-O(1)-C(1)	123.0(8)°	120.9(5)°	121.4(5)°
Sn-O(2)-C(1)	122.8(9)°	120.2(5)°	120.3(5)°
O(1)-C(1)-O(2)	125.5(10)°	129.5(7)°	129.9(6)°
O(1)-C(1)-C(2)	112.5(13)°	114.0(7)°	115.9(8)°
O(2)-C(1)-C(2)	122.0(14)°	115.4(7)°	114.2(8)°

\*Carbon atom of the methyl group.

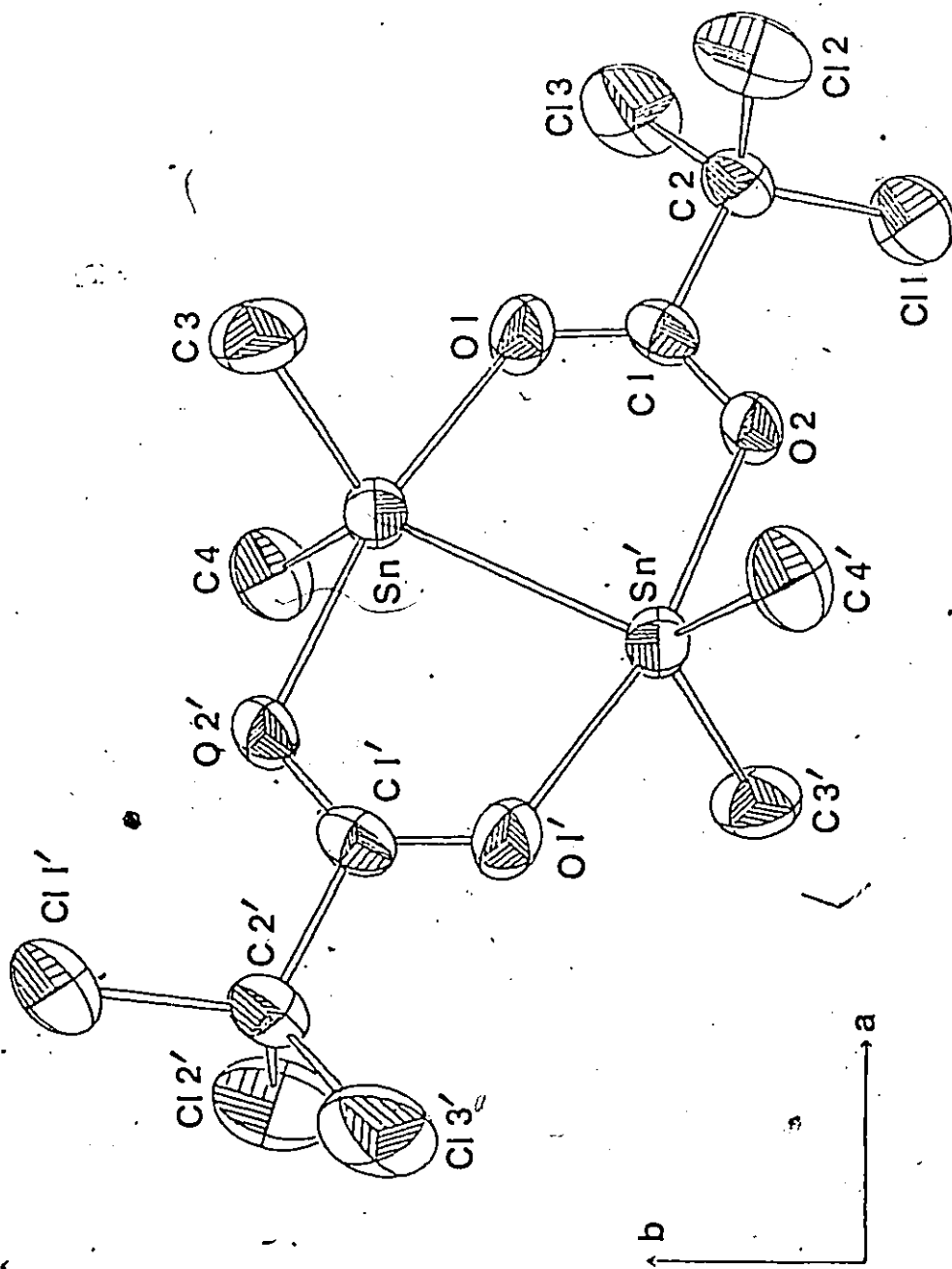


Figure 4.1. A view of  $(\text{CH}_3)_4\text{Sn}_2(\text{O}_2\text{CCCCl}_3)_2$  down the  $c$  axis.

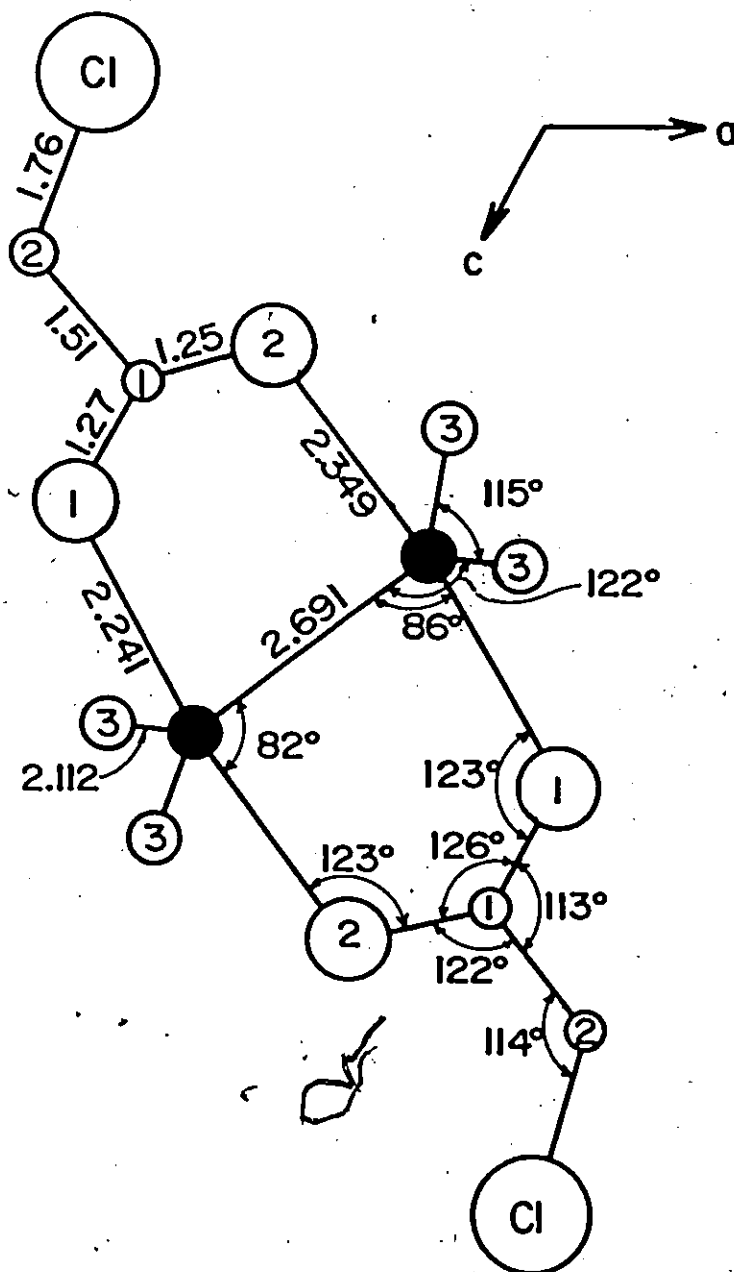


Figure 4.2.  $(\text{CH}_3)_4\text{Sn}_2(\text{O}_2\text{CCH}_2\text{Cl})_2$  viewed down the two fold axis.  
 The large numbered circles are O, the small numbered circles are C, the shaded circles are Sn.

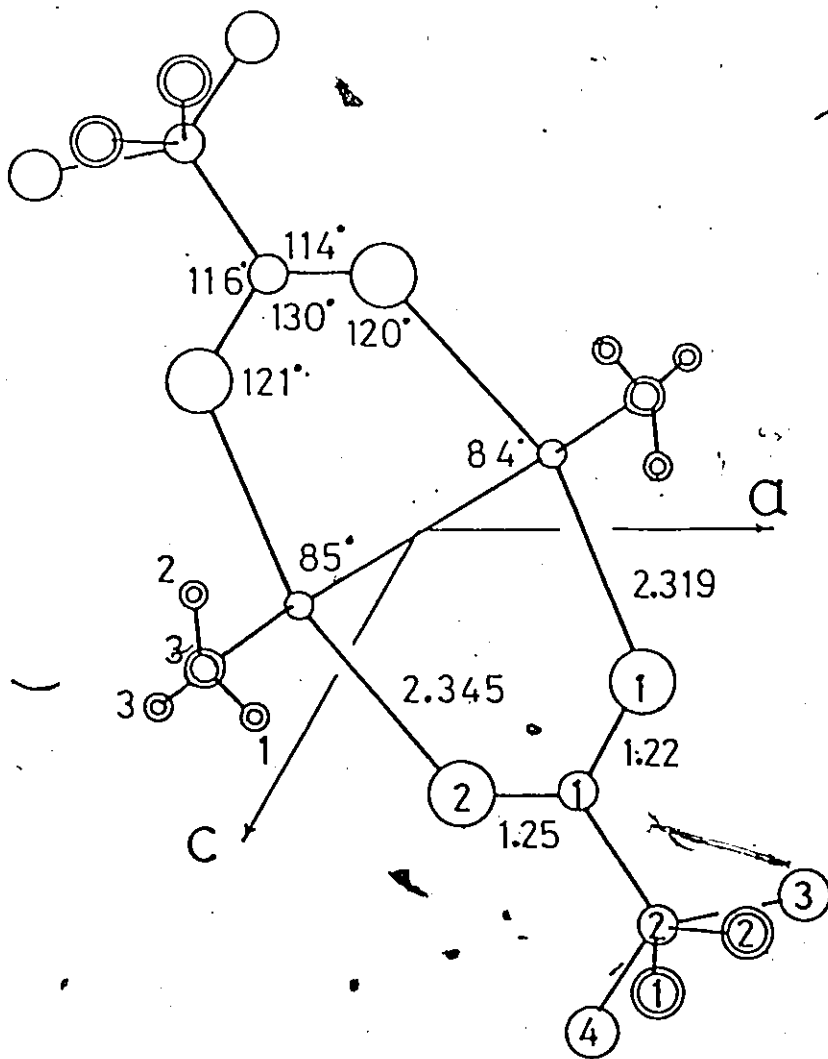


Figure 4.3. A view of  $(\text{CH}_3)_4\text{Sn}_2(\text{O}_2\text{CCF}_3)_2$ . The circles in decreasing order of size represent O, F, C, Sn and H. Double circles represent atoms lying both above and below the molecular plane. All the F positions shown are half occupied.

grey tin, tetrahedral).<sup>85</sup> The tin-tin distance in the monochloride and trifluoride is similar to that found in  $(C_6H_5)_4Sn_2(O_2CCH_3)_2$  (2.69(1)Å),<sup>69</sup> but this distance in the trichloride derivative (2.711(1)Å) is appreciably larger and is very close to the sum of the covalent radii. It is also similar to that for the tetrahedral tin atoms in  $[(C_6H_5)_2Sn]_6$ <sup>86</sup> and  $(C_6H_5)_6Sn_2$ .<sup>87</sup> The major distortion in the equatorial plane of these trigonal bipyramidal configurations is an apparent reduction of the C-Sn-C angle at the expense of an increase of the C-Sn-Sn angle. This approximately 5°-reduction of the C-Sn-C angle from the ideal 120° trigonal angle, is a simple reflection of the large bulk of the  $Sn(CH_3)_2$  unit with respect to the relatively smaller methyl group. The structural data for the three tetramethylditin carboxylates are consistent with the spectroscopic results in that the tetramethylditin moiety is similar in all three compounds. In each molecule, the oxygen atoms are bonded to the tin atom in the axial positions to complete a trigonal bipyramidal arrangement.

The O-Sn-O linkage is not linear and provides a major distortion at the tin sites. The ~ 10° reduction of the O-Sn-O angle from 180° is necessitated by the fact that the bite of the carboxylate group is much smaller than the tin-tin distance, ~ 2.7Å, in these compounds. The small reduction of the tin-tin distance from that in  $(C_6H_5)_6Sn_2$  is probably a result of the constraint of the small  $CO_2$  bite distance. A simple geometric calculation shows that an almost linear O-C-O linkage, or a tin-tin distance of ~ 2.5Å, would be required to give an O-Sn-O angle of 180°. However, neither of these constraints is realistic, and a compromise is reached.

The three  $(\text{CH}_3)_4\text{Sn}_2(\text{O}_2\text{CR})_2$  complexes have two independent Sn-O bond lengths which are given in Table 4.6. These Sn-O bonds are trans to one another, so that each tin atom has one short and one long Sn-O bond. Not only are the two independent Sn-O distances significantly different, but the difference between them (0.026(6), 0.0478(8), 0.108(10)) increases in the order:  $\text{R}' = -\text{CF}_3, -\text{CCl}_3, -\text{CH}_2\text{Cl}$ . This is in direct contrast to the trimethyltin carboxylates, where the difference in Sn-O bond lengths decreases from the  $-\text{CF}_3$  (0.281(21)) to the  $-\text{CCH}_3$  (0.186(5)) derivative.<sup>61</sup>

Poder and Sams<sup>55</sup> have suggested that the increase in asymmetry of the Sn-O linkage in trimethyltin carboxylates is a direct result of the increase of double bond character of the carbonyl C=O bond over the other C-O bond as the electronegativity of the R group of the carboxylato group increases. The increase in Mössbauer quadrupole splitting values as the electronegativity of the R group increases is interpreted here as a result of an increase in the difference in the Sn-O distances.<sup>55</sup> Although the quadrupole splitting values in both the trimethyltin and tetramethylditin series increase with electronegativity of the R group, the asymmetry in tin-oxygen distances decreases from the  $-\text{CF}_3$  to the  $-\text{CH}_2\text{Cl}$  derivative for the tetramethylditin carboxylates. A localized bonding scheme for the carboxylate does not appear to approximately account for the asymmetry of Sn-O distances, and we must look elsewhere for the cause.



A comparison of the "short" Sn-O distances, Sn-O(1), in the tetramethylditin carboxylates (Table 4.6) shows a small, but significant, increase in bond length as the electronegativity of the R group increases. However, the "long" Sn-O distances, Sn-O(2), appear to be almost independent of the R group. Such behaviour is only possible if other bonding interactions are also present which have yet to be accounted for. The consistency of the "long" Sn-O distance is believed to be the result of weak intermolecular H---O interactions.

The increase in the quadrupole splitting values as the electronegativity of the R group increases for the series of halocarboxylates,  $(\text{CH}_3)_4\text{Sn}_2(\text{O}_2\text{CR})_2$ , is a reflection of the increase in magnitude of  $V_{zz}$ . Since the sign of  $V_{zz}$  is probably negative, the increase in quadrupole splitting is a reflection of a decrease in electron density along the z axis, which contains the O-Sn-O linkage. The increase in length observed for the "short" Sn-O distance in these compounds supports the view that the increase in magnitude of the quadrupole splitting values in the  $(\text{CH}_3)_4\text{Sn}_2(\text{O}_2\text{CR})_2$  series is a direct result of the increase in electron withdrawing power of the R group. Little or no change is observed in the "long" Sn-O bond perhaps because of the added complications of weak hydrogen bonding.

In  $(\text{CH}_3)_4\text{Sn}_2(\text{O}_2\text{CCF}_3)_2$  the methyl hydrogens were located in the electron difference map at  $R_w = 0.047$ , allowing the positional but not the temperature parameters ( $U = 0.08\text{\AA}$ ), to be refined. There are two weak hydrogen bonding interactions present at 3.2\text{\AA} between the oxygen involved in the "long" Sn-O(2) bond and two H(3) atoms of the methyl

groups of the molecule related by a (0,0,1) translation. The interbond angles of the carboxylate group vary in a way which confirms that the bonding at this oxygen is weaker. Although the methyl hydrogen atom positions were not observable in  $(\text{CH}_3)_4\text{Sn}_2(\text{O}_2\text{CCH}_2\text{Cl})_2$ , the hydrogen atom positions of the  $-\text{CH}_2\text{Cl}$  group were deduced from chemical considerations, and corresponded to a peak of  $0.5 \text{ e/\AA}^3$  in the final difference synthesis. The oxygen involved in the "long" Sn-O(2) bond is weakly bonded to one hydrogen atom of one  $-\text{CH}_2\text{Cl}$  group of two other molecules at 3.06Å. The substantial reduction of the Sn-Sn-O(2) angle from  $90^\circ$  to  $86^\circ$  is consistent with such an interaction being present. Unfortunately, the methyl hydrogens were not located in the  $(\text{CH}_3)_4\text{Sn}_2(\text{O}_2\text{CCl}_3)_2$  structure. Presumably, the methyl hydrogens in  $(\text{CH}_3)_4\text{Sn}_2(\text{O}_2\text{CCl}_3)_2$  give rise to a similar interaction causing the asymmetry in the Sn-O distances and a distortion in the interbond angles of the carboxylate group.

The chlorine atoms in  $(\text{CH}_3)_4\text{Sn}_2(\text{O}_2\text{CCl}_3)_2$  lie out of the plane of the C-CO<sub>2</sub> group, whereas in  $(\text{CH}_3)_4\text{Sn}_2(\text{O}_2\text{CCH}_2\text{Cl})_2$  the chlorine atom lies in the C-CO<sub>2</sub> plane. The orientation of the  $-\text{CH}_2\text{Cl}$  group is such as to allow for weak H---O(2) intermolecular interactions. Each O(2) atom has two weak hydrogen bonding interactions of 3.06Å. The increase of the O(2)-C(1)-C(2) angle may be the result of both this weak H---O(2) interaction and the need to minimize the O(2), Cl interactions. Both effects appear to contribute to this distortion since there is no angular distortion in the  $-\text{CCl}_3$  derivative, and all three chlorine atoms lie out of the C-CO<sub>2</sub> plane.

Although the hydrogen atom positions in  $(\text{CH}_3)_4\text{Sn}_2(\text{O}_2\text{CCF}_3)_2$  are well defined, the  $-\text{CF}_3$  groups are either disordered or rotating. The six half-fluorine atoms included in the refinement have temperature factors that indicate an easy rotation. The distribution of electrons is much like a doughnut, centered above and about the C-C axis. Hydrogens H(1) and H(2) can form weak intermolecular hydrogen bonds to the fluorine atoms related by the translations  $(1/2, 1/2, 1)$  and  $(-1/2, 1/2, -1)$ . H(3) interacts with fluorine atoms related by a  $(0, 0, 1)$  translation. In the  $(2, 0, 1)$  plane, the molecules form a layer in which they key into each other, with the H...F interactions providing weak bonding. The ill-defined positions of the fluorine atoms arise from the fact that the three F atoms of the  $-\text{CF}_3$  group interact with four H atoms of methyl groups in neighbouring molecules.

D. Crystal Structure of  $\{[(\text{CH}_3)_2\text{Sn}(\text{O}_2\text{CCF}_3)]\text{O}\}_2$  and  $\{[(\text{CH}_3)_2\text{Sn}(\text{O}_2\text{CCCl}_3)]\text{O}\}_2$

(i) Introduction

Crystals of an unknown product were obtained from the crystallization of  $(\text{CH}_3)_4\text{Sn}_2(\text{O}_2\text{CCF}_3)_2$  from chloroform. Characterization by X-ray analysis was carried out since only a few crystals of the unknown product could be prepared, and spectroscopic analysis of such a minute quantity of material did not seem appropriate. Characterization by single-crystal X-ray analysis showed that these crystals were in fact  $\{[(\text{CH}_3)_2\text{Sn}(\text{O}_2\text{CCF}_3)]\text{O}\}_2$ . Since the crystal and molecular structure of  $\{[(\text{CH}_3)_2\text{Sn}(\text{O}_2\text{CCF}_3)]\text{O}\}_2$  showed some structural similarity to both

$(\text{CH}_3)_4\text{Sn}_2(\text{O}_2\text{CCF}_3)_2$  (this chapter) and  $[\text{Sn(II)Sn(IV)O}(\text{O}_2\text{CCF}_3)_4]_2\text{C}_6\text{H}_5$  (Chapter 6) a detailed analysis of the structure of  $\{[(\text{CH}_3)_2\text{Sn}(\text{O}_2\text{CCF}_3)]_2\text{O}\}_2$  is presented.

(ii) Crystal Structure Data for Di- $\mu_3$ -oxo-bis( $\mu$ -trifluoroacetato- $0,0'$ )-bis(trifluoroacetato)tetrakis[dimethyltin(IV)] and Di- $\mu_3$ -oxo-bis( $\mu$ -trichloroacetato)tetrakis[dimethyltin(IV)]

The complexes  $\{[(\text{CH}_3)_2\text{Sn}(\text{O}_2\text{CCF}_3)]_2\text{O}\}_2$  and  $\{[(\text{CH}_3)_2\text{Sn}(\text{O}_2\text{CCCl}_3)]_2\text{O}\}_2$  were obtained from the crystallization of  $(\text{CH}_3)_4\text{Sn}_2(\text{O}_2\text{CCF}_3)_2$  and  $(\text{CH}_3)_4\text{Sn}_2(\text{O}_2\text{CCCl}_3)_2$  from chloroform. Fibrous, crystalline needles of  $\{[(\text{CH}_3)_2\text{Sn}(\text{O}_2\text{CCF}_3)]_2\text{O}\}_2$  were found to be present in small amounts in the bulk solid product, which consisted of rhombohedral shaped crystals of  $(\text{CH}_3)_4\text{Sn}_2(\text{O}_2\text{CCF}_3)_2$ . When  $(\text{CH}_3)_4\text{Sn}_2(\text{O}_2\text{CCCl}_3)_2$  was recrystallized from  $\text{CHCl}_3$  fibrous, crystalline needles of  $\{[(\text{CH}_3)_2\text{Sn}(\text{O}_2\text{CCCl}_3)]_2\text{O}\}_2$  were the major product.

Suitable crystals of both  $\{[(\text{CH}_3)_2\text{Sn}(\text{O}_2\text{CCCl}_3)]_2\text{O}\}_2$  and  $\{[(\text{CH}_3)_2\text{Sn}(\text{O}_2\text{CCF}_3)]_2\text{O}\}_2$  were selected for X-ray analysis.

The crystallographic work on the  $-\text{CF}_3$  and  $-\text{CCl}_3$  derivatives of  $\{[(\text{CH}_3)_2\text{Sn}(\text{O}_2\text{CR})]_2\text{O}\}_2$  was performed by R. Faggiani and by Dr. I. D. Brown of the Institute for Materials Research of this University. Information on the X-ray intensity measurements and information on the solution and refinement of  $\{[(\text{CH}_3)_2\text{Sn}(\text{O}_2\text{CCF}_3)]_2\text{O}\}_2$  is published elsewhere.<sup>88</sup>

$\{[(\text{CH}_3)_2\text{Sn}(\text{O}_2\text{CCF}_3)]_2\text{O}\}_2$  has the same monoclinic space group,  $C_{2/m}$ , as the parent compound  $(\text{CH}_3)_4\text{Sn}_2(\text{O}_2\text{CCF}_3)_2$ . The crystal data are as follows:  $\{[(\text{CH}_3)_2\text{Sn}(\text{O}_2\text{CCF}_3)]_2\text{O}\}_2$ ,  $M_r = 2 \times 539.4$ , monoclinic space group

Table 4.7

Interatomic Distances (Å) and Angles (°) for  $[(\text{CH}_3)_2\text{Sn}(\text{O}_2\text{CCF}_3)]_2\text{O} \cdot 2$ 

<u>Tin Co-ordination</u>			
(a) Bond Lengths (Å)			
Sn(1)-C(5)	2.104(10)x2	Sn(2)-C(6)	2.107(9)x2
Sn(1)-O(5)	2.039(5)	Sn(2)-O(5)	2.040(4)
Sn(1)-O(5)'	2.137(4)	Sn(2)-O(4)	2.253(5)
Sn(1)-O(1)	2.367(5)	Sn(2)-O(2)	2.215(5)
Sn(1)-O(4)'	2.727(5)	Sn(2)-O(3)*	2.996(6)
		Sn(2)-O(3)	3.164(7)
(b) Bond Angles (°)			
C(5)-Sn(1)-C(5)'	147.5(3)	C(6)-Sn(2)-C(6)'	148.9(2)
C(5)-Sn(1)-O(5)	105.7(2)x2	C(6)-Sn(2)-O(5)	105.9(2)
O(5)'-Sn(1)-C(5)	99.3(2)x2	O(4)-Sn(2)-C(6)	92.9(2)x2
O(5)'-Sn(1)-O(5)	77.5(2)	O(4)-Sn(2)-O(5)	78.9(2)
O(1)-Sn(1)-C(5)	83.7(2)x2	O(2)-Sn(2)-C(6)	89.5(2)x2
O(1)-Sn(1)-O(5)	90.5(2)	O(2)-Sn(2)-O(5)	92.2(2)
O(1)-Sn(1)-O(5)'	168.0(3)	O(4)-Sn(2)-O(2)	171.2(4)
O(4)'-Sn(1)-O(5)'	67.1(2)	O(3)*-Sn(2)-O(4)	64.3(2)
O(4)'-Sn(1)-C(5)	81.5(2)x2	O(3)*-Sn(2)-C(6)	74.6(2)x2
		O(3)-Sn(2)-O(4)	44.1(2)
		O(3)-Sn(2)-C(6)	81.5(1)x2
Sn(1)-O(5)-Sn(1)'	102.5(2)	C(1)-O(1)-Sn(1)	133.0(5)
Sn(1)-O(5)-Sn(2)	136.6(2)	C(1)-O(2)-Sn(2)	137.6(5)
Sn(1)''-O(5)-Sn(2)	120.8(3)	C(3)-O(4)-Sn(2)	115.8(4)
		C(3)-O(4)-Sn(1)'	151.0(4)
		C(3)-O(3)-Sn(2)*	171.9(6)
		C(3)-O(3)-Sn(2)	72.4(5)

..... continued

Table 4.7 continued

## Trifluoroacetate

(a) Bond Lengths ( $\text{\AA}$ )

C(1)-O(1)	1.212(11)	C(3)-O(3)	1.190(9)
C(1)-O(2)	1.213(10)	C(3)-O(4)	1.263(10)
C(1)-C(2)	1.552(11)	C(3)-C(4)	1.541(10)
C(2)-F(1)	1.245(15)	C(4)-F(5)	1.269(21)
C(2)-F(2)	1.291(11)x2	C(4)-F(6)	1.304(13)x2
C(2)-F(3)	1.315(22)	C(4)-F(8)	1.329(10)
C(2)-F(4)	1.262(14)x2	C(4)-F(7)	1.249(16)x2

(b) Bond Angles ( $^{\circ}$ )

O(1)-C(1)-O(2)	130.1(7)	O(3)-C(3)-O(4)	127.7(8)
O(1)-C(1)-C(2)	114.8(8)	O(3)-C(3)-C(4)	117.8(8)
O(2)-C(1)-C(2)	115.1(7)	O(4)-C(3)-C(4)	114.5(7)
C(1)-C(2)-F(1)	115.3(9)	C(3)-C(4)-F(5)	116.0(10)
C(1)-C(2)-F(2)	112.0(6)x2	C(3)-C(4)-F(6)	110.5(7)x2
C(1)-C(2)-F(3)	113.5(10)	C(3)-C(4)-F(8)	113.1(12)
C(1)-C(2)-F(4)	113.0(7)x2	C(3)-C(4)-F(7)	113.4(7)x2
F(1)-C(2)-F(2)	109.1(7)x2	F(5)-C(4)-F(6)	110.3(8)x2
F(2)-C(2)-F(2)'	98.0(9)	F(6)-C(4)-F(6)'	97.7(10)
F(3)-C(2)-F(4)	107.1(9)x2	F(8)-C(4)-F(7)	106.5(10)x2
F(4)-C(2)-F(4)'	102.2(11)	F(7)-C(4)-F(7)'	103.1(12)

..... continued

Table 4.7 continued

Methyl Group

	Bond Lengths (Å)	Bond Angles (°)	Interaction Distance (Å)	Interaction Angles (°)	Interatomic Distance (Å)
	C-H	Sn-C-H	H---F	C-H---F	C---F
C(5)H(1)F(6)	0.95(8)	94(7)	2.62(8)	157(7)	3.50(2)
F(8)			2.77(8)	146(7)	3.60(2)
C(5)H(2)F(2)	0.77(12)	114(10)	2.86(12)	127(10)	3.27(1)
F(3)			2.92(12)	132(10)	3.48(2)
C(5)H(3)F(6)	1.06(18)	87(11)	2.88(16)	110(10)	3.39(1)
C(6)H(4)	0.76(18)				
C(6)H(5)F(4)	1.00(18)	108(15)	2.84(15)	118(10)	3.42(2)
C(6)H(6)F(4)	0.77(20)	118(10)	2.97(57)	120(45)	3.42(2)
F(7)		96(12)	2.98(21)	141(7)	3.62(2)

Prime denotes symmetry-related atom.

Fluorine has the occupancy of half an atom.

\*Intermolecular.

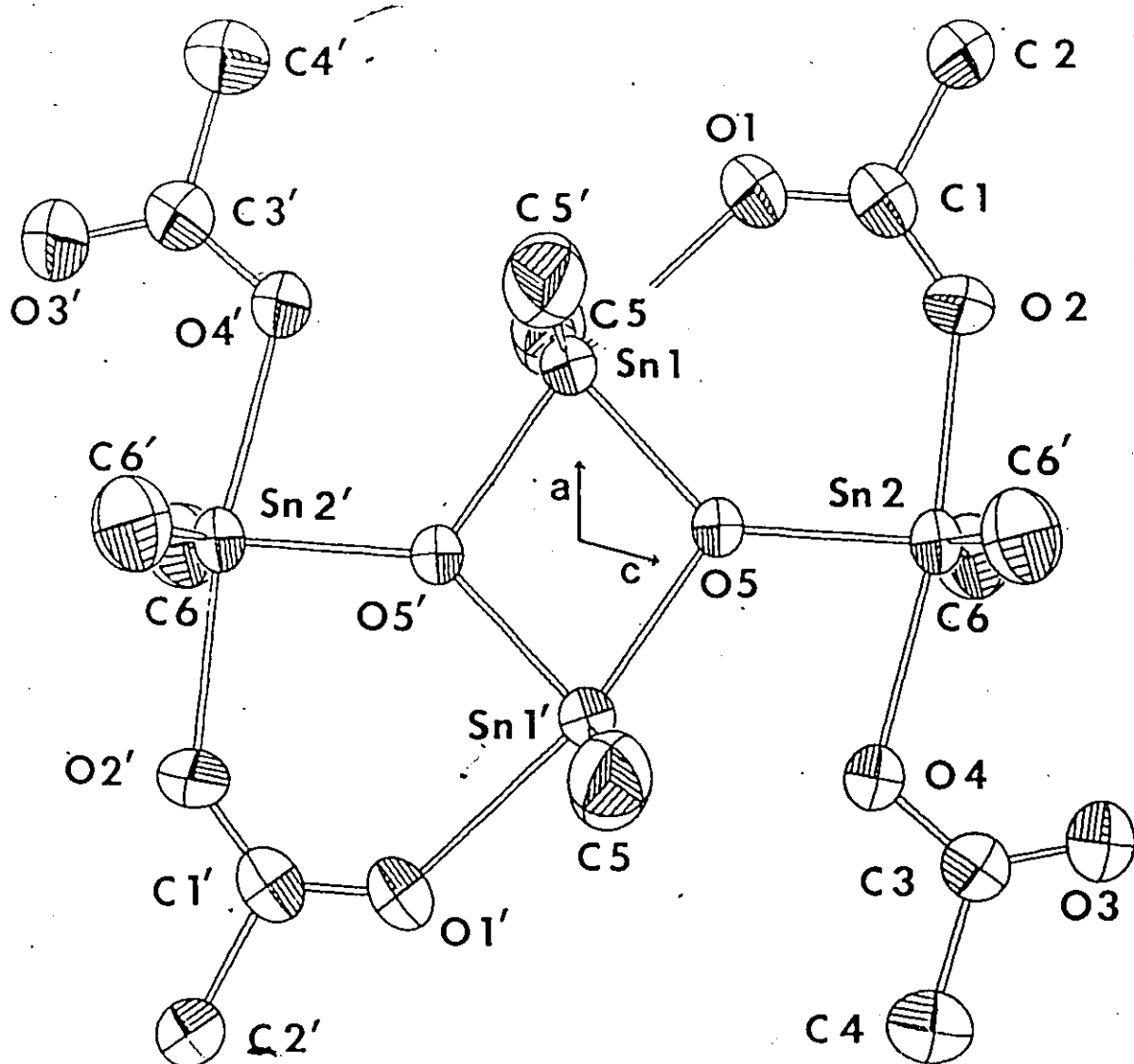


Figure 4.4. A view of  $[(\text{CH}_3)_2\text{Sn}(\text{O}_2\text{CCF}_3)]_2\text{O}_2$  down the  $b$  axis. The hydrogen and fluorine atoms have been omitted for clarity.



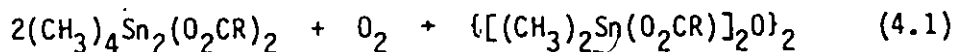
$C_{2/m}$ ,  $a = 16.887(5)$ ,  $b = 8.649(3)$ ,  $c = 11.502(2)$ ,  $\beta = 103.23(2)$ ,  $D_x = 2.19 \text{ g cm}^{-3}$ ,  $Z = 4$ . The structure was refined from X-ray diffractometer measurements to give  $R_w = 0.026$ . The molecular geometry of one dimeric unit is shown in Figure 4.4 with the fluorine and hydrogen atoms being excluded for clarity. The interatomic distances and angles are given in Table 4.7. The packing of the molecule and labelling scheme for non-hydrogen atoms are shown in Figure 4.5.

The final refined structure of  $\{[(CH_3)_2Sn(O_2CCCl_3)]_2O\}_2$  is not yet available. The preliminary data,  $R = 0.08$ , indicate that the molecular structure is similar to that of the  $-CF_3$  derivative.

### (iii) Preparation and Chemical Properties

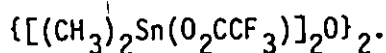
In general, for those reactions giving  $(CH_3)_4Sn_2(O_2CR)_2$  compounds the crude reaction product was purified by washing with warm distilled water. The  $(CH_3)_4Sn_2(O_2CR)_2$  complexes so isolated are white solids and are extremely shelf stable. Some decomposition does occur over periods in excess of one year. However, these impurities can be conveniently removed by washing the solids with distilled water. The stability of the compound in solution which had not been degassed depended on the R group. These reactions can be followed by proton n.m.r. The relative reactivity appeared to vary with the solubilities of these compounds. The solubility at room temperature, mg/ml, in  $CHCl_3$ , decreased from the  $-CCl_3$  to the  $-CH_2Cl$  derivative (427,  $CCl_3$ ; 105,  $CHCl_2$ ; 93,  $CF_3$ ; 26,  $CH_2Cl$ ).

Oxidative insertion reactions are a very common feature of organotin chemistry.<sup>2</sup> The extent of the reaction varies and depends upon the R group.



For example, the  $-\text{CH}_2\text{Cl}$  derivative recrystallizes from chloroform without apparent decomposition, the  $-\text{CF}_3$  with a small amount of decomposition, < 1%, and the  $-\text{CCl}_3$  compound undergoes complete reaction to give the oxo species. Heating a chloroform solution of  $(\text{CH}_3)_4\text{Sn}_2(\text{O}_2\text{CCF}_3)_2$  also results in complete cleavage of the tin-tin bond. A small amount of surface coating on the  $(\text{CH}_3)_4\text{Sn}_2(\text{O}_2\text{CR})_2$  single crystals was also observed to increase with exposure to air, and was attributed to formation of the oxo species.

(iv) Discussion of the Crystal and Molecular Structure of



The molecular geometry of the  $-\text{CF}_3$  and  $-\text{CCl}_3$  derivatives is virtually identical to that of  $\{[(\text{C}_4\text{H}_9)_2\text{Sn}(\text{O}_2\text{CCCl}_3)]_2\text{O}\}_2$ <sup>89</sup> and  $\{[(\text{CH}_2=\text{CH})_2\text{Sn}(\text{O}_2\text{CCF}_3)]_2\text{O}\}_2$ <sup>90</sup>. In  $\{[(\text{CH}_3)_2\text{Sn}(\text{O}_2\text{CCF}_3)]_2\text{O}\}_2$  all atoms, except the methyl groups and two-thirds of the F atoms, lie in the mirror plane, Figure 4.5. Each dimer contains four Sn atoms, of which two are crystallographically distinct. The four tin atoms are held in place by two tridentate oxygen atoms, forming a planar  $\text{Sn}(1)-\text{O} \begin{array}{c} \text{Sn}(2) \\ \text{O}-\text{Sn}(1) \\ \text{Sn}(2) \end{array}$  unit.

The  $\text{Sn}_4\text{O}_2$  unit is not symmetric. The  $\mu_3$  oxygen atom makes two chemically equivalent bonds (2.039, 2.040Å) with Sn(1) and Sn(2), and one slightly longer axial bond to Sn(1)' (2.13Å). The angles subtended at tin in the  $\text{Sn}_2\text{O}_2$  four-membered ring are quite acute, 77.5°, with more open angles of 102.5° at oxygen.

The tin atoms of the same asymmetric unit are also linked by two trifluoroacetates which are quite different. One forms an almost symmetric carboxylate bridge between Sn(1) and Sn(2). The difference in the Sn-O linkage for this bidentate carboxylate, Sn(1)-O(1), 2.367(5)Å; Sn(2)-O(2), 2.215(5)Å; is similar to that observed for  $(\text{CH}_3)_4\text{Sn}_2(\text{O}_2\text{CCF}_3)_2$ , Sn-O(1), 2.319(5)Å; Sn-O(2), 2.345(4)Å; however, the cause of the asymmetry is quite different. Weak hydrogen bonding accounts for the asymmetry in the latter compound whereas in the compound described here, the relative weakness of the Sn(1)-O(1) bond may be related to the fact that O(1) is trans to the very strong Sn(1)-O(5) bond. However, it is interesting to note that in both compounds the trifluoroacetate occupies the axial coordination sites of the two five-coordinate tin atoms, and the average tin-oxygen distances are quite similar,  $\sim 2.30\text{Å}$ . The other trifluoroacetate is very different, and may be regarded primarily as a monodentate group with one strong bond to Sn(2), Sn(2)-O(4), 2.253(50)Å. However, O(4) also bonds to Sn(1), Sn(1)-O(4), 2.727(5)Å, and O(3) forms bonds to Sn(2), Sn(2)-O(3), 3.164(7)Å and to Sn(2) in the adjacent dimer, Sn(2)-O(3), 2.996(4)Å, linking the molecules into chains running along the C axis, Figure 4.5. Each oxygen atom bonds to two tin atoms yielding a very asymmetric species. Support for a monodentate linkage is provided by the C-O distances which are 1.190(9) and 1.263(10)Å. Comparison to those found in  $(\text{CH}_3)_4\text{Sn}_2(\text{O}_2\text{CCF}_3)_2$ , 1.218(12) and 1.251(12)Å, shows they are very similar. The long Sn-O distances, 2.727, 2.996 and 3.164Å, may not be

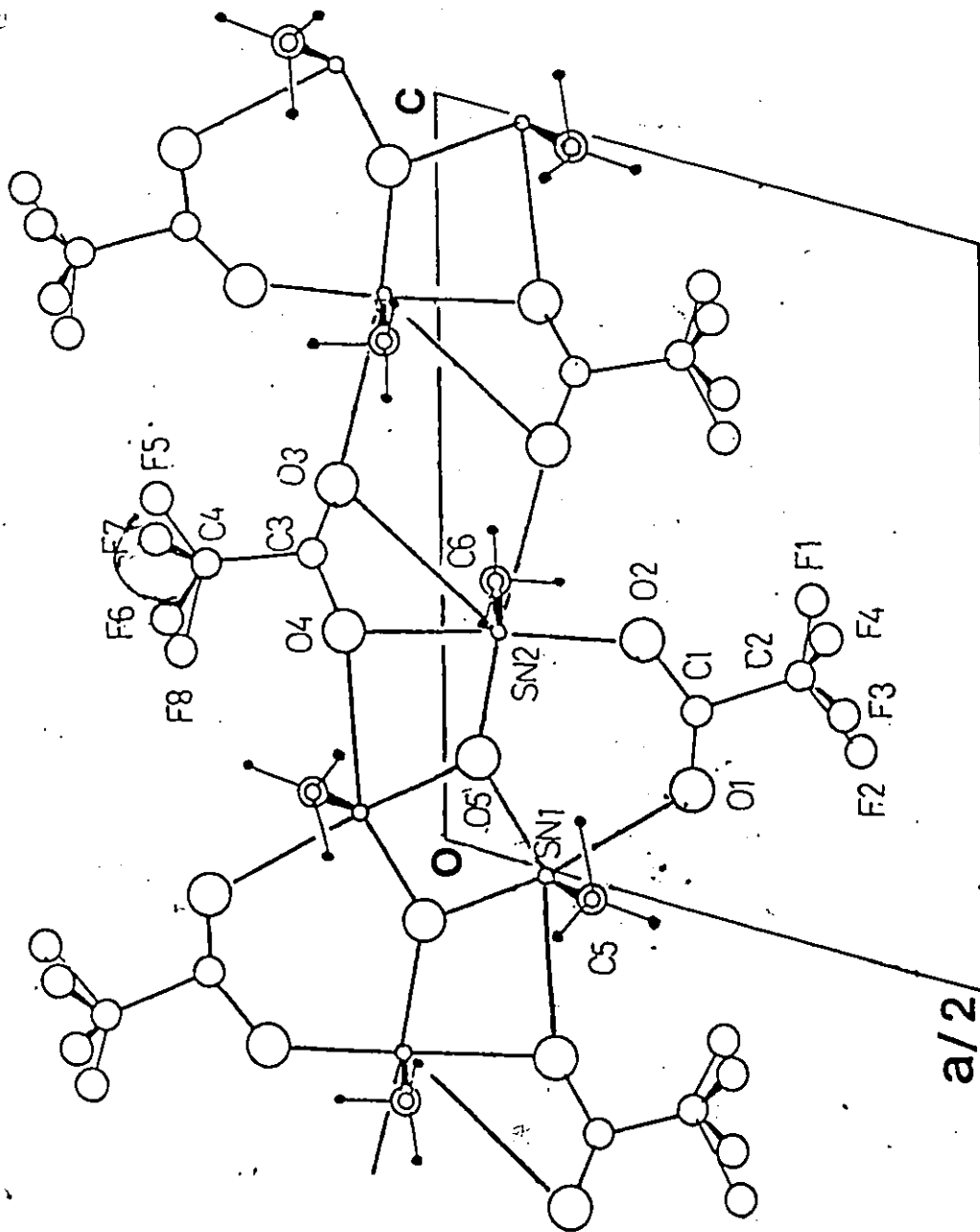


Figure 4.5. Molecular packing of  $[[(\text{CH}_3)_2\text{Sn}(\text{O}_2\text{CCF}_3)_2\text{O}]_2]_2$  as viewed along the  $b$  axis.

The circles represent in decreasing order of size O, F, C and Sn. H atoms are shown as dots.

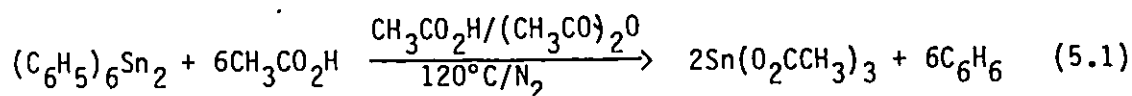
considered as primary bonds but they are much less than the sum of the van der Waals radii, 3.4Å. Inclusion of these into the coordination spheres of the tin atoms increased that of Sn(1) to six, and Sn(2) to coordination number seven.

## CHAPTER FIVE

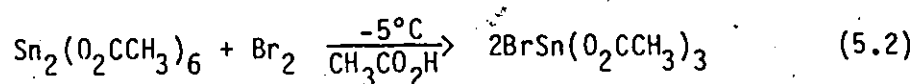
### ACID SOLVOLYSIS OF HEXAPHENYLDITIN AND TETRAPHENYLTIN.

#### A. Introduction

Hexamethylditin has been shown to react with carboxylic acids. Cleavage of the tin-tin bond may occur with formation of the trimethyltin carboxylates, or the tin-tin bond can be preserved and  $(\text{CH}_3)_4\text{Sn}_2(\text{O}_2\text{CR})_2$  complexes are formed. Although the analogous tetraphenylditin carboxylates are known,<sup>63-65,69</sup> this type of product is not isolated from the reaction of hexphenylditin with acetic acid.<sup>91</sup> Hexaphenylditin undergoes complete cleavage of all carbon-tin bonds in acetic acid to produce, quantitatively, a white solid of composition  $\text{Sn}(\text{O}_2\text{CCH}_3)_3$ <sup>91</sup> according to (5.1).



It has been proposed by Wiberg and Behringer,<sup>91</sup> that this compound be formulated as the ditin complex  $\text{Sn}_2(\text{O}_2\text{CCH}_3)_6$ , rather than a simple mixture of  $\text{Sn}(\text{II})(\text{O}_2\text{CCH}_3)_2$  and  $\text{Sn}(\text{IV})(\text{O}_2\text{CCH}_3)_4$ , since it did react stoichiometrically with one mole of  $\text{Br}_2$ , equation (5.2), a reaction characteristic of ditin compounds.<sup>91,64</sup>



The high thermal stability of  $\text{Sn}_2(\text{O}_2\text{CCH}_3)_6$  (m.p.  $> 300^\circ\text{C}$ ) compared to that of  $\text{Sn}(\text{O}_2\text{CCH}_3)_4$  (m.p.  $238^\circ\text{C}$ ) supported this contention. The absorptions in the infrared spectrum of  $\text{Sn}(\text{O}_2\text{CCH}_3)_4$  ( $1710, 1635 \text{ cm}^{-1}$ ) and those of  $\text{Sn}_2(\text{O}_2\text{CCH}_3)_6$  ( $1590, 1510 \text{ cm}^{-1}$ ) also indicated that  $\text{Sn}_2(\text{O}_2\text{CCH}_3)_6$  was not a simple mixture which contained  $\text{Sn}(\text{O}_2\text{CCH}_3)_4$ . The reaction of  $\text{Sn}_2(\text{O}_2\text{CCH}_3)_6$  with  $\text{HCl}$  in ether at  $-100^\circ\text{C}$  produced the expected ditin complex  $\text{Sn}_2\text{Cl}_4(\text{O}_2\text{CCH}_3)_2$ .<sup>91</sup> When this latter compound was reacted with liquid  $\text{HCl}$  at  $-100^\circ\text{C}$ ,  $\text{SnCl}_2$  and  $\text{SnCl}_4$  were produced, but when reacted with one mole of chlorine a mixture of  $\text{SnCl}_4$  and  $\text{SnCl}_2(\text{O}_2\text{CCH}_3)_2$  was obtained.<sup>91</sup>

A structure similar to that established for the tetramethylditin carboxylates with unidentate carboxylate ligands replacing the methyl groups was proposed for  $\text{Sn}_2(\text{O}_2\text{CCH}_3)_6$ .<sup>91</sup> However, little spectroscopic evidence was presented to support this contention, which was based primarily on the "expected" chemical reactivity of tin carboxylates. The interest in the acid solvolysis of hexa-organoditins led to a re-examination of this reaction. It will be shown here that the compound of composition  $\text{Sn}(\text{O}_2\text{CCH}_3)_3$  and the six newly prepared carboxylates of composition  $\text{Sn}(\text{O}_2\text{CR})_3$  are indeed not simple mixtures of tin(II) and tin(IV) carboxylates. The analytical data presented by Wiberg and coworkers for  $\text{Sn}_2(\text{O}_2\text{CCH}_3)_6$  only establish the composition  $\text{Sn}(\text{O}_2\text{CCH}_3)_3$ . The reaction of  $\text{Sn}(\text{O}_2\text{CCH}_3)_3$  with bromine indicates either that a tin-tin bond is present or that the ratio of tin(II) to tin(IV) is one to one. The  $\text{Sn}(\text{O}_2\text{CR})_3$  series could have the following mixed oxidation state tin carboxylate formulations,  $[\text{Sn}(\text{II})\text{Sn}(\text{IV})\text{O}(\text{O}_2\text{CR})_4\text{O}(\text{OCR})_2]_x$ ,

$[\text{Sn(II)Sn(IV)(O}_2\text{CR)}_6]_x$  or  $[\text{Sn(II)Sn(IV)O(O}_2\text{CR)}_4 \cdot 2\text{HO}_2\text{CR}]_x$ . The nature of the bonding, and the possibility of this preparative method as a general route to the preparation of specific mixed oxidation state tin compounds, is of current interest. It will be proposed, based on spectroscopic evidence, that the  $\text{Sn(O}_2\text{CR)}_3$  series is best formulated as  $[\text{Sn(II)Sn(IV)O(O}_2\text{CR)}_4\text{O(OCR)}_2]_2$ .

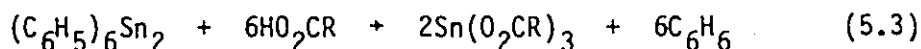
The solvolysis of tetraphenyltin in trifluoroacetic acid at 40°C produces  $\text{Sn(O}_2\text{CCF}_3)_4$  as a minor product.<sup>92</sup> The infrared spectrum of the solid has a carbonyl absorption at  $1750 \text{ cm}^{-1}$ .<sup>92</sup> The tin(IV) haloacetate,  $\text{Sn(O}_2\text{CCH}_2\text{Cl)}_4$  was reported to be a black solid and  $\text{Sn(O}_2\text{CCHCl}_2)_4$  to be a brown viscous liquid.<sup>93</sup> These halo-acetates have been prepared by the transacylation reaction of  $\text{Sn(O}_2\text{CCH}_3)_4$  with the appropriate chloroacetic acid.<sup>93</sup> Characterization was based on the stoichiometry of this reaction with the halo-acetic acids, and % tin content of the final product.<sup>93</sup> The infrared spectrum of  $\text{Sn(O}_2\text{CCHCl)}_4$  and that of  $\text{Sn(O}_2\text{CCHCl}_2)_4$  show an absorption around  $1700 \pm 24 \text{ cm}^{-1}$  which was assigned to unidentate carboxylate groups.<sup>93</sup> In addition, the infrared spectrum of  $\text{Sn(O}_2\text{CCHCl}_2)_4$  showed absorptions around 1550 and  $1450 \text{ cm}^{-1}$  which were assigned to bidentate carboxylate ligands.<sup>93</sup> The solvolysis of tetraphenyltin in halo-acetic acids was investigated to establish the major product in these solvolysis reactions.



## B. Results and Discussion

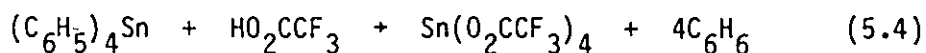
### (i) Preparation and Chemical Properties

Hexaphenylditin reacts with a wide range of carboxylic acids,  $\text{RCO}_2\text{H}$ , where  $\text{R} = \text{CF}_3, \text{C}_3\text{F}_7, \text{CCl}_3, \text{CHCl}_2, \text{CH}_2\text{Cl}, \text{CH}_3$  and  $\text{C}(\text{CH}_3)_3$ , to produce compounds with an empirical formula  $\text{Sn}(\text{O}_2\text{CR})_3$  according to:



No other products were detected by  $^1\text{H}$  n.m.r. or by  $^{119}\text{Sn}$  Mössbauer spectroscopy. These reactions apparently produced only one tin product, namely  $\text{Sn}(\text{O}_2\text{CR})_3$ , generally as a white solid, in high yield. The reaction of hexaphenylditin with the stronger carboxylic acids, ( $\text{pK}_a < 1.48$ ),  $\text{R} = \text{CF}_3, \text{CF}_3(\text{CF}_2)_2, \text{CCl}_3, \text{CHCl}_2$ , proceeds smoothly in evacuated vessels at ambient temperature without any apparent gas evolution. The lack of gaseous evolution, together with a product of composition  $\text{Sn}(\text{O}_2\text{CR})_3$ , rules out homolytic cleavage of the tin-tin bond, as has been observed for other organoditin compounds. The weaker carboxylic acids ( $\text{pK}_a > 2.85$ )  $\text{R} = \text{C}(\text{CH}_3)_3, \text{CH}_3$  and  $\text{CH}_2\text{Cl}$ , did not react at room temperature based on  $^{119}\text{Sn}$  Mössbauer spectroscopy of the reaction mixtures. The reaction did proceed to completion at  $80^\circ\text{C}$  for  $\text{CH}_2\text{ClCO}_2\text{H}$ , and  $100^\circ\text{C}$  for both  $\text{CH}_3\text{CO}_2\text{H}$  and  $(\text{CH}_3)_3\text{CCO}_2\text{H}$ . More vigorous conditions with the lower acidity carboxylic acids was expected based on an electrophilic Sn-C bond cleavage mechanism, and on comparable reactions of  $(\text{C}_6\text{H}_5)_4\text{Sn}$  and  $(\text{CH}_2\text{CH})_4\text{Sn}$  with aliphatic carboxylic acids.<sup>76</sup>

For comparative purposes tetraphenyltin was reacted with halocarboxylic acids under similar conditions. Trifluoroacetic acid produced  $\text{Sn}(\text{O}_2\text{CCF}_3)_4$  as the major product.



The other halocarboxylic acids used in this study based on  $^{119}\text{Sn}$  Mössbauer spectroscopy of the reaction mixture, afforded  $\text{Sn}(\text{O}_2\text{CR})_4$  as the only tin-containing product.

Both hexaphenylditin and tetraphenyltin react with complete cleavage of all carbon-tin bonds with high acid strength carboxylic acids ( $\text{pK}_a < 2.85$ ). However with the weaker carboxylic acids no C-Sn cleavage occurs at room temperature.

The contrast in the high solubility of  $\text{Sn}(\text{IV})(\text{O}_2\text{CCF}_3)_4$  and  $\text{Sn}(\text{IV})(\text{O}_2\text{CCCl}_3)_4$  in the reaction medium compared to the low solubility of the analogous  $\text{Sn}(\text{O}_2\text{CR})_3$  compounds, suggests that the latter are not simple mixtures containing tin(II) and tin(IV) carboxylates. This could only be confirmed for the solid trifluoroacetate derivatives. Whereas  $\text{Sn}(\text{O}_2\text{CCF}_3)_4$  appeared to be almost infinitely soluble in both benzene and trifluoroacetic acid,  $\text{Sn}(\text{O}_2\text{CCF}_3)_3$  did not dissolve to any appreciable extent. The compound  $\text{Sn}(\text{O}_2\text{CCF}_3)_3$  must be regarded as a unique compound.

Several of the  $\text{Sn}(\text{O}_2\text{CR})_3$  compounds dissolve in carboxylic acid anhydrides, other than that of the parent acid from which the compound was derived. Decomposition reactions were apparent, evidenced by the development of a deep red colour for the  $-\text{CH}_3$  derivative in trifluoroacetic anhydride, and also for the  $-\text{CF}_3$  derivative in acetic anhydride.

The carbon-13 n.m.r. data for these reaction mixtures, and that of the  $-\text{CCl}_3$  derivative in acetic anhydride, are presented in Table 5.1. The methyl  $^{13}\text{C}$  n.m.r. region of both the  $-\text{CF}_3$  and  $-\text{CCl}_3$  mixed oxidation state tin carboxylates in acetic anhydride consists of three peaks: a high intensity signal assigned to free acetic anhydride, and two lower, almost equal intensity signals corresponding to bound anhydride or to acetate ligands attached to tin. The  $-\text{CF}_3$  derivative also has two sets of peaks which may be assigned to two types of  $\text{CF}_3$  groups. However, whether these peaks are from trifluoroacetate bound to tin or to an exchange product is not clear. The  $-\text{CH}_3$  derivative in trifluoroacetic anhydride has similar features in the  $^{13}\text{C}$  n.m.r. spectra. These spectra are consistent with the coordination of anhydride to tin or to exchange of carboxylate groups attached to tin with the anhydrides.

In general, polar solvents dissolve these compounds with subsequent decomposition. No non-polar solvents were found for these compounds thereby preventing a detailed n.m.r. study of these compounds in solution.

All of the tin carboxylates were analyzed for both total tin (as  $\text{SnO}_2$ ), and percentage acid ligand. The percentage acid ligand is based on the quantitative base hydrolysis of the tin carboxylate in standard aqueous hydroxide solution. The relative consistency of the results tabulated in Table 2.1 for mixed oxidation state carboxylates, and the data presented in the experimental section of this work for tin carboxylates, suggest that this is a reasonable technique for the analysis of these compounds.

Table 5.1.  $^{13}\text{C}$  N.M.R. Data for  $\text{Sn}(\text{O}_2\text{CR})_3$  in a Solution of  $(\text{RCO})_2\text{O}$  and  $\text{C}_6\text{D}_6$

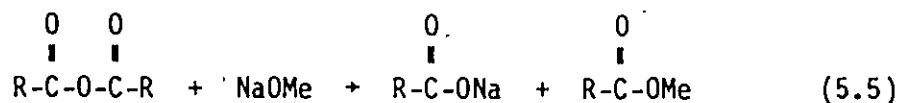
Sample Solution <sup>b</sup>	Chemical Shift $^{13}\text{C}$ (T.M.S. = 0)		Coupling Constant (Hz)
	Group = ( $\text{CH}_3\text{CO}-$ ) $\delta_{\text{CH}_3}$	Group = ( $\text{CF}_3\text{CO}-$ ) $\delta_{\text{CF}_3}$	
$\text{Sn}(\text{O}_2\text{CCH}_3)_3$ (1.7)	$(\text{CF}_3\text{CO})_2\text{O}$ (7.1)	$\delta_{\text{CO}}$ 199.7	$\delta_{\text{CO}}$ 149.7
		$\delta_{\text{CO}}$ 20.2	$\delta_{\text{CO}}$ 113.6
$\text{Sn}(\text{O}_2\text{CCF}_3)_3$ (0.9)	$(\text{CH}_3\text{CO})_2\text{O}$ (5.3)	$\delta_{\text{CO}}$ 166.6	$\delta_{\text{CO}}$ 161.3
		$\delta_{\text{CO}}$ 20.5	$\delta_{\text{CO}}$ 114.3
		$\delta_{\text{CO}}$ 18.1	$\delta_{\text{CO}}$ 162.3
$\text{Sn}(\text{O}_2\text{CCCl}_3)_3^b$ (0.4)	$(\text{CH}_3\text{CO})_2\text{O}$ (5.3)	$\delta_{\text{CO}}$ 166.4	$\delta_{\text{CO}}$ 152.6
		$\delta_{\text{CO}}$ 20.5	$\delta_{\text{CO}}$ 114.3
		$\delta_{\text{CO}}$ 17.9	$\delta_{\text{CO}}$ 163.1
			$J_{^{13}\text{C}-^{19}\text{F}}$
			$J_{^{13}\text{C}-^{19}\text{F}}$
			$J_{^{13}\text{C}-^{19}\text{F}}$

<sup>a</sup>In approximately 2.0 to 2.5 g of  $\text{C}_6\text{D}_6$ .

<sup>b</sup>No signals observed for a  $(\text{CCl}_3\text{CO}-)$  group.

<sup>c</sup>The mmoles of  $\text{Sn}(\text{O}_2\text{CR})_3$  and  $(\text{RCO})_2\text{O}$  is given in parentheses.

The total tin, percentage acid ligand, and standard carbon, hydrogen and halogen analysis indicate that the compounds prepared are of composition  $\text{Sn}(\text{O}_2\text{CR})_3$ . However, it is not possible to distinguish between the two possible formulations,  $[\text{Sn}(\text{II})\text{Sn}(\text{IV})(\text{O}_2\text{CR})_6]_x$  and  $[\text{Sn}(\text{II})\text{Sn}(\text{IV})\text{O}(\text{O}_2\text{CR})_4\text{O}(\text{OCR})_2]_x$ , for the mixed oxidation state tin carboxylates. Attempts to analyze the percentage anhydride present by titration with standard NaOMe in tetrahydrofuran with phenolphthalein as an indicator were unsuccessful. This technique is well established for the analysis of anhydrides,<sup>94</sup> and is based on the reaction of NaOMe with anhydride according to (5.5).



$[\text{Sn}(\text{II})\text{Sn}(\text{IV})\text{O}(\text{O}_2\text{CR})_4\text{O}(\text{OCR})_2]_x$  should react with five moles of NaOMe, whereas  $[\text{Sn}(\text{II})\text{Sn}(\text{IV})(\text{O}_2\text{CR})_6]_x$  would be expected to react with six moles of NaOMe. The ratio of the number of moles of NaOMe per mole of mixed oxidation state compound were found to be:  $\text{CF}_3$ , 5.89, 6.61;  $\text{C}(\text{CH}_3)_3$ , 6.54;  $\text{CH}_3$ , 6.29; clearly inconsistent with either formulation. However, the ratio was found to be 4.05 for  $\text{Sn}(\text{IV})(\text{O}_2\text{CF}_3)_4$ , which suggests that the esters formed during the reaction with the mixed oxidation state compounds are not undergoing hydrolysis. It is possible that some other reaction involving Sn(II) interferes with this type of analysis. The results neither confirm nor disprove the presence or absence of anhydrides in the mixed oxidation state tin carboxylates.

The melting points and/or decomposition points of the  $\text{Sn}(\text{O}_2\text{CCR})_3$  series are presented in Chapter 2, Table 2.1. These temperatures are much higher than for the corresponding tin(IV) carboxylates:

$\text{Sn}(\text{O}_2\text{CCH}_3)_4$ , 238°C;<sup>91</sup>  $\text{Sn}(\text{O}_2\text{CCHCl}_2)_4$ , < 25°C;<sup>93</sup>  $\text{Sn}(\text{O}_2\text{CCF}_3)_4$ , 112°C.<sup>92</sup>

These temperatures suggest that  $\text{Sn}(\text{O}_2\text{CCH}_3)_3$ ,  $\text{Sn}(\text{O}_2\text{CCHCl}_2)_3$  and  $\text{Sn}(\text{O}_2\text{CCF}_3)_3$  are unique compounds. Unfortunately similar data for the other tin(IV) carboxylates are not available.

(ii) Tin-119 Mössbauer Data

The tin-119 Mössbauer data for the  $\text{Sn}(\text{O}_2\text{CR})_3$  series are presented in Table 5.2. Typical spectra of the trifluoroacetate and acetate derivatives are shown in Figures 5.1 and 5.2, respectively. It is immediately apparent from these spectra that there is more than one tin environment. Careful analysis of the spectra in terms of peak positions, line widths and relative areas, leads to the conclusion that these spectra arise from a tin(IV) in a slightly distorted environment and a tin(II) in a very distorted environment.

The tin-119 Mössbauer data for the tin(IV) carboxylates prepared in this study together with literature data for the tin(II) carboxylates<sup>95</sup> and tin(IV) tetra-acetate,<sup>96</sup> are presented in Table 5.2. Careful comparison of these data with those of the  $\text{Sn}(\text{O}_2\text{CR})_3$  series indicate that the latter cannot be simple mixtures of tin(II) and tin(IV) carboxylates.

Table 5.2

 $^{119}\text{Sn}$  Mössbauer Data for  $\text{Sn}(\text{O}_2\text{CR})_3$ ,  $\text{Sn}(\text{O}_2\text{CR})_4$  and Related Tin Compounds

Compound	Temp. K	$\delta$			Relative Area Sn(IV)/Sn(II)	$\chi^2/\text{degree}$ of freedom
		$\delta$ $\text{mm s}^{-1}$	$\delta$	$\Gamma$		
$\text{Sn}(\text{O}_2\text{CCF}_3)_3$	77	-0.03 3.94	-0.52 1.11	0.81 0.85	1.16	1.01
	4	-0.02 3.93	0.52 1.20		0.91	1.15
$\text{Sn}(\text{O}_2\text{CCF}_3)_4$	77	-0.04	1.56	0.95		0.91
$\text{Sn}(\text{O}_2\text{CCF}_3)_2^{95}$	77	3.16	1.76			
$\text{Sn}(\text{O}_2\text{CC}_3\text{F}_7)_3$	77	-0.03 3.88	- 1.14	0.96 0.84	1.13	1.08
	77	0.03	1.27	0.97		1.00
$\text{Sn}(\text{O}_2\text{CCCl}_3)_3$	77	-0.01 3.98	- 1.05	0.97 0.95	1.22	1.24
	77	0.15	0.91	0.96		1.04
$\text{Sn}(\text{O}_2\text{CCCl}_3)_2^{95}$	77	3.29	1.78			
$\text{Sn}(\text{O}_2\text{CCHCl}_2)_3$	77	0.07 3.80	0.54 1.81	0.95 1.09	1.31	1.23
	77	-0.01	0.79	1.04		0.96
$\text{Sn}(\text{O}_2\text{CCHCl}_2)_2^{95}$	77	3.48	1.64			
$\text{Sn}(\text{O}_2\text{CGH}_2\text{Cl})_3$	77	0.13 3.56	0.79 1.71	0.98 1.11	1.25	1.17
	77	0.29	0.55	1.13		1.17
$\text{Sn}(\text{O}_2\text{CCH}_2\text{Cl})_2^{95}$	77	3.10	1.66			
$\text{Sn}(\text{O}_2\text{CCH}_3)_3$	77	0.14 3.48	0.47 1.83	0.90 0.85	0.68	1.06
	4	0.20 3.49	0.45 1.83	0.89 0.91	0.75	0.97
$\text{Sn}(\text{O}_2\text{CCH}_3)_4^{96}$	77	0.08	-	1.45		
$\text{Sn}(\text{O}_2\text{CCH}_3)_2^{95}$	77	3.31	1.77			
$\text{Sn}(\text{O}_2\text{CC}(\text{CH}_3)_3)_3$	77	0.18 3.32	0.50 2.20	0.83 0.83	0.74	1.12
	77	3.25	1.88			
$[\text{Sn}_2\text{O}(\text{O}_2\text{CR})_4 \cdot \text{THF}]_2^{105}$	77	0.07 3.60	- 1.82	1.18 0.85	1.36	

 $\text{R} = (\text{o-NO}_2)\text{C}_6\text{H}_4$ 

\*Excess acid present in product, see Chapter 2.

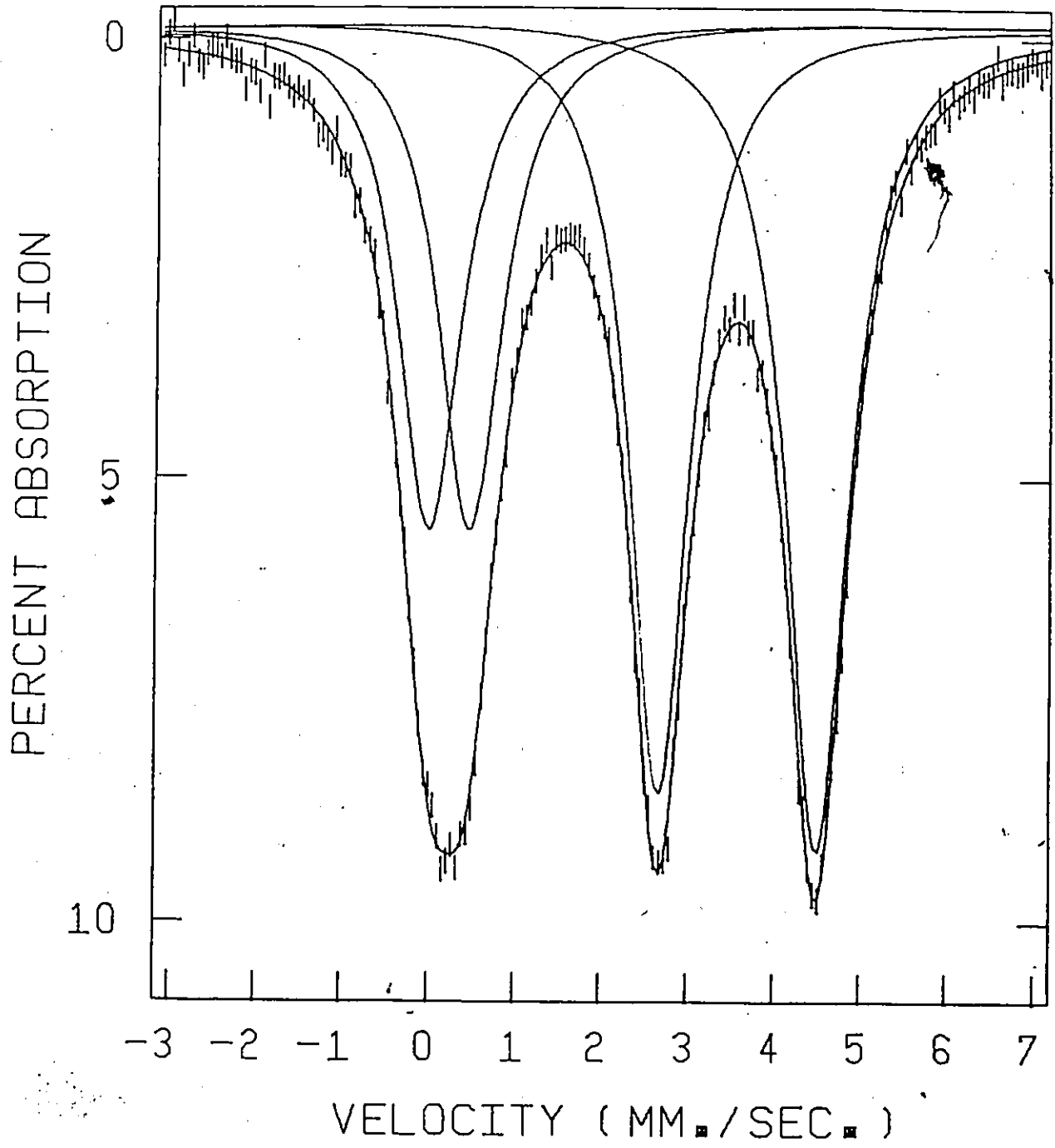


Figure 5.1.  $^{119}\text{Sn}$  Mössbauer spectrum of  $\text{Sn}(\text{O}_2\text{CCH}_3)_3$  at  $77^\circ\text{K}$ .



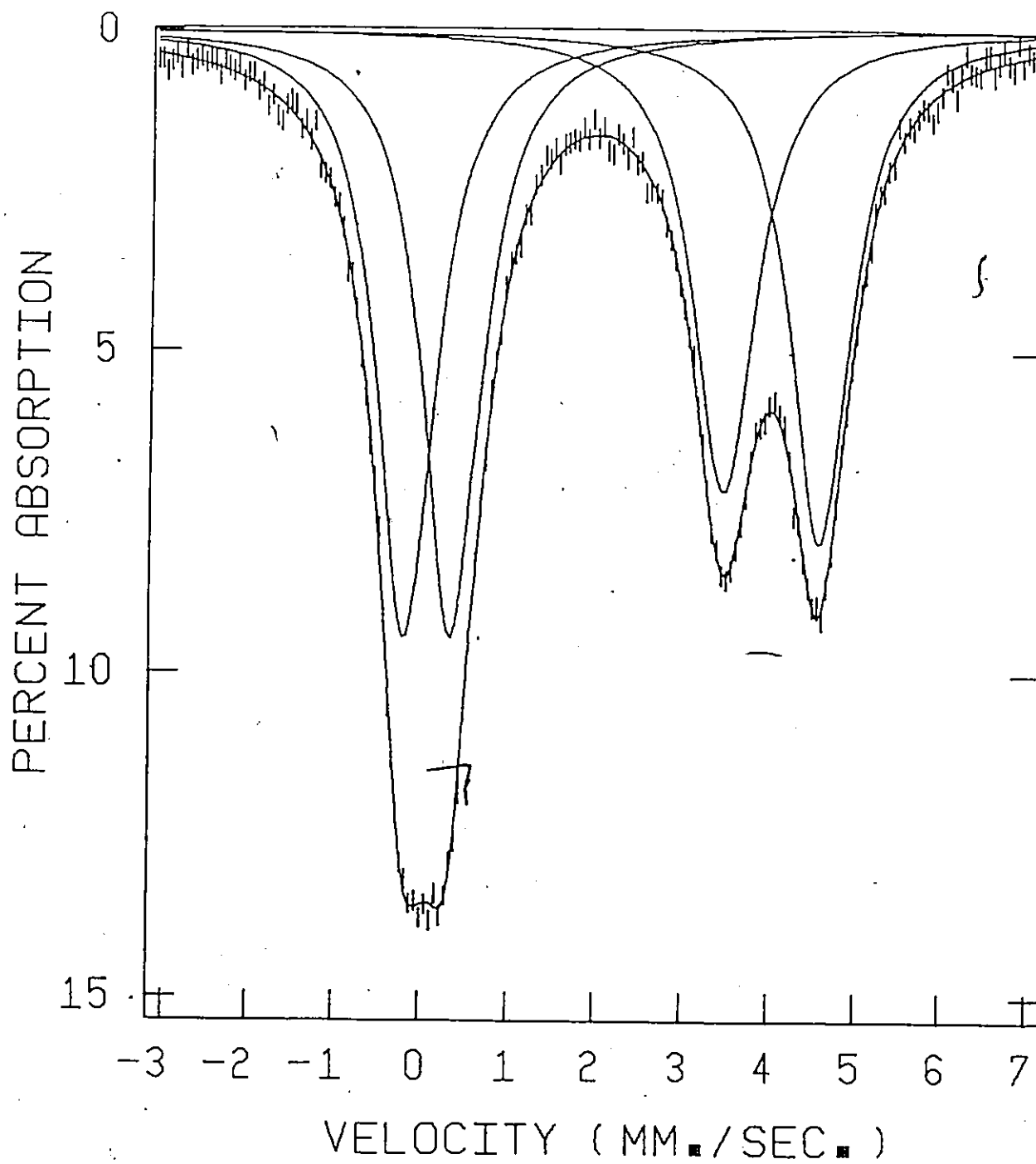


Figure 5.2.  $^{119}\text{Sn}$  Mössbauer spectrum of  $\text{Sn}(\text{O}_2\text{CCF}_3)_3$  at  $77^\circ\text{K}$ .

## (iii) Tin(II) Mössbauer Region

The Mössbauer spectra of the tin(II) carboxylates and the tin(II) region of the mixed oxidation state tin carboxylates are similar in appearance. Both series show spectra consisting of well resolved quadrupole doublets, but with the isomer shifts, and in some cases the quadrupole splittings, being quite different. The isomer shift, and therefore the s-electron density at the tin nucleus observed for the tin(II) sites in the mixed oxidation state tin carboxylates are significantly larger than those reported for the tin(II) carboxylates, and this difference increases from the acetate to the trihaloacetate.

The quadrupole splittings for both series of compounds are very similar for the  $-\text{CH}_3$ ,  $-\text{CH}_2\text{Cl}$  and  $-\text{CHCl}_2$  carboxylates, however a marked decrease in quadrupole splittings, of  $\sim 0.7 \text{ mm s}^{-1}$ , is observed for the tin(II) site of the mixed oxidation state tin carboxylates of the trichloro- and trifluoroacetates compared to the analogous tin(II) compound. It should be pointed out that several of the tin(II) carboxylates have not been isolated pure but their spectra were recorded as frozen solutions in the parent acids.<sup>95</sup> In the solid state, the structures of these compounds, and hence their Mössbauer parameters, may be quite different, although control experiments would seem to rule out this possibility.<sup>95</sup>

Unlike the tin(II) carboxylates, the Mössbauer parameters for the tin(II) site in the mixed oxidation state tin compounds do change in a systematic manner as R is varied. The isomer shift increases (3.32 to  $3.93 \text{ mm s}^{-1}$ ), while the quadrupole splittings decrease (2.20 to

1.05 mm s<sup>-1</sup>), from the trimethylacetate to the trihaloacetate compounds. In fact, a reasonably smooth correlation exists between isomer shift and quadrupole splitting, with the exception of the dichloroacetate compound which deviates slightly from the "least squares line", Figure 5.3. The data for the tin(II) site in the dichloroacetate compound may be slightly in error since the spectrum of this compound was rather poorly resolved in the tin(II) region, perhaps due to an impurity. There is a definite increase in isomer shift and hence in s-electron density, as the electronegativity of the R group of the carboxylate ligand is increased. At the same time, the electron distribution about the tin(II) site is becoming more symmetric, which is reflected by a smaller quadrupole splitting.

The isomer shift of the tin(II) site in these compounds appears to be quite sensitive to the type of R group. The isomer shift (s electron density) is plotted against the ionization constant of the parent acid,<sup>97</sup> in Figure 5.4, the pK<sub>a</sub> being a measure of the inductive effect or the electronegativity of the R group.<sup>98</sup> From the least electronegative ligand, R = C(CH<sub>3</sub>)<sub>3</sub>, to the most electronegative ligand, R = CF<sub>3</sub>, the isomer shift increases by 0.62 mm s<sup>-1</sup>. The isomer shift of the tin(II) site in these compounds is plotted against the Taft inductive factor, σ\*,<sup>98</sup> Figure 5.5, and again an essentially linear correlation is found. The linear correlation is significant in establishing that inductive effects are important in determining the trend in isomer shifts for these compounds.

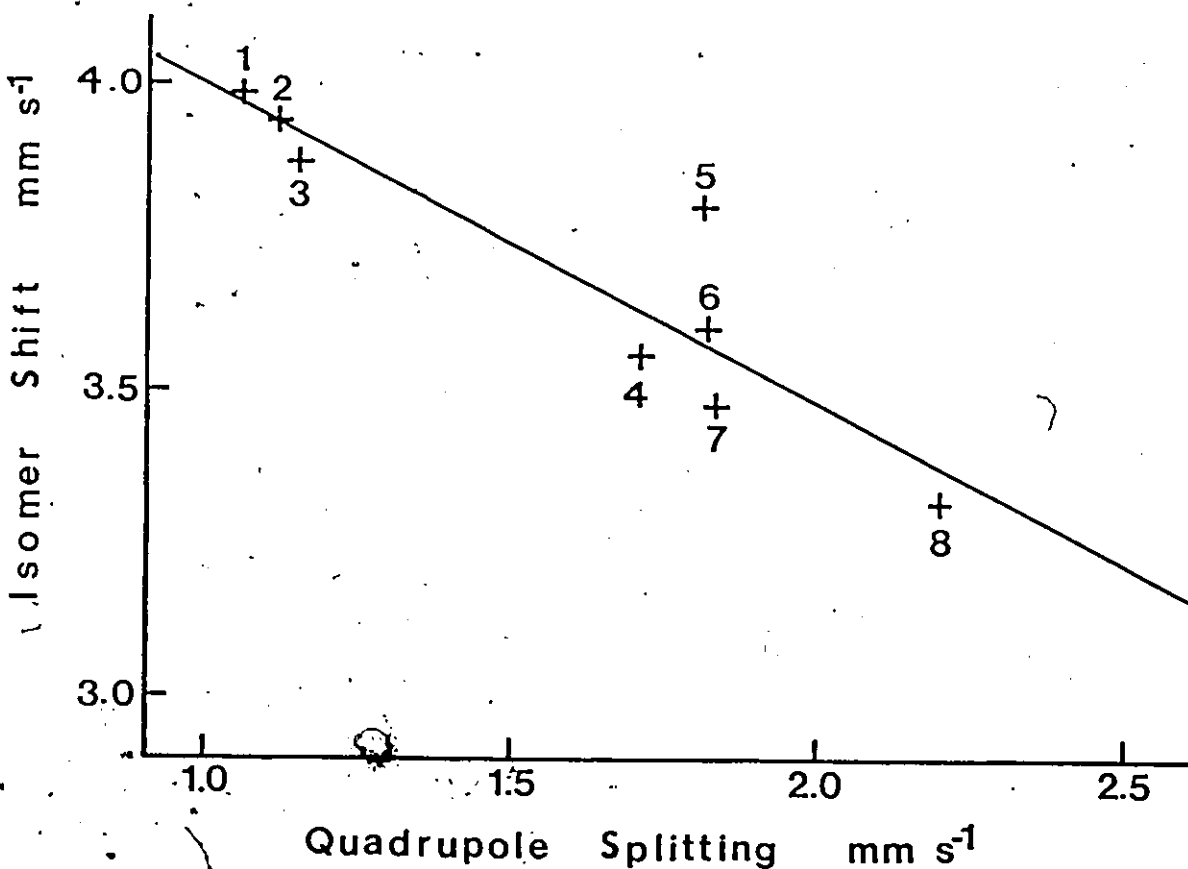


Figure 5.3. A plot of the isomer shift of the tin(II) site versus the quadrupole splitting of this site for the series  $\text{Sn}(\text{O}_2\text{CR})_3$ : 1,  $\text{R}=\text{CCl}_3$ ; 2,  $\text{R}=\text{CF}_3$ ; 3,  $\text{R}=\text{C}_3\text{F}_7$ ; 4,  $\text{R}=\text{CH}_2\text{Cl}$ ; 5,  $\text{R}=\text{CHCl}_2$ ; 7,  $\text{R}=\text{CH}_3$ ; 8,  $\text{R}=\text{C}(\text{CH}_3)_3$ . The line drawn is the best least squares fit to the data.  $[\text{Sn}(\text{II})\text{Sn}(\text{IV})\text{O}(\text{O}_2\text{CR})_4 \cdot \text{THF}]_2$ : 6,  $\text{R}=(\text{o}-\text{NO}_2)\text{C}_6\text{H}_4$  is included in the best least squares fit to the data.

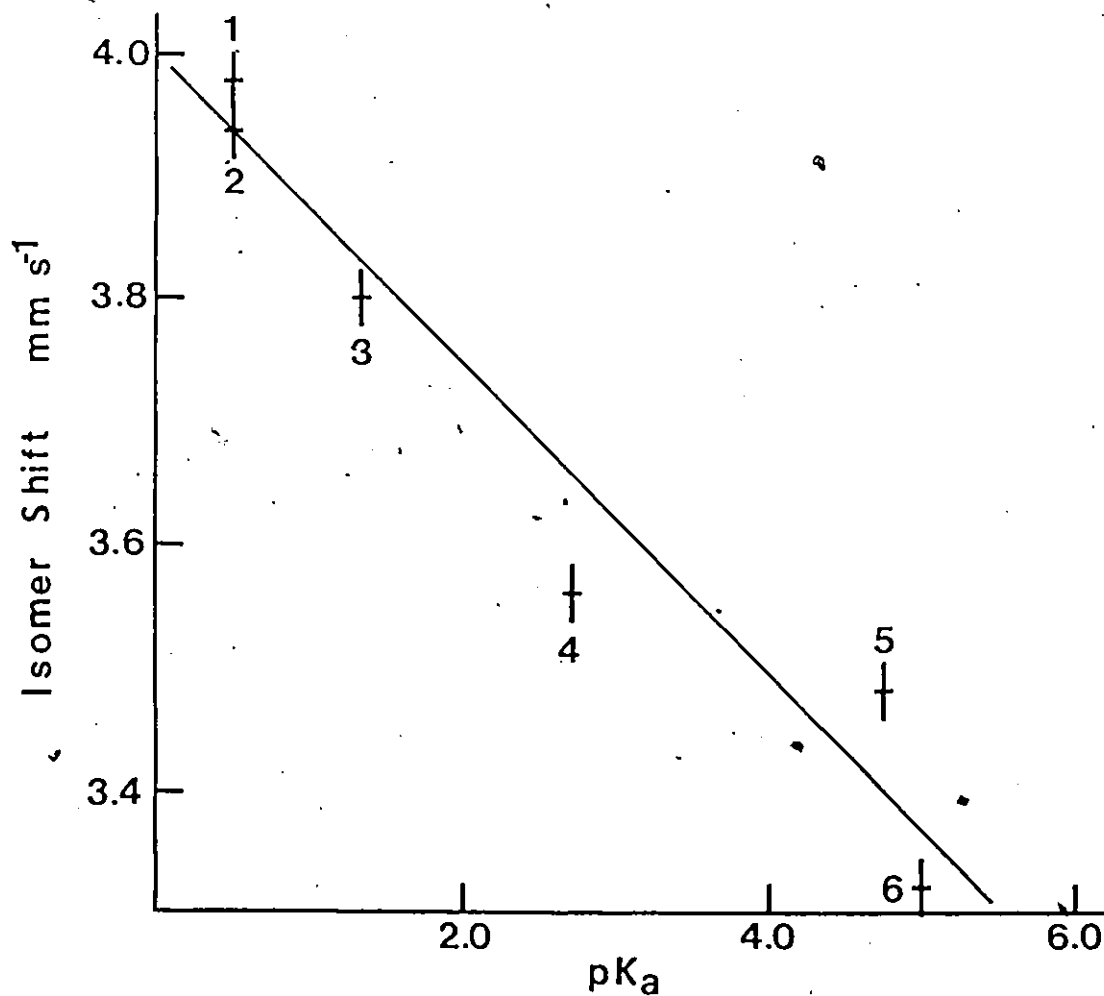


Figure 5.4. A plot of the isomer shift of the tin(II) site against the  $pK_a^{97}$  of the acid for the series  $Sn(O_2CR)_3$ :  
 1,  $R=CCl_3$ ; 2,  $R=CF_3$ ; 3,  $R=CHCl_2$ ; 4,  $R=CH_2Cl$ ; 5,  $R=CH_3$ ;  
 6,  $R=C(CH_3)_3$ . The line drawn is the best least squares fit to the data.

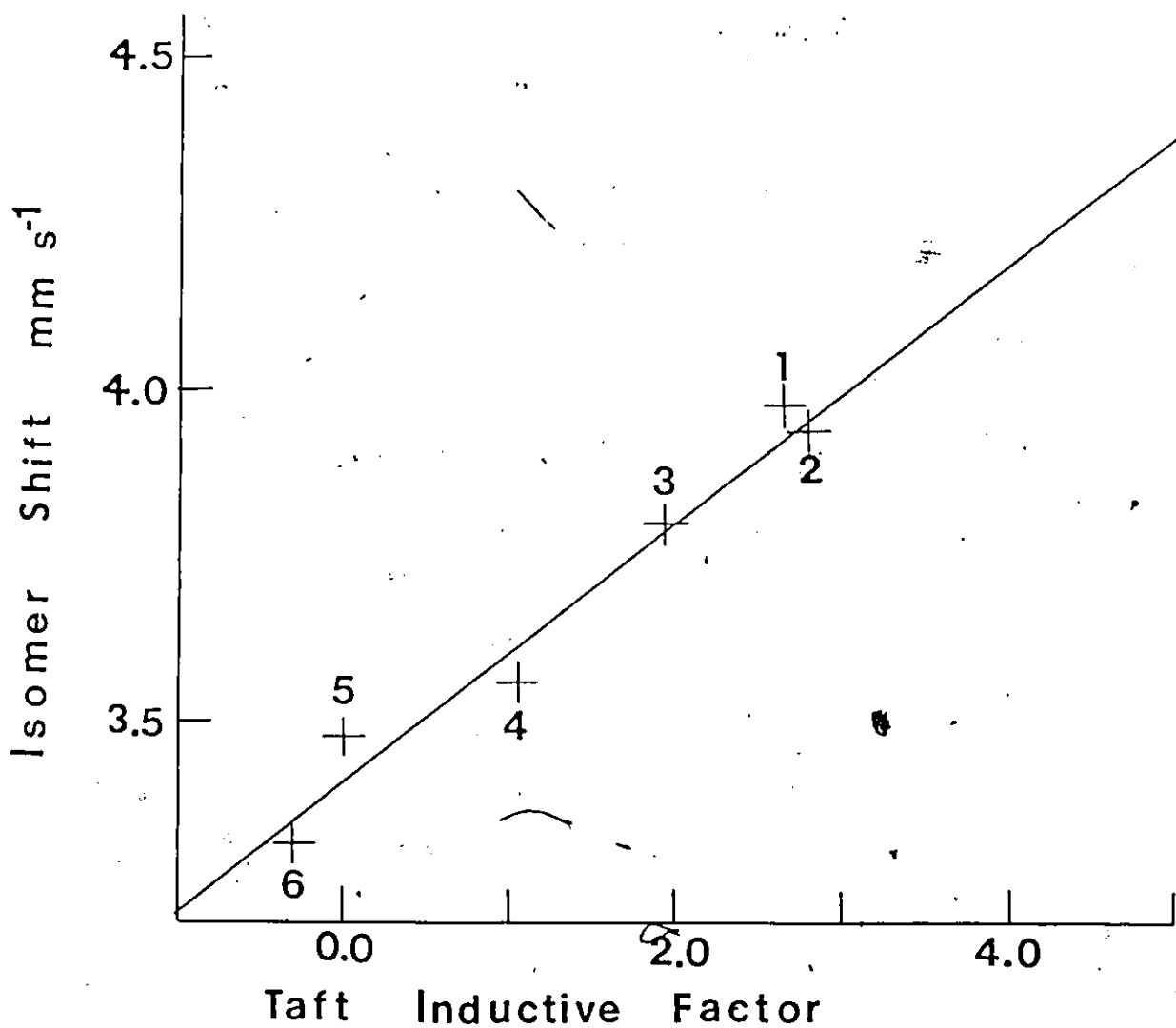


Figure 5.5. A plot of the isomer shift of the tin(II) site against the Taft inductive factor  $\sigma^*$ <sup>98</sup> of the R groups for the series  $\text{Sn}(\text{O}_2\text{CR})_3$ : 1, R=CCl<sub>3</sub>; 2, R=CF<sub>3</sub>; 3, R=CHCl<sub>2</sub>; 4, R=CH<sub>2</sub>Cl; 5, R=CH<sub>3</sub>; 6, R=C(CH<sub>3</sub>)<sub>3</sub>. The line drawn is the best least squares fit to the data.

The similar Mössbauer parameters for the tin(II) site in the mixed oxidation state tin carboxylates, and the correlation between the isomer shift and quadrupole splittings with increasing electronegativity of the R group, strongly suggests that the same geometry persists throughout this series of compounds, with only small changes in bonding occurring to cause the observed variation in Mössbauer parameters.

The  $^{119}\text{Sn}$  Mössbauer parameters of a series of tin(II) bis( $\beta$ -ketoenolates),  $\text{Sn}(\text{OCRCHCR}'\text{O})_2$  ( $R = R' = \text{CH}_3$ :  $\delta = 3.10 \text{ mm s}^{-1}$ ,  $\Delta = 2.02 \text{ mm s}^{-1}$ ;  $R = \text{CH}_3$ ,  $R' = \text{CF}_3$ :  $\delta = 3.40 \text{ mm s}^{-1}$ ,  $\Delta = 1.87 \text{ mm s}^{-1}$ ;  $R = R' = \text{CF}_3$ :  $\delta = 3.60 \text{ mm s}^{-1}$ ,  $\Delta = 1.66 \text{ mm s}^{-1}$ )<sup>99</sup> follow a similar trend with the electronegativity of the R groups. Based on spectroscopic evidence these tin(II) bis( $\beta$ -ketoenolates) are proposed to have tin(II) in a distorted trigonal-pyramidal environment with two axial and two equatorial oxygen atoms as has been established for  $\text{Sn}(\text{OCRCHCR}'\text{O})_2$ , ( $R = \text{CH}_3$ ,  $R' = \text{C}_6\text{H}_5$ ).<sup>100</sup> There are other series of tin(II) compounds in which there is a correlation of the type shown in Figure 5.3. Such a series are the  $[\text{SnX}_3]^-$  compounds, where X can be a halide or another anion.<sup>101</sup> There is no reason to expect such a correlation if the compounds are not structurally related.

The Mössbauer parameters observed for the simple tin(II) carboxylates vary over a small range ( $\delta = 3.10\text{-}3.49 \text{ mm s}^{-1}$ ;  $\Delta = 1.56\text{-}2.03 \text{ mm s}^{-1}$ ) and there appears to be no consistent agreement between these parameters and the ionization constants of the parents acids.<sup>95</sup> On the basis of the spectroscopic data it was proposed that the tin(II) carboxylates were trigonal-pyramidal with bridging and/or chelating

carboxylate groups.<sup>95,102</sup> The recent X-ray crystal structure of tin(II) formate shows that this inference is not valid at least in the case of the formate.<sup>103</sup> The "local" stereochemistry at tin is that of a distorted trigonal-bipyramid.

The Mössbauer parameters of the tin(II) atom in the mixed oxidation state tin carboxylates span the range observed for uncharged tin(II) oxygen compounds.<sup>13</sup> The quadrupole splitting value of  $2.20 \text{ mm s}^{-1}$  observed for the trimethylacetate is among the highest recorded for a tin(II) compound. The environment of the tin(II) atom must be very distorted in terms of the imbalance of p and/or d orbital electron density. The tin(II) atom of the trihaloacetate compounds, on the other hand, exhibits a high isomer shift,  $\sim 3.9\text{-}4.0 \text{ mm s}^{-1}$ , with much smaller quadrupole splittings,  $\sim 1.0\text{-}1.2 \text{ mm s}^{-1}$ . These are atypical of tin(II) carboxylates and are normally found for compounds containing the more electronegative ligands, for example  $\text{Sn(II)SO}_4$ ,  $\text{Sn(II)(SO}_3\text{F)}_2$  and  $\text{Sn(II)(SO}_3\text{Cl)}_2$ .<sup>104</sup>

The Mössbauer parameters for the tin(II) site in the ortho-nitrobenzoate mixed oxidation state tin carboxylate  $[\text{Sn(II)Sn(IV)O}(\text{O}_2\text{CC}_6\text{H}_4\text{NO}_2\text{-o})_4\text{THF}]_2$ ,<sup>105</sup> are similar to those of the compounds discussed here (Table 5.1). The Mössbauer parameters reported for this compound correlate reasonably well with the data shown in Figure 5.3, suggesting a similarity in the environments of the tin(II) atoms. The geometry about the tin(II) site in this molecule,<sup>105</sup> Figure 5.6, is that of a slightly distorted pentagonal pyramid with five oxygens in the equatorial plane, four from tin(IV)-tin(II) carboxylate bridges, the fifth from coordinated tetrahydrofuran (THF). The axial



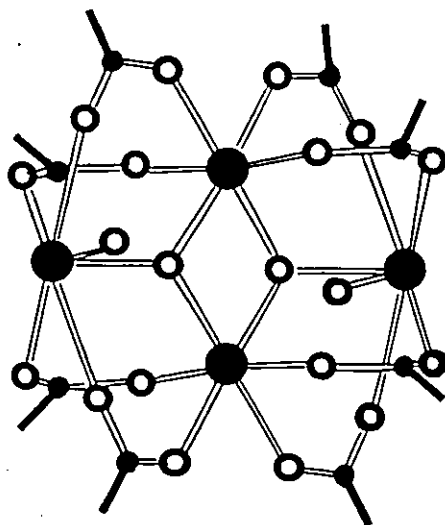


Figure 5.6. A diagram of the tetranuclear skeleton of  $[\text{Sn(II)Sn(IV)O}(\text{O}_2\text{CC}_6\text{H}_4\text{NO}_2\text{-o})_4\text{THF}]_2$ . The large shaded circles are Sn, the small shaded circles C, the open circles O.

oxygen is supplied from a  $\mu_3$ -oxygen atom which bridges two tin(IV) and the tin(II) atoms. The mixed oxidation state tin carboxylates discussed here could have a similar structure, with anhydride replacing the THF molecule. Their formula would then be  $[\text{Sn(II)Sn(IV)O(O}_2\text{CR)}_4\text{O(OCR)}_2]_2$ .

The origin of the quadrupole splitting for tin(II) compounds has not been satisfactorily explained to date.<sup>13,100,101,104</sup> The available evidence seems to favour an interpretation with a dominant contribution from a stereochemically active lone pair. The lone pair provides an excess of electron density in a p and/or d orbital which is generally taken to be along the z axis of the molecule. Tin(II) compounds which exhibit a resolvable quadrupole splitting have invariably been shown crystallographically to have a structure consistent with a covalent model for bonding with a stereochemically active lone pair.<sup>16</sup> Further, the sign at the electric field gradient tensor,  $V_{zz}$ , and therefore the quadrupole splitting when determined, is consistent with an excess of electron density along the axis which would contain the lone pair.<sup>106,107</sup> The large quadrupole splittings for the tin(II) in the mixed oxidation state carboxylates suggest the presence of a stereochemically active lone pair.

The quadrupole splitting is made up of a valence contribution, dominated by the lone pair, and a lattice or ionic contribution from ligands. For tin(II) compounds as a whole, the lack of a general relationship between isomer shift and quadrupole splitting may be due to the geometries which vary from compound to compound, and which result in lattice contributions which are independent of the valence contributions.

In a series of isostructural compounds such as are discussed here, the lattice contributions to the quadrupole splitting which arise from the external ligand charges, would be expected to be similar and hence may be neglected in a discussion of the changes observed. Changes in the magnitude of the quadrupole splitting arise from the variation in the non-cubic electric field about the tin atom due to the unequal population of the non-spherical p and/or d orbitals. The geometry and the sp or spd hybridization of the tin(II) site would be expected to be similar in this series and any changes that occur in isomer shift and quadrupole splitting should arise from variation in bonding characteristics of the ligands. A general relationship between the s electron density and imbalance of the electron density at the tin(II) site is expected, since the imbalance should be caused by a similar type of geometric distortion or electronegativity effect.

An increase of s electron density at the tin(II) occurs with an increase in ligand electronegativity and is accompanied by a corresponding decrease in the disparity and imbalance of p and/or d electron density.

An increase in ligand electronegativity would be expected to result in a removal of electron density through the tin-oxygen bonds. The observed increase in isomer shift with ligand electronegativity suggests that the removal of electron density from the tin(II), via the tin-oxygen bonds in the x-y plane, must occur through orbitals of predominantly p and/or d character. The s electron density must be mainly concentrated in the lone pair and the bonds to the apical oxygen in the z direction. A stereochemically active lone pair implies the

participation of the 5s electrons in bonding and hence the isomer shift of tin(II) compounds would be strongly influenced by this participation. A significant involvement of the 5s electrons in the tin-oxygen bonds in the x-y plane would result in a decrease in s electron density at the tin nucleus and a decrease in isomer shift, when the electronegativity of the ligand is increased. This decrease is not observed. In fact, the reverse of this trend occurs, indicating that the increase in isomer shift is the result of the removal of predominantly p and/or d electron density.

The removal of electron density through the tin-oxygen bonds will result in deshielding of the tin atom and a contraction of the 5s orbital which would increase the s electron density. A small percentage of s character to the bonds in the x-y plane cannot be ruled out, but this must be quite small because of the observed trends in the isomer shift.

The increase in isomer shift is accompanied by a reduction in the quadrupole splitting. This indicates that as the s electron density increases the tin environment becomes more symmetric. This could be accomplished by a reduction of p, and to a lesser extent d, orbital imbalance about the tin(II) and a trend towards decreased participation of the 5s electrons in the bonding. More electronegative ligands would reduce the repulsions between the Sn-O bonds and the lone pair and would allow the lone pair to increase the amount of space it occupies and perhaps eventually become spherical. Confirmation of this might be obtained from a careful comparison of the structures of the  $-\text{C}(\text{CH}_3)_3$  and  $-\text{CF}_3$  mixed oxidation state compounds. To date, only the structure of a derivative of the latter compound is known.

Both the structure and the sign of the quadrupole splitting for several derivatives of the mixed oxidation state tin carboxylates is required before any final interpretation can be made of the observed trends in the Mössbauer parameters at the tin(II) site. Such data may provide an insight for the interpretation of Mössbauer data for tin(II) compounds in general.

#### (iv) Tin(IV) Mössbauer Region

The isomer shifts for the tin(IV) site in the mixed oxidation state tin carboxylates behave in the expected manner. The isomer shift becomes more negative, indicating that there is less s electron density at the tin nucleus as the electronegativity of the carboxylate ligand increases. Those compounds prepared from the weaker carboxylic acids ( $\text{RCO}_2\text{H}$  where  $\text{R} = \text{C}(\text{CH}_3)_3, \text{CH}_3, \text{CH}_2\text{Cl}$ ), have positive isomer shifts of  $\sim 0.14 \text{ mm s}^{-1}$ , and those compounds derived from the stronger carboxylic acids ( $\text{R} = \text{CF}_3, \text{CCl}_3, \text{CF}_3(\text{CF}_2)_2$ ), have negative isomer shifts of  $\sim -0.03 \text{ mm s}^{-1}$ . The  $\text{CHCl}_2$  compound appears to be intermediate with an isomer shift of  $0.07 \text{ mm s}^{-1}$ . Although the reductions in isomer shift are small with respect to the increase in ligand electronegativity, the trend is quite apparent. The isomer shift is not as sensitive to changes in the carboxylate ligand as is observed for the tin(II) site because the valence s electrons of the tin(IV) atom are involved in bonding and not localized in a lone pair. This relative insensitivity of isomer shift with increasing electronegativity of the ligands is to be expected since removal of s electron density is compensated for by removal of p and/or d electron density.

No clearly resolvable quadrupole splittings were observed (Figures 5.1 and 5.2). Small quadrupole splittings are probably present in all cases except when  $R = C_3F_7$  and  $CCl_3$  since fitting the tin(IV) absorption to only one line gives a line width of  $1.2 \text{ mm s}^{-1}$  which is broader than that observed for the analogous tin(II) site in these compounds ( $0.8\text{-}1.0 \text{ mm s}^{-1}$ ). Such unresolved splittings are the rule rather than exception for tin(IV) sites where the coordinating ligands are the same.

The low isomer shifts for the tin(IV) site of the mixed oxidation state tin carboxylates are consistent with coordination by electro-negative atoms such as oxygen. When the coordinating atoms are oxygen, six and eight coordinate environments for tin(IV) are common, whereas seven coordinate environments are rare.<sup>16</sup>

The small or zero quadrupole splittings indicate a fairly regular environment about the tin(IV) site, such as would occur in a slightly distorted octahedral, pentagonal bipyramidal or dodecahedral geometry at tin. The similarity of the Mössbauer parameters for the tin(IV) in these compounds strongly suggests that the same geometry persists throughout this series of the mixed oxidation state tin carboxylates. The rather large line width of the tin(IV) resonance for  $[Sn(II)Sn(IV)O(O_2CC_6H_4NO_2-o)_4THF]_2$ ,  $1.18 \text{ mm s}^{-1}$ <sup>105</sup> would be consistent with it also having an unresolved quadrupole splitting and the slightly distorted octahedral tin(IV) environment in this compound. Clearly both  $[Sn(II)Sn(IV)O(O_2CC_6H_4NO_2-o)_4THF]_2$  and the  $Sn(O_2CR)_3$  series are structurally related based on the interpretation of the  $^{119}\text{Sn}$  Mössbauer parameters for these compounds.

In contrast to the data for the tin(IV) sites in the mixed oxidation state tin carboxylates, the  $^{119}\text{Sn}$  Mössbauer data presented for the  $\text{Sn}(\text{O}_2\text{CR})_4$  series are quite different. The isomer shifts, although all are fairly small as expected, do not follow the same general pattern observed for the mixed oxidation state tin carboxylates with respect to the electronegativity of the carboxylato ligand. Several of the tin(IV) carboxylates, particularly the  $-\text{CCl}_3$ ,  $-\text{CHCl}_2$  and  $-\text{CH}_2\text{Cl}$  derivatives, have significantly different isomer shifts from those observed for the tin(IV) sites in the mixed oxidation state tin carboxylates. This, coupled with the well resolved quadrupole splittings observed for the tin(IV) carboxylates derived from the stronger carboxylic acids ( $\text{R} = \text{CHCl}_2$ ,  $\text{CCl}_3$ ,  $\text{CF}_3$ ,  $\text{C}_3\text{F}_7$ ), eliminates the possibility that the tin(IV) site in the mixed oxidation state tin carboxylates has the same geometry.

The spectrum of tin(IV) acetate was fitted to a single line,<sup>96</sup> though the rather large line width suggests the presence of a small splitting of  $\sim 0.6 \text{ mm s}^{-1}$ . This splitting would also be consistent with the recent crystal structure of  $\text{Sn}(\text{OAc})_4$ .<sup>108</sup> Tin(IV) tetra-acetate consists of independent  $\text{Sn}(\text{IV})(\text{OAc})_4$  molecules with the tin in an eight coordinate dodecahedral environment, achieved by four bidentate carboxylato groups. A similar non-polymeric dodecahedral structure has been observed for  $\text{Sn}(\text{NO}_3)_4$ ,<sup>109</sup> the Mössbauer spectrum of which has been interpreted in terms of a small unresolved quadrupole splitting.<sup>110</sup> Tin(IV) monochloroacetate has a small unresolved quadrupole splitting and likely has the same geometry.

Unexpectedly, the tin(IV) carboxylates derived from the stronger carboxylic acids all show a well resolved quadrupole splitting, that of tin(IV) trifluoroacetate being the largest in magnitude,  $1.56 \text{ mm s}^{-1}$ , Figure 5.7. The only previously reported compound to have a resolved quadrupole splitting, where all the coordinating ligands are oxygen, is  $\text{Sn}(\text{SO}_3\text{F})_4$  ( $\Delta = 1.34 \text{ mm s}^{-1}$ ).<sup>111</sup> While there is as yet no crystallographic data for this latter molecule, the spectroscopic evidence suggests that tin(IV) fluorosulphate is six coordinate with two unidentate axial fluorosulphates and bidentate bridging equatorial fluorosulphates, giving a polymeric structure. The difference in electron withdrawing power by terminal and bridging fluorines also gives rise to a similar resolved quadrupole splitting in  $\text{SnF}_4$ <sup>112</sup> ( $\Delta = 1.80 \text{ mm s}^{-1}$ ), which consists of octahedral  $\text{SnF}_6$  groups that form infinite layers by sharing four equatorial fluorine atoms (Sn-F bridging 2.20Å, Sn-F terminal 1.88Å).<sup>113</sup> A similar structure could account for the observed quadrupole splittings in the tin(IV) carboxylates of the more electronegative carboxylates, however, several other possibilities must be considered. Such a geometry has been suggested for tin(IV) carboxylates.<sup>93</sup>

Tin, when bonded to more electronegative groups, has a strong tendency to increase its coordination number to compensate for the increase in effective nuclear charge at the central metal atom. For  $\text{SnL}_4$  compounds, where L may be unidentate or bidentate, a coordination number of four is rare, with six and eight being more common.<sup>16</sup> Both



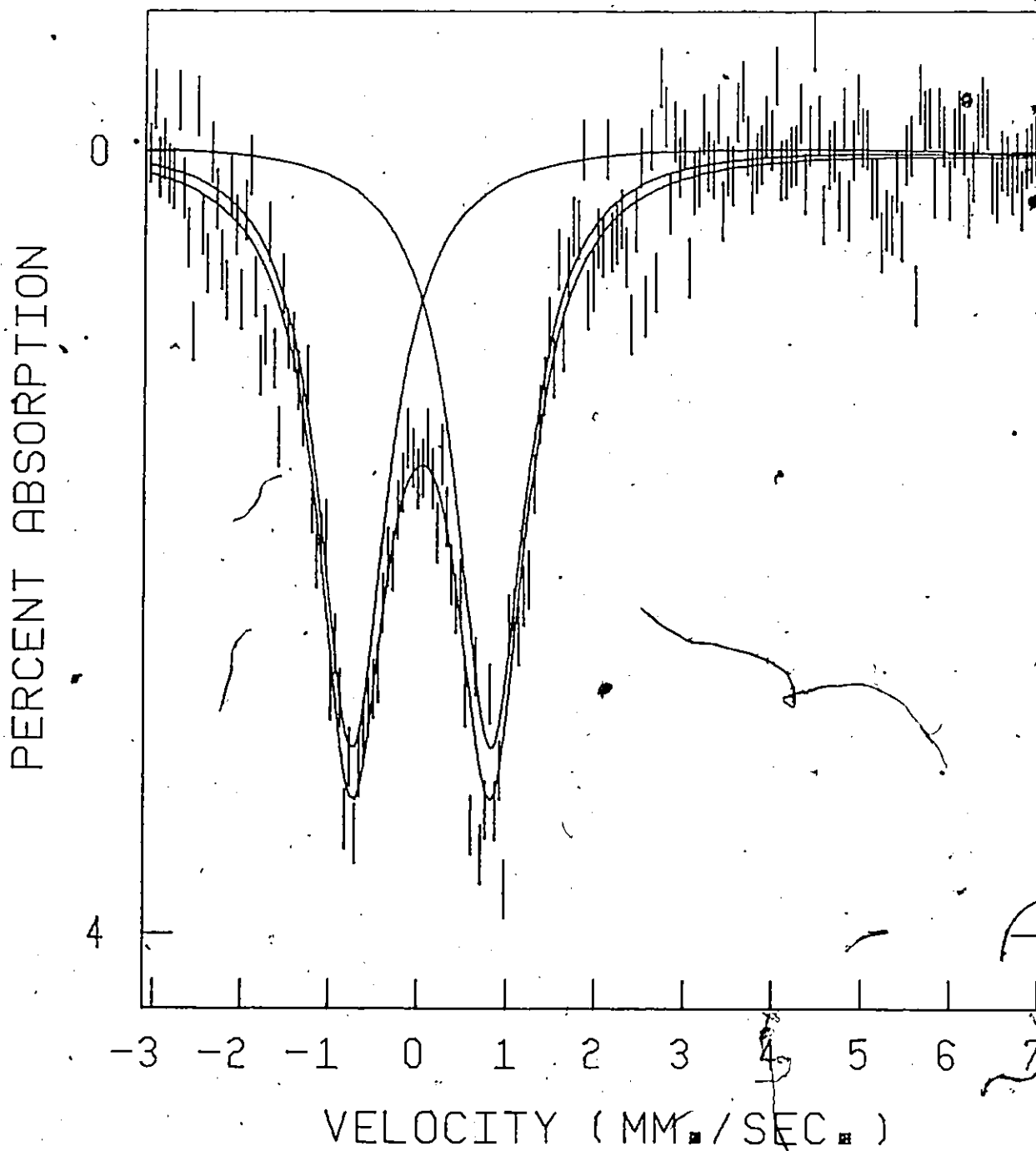


Figure 5.7.  $^{119}\text{Sn}$  Mössbauer spectrum of  $\text{Sn}(\text{O}_2\text{CCF}_3)_4$  at  $77^\circ\text{K}$ .

distorted octahedral and dodecahedral structures have been shown to give rise to a quadrupole splitting, although rather small in the latter case.<sup>96, 110</sup>

A non-cubic electric field about the tin atom gives rise to a quadrupole splitting and this could also be achieved with a coordination number of seven. Until recently, no crystallographic evidence for such a coordination number has existed and so this coordination number has been ignored. However, the crystal structure of  $[(\text{CH}_3)_4\text{N}][\text{Sn}(\text{OAc})_5^-]$  consists of independent  $[\text{Sn}(\text{OAc})_5^-]$  units which contain seven coordinate tin in a pentagonal-bipyramidal geometry, with two bi- and one unidentate acetate groups around the equatorial plane, and two unidentate axial acetates.<sup>114</sup> Such a structure would be expected to give rise to a quadrupole splitting, the magnitude of which is difficult to estimate. It is indeed possible that tin(IV) carboxylates of the more electronegative carboxylato groups may have a structure similar to that found for  $\text{Sn}(\text{OAc})_5^-$ , or they could have a polymeric structure based on this geometry.

Since  $\text{Sn}(\text{OAc})_4$  has an eight coordinate dodecahedral structure it seems likely that the tin(IV) carboxylates derived from the weaker acid strength carboxylic acids are also non-polymeric solids of the same type. The lack of a large room temperature Mössbauer effect, together with the appreciable solubility of these compounds in non-polar solvents such as benzene, the low melting point and high volatility of  $\text{Sn}(\text{IV})(\text{O}_2\text{CCF}_3)_4(\text{s})$  in particular,<sup>92</sup> suggests that all of the tin(IV) carboxylates could be non-polymeric. The Mössbauer parameters indicate

that a significant structural change must occur with the more electronegative carboxylate ligands. Crystallographic studies on tin compounds<sup>16</sup> indicate that increased coordination achieved from chelation of potential bidentate ligands occurs with a reduction in steric bulk of these ligands. Furthermore, reduction in steric bulk allows chelates to open into bridges to form polymeric solids. These trends are consistent with the dodecahedral structure of  $\text{Sn}(\text{OAc})_4$  and suggest that as the bulk of the carboxylate ligand increases one bidentate carboxylate group becomes unidentate, to produce a seven coordinate pentagonal bipyramidal structure. Further increase in steric bulk would logically lead to a six coordinate octahedral structure with two bidentate and two unidentate carboxylate groups. These results strongly suggest a non-polymeric six or seven coordinate tin(IV) site for the tin(IV) carboxylates having the more electronegative R groups ( $\text{CF}_3$ ,  $\text{CCl}_3$ ,  $\text{C}_3\text{F}_7$ ).

#### (v) Temperature Dependent Mössbauer Effect

Attempts to observe the Mössbauer effect for the mixed oxidation state tin carboxylates  $[\text{Sn}(\text{II})\text{Sn}(\text{IV})\text{O}(\text{O}_2\text{CR})_4\text{O}(\text{OCR})_2]_2$  at room temperature were unsuccessful. Polymeric solids such as  $\text{Sn}(\text{SO}_3\text{F})_4$  and  $\text{SnF}_4$  exhibit a strong room temperature resonance.<sup>111</sup> It has been suggested that the absence of a room temperature effect in no way allows the elimination of an associated structure.<sup>47</sup> However, in octahedrally coordinated tin compounds when four or more of the coordinated atoms are oxygen atoms from four ligands which bridge adjacent tin atoms, a room temperature effect is observed.<sup>41</sup> This would seem to rule out the

possibility that the mixed oxidation state tin carboxylates are "highly" polymeric solids. Further information may be gained from the temperature dependence of the Mössbauer effect for the mixed oxidation state tin carboxylates.

Examination of data in Table 5.2 shows that for both the acetate and trimethylacetate the area under the Sn(II) absorption is greater than that for the Sn(IV) absorption at 77°K. For the haloacetates, the reverse is true. This is apparent by visual comparison of the spectra of the acetate, Figure 5.1, and the trifluoroacetate, Figure 5.2. At liquid helium temperature, the relative areas change somewhat, with an increase in the Sn(IV)/Sn(II) ratio for the acetate, Table 5.2, Figures 5.1 and 5.8. The Debye temperature of the Sn(II) site is higher than that of the Sn(IV) site, indicating that it is more rigidly bound in the lattice. For the  $-CF_3$  derivative (Figures 5.2 and 5.9) at 77°K the Sn(IV) atom is more strongly bound, and it is only at 4°K that the area under the Sn(II) absorption becomes greater than that under the Sn(IV) absorption, though the ratio does not reach that observed for the  $-CH_3$  compound. These facts are consistent with a more ionic situation for the  $-CF_3$  derivative than for the  $-CH_3$  derivative.

There appears to be no simple dependence of the Sn(IV)/Sn(II) ratio as electronegativity of the R group increases. However, there is a dependence of the Sn(IV)/Sn(II) ratio on the type of R group. At 77°K the ratio of Sn(IV)/Sn(II) is  $< 0.8$  for non-haloacetates,  $\sim 1.1-1.2$  for fluoroacetates, and  $> 1.2$  for chloroacetates. The cause of such a dependence is not clear. A more extensive temperature-dependence study

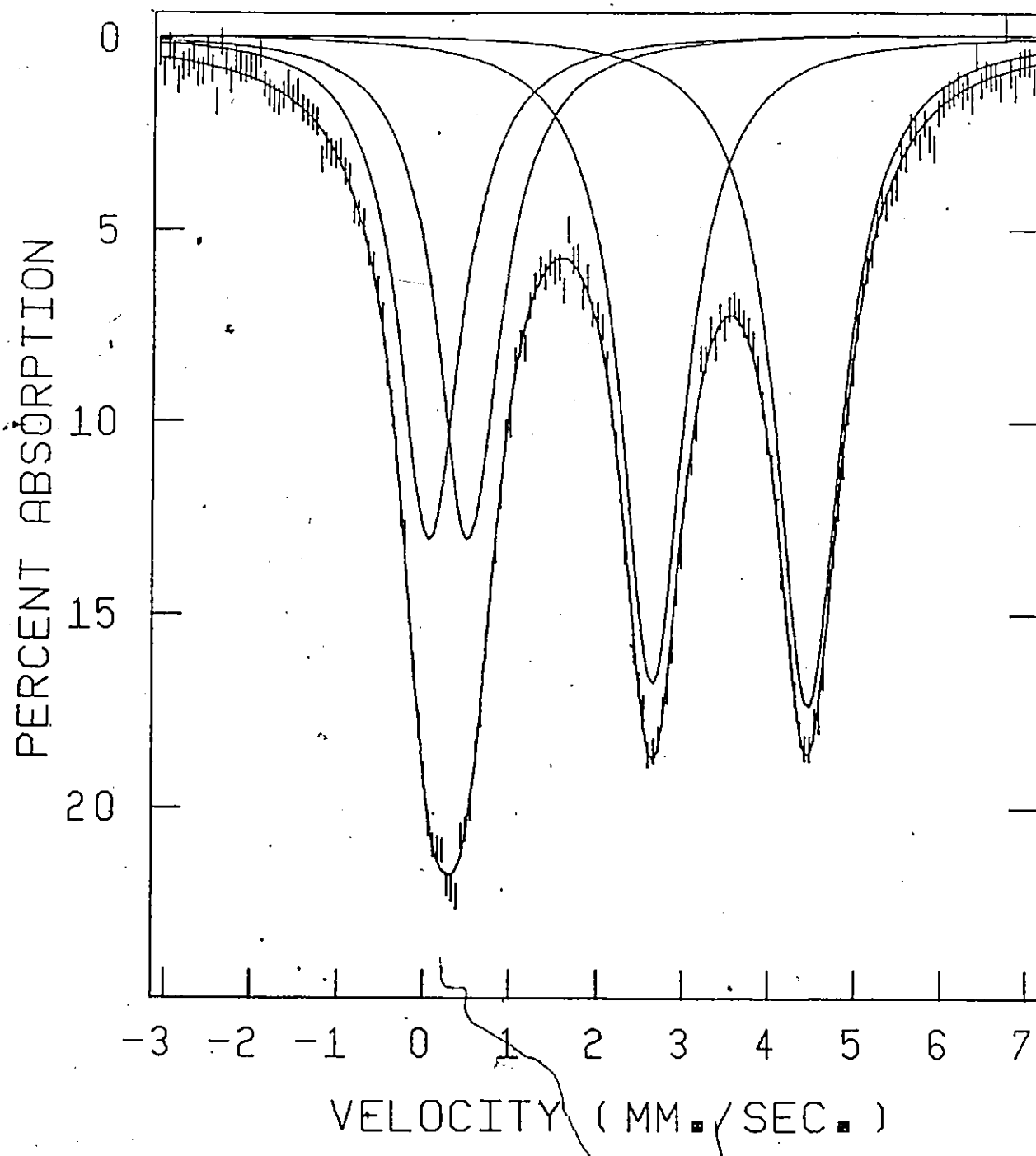


Figure 5.8.  $^{119}\text{Sn}$  Mössbauer spectrum of  $\text{Sn}(\text{O}_2\text{CCH}_3)_3$  at  $4^\circ\text{K}$ .

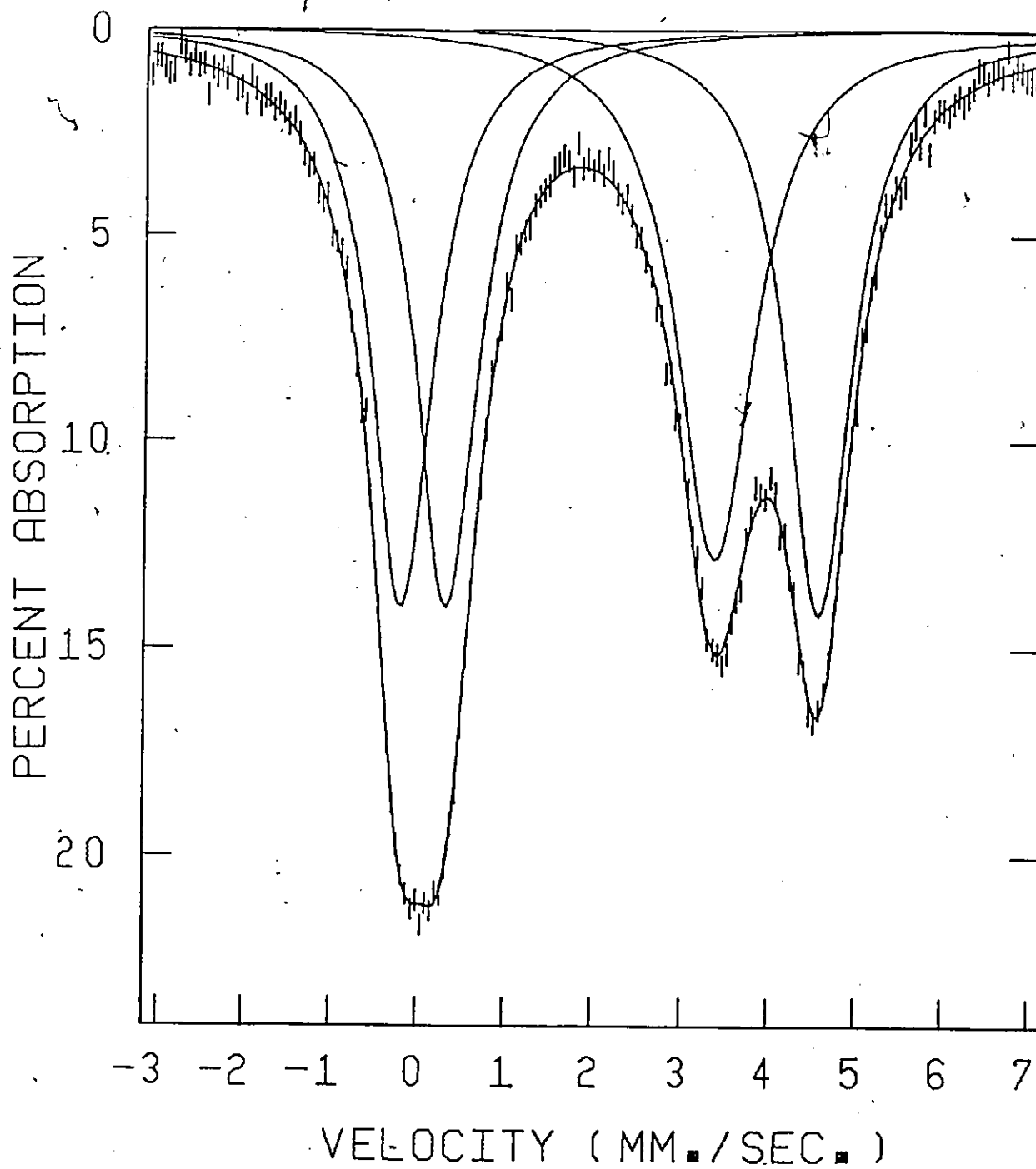


Figure 5.9.  $^{119}\text{Sn}$  Mössbauer spectrum of  $\text{Sn}(\text{OC}_2\text{CF}_3)_3$  at  $4^\circ\text{K}$ .

would allow an estimation of the Debye temperature for the tin(II) and tin(IV) atoms for this series of compounds and perhaps a more definitive statement about the lattice dynamics could then be made.

(vi) Vibrational Data

The vibrational data for the  $\text{Sn}(\text{O}_2\text{CR})_3$  series are presented in Table 5.3. Spectroscopic data for  $\text{Sn}(\text{O}_2\text{CCF}_3)_4$  are also given in Table 5.3. All spectroscopic data in Table 5.3 are for the compounds in the solid state. Infrared spectra were recorded for all the compounds, but only some of the compounds gave satisfactory Raman spectra due to fluorescence problems. Vibrational data are not reported for the other  $\text{Sn}(\text{O}_2\text{CR})_4$  compounds because these compounds could not be isolated free of excess acid (Chapter 2).

Ambiguous assignments, particularly in the infrared, where overtones and combination bands are likely, could be avoided in part when Raman data were obtainable. Although the complexity of the spectra makes a total vibrational assignment for these compounds difficult, certain spectral features are readily identifiable and provide structurally significant information. All vibrations to be assigned are based on both the frequency and intensity of the observed bands. Complete vibrational spectra for the sodium salts  $\text{NaO}_2\text{CR}$  are available.<sup>115,116</sup> Even in these simple compounds there is considerable controversy over the description of some of these modes and their assignments to the observed bands in the vibrational spectra.<sup>115,116</sup> However, in the stretching region for the

Table 5.3

Infrared and Raman Data for  $\text{Sn}(\text{O}_2\text{CCF}_3)_4$  and the Tin Carboxylates,  $\text{Sn}(\text{O}_2\text{CR})_3$ 

## Part A

$\text{Sn}(\text{O}_2\text{CCF}_3)_4$		$\text{R} = \text{CF}_3$		$\text{C}_3\text{F}_7$	$\text{CCl}_3$		Assignment
IR	Raman	IR	Raman	IR	IR	Raman	
1760(s)	1763(37)	1765(s)	1764(25)	1755(s)	1740(s)	1733(32)	as CO <sub>2</sub>
1670(s,sh)		1720(m,sh)	1720(22)	1690(s)	1712(w)	1709(17)	
1600(s)		1680(s)	1629(42)	1660(s)	1675(m,sh)	1622(32)	vC=O
	1580(17)	1650(s)	1616(33)	1610(s,b)	1650(s)	1607(19)	
1490(m)	1503(43)		1575(4)				v <sub>s</sub> CO <sub>2</sub>
		1480(m)	1482(52)				
		1463(s)	1466(15)				
		1450(s)	1449(11)				
1365(s)	1370(20)	1370(s)	1368(10)	1415(s)		1395(11)	vC-O
					1365(s)		
				1340(s)	1350(s)		vC-O,
				1270(s,sh)			
1240(s,sh)		1220(s)	1227(5)	1215(s)	1255(m)	1245(w,sh)	v <sub>as</sub> CF <sub>3</sub>
1180(vs)		1190(s)	1180(6)	1180(s)			
		1150(s)	1153(2)	1150(s)			v <sub>s</sub> CF <sub>3</sub>
		1130(s)		1120(s)			
985(m)				1080(s)			vCF <sub>2</sub>
830(w)							
				965(s)	970(w,sh)	968(13)	δCO <sub>2</sub>
				925(s)	965(w)	951(8)	
870(w)	876(29)	869(w)	865(100)		952(w)		vC-C
850(m)	846(23)	855(m)					
		850(m)	848(35)		850(s)	855(21)	vC-C,
		840(m)			830(s)	830(25)	
				810(s)	825(w,sh)		v <sub>as</sub> CCl <sub>3</sub>
780(m)		789(m)	782(2)				v <sub>s</sub> CCl <sub>3</sub>
		785(m)					
		778(m)					δCO <sub>2</sub>
				755(m)	749(s)	761(53)	
					740(m,sh)	743(74)	vSn-O-Sn
					680(s)	680(15)	
730(s)	730(9)	729(s)	726(8)	735(s)			δCO <sub>2</sub>
655(w,sh)	643(100)	701(s)	715(3)	710(s)			
635(m,sh)		629(m)	635(36)	645(m)			vSn-O-Sn
620(m)		619(m)					
		585(w)		600(m)			vSn-O-Sn
550(w)	540(43)				565(w)	567(15)	
520(w)		525(m)	591(15)	550(m)	550(w)		δCX <sub>3</sub>
500(w)		500(w)	514(22)	520(m)			
	500(17)	492(9)	492(9)				δCO <sub>2</sub>
	435(29)	452(w)	450(12)	475(w)			
	425(31)	432(w)	430(6)				δCO <sub>2</sub>
			424(8)				
						384(32)	δCO <sub>2</sub>
	313(51)		331(39)			296(64)	δCO <sub>2</sub>
	270(9)		289(6)			278(100)	
			263(13)				δCO <sub>2</sub>
			237(13)				
			219(27)				δCO <sub>2</sub>
			189(23)				
	190(26)						δCO <sub>2</sub>
	148(37)						
	135(20)						δCO <sub>2</sub>
	105(9)						

\*Infrared were recorded from 4000 to 400 cm<sup>-1</sup>.

..... continued



Table 5.3 (continued)

## Part B

R = CHCl <sub>2</sub>	CH <sub>2</sub> Cl	CH <sub>3</sub>	C(CH <sub>3</sub> ) <sub>3</sub>	Assignment
IR	IR	IR	Raman	IR
3020(w)		3000(w)	3015(24) 3001(27)	} $\nu_{as} CH_3$ $\nu C-H$
2990(w)				
		2920(w)	2952(100) 2936(92)	} $\nu_s CH_3$ $\nu C-H$
2220(w,b) 2100(w,b)	2200(m,b) 2060(m,b)		2731(1)	
			2970(m) 2930(w) 2880(w) 2720(w) 2200(w) 2100(w)	
1745(m)	1720(w,sh)		1638(1)	} $\nu_{as} CO_2$ $\nu C=O$
1640(vs) 1560(m,sh)	1625(s) 1520(s)	1590(m,sh) 1520(s)	1594(4) 1536(14) 1517(12)	
			1475(14)	
			1485(vs) 1460(m)	
1400(sh)	1420(m,sh)	1435(sh) 1400(s)	1433(10) 1401(16)	} $\nu_s CO_2$ $\nu C-O$ $\delta CH_3$
1360(s)	1380(s) 1315(m,sh)	1350(m,sh) 1334(m,sh)	1358(6) 1335(7)	
1225(m) 1210(m) 1195(m)	1240(s)			} $\delta C-H$ $\nu C-O$
			1047(w) 1012(m)	
950(m)	925(s)	965(w) 930(w)	975(91) 937(67)	} $\nu C-C$
825(m) 815(m) 795(w) 780(w)				
	790(s)			} $\nu_{as} CX_2$ $\delta CO_2$ $\nu_s CX_2$ $\nu_{as} CC_3$ $\nu C-X$
			820(m) 795(m) 780(m)	
730(w) 715(m) 705(m) 680(s)	700(s) 680(s)	705(m)	726(7)	} $\delta CO_2$ $\nu Sn-O-Sn$
			670(6) 627(3)	
620(w) 600(w)	620(w)	657(m) 625(w) 610(w)	620(8) 610(2)	
			610(vs)	
550(m)	565(vs) 495(vs)			} $\nu_{as} CH_3$ $\nu C-H$
		430(m)	485(22) 430(w)	
			333(15) 300(54) 271(29) 241(16)	

\* Infrared were recorded from 4000 to 400 cm<sup>-1</sup>.

$\text{NaO}_2\text{CR}$  series assignments are well established, there being uncertainty in the assignments only in the lower frequency range, 700 to  $200\text{ cm}^{-1}$ .

Stretching vibrations in the range  $4000$  to  $700\text{ cm}^{-1}$  of the R substituent of the carboxylate group are readily identified on the basis of their characteristic frequencies and intensities. These frequencies are generally insensitive to the mode of coordination of the carboxylate group. These bands are indicated in Table 5.3. None of the mixed oxidation state tin compounds, that is the  $\text{Sn}(\text{O}_2\text{CR})_3$  series, nor  $\text{Sn}(\text{O}_2\text{CCF}_3)_4$  show any bands in the OH region of the infrared spectra, indicating there is no free or coordinated acid present in these compounds. The vibrational modes from the  $\text{CO}_2$  group are the most sensitive to the type of carboxylate group since these are directly bonded to the tin. Of these modes, the  $\text{CO}_2$  stretching frequencies are the most useful since these generally intense infrared absorptions occur in characteristic regions of the spectrum. Such is not the case for the other  $\text{CO}_2$  modes, which are generally of little diagnostic value. The  $\nu_{\text{as}}\text{CO}_2$  modes,  $1770$  to  $1500\text{ cm}^{-1}$ , observed for the spectra of the compounds presented in Table 5.3, span the entire range for all types of carboxylate bonded to tin.

The occurrence of two  $\nu_{\text{as}}\text{CO}_2$  modes in the infrared spectra of  $\{[(\text{CH}_2=\text{CH})_2\text{Sn}(\text{O}_2\text{CCF}_3)]_2\text{O}\}_2$ <sup>90</sup> and that of  $\{[(n\text{-C}_4\text{H}_9)_2\text{Sn}(\text{O}_2\text{CCF}_3)]_2\text{O}\}_2$ <sup>89</sup> has been interpreted in terms of two types of carboxylate ligands in these molecules and has been confirmed by X-ray crystallographic analysis of these compounds. The Raman spectrum of  $\text{Sn}(\text{O}_2\text{CCF}_3)_4$  consists of several

bands in the  $\text{CO}_2$  asymmetric stretching region. The  $\nu_{\text{as}}\text{CO}_2$  mode at  $1763\text{ cm}^{-1}$  is assigned to unidentate carboxylate ligands and the lower frequency band, at  $1580\text{ cm}^{-1}$ , to bidentate, chelating or bridging carboxylate ligands.

The  $1763\text{ cm}^{-1}$  band is similar in frequency to the  $1713\text{ cm}^{-1}$  band in the infrared spectrum of  $(\text{CH}_2=\text{CH})_2\text{Sn}(\text{O}_2\text{CCF}_3)_2(\text{C}_{10}\text{H}_9\text{N}_2)^{1,17}$  which is confirmed to have only unidentate carboxylate ligands.

The  $1580\text{ cm}^{-1}$  band in the Raman spectrum of  $\text{Sn}(\text{O}_2\text{CCF}_3)_4$  is similar in frequency to the  $1619\text{ cm}^{-1}$  band for  $(\text{CH}_3)_4\text{Sn}_2(\text{O}_2\text{CCF}_3)_2$  (Chapter 3) which is confirmed as having bridging trifluoroacetate ligands (Chapter 4). The corresponding symmetric  $\text{CO}_2$  stretching frequencies,  $\nu_{\text{s}}\text{CO}_2$ , for  $\text{Sn}(\text{O}_2\text{CCF}_3)_4$  are assigned to the bands at  $1503\text{ cm}^{-1}$  and  $1370\text{ cm}^{-1}$ . The relative intensities of the  $\nu\text{CO}_2$  modes in the Raman spectrum of  $\text{Sn}(\text{O}_2\text{CCF}_3)_4$  indicate that the  $\nu_{\text{as}}\text{CO}_2/\nu_{\text{s}}\text{CO}_2$  modes at  $1763\text{ cm}^{-1}/1503\text{ cm}^{-1}$  for this compound are associated with unidentate carboxylates, while those at  $1580\text{ cm}^{-1}/1370\text{ cm}^{-1}$  are assigned to bidentate carboxylates.

The two intense Raman bands at  $876$  and  $846\text{ cm}^{-1}$  are assigned to C-C stretching frequencies. The frequency of the  $\nu\text{C-C}$  mode is sensitive to the type of carboxylate group. The  $846\text{ cm}^{-1}$  band in the Raman spectrum of  $\text{Sn}(\text{O}_2\text{CCF}_3)_4$  is very similar in frequency to the  $844\text{ cm}^{-1}$  band observed in the spectrum of  $(\text{CH}_3)_4\text{Sn}_2(\text{O}_2\text{CCF}_3)_2$ .

The infrared spectra of the  $\text{Sn}(\text{O}_2\text{CR})_3$  series in the C-C stretching region  $930$  to  $850\text{ cm}^{-1}$  have several sharp, medium to weak, intensity absorptions which can be assigned to this mode. However,

reliable assignment is only possible in the Raman spectrum where the  $\nu(\text{C-C})$  stretch occurs as an intense band. For the majority of the compounds studied in the  $\text{Sn}(\text{O}_2\text{CR})_3$  series at least two C-C stretching absorptions were observed, indicative of more than one type of carboxylate ligand.

The vibrational modes, 1770 to  $1500\text{ cm}^{-1}$ , observed for the vibrational spectra of the mixed oxidation state tin carboxylates span the entire range of  $\nu_{\text{as}}\text{CO}_2$  for all types of carboxylate bonded to tin. There are several absorptions in the  $\nu_{\text{as}}\text{CO}_2$  region 1690 to  $1500\text{ cm}^{-1}$  which can be attributed to carboxylate ligands bridging two adjacent tin atoms. Carboxylate groups which bridge both tin(II) and tin(IV) are present in  $[\text{Sn}(\text{II})\text{Sn}(\text{IV})\text{O}(\text{O}_2\text{CC}(\text{H})\text{NO}_2-\text{o})_4\text{THF}]_2$ <sup>105</sup> which has  $\nu_{\text{as}}\text{CO}_2$  at  $1530\text{ cm}^{-1}$ .<sup>118</sup>

There are several bands in the vibrational spectra of the mixed oxidation state tin carboxylates in the 1770 to  $1700\text{ cm}^{-1}$  range which are usually associated with unidentate carboxylates bonded to tin(IV). These frequencies are too high to be assigned to unidentate carboxylates linked to tin(II). For example,  $\text{K}[\text{Sn}(\text{II})(\text{O}_2\text{CCH}_3)_3]$ , which is confirmed to have only unidentate carboxylates,<sup>119</sup> has  $\nu_{\text{as}}\text{CO}_2$  at  $1587\text{ cm}^{-1}$ .<sup>120</sup> and the  $\text{K}[\text{Sn}(\text{O}_2\text{CCH}_2\text{Cl})_3]$  analogue has  $\nu_{\text{as}}\text{CO}_2$  at  $1625\text{ cm}^{-1}$ .<sup>120</sup> The tin(II) carboxylates  $\text{Sn}(\text{II})(\text{O}_2\text{CR})_2$ <sup>102</sup> (R = H,  $\text{CH}_3$ ,  $\text{CH}_2\text{Cl}$ ,  $\text{CHCl}_2$ ,  $\text{CH}_2\text{F}$ ,  $\text{CF}_2\text{H}$ ) have  $\nu_{\text{as}}\text{CO}_2$  in the  $1570$  to  $1520\text{ cm}^{-1}$  range which coincides with the normal range for bidentate carboxylate ligands for organotin(IV) carboxylates.

However, the assignment of the  $\nu_{\text{as}}\text{CO}_2$  modes in the range 1770 to  $1700\text{ cm}^{-1}$  to unidentate carboxylates for the mixed oxidation state tin carboxylates here is unlikely, since this would imply the presence of

both unidentate and bidentate carboxylates bonded to tin(IV) and would lead to a large quadrupole splitting as observed in the Mössbauer spectra for several of the tin(IV) carboxylates (Table 5.2). In the mixed oxidation state tin carboxylates these bands are in the right range to arise from an anhydride coordinated to a tin(II). Free anhydrides generally display two C=O stretching modes separated by  $\sim 65 \text{ cm}^{-1}$  in the range 1885 to  $1725 \text{ cm}^{-1}$ .<sup>121</sup>

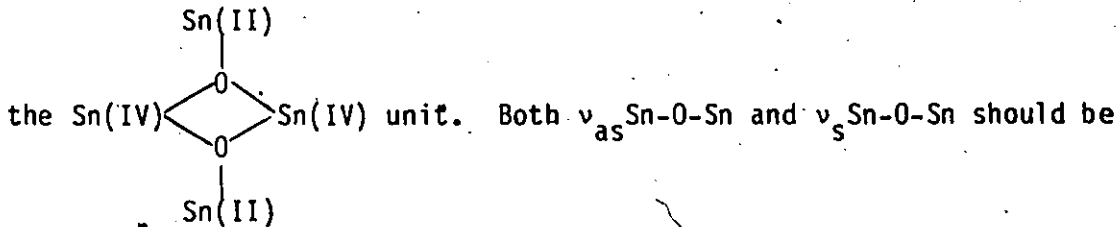
One might reasonably expect these to shift to lower values upon coordination to a tin(II). This behaviour has been reported for  $\text{Sn(IV)X}_4 \cdot 2\text{O}(\text{CCH}_3)_2$  ( $\text{X} = \text{Cl}, \text{Br}$ ) complexes,<sup>122</sup> for which  $\nu\text{C=O}$  shifts from free anhydride 1820,  $1775 \text{ cm}^{-1}$  to 1742,  $1688 \text{ cm}^{-1}$ , upon complex formation. The coordination of anhydride to the tin(IV) is unlikely here since this would produce a more distorted environment than suggested by the Mössbauer spectrum for the  $\text{Sn}(\text{O}_2\text{CR})_3$  series. In any case, the coordination of anhydride to a tin(IV) atom is unlikely on the basis of the similar Mössbauer parameters for  $[\text{Sn(II)Sn(IV)O}(\text{O}_2\text{C}_6\text{H}_4\text{NO}_2\text{-o})\text{THF}]_2$  to those of the  $\text{Sn}(\text{O}_2\text{CR})_3$  series.

Complexed and free anhydrides also have characteristic bands, 1350 to  $900 \text{ cm}^{-1}$ , due to C-O stretching vibrations of the  $\text{O}(\text{OCC})_2$  unit, and all the compounds examined here have bands in this region. Unfortunately, carboxylates with C-H or C-F bonds also display intense bands in this region. In the case where  $\text{R} = \text{CCl}_3$ , the presence of anhydride is suggested by the band at  $1255 \text{ cm}^{-1}$ . This band is abnormally low to be assigned to  $\nu_s \text{CO}_2$ .

Some further support for the presence of anhydride in the mixed oxidation state tin compounds comes from a closer examination of the relative areas of the  $\nu_s \text{CO}_2$  and  $\nu_{as} \text{CO}_2$  bands in the Raman spectra of the  $-\text{CCl}_3$  and  $-\text{CF}_3$  derivatives. Both derivatives display a similar pattern of four bands in the  $1760$  to  $1600 \text{ cm}^{-1}$  range, which must be assigned to anhydride which is coordinated to tin(II). If these bands are not anhydride coordinated to tin(II), then the total intensity of  $\nu_{as} \text{CO}_2$  modes would be greater than that of the  $\nu_s \text{CO}_2$  modes. This is particularly apparent for the  $-\text{CCl}_3$  derivatives for which no  $\nu_s \text{CO}_2$  modes are observed in the Raman.

In  $(\text{CH}_3)_4\text{Sn}_2(\text{O}_2\text{CCF}_3)_2$  and  $(\text{CH}_3)_4\text{Sn}_2(\text{O}_2\text{CCCl}_3)_2$  (Chapter 3),  $\nu_{as} \text{CO}_2$  is less intense than  $\nu_s \text{CO}_2$ . The absence of  $\nu \text{CO}_2$  modes in the Raman spectra, as is apparently the case for the  $-\text{CCl}_3$  derivative, is not uncommon since these are generally weak in intensity. In  $\text{Sn}(\text{O}_2\text{CCF}_3)_4$ , which contains unidentate and bidentate or bridging carboxylates,  $\nu_{as} \text{CO}_2$  is less intense than  $\nu_s \text{CO}_2$  and the mixed oxidation state tin carboxylates can only be rationalized if the bands in the region  $1770$  to  $1600 \text{ cm}^{-1}$ , are attributed to anhydride.

One might expect to observe  $\mu_3$ -oxo-tin vibrations associated with



present in the vibrational spectra of the mixed oxidation state tin carboxylates. Vibrations associated with an oxygen bridging two or more

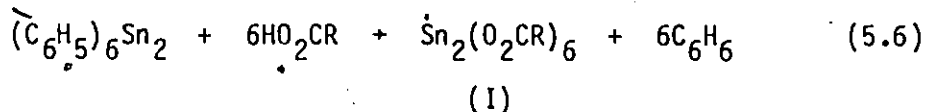
tin atoms occur in the region 700 to 400  $\text{cm}^{-1}$ .<sup>123</sup> Unfortunately, this region contains a number of vibrations which arise from modes due to the R substituent and other vibrations of the C-CO<sub>2</sub> group. It is not particularly apparent which of the observed bands are associated with the  $\mu_3$ -oxo-bridge.

The infrared spectra of  $[(\text{CH}_3)_2\text{Sn}(\text{O}_2\text{CR})]_2\text{O}$ , which are proposed to have a  $\mu_3$ -oxo bridge, are similar to those spectra reported here. The band at  $\sim 625 \text{ cm}^{-1}$  in the infrared spectra of  $[(\text{CH}_3)_2\text{Sn}(\text{O}_2\text{CR})]_2\text{O}$  has been assigned to both  $\delta\text{CO}_2$  and  $\nu\text{Sn-O-Sn}$ .<sup>124</sup> The vibration of the tin-oxo unit cannot be assigned with any certainty. Several bands occur in the 500-400  $\text{cm}^{-1}$  range in the vibrational spectrum of each compound in Table 5.3. Some of these are associated with  $\nu_{\text{as}}\text{Sn-O}$ . The Raman spectrum of the compounds exhibit bands  $< 400 \text{ cm}^{-1}$  which may be associated with  $\nu_{\text{s}}\text{Sn-O}$ . However, because of the large number of bands in the 500 to 20  $\text{cm}^{-1}$  region of the Raman spectra it is not possible to distinguish  $\nu\text{Sn-O}$  from vibrations of the carboxylate group.

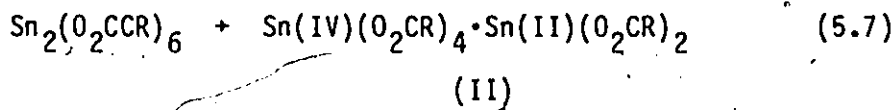
(vii) Mechanism of Formation of  $[\text{Sn}(\text{II})\text{Sn}(\text{IV})\text{O}(\text{O}_2\text{CR})_4\text{O}(\text{OCR})_2]_2$

The formation of  $[\text{Sn}(\text{II})\text{Sn}(\text{IV})\text{O}(\text{O}_2\text{CR})_4\text{O}(\text{OCR})_2]_2$  from the solvolysis of  $(\text{C}_6\text{H}_5)_6\text{Sn}_2$  by carboxylic acids requires the occurrence of three types of reactions. These are, acid cleavage of all carbon-tin bonds, disproportionation of a ditin species into a tin(IV) and a tin(II) species, and production of anhydride by elimination of  $\text{O}^{2-}$  to produce a tin-oxo species. The exact sequence in which these reactions occurs has

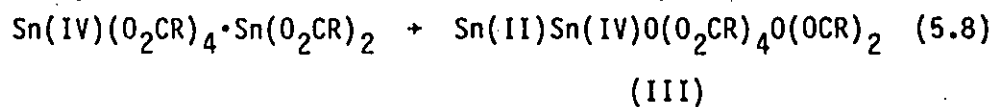
not been established here. However, the solvolysis of  $(C_6H_5)_6Sn_2$  by carboxylic acids is thought to proceed by complete cleavage of all carbon-tin bonds (equation (5.6)) to produce an unstable ditin intermediate (I).



The intermediate (I) was thought to be stable, and the final product of the solvolysis of hexaphenylditin by acetic acid by Wiberg and coworkers.<sup>91</sup> The intermediate (I) might be expected to be unstable because ditin compounds, where all of the atoms bonded to tin are very electronegative, are not known. Asymmetric cleavage of the tin-tin bond of (I) occurs (equation (5.7)) to produce a tin(IV) and a tin(II) carboxylate perhaps associated via the bridging carboxylate ligands.

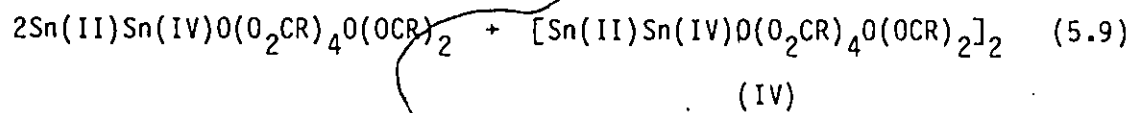


The production of anhydride by elimination of  $O^{2-}$  (equation (5.8)) would produce (III), the monomeric oxo-bridged tin complex.





Dimerization (equation (5.9)) would produce (IV), the oxo-bridged mixed oxidation state tin complex as the final product.



## CHAPTER SIX

### CRYSTAL STRUCTURE OF $[\text{Sn(II)Sn(IV)O}(\text{O}_2\text{CCF}_3)_4]_2\text{C}_6\text{H}_6$

#### A. Introduction

On the basis of the spectroscopic results and physical properties the mixed oxidation state tin carboxylates have been established as true compounds, rather than as simple mixtures of the Sn(II) and Sn(IV) carboxylates (Chapter 5). On the basis of the spectroscopic results it was possible to clearly distinguish between the structural isomers  $[\text{Sn(II)Sn(IV)O}(\text{O}_2\text{CR})_4\text{O}(\text{OCR})_2]_2$  and  $[\text{Sn(II)Sn(IV)}(\text{O}_2\text{CR})_6]_x$ . An X-ray crystallographic investigation was initiated to establish the correct molecular formulation. Although a number of the mixed oxidation state tin carboxylates were found to be soluble to varying degrees in the parent acid and the reaction medium, only fibrous solids were isolated. The trifluoroacetato derivatives could be sublimed without apparent decomposition but only a fibrous solid was obtained. Crystals suitable for single crystal X-ray crystallographic analysis were obtained by carrying out the solvolysis by first dissolving hexaphenylditin in benzene prior to its addition to trifluoroacetic acid, followed by slow crystallization of the soluble product. The bulk crystalline material had  $^{119}\text{Sn}$  Mössbauer parameters indistinguishable from the mixed oxidation state tin trifluoroacetate. Characterization by single crystal X-ray diffraction shows that these crystals are in fact

$[\text{Sn(II)Sn(IV)O}(\text{O}_2\text{CCF}_3)_4]_2\text{C}_6\text{H}_6$ . Several attempts to repeat this preparation failed, preventing further investigation of this product.

B. Experimental for the Crystal Structure of Di- $\mu_3$ -oxo-octakis- $\mu$ -  
(trifluoroacetato)-ditin(II)ditin(IV)-Benzene (1/1)

Good quality single crystals of  $[\text{Sn(II)Sn(IV)O}(\text{O}_2\text{CCF}_3)_4]_2\text{C}_6\text{H}_6$  were obtained from the reaction of hexaphenylditin with trifluoroacetic acid, by the following procedure. Hexaphenylditin, 0.5 g, was added to one side of a two-bulb reaction vessel and 5 cm<sup>3</sup> of dry benzene were condensed onto it. Trifluoroacetic acid, 4 cm<sup>3</sup>, was added to the opposite side of the vessel, separated from the first side by a glass frit. All additions were made in a dry atmosphere glove box. The benzene solution was then filtered to the acid side of the vessel after the solvents had been degassed. After one day, the solvent was slowly condensed to the empty side of the vessel by immersing that side in cold running water overnight. In this way, ninety per cent of the solvent was removed from the solution leaving a pale yellow liquid and clear crystals. The remaining liquid was removed by filtration and the solvent side of the vessel was sealed. The crystals were then pumped dry on a vacuum line. Most of the material was present as thin, clear, crystalline needles. Several crystals were selected for X-ray analysis. The remaining material was used as a sample for <sup>119</sup>Sn Mössbauer spectroscopy at 77°K. Unfortunately, the sample decomposed when warmed to room temperature. The <sup>119</sup>Sn Mössbauer spectrum of the solid was indistinguishable from the product isolated from the direct reaction of hexaphenylditin with trifluoroacetic acid.

In an attempt to reproduce this preparation, 1.96 g of hexaphenylditin were dissolved in 30 cm<sup>3</sup> of dry benzene and reacted with trifluoroacetic acid, 5 cm<sup>3</sup>, for one month. After removal of the yellow solvent by filtration, a white solid was obtained. Tin analysis was inconsistent with the presence of only the title compound, i.e. 25.94% Sn found, 31.91% Sn calculated. However, this analysis is consistent with the product being the original mixed oxidation state compound. The following crystal data were obtained:

$C_{22}H_6F_{24}O_8Sn_4$ ,  $M = 1488.22$ , monoclinic,  $a = 24.182(10) \text{ \AA}$ ,  $b = 9.828(3) \text{ \AA}$ ,  $c = 17.882(6) \text{ \AA}$ ,  $\beta = 104.77(3)$ ,  $U = 4109.40 \text{ \AA}^3$ ,  $Z = 4$ ,  $D_c = 2.405 \text{ g cm}^{-3}$ ,  $F(0,0,0) = 2792$ ,  $\lambda(\text{Mo-K}\alpha) = 0.71069 \text{ \AA}$  and  $\mu(\text{Mo-K}\alpha) = 27 \text{ cm}^{-1}$ .

The unit cell parameters were obtained from a least squares refinement of 15 well-centered reflections with  $8.6^\circ < 2\theta < 23.9^\circ$ . The diffractometer data indicated that reflections were absent for  $hkl$  when  $\underline{h} + \underline{k} = 2n + 1$ , for  $h0l$  when  $\underline{l} = 2n + 1$  or  $\underline{h} = 2n + 1$ , and for  $0k0$  when  $\underline{k} = 2n + 1$ , characteristic of the space group  $C_c$  and  $C_{2/c}$ . The equivalent positions for  $C_{2/c}$  are  $x, y, z$  and  $\bar{x}, y, 1/2 - z$ . A total of 3718 reflections with  $0 < \underline{h} < 30$ ,  $0 < \underline{k} < 12$ ,  $-23 < \underline{l} < 22$  and  $0 < 2\theta < 55$  was obtained after the equivalent reflections were averaged, and reflections, systematically absent, along with those whose intensities were less than the standard counting error,  $\sigma(I)$ , were removed from the initial data set. Of these 3718 reflections, 628 had intensities less than  $3\sigma(I)$ . Two standard reflections which were measured every 48 reflections showed no

Table 6.1

Atomic Coordinates ( $\times 10^4$ ) for  $[\text{Sn(II)Sn(IV)O}(\text{O}_2\text{CCF}_3)_4]_2\text{C}_6\text{H}_6$ 

	y/b	x/a	z/c
Sn(1)	985(7)	2691(2)	-67(3)
Sn(2)	3005(8)	3637(3)	1524(4)
O(1)	2599(6)	2858(2)	673(3)
O(2)	5124(7)	2916(3)	4583(3)
O(3)	4766(8)	3668(3)	603(4)
C(1)	78(11)	1576(4)	5066(6)
C(2)	821(14)	1219(6)	5517(7)
F(1)	2865(10)	3679(4)	4482(6)
F(2)	4507(11)	3655(4)	3769(5)
F(3)	4313(12)	4316(3)	4765(6)
O(4)	4563(8)	2984(3)	1938(4)
O(5)	537(7)	2554(3)	4125(4)
C(3)	447(10)	2327(4)	3389(6)
C(4)	1623(14)	2469(6)	2942(7)
F(4)	1670(11)	2168(5)	2246(5)
F(5)	1583(9)	3001(4)	2922(5)
F(6)	2817(7)	2416(3)	3258(5)
O(6)	545(8)	3542(3)	1732(4)
O(7)	4574(7)	1756(3)	4426(4)
C(5)	349(11)	3538(4)	6258(6)
C(6)	3466(14)	1053(6)	3493(7)
F(7)	2348(9)	1293(4)	3591(8)
F(8)	3461(12)	679(4)	3876(7)
F(9)	3547(12)	9238(6)	2201(5)
O(8)	3519(7)	1659(3)	579(4)
O(9)	3105(8)	9026(3)	5502(4)
C(7)	1674(11)	3855(4)	9822(6)
C(8)	1606(17)	4489(7)	9348(9)
F(10)	1848(17)	4786(4)	9792(6)
F(11)	2456(15)	4184(5)	8790(8)
F(12)	4506(14)	712(5)	980(8)
C(9)	4481(18)	5064(7)	2143(10)
C(10)	3256(26)	5111(6)	1797(8)
C(11)	2056(18)	5062(5)	2162(8)

Table 6.2. Thermal Parameters<sup>a</sup> for [Sn(II)Sn(IV)O(O<sub>2</sub>CCF<sub>3</sub>)<sub>4</sub>]<sub>2</sub> C<sub>6</sub>H<sub>6</sub>

	U <sub>11</sub>	U <sub>22</sub>	U <sub>33</sub>	U <sub>12</sub>	U <sub>13</sub>	U <sub>23</sub>
Sn( 1)	353( 3)	475( 4)	402( 3)	-6( 3)	55( 2)	-31( 3)
Sn( 2)	419( 4)	622( 5)	436( 4)	5( 3)	1( 3)	-41( 3)
F( 1)	2506( 93)	1801( 73)	2147( 79)	512( 70)	615( 70)	-285( 64)
F( 2)	1945( 67)	2950(110)	1524( 53)	750( 71)	737( 50)	223( 62)
F( 3)	1240( 47)	3317(129)	2253( 82)	279( 64)	425( 48)	-655( 82)
F( 4)	3400(126)	2217( 86)	1356( 51)	-1122( 85)	-289( 66)	527( 54)
F( 5)	2250( 82)	1878( 68)	2208( 78)	-54( 61)	1191( 68)	215( 60)
F( 6)	1996( 64)	1377( 52)	1980( 62)	0( 47)	647( 52)	252( 45)
F( 7)	1907( 73)	1273( 56)	3799(146)	-182( 52)	462( 86)	-53( 71)
F( 8)	1894( 74)	3084(127)	2785(104)	-1079( 85)	1100( 76)	-698( 98)
F( 9)	3431(139)	2351(101)	1664( 68)	1050( 98)	-470( 80)	192( 65)
F(10)	1360( 57)	5085(215)	2280( 94)	-448( 92)	789( 62)	-664(117)
F(11)	2509(109)	3403(167)	2767(118)	513(107)	1563(102)	1071(119)
F(12)	2417(107)	2889(136)	2585(153)	-311( 98)	1754(110)	-1371(131)
C( 9)	775(108)	1296(138)	1460(195)	-229(127)	-279(147)	605(114)
C(10)	472( 70)	2377(246)	579( 83)	-332(131)	41( 58)	146(121)
C(11)	297( 57)	1525(139)	1118( 52)	15( 83)	-6( 74)	-426(104)

..... continued

Table 6.2 continued

	$U(\text{\AA}^2)$
O(1)	406(13)
O(2)	499(15)
O(3)	680(20)
C(1)	558(25)
C(2)	734(32)
O(4)	687(20)
O(5)	532(17)
C(3)	518(24)
C(4)	735(33)
O(6)	668(20)
O(7)	538(16)
C(5)	530(24)
C(6)	710(31)
O(8)	503(16)
O(9)	679(20)
C(7)	516(24)
C(8)	880(40)

<sup>a</sup>Temperature factors ( $\times 10^4$ ) in the form  $\exp(-2\pi^2 \sum_{ij} U_{ij} H_i H_j a_i^* a_j^*)$  with standard deviations in parentheses.

significant variation during data collection. No correction for absorption was necessary since  $\mu(\text{Mo-K}\alpha) = 26 \text{ cm}^{-1}$ .

The structure was determined by a procedure similar to that described in Chapter 4 of this thesis. The least squares refinement converged at  $R = 0.054$  and  $R' = 0.058$ . The secondary extinction correction defined by Larson<sup>81</sup> with  $F^* = F[1+0.36 \times 10^{-8} \times \beta(2\sigma)F^2]^{1/2}$  and weighting scheme defined by  $\omega = |\sigma^2 + (0.025F_0)^2|^{-1}$  were used. The maximum value of the shift over error was 0.058 for the U(1,1) of the C(10) atom, while the average shift over error for all variables was 0.0096. The final value of  $[\Sigma\omega(|F_o| - |F_c|)^2 / (N_F - N_p)]^{1/2} = 1.29$  where  $N_p = 223$ . A final difference map did not reveal the positions of the hydrogen atoms of the benzene ring. The largest feature was  $0.5 \text{ e } \text{Å}^{-3}$  in the vicinity of the tin atoms. Atomic scattering factors corrected for anomalous dispersion were taken from reference 82. The final atomic coordinates of the atoms in the asymmetric unit are given in Table 6.1. The temperature factors are given in Table 6.2. Structure factors are presented in Table 2, J. P. Johnson, McMaster University Thesis Tables #1, June 1983, and are available from Thode Library, McMaster University.

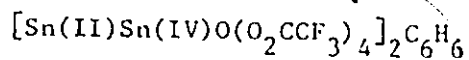
### C. Results and Discussion

#### (i) Crystal Structure of $[\text{Sn(II)Sn(IV)O}(\text{O}_2\text{CCF}_3)_4]_2\text{C}_6\text{H}_6$

The bond lengths and bond angles for  $[\text{Sn(II)Sn(IV)O}(\text{O}_2\text{CCF}_3)_4]_2\text{C}_6\text{H}_6$  are given in Table 6.3. Deviation in Å of atoms from least squares planes are given in Table 6.4.



Table 6.3. Bond Lengths (Å) and Bond Angles (°) for

Tin Co-ordination

## (a) Bond lengths (Å)

Sn(1)-O(1)	2.040(6)	Sn(2)-O(1)	2.136(5)
Sn(1)-O(1)'	2.035(5)	Sn(2)-O(3)	2.403(8)
Sn(1)-O(2)	2.065(7)	Sn(2)-O(4)	2.446(8)
Sn(1)-O(5)	2.047(6)	Sn(2)-O(6)	2.466(8)
Sn(1)-O(7)	2.060(6)	Sn(2)-O(9)	2.509(8)
Sn(1)-O(8)	2.070(7)	Sn(2)-C(9)'	3.720(12)
Sn(2)-C(9)	3.645(17)	Sn(2)-C(10)'	3.689(12)
Sn(2)-C(10)	3.481(14)	Sn(2)-C(11)'	3.538(12)
Sn(2)-C(11)	3.470(12)		

## (b) Bond angles (°)

O(1)-Sn(1)-O(1)'	78.93 (21)	O(1)-Sn(2)-O(3)	79.77 (22)
O(1)-Sn(1)-O(2)	95.20 (25)	O(1)-Sn(2)-O(4)	79.17 (22)
O(1)-Sn(1)-O(5)	174.92 (26)	O(1)-Sn(2)-O(6)	79.93 (21)
O(1)-Sn(1)-O(7)	99.72 (23)	O(1)-Sn(2)-O(9)	80.00 (23)
O(1)-Sn(1)-O(8)	93.22 (25)	O(3)-Sn(2)-O(4)	83.80 (27)
O(1)'-Sn(1)-O(2)	93.81 (24)	O(3)-Sn(2)-O(6)	146.10 (25)
O(1)'-Sn(1)-O(5)	99.10 (23)	O(3)-Sn(2)-O(9)	74.40 (26)
O(1)'-Sn(1)-O(7)	178.42 (25)	O(4)-Sn(2)-O(6)	118.40 (27)
O(1)'-Sn(1)-O(8)	93.99 (24)	O(4)-Sn(2)-O(9)	152.11 (23)
O(2)-Sn(1)-O(5)	89.58 (26)	O(6)-Sn(2)-O(9)	75.54 (26)
O(2)-Sn(1)-O(7)	85.48 (26)		
O(2)-Sn(1)-O(8)	169.49 (26)	C(9)-Sn(2)-C(10)	22.0 (5)
O(5)-Sn(1)-O(7)	82.32 (24)	C(10)-Sn(2)-C(11)	22.1 (5)
O(5)-Sn(1)-O(8)	82.23 (26)	C(11)-Sn(2)-C(11)'	21.6 (4)
O(7)-Sn(1)-O(8)	86.90 (26)	C(11)'-Sn(2)-C(10)'	21.7 (5)
		C(10)'-Sn(2)-C(9)'	21.3 (5)
Sn(1)-O(1)-Sn(1)	101.07 (21)	C(9)'-Sn(2)-C(9)	21.7 (5)
Sn(1)-O(1)-Sn(2)	126.94 (28)	C(9)'-Sn(2)-C(11)	44.9 (4)
Sn(1)-O(1)-Sn(2)	126.04 (27)	C(9)-Sn(2)-C(11)'	44.8 (4)
		C(10)-Sn(2)-C(10)	44.2 (3)
Sn(1)-O(2)-C(1)	124.7 (6)		
Sn(2)-O(3)-C(1)	139.0 (7)	O(1)-Sn(2)-C(9)	152.3 (3)
Sn(1)-O(5)-C(3)	128.2 (6)	O(1)-Sn(2)-C(10)	143.0 (3)
Sn(2)-O(4)-C(3)	132.8 (7)	O(1)-Sn(2)-C(11)	143.7 (3)
Sn(1)-O(7)-C(5)	129.1 (7)	O(1)-Sn(2)-C(9)'	167.6 (4)
Sn(2)-O(6)-C(5)	125.8 (7)	O(1)-Sn(2)-C(10)'	169.7 (4)
Sn(1)-O(8)-C(7)	121.7 (6)	O(1)-Sn(2)-C(11)'	153.8 (3)
Sn(2)-O(9)-C(7)	135.9 (7)		

..... continued

Table 6.3 continued

Trifluoroacetate

## (a) Bond lengths (Å)

C(1)-O(2)	1.245(11)	C(5)-O(7)	1.250(13)
C(1)-O(3)	1.229(11)	C(5)-O(6)	1.219(13)
C(1)-C(3)	1.510(18)	C(5)-C(6)	1.520(16)
C(2)-F(1)	1.315(17)	C(6)-F(7)	1.244(16)
C(2)-F(2)	1.278(15)	C(6)-F(8)	1.267(19)
C(2)-F(3)	1.272(14)	C(6)-F(9)	1.262(15)
C(3)-O(5)	1.293(11)	C(7)-O(8)	1.279(11)
C(3)-O(4)	1.199(12)	C(7)-O(9)	1.200(12)
C(3)-C(4)	1.494(18)	C(7)-C(8)	1.510(21)
C(4)-F(4)	1.271(14)	C(8)-F(10)	1.240(16)
C(4)-F(5)	1.298(18)	C(8)-F(11)	1.277(21)
C(4)-F(6)	1.323(16)	C(8)-F(12)	1.241(22)

## (b) Bond angles (°)

O(2)-C(1)-O(3)	128.1 (10)	O(6)-C(5)-O(7)	128.8 (9)
O(2)-C(1)-C(2)	115.6 (9)	O(6)-C(5)-C(6)	117.3 (8)
O(3)-C(1)-C(2)	116.2 (9)	O(7)-C(5)-C(6)	114.0 (9)
C(1)-C(2)-F(1)	110.1 (12)	C(5)-C(6)-F(7)	113.3 (10)
C(1)-C(2)-F(2)	113.0 (11)	C(5)-C(6)-F(8)	110.3 (11)
C(1)-C(2)-F(3)	113.4 (11)	C(5)-C(6)-F(9)	113.5 (12)
F(1)-C(2)-F(2)	104.4 (11)	F(7)-C(6)-F(8)	107.0 (13)
F(1)-C(2)-F(3)	105.9 (12)	F(7)-C(6)-F(9)	108.5 (13)
F(2)-C(2)-F(3)	109.5 (12)	F(8)-C(6)-F(9)	103.7 (12)
O(4)-C(3)-O(5)	126.6 (10)	O(8)-C(7)-O(9)	129.1 (10)
O(4)-C(3)-C(4)	120.0 (9)	O(8)-C(7)-C(8)	113.2 (9)
O(5)-C(3)-C(4)	113.4 (9)	O(9)-C(7)-C(8)	117.7 (9)
C(3)-C(4)-F(4)	113.6 (11)	C(7)-C(8)-F(10)	114.0 (13)
C(3)-C(4)-F(5)	110.8 (10)	C(7)-C(8)-F(11)	112.4 (13)
C(3)-C(4)-F(6)	113.4 (11)	C(7)-C(8)-F(12)	112.8 (14)
F(4)-C(4)-F(5)	107.4 (13)	F(10)-C(8)-F(11)	105.5 (15)
F(4)-C(4)-F(6)	107.0 (11)	F(10)-C(8)-F(12)	108.0 (15)
F(5)-C(4)-F(6)	104.0 (11)	F(11)-C(8)-F(12)	103.3 (15)

Benzene

## (a) Bond lengths (Å)

C(9)-C(9)'	1.389(27)
C(9)-C(10)	1.372(30)
C(10)-C(11)	1.368(29)
C(11)-C(11)'	1.317(22)

## (b) Bond angles (°)

C(9)-C(9)-C(10)	118.6 (17)
C(9)-C(10)-C(11)	120.9 (15)
C(11)-C(11)-C(10)	120.4 (17)

Primes denote symmetry related atoms.

Table 6.4. Deviations in Å, of Atoms From a Least Squares Plane

Tin(II)Tin(IV)<sub>2</sub>-oxo plane

Sn( 1)	-0.001( 6)	Sn( 1)'	0.001( 5)
Sn( 2)	-0.095( 5)	Sn( 2)'	0.095( 5)
O( 1)	0.253( 5)	O( 1)'	-0.253( 5)

Tin(II)-oxvqen basal plane

*Sn( 2)	0.440( 8)	O( 6)	0.007( 8)
O( 3)	0.009( 8)	O( 9)	-0.010( 8)
O( 4)	-0.006( 8)		

Benzene ring

C( 9)	-0.01( 3)	C( 9)'	-0.01( 3)
C(10)	-0.01( 3)	C(10)'	0.01( 3)
C(11)	0.01( 3)	C(11)'	-0.01( 3)
*Sn( 2)	-3.30( 1)	*Sn( 2)'	3.30( -1)

Tin(IV)-oxvqen planes

Sn( 1)	-0.056( 6)	O( 7)	-0.040( 6)
O( 1)	0.056( 6)	O( 5)	0.055( 6)
O( 1)'	-0.043( 5)		
Sn( 1)	0.032( 7)	O( 1)	0.061( 6)
O( 8)	-0.086( 7)	O( 5)	-0.073( 6)
O( 2)	-0.081( 7)		
Sn( 1)	0.042( 7)	O( 7)	0.071( 6)
O( 1)'	0.060( 5)	O( 8)	-0.086( 7)
O( 2)	-0.087( 7)		

Trifluoroacetate

O( 2)	0.00( 1)	*F( 1)	-1.22( 2)
O( 3)	0.00( 1)	*F( 2)	0.69( 2)
C( 1)	0.01( 2)	*F( 3)	0.37( 1)
C( 2)	0.00( 2)		
O( 4)	0.00( 1)	*F( 4)	0.23( 1)
O( 5)	0.00( 1)	*F( 5)	-1.13( 2)
C( 3)	-0.01( 2)	*F( 6)	0.69( 2)
O( 6)	0.00( 1)	*F( 7)	-0.93( 2)
O( 7)	0.00( 1)	*F( 8)	1.08( 2)
C( 5)	-0.01( 2)	*F(-9)	-0.02( 2)
C( 6)	0.00( 2)		
O( 8)	0.00( 1)	*F(10)	0.06( 2)
O( 9)	0.00( 1)	*F(11)	0.99( 2)
C( 7)	0.00( 2)	*F(12)	-0.98( 2)
C( 8)	0.00( 2)		

\*These atoms were not used in the calculation of the least squares plane.

Prime denotes symmetry-related atoms.

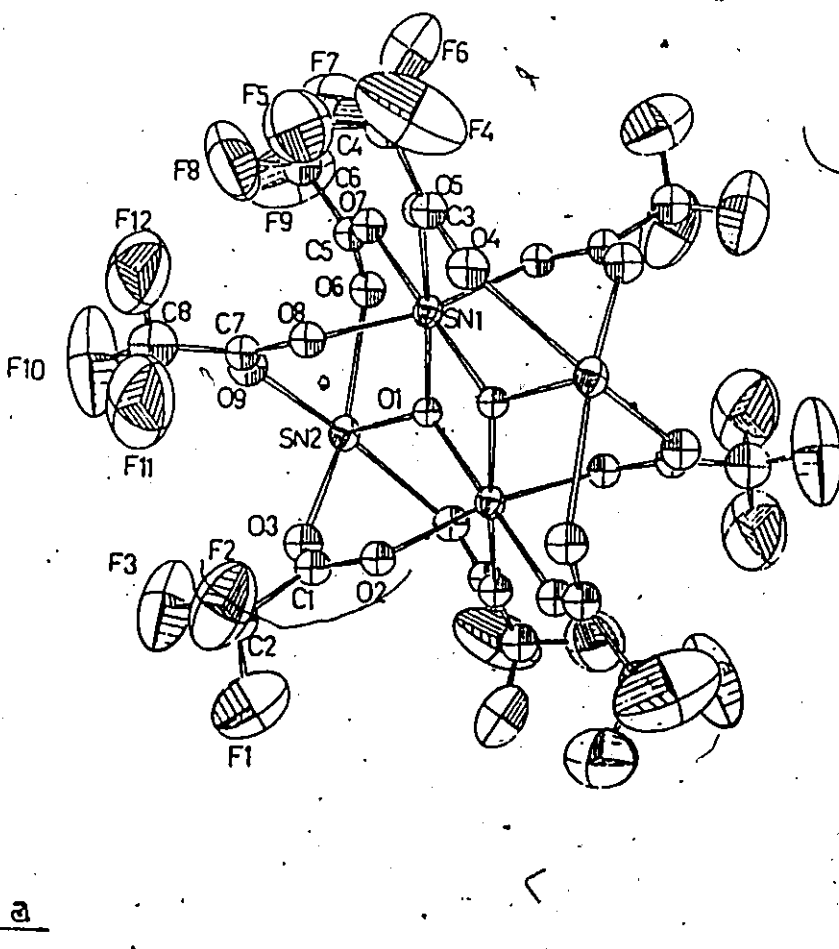


Figure 6.1. The molecular structure of the  $[\text{Sn}(\text{II})\text{Sn}(\text{IV})\text{O}(\text{OOCCF}_3)_4]_2$ , view down the  $c$  axis, with 10% probability vibration ellipsoids for the atoms. The benzene molecules have been omitted for clarity.

The molecular structure of octakis- $\mu$ -(trifluoroacetato)-di- $\mu_3$ -oxo-ditin(II)-ditin(IV)-1-benzene consists of independent centrosymmetric  $[\text{Sn(II)Sn(IV)O}(\text{O}_2\text{CCF}_3)_4]_2$  units; Figure 6.1. The central feature of the cluster is a  $\text{Sn(IV)}_2\text{O}_2$  ring in which two  $\mu_3$  oxygen atoms form a bridge to two symmetry related tin(IV) atoms. Octahedral coordination at tin(IV) is completed by four independent trifluoroacetato groups which bridge both a tin(IV) and a tin(II) atom. The remaining coordination site of the three coordinate oxygen atom is occupied by a tin(II) atom of the cluster to yield an almost planar  $\text{Sn(II)-O} \begin{array}{c} \text{Sn(IV)} \\ \diagup \quad \diagdown \\ \text{O} \end{array} \text{O-Sn(II)}$  unit. The tin(II) atoms have a distorted square pyramidal geometry with the apical site occupied by a  $\mu_3$  oxygen atom, and the basal positions by oxygens from bridging trifluoroacetates. The remaining apical site is presumably occupied by a non-bonding electron pair.

Three coordinate oxygen atoms are a common feature in oxo-organo-tin(IV)<sup>89,90</sup> compounds. The  $\text{Sn(II)-O} \begin{array}{c} \text{Sn(IV)} \\ \diagup \quad \diagdown \\ \text{O} \end{array} \text{O-Sn(II)}$  unit is similar to the planar tin(IV)-oxo units in  $\{[(\text{CH}_3)_2\text{Sn}(\text{O}_2\text{CCF}_3)]_2\text{O}\}_2$  (Chapter 4), where the tin(II) atoms are replaced by tin(IV) atoms. In fact, both the tin-oxygen bond distances,  $\text{Sn-O} \sim 2.1\text{\AA}$ , and geometry of the tin-oxo unit ( $\text{O-Sn-O}$ ,  $78^\circ$ ;  $\text{Sn-O-Sn}$ ,  $102^\circ$ ), appear to be independent of the oxidation state of the tin atom and the ligands which satisfy the remaining coordination sites of the atoms. Based on the structural data for  $\{[(\text{CH}_3)_2\text{Sn}(\text{O}_2\text{CR})]_2\text{O}\}_2$  ( $\text{R} = \text{CCl}_3, \text{CF}_3$ , this work),  $\{[(n\text{-Bu})_2\text{Sn}(\text{O}_2\text{CCl}_3)]_2\text{O}\}_2$ ,<sup>89</sup>  $\{[(\text{CH}_2=\text{CH})_2\text{Sn}(\text{O}_2\text{CCF}_3)]_2\text{O}\}_2$ ,<sup>90</sup> and the mixed oxidation state tin carboxylate  $[\text{Sn(II)Sn(IV)O}(\text{O}_2\text{CC}_6\text{H}_4\text{NO}_2\text{-o})_4\text{THF}]_2$ ,<sup>105</sup> the geometry of these molecules is built around an essentially planar  $\text{Sn}_4\text{O}_2$  unit.

Two of the four independent trifluoroacetato groups of the molecular unit are approximately coplanar with the  $\text{Sn(IV)}_2\text{O}_2$  ring. The oxygen atoms of the coplanar trifluoroacetato groups, O(5) and O(7), are trans with respect to the  $\mu_3$  oxygen atoms attached to the tin(IV) atom. One of each type of trifluoroacetato groups is very asymmetric. The C-O groups bonded to tin(II), C(3)-O(4), 1.199(12)Å; C(7)-O(9), 1.200(12)Å, are 0.09Å shorter than those bonded to tin(IV), C(3)-O(5), 1.293(11)Å; C(7)-O(8), 1.279(11)Å. This shortening is a consequence of the greater degree of covalent character in the tin(IV) oxygen bonds, Sn(IV)-O = 2.06Å, compared to the tin(II) oxygen bonds, Sn(II)-O = 2.45Å. The other two carboxylates follow the same pattern. The C-O distances are

consistent with a  $\text{Sn(IV)-O}-\overset{\text{R}}{\text{C}}=\text{O}+\text{Sn(II)}$  bonding arrangement and compare reasonably well with the C=O and C-O distances, 1.190(9) and 1.263(10)Å, found in  $\{[(\text{CH}_3)_2\text{Sn}(\text{O}_2\text{CCF}_3)]_2\text{O}\}_2$ . The bridging carboxylates in the above compound have C-O distances of 1.212(11) and 1.213(10)Å. The

$\text{Sn(IV)-O}-\overset{\text{R}}{\text{C}}=\text{O}+\text{Sn(II)}$  pattern is also observed in  $[\text{Sn(II)Sn(IV)O}(\text{O}_2\text{CC}_6\text{H}_4\text{NO}_2-\text{o})_4\text{THF}]_2^{105}$  with the C=O to the Sn(II) distances of ~ 1.21(1)Å and the C-O to the Sn(IV) distances, 1.26(2)-1.30(1)Å. The difference in C-O bond lengths also causes a distortion in the C-C-O angles. The short C-O bond, that is the one bonded to the tin(II) atom, has more double bond character, and this results in an increase in one C-C-O angle at the expense of the other, O(4)-C(3)-C(4), 120.0(9)°; O(5)-C(3)-C(4), 113.4(9)°, because of the difference in bond-bond repulsions. Only C(2)-C(1)  $\begin{matrix} \text{O(3)} \\ \text{O(2)} \end{matrix}$  does not follow this pattern.

However, the complex  $[\text{Sn(II)Sn(IV)O}(\text{O}_2\text{CC}_6\text{H}_4\text{NO}_2\text{-o})_4\text{THF}]_2$ ,<sup>105</sup> although different in structure to that reported here, also shows these distortions in the angles.

The tin(IV) atom has a distorted octahedral arrangement of oxygen atoms with the O-Sn-O bond angles ranging from  $78.91(21)^\circ$  to  $99.72(23)^\circ$ . The Sn(IV)-O distances are quite short and vary over the narrow range 2.040(6) to 2.070(7)Å. The tin-oxo bridged distances are at the lower end of this range. The tin(IV)-carboxylate oxygen distances are at the lower end of the range of such distances (1.88-2.46Å) found for Sn(IV)-carboxylate compounds. The average tin(IV)-oxygen distance of 2.3Å found in  $(\text{CH}_3)_4\text{Sn}(\text{O}_2\text{CCF}_3)_2$  and  $\{[(\text{CH}_3)_2\text{Sn}(\text{O}_2\text{CCF}_3)]_2\text{O}\}_2$  and related organotin(IV) trifluoroacetates is significantly longer than the distances found here. The related mixed oxidation state tin carboxylate  $[\text{Sn(II)Sn(IV)O}(\text{O}_2\text{CC}_6\text{H}_4\text{NO}_2\text{-o})_4\text{THF}]_2$ <sup>105</sup> has the same stereochemistry at the tin(IV) site. Both the ortho-nitrobenzoato mixed oxidation state tin compound and the compound discussed here have virtually identical Sn(IV)-O distances at 2.056(8) to 2.067(7)Å.

Each tin(II) in the  $[\text{Sn(II)Sn(IV)O}(\text{O}_2\text{CCF}_3)_4]_2$  molecular unit is bonded to five oxygen atoms in a distorted square pyramidal arrangement. The Sn(II)-O apical distance of 2.136(5)Å is substantially shorter than the Sn(II)-O basal distances which range from 2.403(8) to 2.509(8)Å, these values being typical Sn(II)-O distances. Coordination number five is not common for tin(II) although it has been observed previously for the compound  $(\text{C}_6\text{H}_5)_3\text{Sn(IV)Sn(II)NO}_3$ ,<sup>125,126</sup> in which tin(IV) occupies one coordination site, the remaining positions being occupied by oxygen atoms

of the nitrate groups. However, the distortion is so severe that it is difficult even to describe the geometry at tin(II).

In the  $[\text{Sn(II)Sn(IV)O}(\text{O}_2\text{CC}_6\text{H}_4\text{NO}_2\text{-o})_4\text{THF}]_2$  complex prepared by Harrison et al.<sup>105</sup> the geometry at the Sn(II) atoms is somewhat different to that observed here, being that of a pentagonal bipyramid with an electron pair presumably occupying the vacant axial position. The arrangement of the five oxygen atoms in the equatorial plane would ideally be with O-Sn(II)-O angles of  $72^\circ$ , but in fact they range from  $68.9(3)^\circ$  to  $76.1(3)^\circ$ . The tin(II) atom lies 0.32Å below the basal plane of these five oxygens and the O(apical)-Sn(II)-O(basal) angle ranges from  $89.5(3)^\circ$  to  $78.4(3)^\circ$ .

The geometry about the tin(II) in the structure discussed here is different. There are only four oxygens in the basal plane which are displaced towards the apical oxygen so that the tin(II) lies 0.440(8)Å below the mean plane of these oxygen atoms, Table 6.4. The O(basal)-Sn(II)-O(apical) angles are substantially reduced from  $90^\circ$ ;  $79.17(22)^\circ$  to  $80.00(23)^\circ$ . The additional reduction of the O(basal)-Sn(II)-O(apical) angles from the pentagonal bipyramid is a reflection of one less oxygen to share the lone pair-bond pair repulsions. The O(basal)-Sn(II)-O(apical) angles of  $\sim 80^\circ$  in the distorted square pyramidal arrangement found here is strong evidence that the non-bonding electron pair of the Sn(II) occupies the second apical position of an octahedron, with the lone pair-bond pair repulsions accounting for the observed distortions. This effect is also reflected in the distortions in the O-Sn(IV)-O angles. Comparison of the symmetrically bridging trifluoroacetate in  $\{[(\text{CH}_3)_2\text{Sn}(\text{O}_2\text{CCF}_3)]\text{O}\}_2$  (Figure 4.4), clearly shows that a lone pair on



one tin site would move the bridging trifluoroacetato group towards the tin(IV) atom. This is manifested in the structure here by large Sn(II)-O-C angles,  $\sim 118^\circ$ , and smaller Sn(IV)-O-C angles,  $\sim 114^\circ$ . The reduction of the O(8)-Sn(IV)-O(2) angles to  $169.49(26)^\circ$  from  $180^\circ$ , and O(7)-Sn(IV)-O(5) angles to  $82.32(24)^\circ$  from  $90^\circ$ , is clearly the result of a lone pair in the second apical site at tin(II). The one O-Sn(IV)-O angle not accounted for is O(1)-Sn(IV)-O(1)' at  $78.93(21)^\circ$  which is typical for a  $\text{Sn(IV)}_2\text{O}_2$  ring.

A more interesting aspect of the structure concerns the distortion of the O(basal)-Sn(II)-O(basal) angles from the ideal value of  $90^\circ$ . These angles are not all equal but vary from  $74.40(26)^\circ$  to  $118.40(27)^\circ$ , the largest of these being between O(4) and O(6). It is not possible to locate the non-bonded electron pair in this space, rather than the position discussed above, and still rationalise the arrangement of atoms about the tin(II) atom. The observed arrangement of the angles in the basal plane is a compromise between the O(basal)-Sn(II) bonds being at  $90^\circ$  to one another in order to minimize bond pair-bond pair repulsions, and the desire for the  $-\text{CO}_2$  groups to be coplanar with the tin(II) and tin(IV) atoms. In order to preserve the coplanarity of the  $\text{Sn(IV)}_2\text{O}_2$  ring and at the same time retain the octahedral arrangement at tin(IV), the bridging trifluoroacetato ligand cannot remain coplanar with the tin(II) and tin(IV) atoms. A coplanar arrangement of, for example, Sn(1)-O(7)-C(5)-O(6)-Sn(2), would result in the O(6)-Sn(2)-O(4)' angle being  $180^\circ$  and coincidence of O(3) and O(9), which desire to be perpendicular to the  $\text{Sn(IV)}_2\text{O}_2$  ring; clearly an impossible situation. The tin trifluoroacetato linkage therefore undergoes a twist, destroying

the potential coplanar arrangement and the O(6)-Sn(2)-O(4)' angle opens up from the ideal of  $90^\circ$  to  $118.40(27)^\circ$ , while the O(3)-Sn(2)-O(9) angle closes down from  $90^\circ$  to  $74.40(26)^\circ$ . As a result, the tin(II) is no longer coplanar with the Sn(IV) $_2$ O $_2$  ring. This arrangement then creates a large open space above the O(6)-Sn(2)-O(4)' angle which could accommodate another ligand. The geometry of the tin(II) appears to be a pentagonal bipyramid with one basal position vacant. In the case of Harrison's ortho-nitrobenzoato complex,<sup>105</sup> this vacant space is used to accommodate a molecule of tetrahydrofuran which results in five oxygens being in the basal plane of the Sn(II) atom and the O(basal)-Sn(II)-O(basal) angles are  $\sim 72^\circ$ . This site is unoccupied in the mixed oxidation state tin trifluoroacetate structure reported here.

There are large open spaces in the unit cell located between regions presumably occupied by a non-bonded pair of the Sn(II) atoms of adjacent  $[\text{Sn(II)Sn(IV)O}(\text{O}_2\text{CCF}_3)_4]_2$  units which accommodate molecules of benzene. Each benzene is shared by two tin(II) atoms on opposite faces of the benzene ring. This arrangement is illustrated in Figure 6.2, the trifluoroacetato groups being omitted for clarity. The Sn(II)-carbon(benzene) distances, although quite long at 3.5Å, are still shorter than the sum of van der Waals radii for Sn(II) and C, i.e. 4Å.<sup>127</sup> These distances are slightly longer than those found in  $\text{C}_6\text{H}_6\text{Sn}(\text{AlCl}_4)_2\text{C}_6\text{H}_6$ , where the tin-carbon distance is 3.08Å.<sup>127</sup> In the latter compound each benzene is coordinated to one tin, whereas here the benzene is shared by two tin atoms. In both compounds the C-C distances are indistinguishable from free benzene. Also, in this case, the metal atom does not lie on

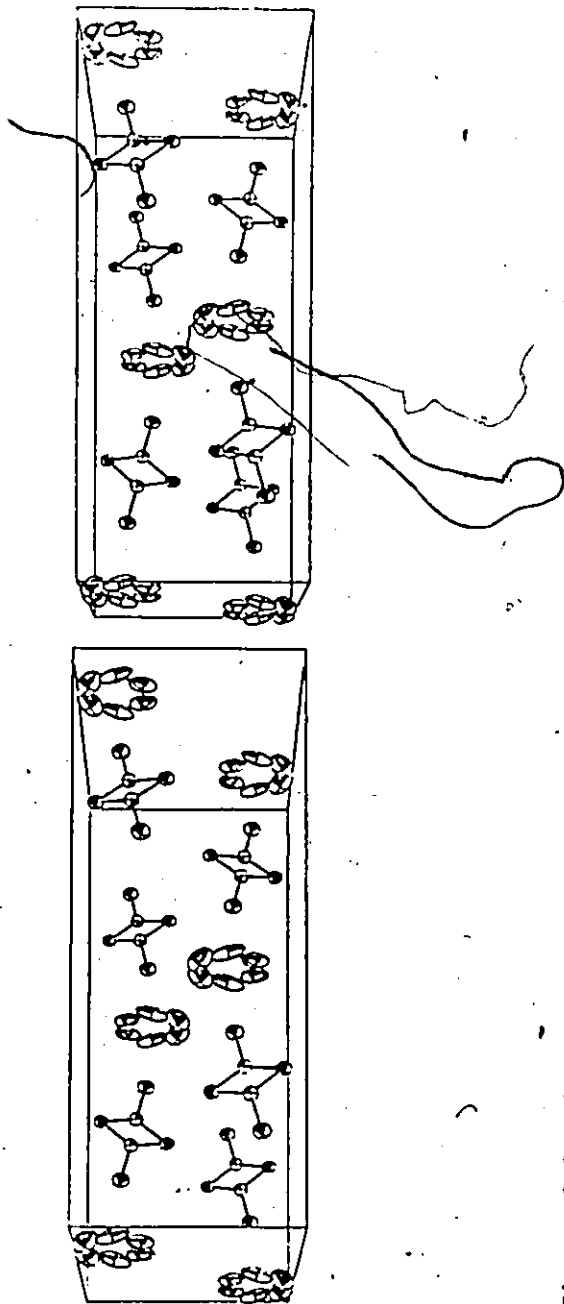
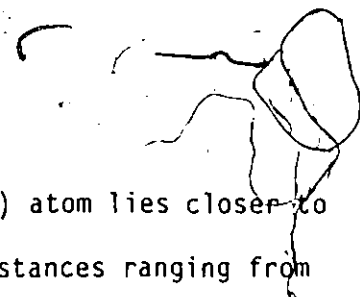


Figure 6.2. A stereoscopic view of the molecular packing of benzene rings and  $\text{Sn}_4\text{O}_2$  units. The contents of one unit cell are shown plus other atoms outside the unit cell to show the packing with 50% probability vibration ellipsoids for the atoms and with trifluoroacetates omitted for clarity. The crystallographic  $a$  axis lies along the horizontal direction, the  $b$  axis on the vertical direction, and the  $c$  axis completes the right handed co-ordinate system.



the six-fold axis of the benzene ring. The tin(II) atom lies closer to C(10), C(11) and C(11)' of the benzene ring, at distances ranging from 3.470(12) to 3.538(12)Å, than it does to the other three carbons, C(9), C(9)' and C(10)'; these latter distances range from 3.645(17) to 3.720(12)Å (Table 6.5). The Sn(II)-O(apical) bond does not lie on the six-fold axis; the projection of the Sn(2)-O(1) bond vector intersects the plane of the benzene ring at an angle of 76°. This results in a zig-zag arrangement of [Sn(II)Sn(IV)O]<sub>2</sub> cluster units and benzene molecules as shown in Figure 6.2. If this arrangement were the result of some interaction between the π electron cloud of the benzene ring with the empty d orbitals on tin(II), one might have expected a more symmetrical location of the benzene ring. However, if the interaction is weak, as indicated by the long Sn(II)-C(benzene) distances compared to cyclopentadienyltin(II) complexes, cf. 2.2Å,<sup>127</sup> only small interactions would be necessary to cause the observed distortion.

One possibility is that there are hydrogen bonded interactions between benzene hydrogen and fluorine atoms of the trifluoroacetato ligands. Estimation of the hydrogen positions (Table 6.5), shows the presence of three significant (i.e. ~ 3Å), hydrogen-fluorine interactions which are longer than the sum of the van der Waals radii of 2.70-3.05Å.<sup>128,129</sup> One of these interactions is between a hydrogen and fluorine in the same zig-zag chain, while the other two hydrogen bonds are to fluorines in adjacent chains. These interactions are probably one reason for the unusual orientation of the benzene in this compound. Hydrogen-fluorine interactions of this kind may account for the fact that

Table 6.5. Estimation of Hydrogen Bonding Interactions

CALCULATED POSITIONS OF HYDROGEN ATOMS OF BENZENE RING

	<u>x/a</u>	<u>y/b</u>	<u>z/c</u>
H( 9)	0.506	0.544	0.187
H(10)	0.511	0.326	0.119
H(11)	0.506	0.106	0.187

BOND LENGTHS (Å) AND BOND ANGLES (°) OF BENZENE RING

C( 9)-H( 9)	1.06	H( 9)-C( 9)-C(10)	125
C(10)-H(10)	1.09	H( 9)-C( 9)-C( 9)'	116
C(11)-H(11)	1.11	H(10)-C(10)-C( 9)	118
		H(10)-C(10)-C(11)	120
		H(11)-C(11)-C(10)	121
		H(11)-C(11)-C(11)'	118

H---F INTERACTIONS (Å)

H(10)---F( 3)	2.67
H(10)---F(10)	2.89*
H(11)---F(12)	2.99

\* Intramolecular

Prime denotes symmetry-related atoms.

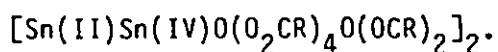
not all of the  $\text{CF}_3$  groups lie in their lowest energy configuration. One might have expected that within each  $\text{F}_3\text{C}-\text{CO}_2$  one fluorine would lie above the  $\text{C}-\text{CO}_2$  plane, while the other two would lie below this plane. This is not the case as can be seen in Table 6.5. There are seven long range F---F repulsive interactions, 2.95(3)-3.27(3)Å, between  $\text{CF}_3$  groups. Presumably a balance between H---F attractions and F---F repulsions determines the orientation of the  $\text{CF}_3$  groups. The large anisotropic temperature factors associated with the fluorine atoms indicate that their positions are not rigid within the lattice, which makes further analysis difficult.

(ii) Mechanism of Formation of  $[\text{Sn(II)Sn(IV)O}(\text{O}_2\text{CCF}_3)_4]_2\text{C}_6\text{H}_6$

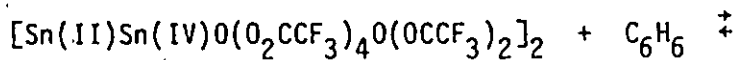
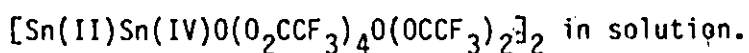
As discussed previously the similarity of the  $^{119}\text{Sn}$

Mössbauer parameters for Harrison's ortho-nitrobenzoato complex  $[\text{Sn(II)Sn(IV)O}(\text{O}_2\text{C}_6\text{H}_4\text{NO}_2\text{-o})_4\text{THF}]_2^{105}$  and the mixed oxidation state tin carboxylates reported in this thesis suggested that the structural isomer  $[\text{Sn(II)Sn(IV)O}(\text{O}_2\text{CR})_2\text{O}(\text{OCR})_2]_2$  was more likely than  $[\text{Sn(II)Sn(IV)}(\text{O}_2\text{CR})_6]_x$ . Both the mixed oxidation state tin ortho-nitrobenzoate and the trifluoroacetato  $[\text{Sn(II)Sn(IV)O}(\text{O}_2\text{CCF}_3)_4]_2\text{C}_6\text{H}_6$  complexes are composed of the same basic  $[\text{Sn(II)Sn(IV)O}(\text{O}_2\text{CR})_4]_2$  unit.<sup>6</sup> The large angle between O(4)-Sn(II)-O(6) in the trifluoroacetate complex could be used to accommodate other base molecules, tetrahydrofuran for example in the ortho-nitrobenzoato complex, with only slight changes in bond angles at tin(II) being necessary. The similarity of the  $^{119}\text{Sn}$  Mössbauer data of the mixed oxidation state tin carboxylates to those

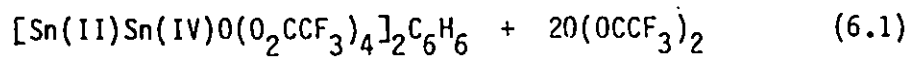
of the trifluoroacetato complex discussed here, strongly suggests that they have the same basic oxo-bridged structure, but with the vacant position in the basal plane being taken up by an oxygen atom of an anhydride molecule. Their molecular formula would then be



The formation of  $[\text{Sn(II)Sn(IV)O}(\text{O}_2\text{CCF}_3)_4]_2\text{C}_6\text{H}_6$  from the solvolysis of hexaphenylditin by trifluoroacetic acid is thought to take place by the displacement of trifluoroacetic anhydride from



(I)



(II)

The molecule of anhydride would be expected to be rather difficult to replace since (I) may be sublimed without apparent change in physical and spectroscopic properties. Incorporation of the benzene molecule into the crystal appears to be either the result of an interaction of the  $\pi$  cloud with empty d orbitals, or more likely, weak hydrogen bonded interactions between the fluorines of the trifluoroacetates and benzene hydrogens.

The equilibrium reaction (6.1) suggests that formation of the benzene complex (II) is most likely in the absence of the anhydride. The crystals of (I) were prepared by slow condensation of the solvent to the

empty side of the evacuated vessel by immersing this side in cold running water overnight. This procedure removed the more volatile trifluoroacetic acid (b.p. 72.4°C),<sup>130</sup> and trifluoroacetic anhydride (b.p. 40°C),<sup>130</sup> leaving benzene (b.p. 80.1°C),<sup>130</sup> behind. The equilibrium (6.1) is shifted to the right allowing formation of the benzene complex (II). The anhydride complex (I) must be the preferred product since it is formed in the presence of a large excess of benzene. Presumably when anhydride is present ordered crystalline material is difficult to obtain. These data are also consistent with the formation of  $[\text{Sn(II)Sn(IV)O(O}_2\text{CR)}_4\text{O(OCR)}_2]_2$  ( $\text{R} = \text{CF}_3, \text{CCl}_3$ ) with benzene as a solvent.

At the completion of the work it was noted that  $[\text{Sn(II)Sn(IV)O(O}_2\text{CC(CH}_3)_3)_4\text{O(OCC(CH}_3)_3)_2]_2$  prepared was crystalline. Hopefully other workers will confirm the predicted structure for these compounds.



## CHAPTER SEVEN

### MIXED OXIDATION STATE TIN COMPOUNDS DERIVED FROM THE REACTION OF HEXAPHENYLDITIN WITH INORGANIC ACIDS

#### A. Introduction

The successful high yield syntheses of the mixed oxidation state tin carboxylates from the reaction of hexaphenylditin with carboxylic acids (this thesis), suggested that acid solvolysis of hexphenylditin may provide a general synthetic route to mixed oxidation state tin compounds. The majority of compounds which contain tin in both the +2 and +4 oxidation state have only recently been prepared by fortuitous methods, in unreported quantities, and generally by proposed partial oxidation or reduction of the appropriate tin reagent. The only specific attempt to prepare a mixed oxidation state tin compound involved isolation of  $\text{Sn}_2\text{S}_3$  from melts of  $\text{SnS}_2$  and  $\text{SnS}$ .<sup>131</sup> The compound  $\text{Sn}_2\text{S}_3$  was characterized by X-ray diffraction and found to contain both tin(II) and tin(IV).<sup>131</sup> The mixed oxidation state tin compounds,  $\text{Sn}_3\text{F}_8$ ,<sup>132</sup>  $(\text{C}_6\text{H}_5)_3\text{Sn-SnNO}_3$ <sup>126</sup> and  $[\text{Sn(II)Sn(IV)O}(\text{O}_2\text{C}_6\text{H}_4\text{NO}_2\text{-o})_4\text{THF}]_4$ <sup>105</sup> have been characterized by X-ray diffraction.

The <sup>119</sup>Sn Mössbauer spectrum of  $\text{Sn}_2\text{S}_3$ ,<sup>133</sup> that of  $\text{Sn}_3\text{F}_8$ <sup>132</sup> and that of  $[\text{Sn(II)Sn(IV)O}(\text{O}_2\text{C}_6\text{H}_4\text{NO}_2\text{-o})_4\text{THF}]_4$ <sup>105</sup> have been used to demonstrate the presence of both tin(II) and tin(IV) in these well established mixed oxidation state tin compounds. The fluoride  $\text{Sn}_3\text{F}_8$ <sup>132</sup> was obtained by partial oxidation of  $\text{SnF}_2$  in HF, while

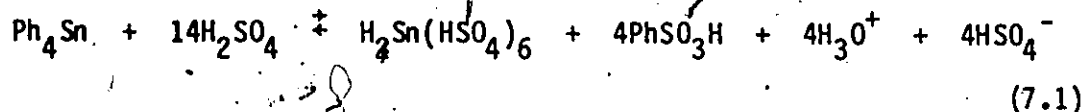
$[\text{Sn(II)Sn(IV)O}(\text{O}_2\text{C}_6\text{H}_4\text{NO}_2)_2\text{THF}]_2$ <sup>105</sup> was obtained from the reaction of bis(methylcyclopentadienyl)tin and two moles of ortho-nitrobenzoic acid in tetrahydrofuran. The novel mixed oxidation state tin compound  $(\text{C}_6\text{H}_5)_3\text{SnSnNO}_3$ <sup>126</sup> was obtained as one of the products of the reaction of  $(\text{C}_6\text{H}_5)_2\text{Sn}(\text{NO}_3)_2$  with  $(\text{C}_6\text{H}_5)_3\text{Sb}$ . The <sup>119</sup>Sn Mössbauer spectrum of the product obtained by heating SnO has been interpreted in terms of a mixed oxidation state tin compound  $\text{Sn}_2\text{O}_3$ <sup>134</sup>. The compound  $\text{Sn}_2\text{O}_3$  was proposed to be isostructural with  $\text{Sn}_2\text{S}_3$ <sup>134</sup>. The oxide,  $\text{Sn}_2\text{O}_3$ , was proposed to contain an octahedrally coordinated tin(IV) atom together with a tin(II) atom at the apex of a trigonal pyramid of oxygen atoms.<sup>134</sup>

The most general preparative method of a series of mixed oxidation state tin compounds involves partial oxidation of tin(II) bis-ketoenolates,  $^{135}(\text{SnL}_2)$ , with 7,7,8,8-tetracyanoquinodimethane, tcnq, to form  $\text{Sn}(\text{tcnq})\text{L}_2$ . However, similar organic electron acceptor molecules such as tetracyanoethylene, tcne, and 2,3,5,6-tetrachlorobenzoquinone, tcbq, completely oxidize tin(II) bis( $\beta$ -ketoenolates) and tin(II) halides to tin(IV) compounds.<sup>135</sup> These reactions are rather specific such that tcne, but not tcnq or tcbq, reacts directly with the metal to form  $\text{Sn}(\text{tcne})_2 \cdot \text{THF}$ , and only excess tcnq converting  $\text{Sn}(\text{pd})_2$  (pd = pentane-2,4-dionato) to  $\text{Sn}(\text{pd})_2(\text{tcnq})_{1.5}$ .<sup>135</sup> <sup>119</sup>Sn Mössbauer spectroscopy has been used to demonstrate the presence of both tin(II) and tin(IV) in the complexes  $\text{Sn}(\text{tcnq})\text{L}_2$ ,  $\text{Sn}(\text{tcne})_2 \cdot \text{THF}$  and  $\text{Sn}(\text{pd})_2(\text{tcnq})_{1.5}$ .<sup>135</sup> Recently, spectroscopic evidence has been presented for the product,  $[(\text{CH}_3)_3\text{SnC}_5\text{H}_4]_2\text{Sn}$ , isolated from the reaction of  $(\text{C}_5\text{H}_5)_2\text{Sn}$  with  $(\text{CH}_3)_3\text{SnN}(\text{CH}_2\text{CH}_3)_2$ .<sup>136</sup> The <sup>119</sup>Sn Mössbauer spectrum of

$[(CH_3)_3SnC_5H_4]_2Sn$  was interpreted in terms of a compound containing organotin(II) and organotin(IV) in one molecule. The compounds  $Sn_7F_{16}$ ,  $Sn_2F_6$  and  $Sn_{10}F_{34}$  have been isolated from melts of  $SnF_2$  and  $SnF_4$ .<sup>137</sup> No spectroscopic evidence was presented to establish the structure of these tin fluorides.

The acid solvolysis of hexaphenylditin in strong acid medium has not been extensively studied. Hexaphenylditin reacts with nitric acid, but the nature of the black solid obtained has not been identified.<sup>138</sup> Hexaphenylditin does react with hydrochloric acid in tetrahydrofuran to produce an unidentified gas and triphenyltin chloride (60%).<sup>138</sup> Sulphuric acid was reported to produce no gas and no reaction was apparent after several days.<sup>138</sup> The behaviour of hexaphenylditin in strong acid medium, based on previously published results, is not clear.

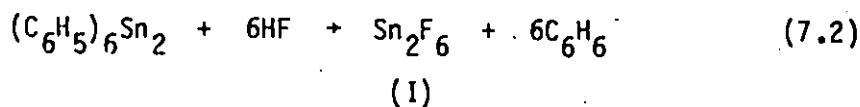
The acid solvolysis of alkyl tin(IV) compounds has been extensively studied,<sup>42,44-46</sup> with the isolation of alkyl tin(IV) compounds.<sup>47,49</sup> Such is not the case for aryl tin(IV) compounds. In general, it appears that all  $Sn-C_6H_5$  bonds are cleaved in strong acid.<sup>44,139</sup> Tetraphenyltin,  $Ph_4Sn$ , reacts with 100% sulphuric acid according to:<sup>44</sup>



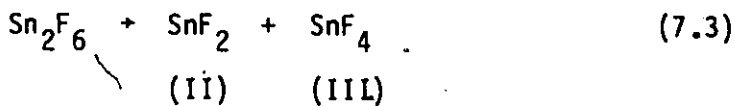
Similarly, at ambient temperature  $Ph_4Sn$ ,  $Ph_3SnCl$  and  $Ph_2SnCl_2$ , react with disulphuric acid yielding the same products.<sup>139</sup>

Divinyl-, dibenzyl-, and diphenyl tin(IV) dichloride react with  $\text{HSO}_3\text{F}$ ,  $\text{HSO}_3\text{CF}_3$ ,  $\text{H}_2\text{PO}_3\text{F}$  or  $\text{HF}$  with extensive side reactions and the formation of black/brown products.<sup>43</sup>

The acid solvolysis of  $(\text{C}_6\text{H}_5)_6\text{Sn}_2$  in  $\text{HF}$  might be expected to produce an unstable  $\text{Sn}_2\text{F}_6$  dimer species, (I) equation (7.2).



Disproportionation of (I) would produce both  $\text{SnF}_2$  (II), and  $\text{SnF}_4$  (III).



However, the interaction of  $\text{SnF}_2$  with strong fluoride acceptors,  $\text{SbF}_5$ ,  $\text{AsF}_6$ ,  $\text{BF}_3$ , produces 1:1 adducts  $\text{SnF}_2 \cdot \text{SbF}_5$ ,  $\text{SnF}_2 \cdot \text{AsF}_5$ ,  $\text{SnF}_2 \cdot \text{BF}_3$ , and  $\text{SbF}_5$  also forms a 1:2 adduct  $\text{SnF}_2 \cdot 2\text{SbF}_5$ .<sup>140</sup> On the basis of their vibrational and  $^{119}\text{Sn}$  Mössbauer spectra these 1:1 adducts have been formulated as salts of the fluorine-bridged cation  $[\text{Sn-F}]_n^{n+}$  with the anions  $[\text{SbF}_6^-]$ ,  $[\text{AsF}_6^-]$  and  $[\text{BF}_4^-]$ , and the 1:2 adduct as  $\text{Sn}(\text{SbF}_6)_2$ . The crystal structure of  $\text{SnF}_2 \cdot \text{AsF}_5$  consists of a planar  $(\text{SnF})_3$  ring, fluorine bridged to octahedral  $[\text{AsF}_6^-]$  species and has been best formulated as  $(\text{SnF})_3 \cdot 3\text{AsF}_6$ .<sup>141</sup> Similarly the crystal structure of  $\text{Sn}_3\text{F}_8$ <sup>132</sup> consists of a  $(\text{Sn(II)F})_n^{n+}$  polymer chain linked to octahedral  $[\text{SnF}_6^{2-}]$  anions. The reaction product from the disproportionation of

$\text{Sn}_2\text{F}_6$  might be expected to be the adduct  $\text{SnF}_2 \cdot \text{SnF}_4$  with a similar  $^{119}\text{Sn}$  Mossbauer spectrum in the tin(II) region to that of  $\text{Sn}(\text{SbF}_6)_2$ . The  $^{119}\text{Sn}$  Mossbauer spectrum of  $\text{SnF}_2 \cdot \text{SnF}_4$  in the tin(IV) region might be expected to be similar to that of  $\text{K}_2\text{SnF}_6$ ,<sup>142</sup> which consists of a single resonance of  $-0.43 \text{ mm s}^{-1}$ . An octahedral  $[\text{SnF}_6^{2-}]$  ion has been established for the  $\text{Na}_2\text{SnF}_6$  salt.<sup>143</sup> The adduct  $\text{SnF}_2 \cdot \text{SnF}_4$  could be formulated as the salt  $\text{Sn(II)[Sn(IV)F}_6]$ . Both vibrational data and the Mössbauer spectrum of a product of composition  $\text{SnF}_3$  should confirm or disprove these contentions.

The solvolysis of  $(\text{C}_6\text{H}_5)_6\text{Sn}_2$  in the highly acidic sulphonic acids ( $\text{RSO}_3\text{H}$ ;  $\text{R} = \text{CF}_3, \text{CH}_3, \text{CH}_2\text{CH}_3, \text{OH}, \text{F}$ ) might be expected to produce a product of composition  $\text{Sn}(\text{SO}_3\text{R})_3$ . A compound of composition  $\text{Sn}(\text{SO}_3\text{CF}_3)_3$  has been reported to be the product from the interaction of  $(\text{CH}_2\text{CH})_4\text{Sn}$  with  $\text{CF}_3\text{SO}_3\text{H}$  in an attempted preparation of  $\text{Sn}(\text{SO}_3\text{CF}_3)_4$ .<sup>96</sup> On the basis of the infrared and  $^{119}\text{Sn}$  Mossbauer spectra,  $\text{Sn}(\text{SO}_3\text{CF}_3)_3$  has been formulated as  $\text{Sn(II)[Sn(IV)(SO}_3\text{CF}_3)_6]$ ,<sup>96</sup> similar to that of  $\text{Sn}(\text{SbF}_6)_2$ . The vibrational spectra for  $\text{Sn}(\text{SbF}_6)_2$  indicate appreciable cation-anion interaction,<sup>140</sup> presumably through extensive fluorine bridging, yet the infrared data suggest little or no cation-anion interaction in  $\text{Sn(II)[Sn(IV)(SO}_3\text{CF}_3)_6]$ .<sup>96</sup> The  $^{119}\text{Sn}$  Mössbauer spectra of  $\text{Sn}(\text{SbF}_6)_2$  and that of  $\text{Sn(II)[Sn(IV)(SO}_3\text{CF}_3)_6]$  exhibit a narrow resonance in the tin(II) region with no evidence of any quadrupole splitting. The higher isomer shift of the tin(II) atom in  $\text{Sn(II)[Sn(IV)(SO}_3\text{CF}_3)_6]$ ,  $4.69 \text{ mm s}^{-1}$ ,<sup>96</sup> compared to that of  $4.44 \text{ mm s}^{-1}$  for  $\text{Sn}(\text{SbF}_6)_2$ ,<sup>140</sup> suggests that the tin(II) in the former compound approximates fairly closely that of a bare  $\text{Sn}^{+2}$  cation.<sup>96</sup>

The  $^{119}\text{Sn}$  Mössbauer spectrum of  $\text{Sn(II)[Sn(IV)(SO}_3\text{CF}_3)_6]_x$  in the tin(IV) region was identical to that of  $\text{K}_2\text{Sn(SO}_3\text{F)}_6$ <sup>144</sup> and supported the proposed formulation for the mixed oxidation state tin compound.

## B. Results and Discussion

### (i) Preparations

Hexaphenylditin reacts with  $\text{HSO}_3\text{X}$  ( $\text{X} = \text{CH}_3, \text{CH}_2\text{CH}_3, \text{OH}, \text{CF}_3, \text{F}$ ) and HF with no apparent gas evolution. Solid products free of excess acid and solvent could only be obtained for the sulphonic acids when  $\text{X} = \text{CF}_3, \text{F}$ , and for anhydrous hydrofluoric acid. The sulphonic acids  $\text{CH}_3\text{CH}_2\text{SO}_3\text{H}$ ,  $\text{CH}_3\text{SO}_3\text{H}$  and  $\text{H}_2\text{SO}_4$  did not produce "dry" solids, even when the reaction was carried out almost stoichiometrically.

The chemical analysis of the product from the fluorosulphuric acid -- hexaphenylditin reaction (Chapter 2) -- indicated a tin(II):tin(IV) ratio of 1:1. The total tin analysis suggested a maximum of 1.35  $\text{SO}_3\text{F}$  groups per tin atom rather than 3  $\text{SO}_3\text{F}$  groups per tin atom expected for a product of composition  $\text{Sn(SO}_3\text{F)}_3$ . A possible composition consistent with the analytical data would be  $\text{Sn(IV)O}\cdot\text{SO}_4\text{Sn(II)(SO}_3\text{F)}_2$ . Spectroscopic data will be presented in this chapter to support the formulation  $[\text{Sn(IV)O}\cdot\text{SO}_4\text{Sn(II)(SO}_3\text{F)}_2]_x$  for this compound. Incomplete carbon-tin bond cleavage is unlikely because of the absence of phenyl group resonances in the  $^1\text{H}$  n.m.r. of a  $\text{HSO}_3\text{F}$  solution of this product.

The solvolysis of hexaphenylditin in fluorosulphuric acid is thought to proceed by complete cleavage of all carbon-tin bonds to produce the intermediate  $[\text{Sn(II)Sn(IV)(SO}_3\text{F)}_6]_x$ . Unfortunately solid

products could only be isolated in sufficient amounts after a period of several days. During this period of time it would appear that  $[\text{Sn(II)Sn(IV)(SO}_3\text{F)}_6]_x$  reacts further to form an insoluble species of approximate composition  $\text{Sn(IV)O}\cdot\text{SO}_4\text{Sn(II)(SO}_3\text{F)}_2$ . Fluorosulphates are known to lose  $\text{S}_2\text{O}_5\text{F}_2$  and higher sulphur oxyfluorides on heating,<sup>145</sup> and it is possible that a species such as  $[\text{Sn(II)Sn(IV)(SO}_3\text{F)}_6]_x$  could decompose in solution after several days to yield an oxo-bridged species, analogous to the carboxylates discussed in Chapter 5. The  $^{19}\text{F}$  n.m.r. of solutions of  $[\text{Sn(IV)O}\cdot\text{SO}_4\text{Sn(II)(SO}_3\text{F)}_2]_x$  in  $\text{HSO}_3\text{F}$  at  $-45^\circ\text{C}$ , consisted of two equal intensity signals (40.9, 41.9 ppm) adjacent to the solvent peak. As temperature was increased to  $35^\circ\text{C}$ , the 40.9 ppm signal decreased in intensity and only the 41.9 ppm signal was observed at  $70^\circ\text{C}$ . The observed chemical shifts  $\sim 40$  ppm are typical of fluorosulphate ( $\text{Me}_3\text{NSO}_3\text{F}$ ,<sup>146</sup>  $[\text{SnF}_4(\text{SO}_3\text{F})_2]^{2-}$ ,<sup>146</sup>  $[\text{Sn}(\text{SO}_3\text{F})_6]^{2-}$ <sup>144</sup>) and exclude the possibility that  $\text{Sn(IV)-F}$  (-130 to -143 ppm)<sup>144,146</sup> or  $\text{Sn(II)-F}$  (-88 ppm)<sup>147</sup> are present in the product. The temperature dependent  $^{19}\text{F}$  n.m.r. suggests that two types of  $\text{SO}_3\text{F}$  groups are present in solution, one perhaps arising from a  $\text{SO}_3\text{F}$  group covalently bonded to tin, and the other from a  $\text{SO}_3\text{F}$  group which is weakly bonded to a tin atom and which exchanges with the solvent.

(ii)  $^{119}\text{Sn}$  Mössbauer Data

The  $^{119}\text{Sn}$  Mössbauer spectra for the reaction products derived from the reaction of hexaphenylditin with  $\text{H}_2\text{SO}_4$ ,  $\text{HSO}_3\text{CH}_3$ , and  $\text{HSO}_3\text{C}_2\text{H}_5$ , are presented in Table 7.1. The  $^{119}\text{Sn}$  Mössbauer spectra of

Table 7.1  $^{119}\text{Sn}$  Mössbauer Data for  $\text{Sn}(\text{SO}_3\text{R})_3$ ,  $\text{Sn}_3\text{F}_2(\text{SO}_3\text{CF}_3)_6$ , $\text{Sn}(\text{IV})\text{O}\cdot\text{SO}_4\text{Sn}(\text{II})(\text{SO}_3\text{F})_2$ ,  $\text{SnF}_3$  and Related Tin Compounds

Compound	Temp. K	$\delta$	$\Delta$ rms $^{-1}$	$\Gamma$	Relative Area Sn(IV)/Sn(II)	$\chi^2/\text{degree}$ of Freedom
$\text{Sn}(\text{SO}_3\text{C}_2\text{H}_5)_3^*$	77	-0.20 4.33	- 0.58	0.89 1.04	1.66	1.71
$\text{Sn}(\text{SO}_3\text{CH}_3)_3^*$	77	-0.22 4.25	- 0.70	0.90 0.97	1.60	1.30
$\text{Sn}(\text{SO}_3\text{OH})_3^*$	77	-0.22 4.06	- 0.96	1.14 1.04	0.97	0.60
$\text{SnSO}_4^{148}$	77	3.90	1.00			
$\text{Sn}(\text{SO}_4)_2^{149}$	77	-0.18	-			
$\text{Sn}(\text{IV})\text{O}\cdot\text{SO}_4\text{Sn}(\text{II})(\text{SO}_3\text{F})_2$	77	-0.27 4.38	- 0.68	1.28 1.20	1.19	1.16
$\text{Sn}(\text{SO}_3\text{F})_2^{140}$	77	4.18	0.68	1.33		
$\text{Sn}(\text{SO}_3\text{F})_4^{111}$	77	-0.27	1.34	1.19		
$\text{K}_2\text{Sn}(\text{SO}_3\text{F})_6^{144}$	77	-0.26	-	1.14		
$\text{Sn}(\text{SO}_3\text{CF}_3)_3$	77	-0.22 4.39	- 0.41	0.97 1.01	1.22	1.11
	298	-0.34	-	0.79		1.01
$\text{Sn}(\text{SO}_3\text{CF}_3)_3^{96}$	77	-0.24 4.69	- -	1.08 1.14	1.67	
	298	-0.29	-	1.12		
$\text{Sn}(\text{SO}_3\text{CF}_3)_2^{96}$	77	4.15	0.84	0.98		
$\text{Sn}(\text{SO}_3\text{CF}_3)_4^{96}$	77	-0.21	-	1.11		
$\text{SnF}_3$	77	-0.36 4.13	0.66 0.60	0.95 1.15	0.98	0.31
	298	-0.37 4.26	0.47 -	0.87 0.99	0.42	1.21
$\text{SnF}_2^{140}$	77	3.49	1.61	1.09		
$\text{SnF}_4^{112,150}$	77	-0.26	1.80			
$\text{K}_2\text{SnF}_6^{148}$	77	-0.43	-	1.59		
$\text{Sn}_3\text{F}_2(\text{SO}_3\text{CF}_3)_6$	77	-0.27 4.30	1.32 0.57	0.84 0.86	0.71	1.04
$(\text{Sn}(\text{II})\text{F})_2\text{Sn}(\text{IV})\text{F}_6^{132}$	77	-0.37 3.82	- 1.34			
$\text{SnFSbF}_6^{140}$	77	3.93	1.45	1.11		
$(\text{SnF})_3\cdot 3\text{AsF}_6^{140}$	77	3.97	1.54	1.00		
$\text{Sn}(\text{SbF}_6)_2^{140}$	77	4.44	-	1.21		
$\text{SnF}_2(\text{SO}_3\text{F})_2^{43}$	77	-0.23	1.96	1.15		

\* Denotes excess acid in product, see Chapter 2.



these products at 77° K consist of a single resonance at  $-0.2 \text{ mm s}^{-1}$  and a quadrupole doublet at 4.0 to 4.3  $\text{mm s}^{-1}$ , clearly representative of tin(IV) and tin(II) respectively. The possibility that these spectra arise from only tin(IV) species is eliminated by the following arguments. If these spectra arise only from tin(IV) species then their isomer shifts must be 1.9 and 2.4  $\text{mm s}^{-1}$  with quadrupole splittings of 3.8 and 4.8  $\text{mm s}^{-1}$  respectively. Neither set of data fall within the range given in the literature for  $\text{R}_3\text{Sn}(\text{SO}_3\text{X})^{42}$  or  $\text{R}_2\text{Sn}(\text{SO}_3\text{X})_2^{44}$ . The isomer shifts are too high for  $\text{R}_3\text{Sn}(\text{SO}_3\text{X})$  compounds and quadrupole splittings too low for  $\text{R}_2\text{Sn}(\text{SO}_3\text{X})_2$ . Although the organotin trisulphonates,  $\text{RSn}(\text{SO}_3\text{X})_3$ , are not known, the Mössbauer data could not be rationalized in terms of such species. In any case, an isomer shift of 2.4  $\text{mm s}^{-1}$  is well outside the accepted region for tin(IV) compounds<sup>17</sup> and would be assigned to a tin(II) compound. Other possible products such as organoditin sulphonates would give rise to spectra similar to those observed for organotin sulphonates. Phenyliditin sulphonates as reaction products would not be consistent with the solvolysis products obtained from the reaction of hexphenyliditin in acid medium described in this thesis. The isomer shift of the tin(II) site in  $\text{Sn}(\text{SO}_3\text{OH})_3$  is more positive than that of  $\text{SnSO}_4$ ,<sup>148</sup> while that of the tin(IV) site is more negative than that for  $\text{Sn}(\text{SO}_4)_2$ .<sup>149</sup> However, these shifts are not significantly different from those of the  $\text{SnSO}_4$  and  $\text{Sn}(\text{SO}_4)_2$  analogues. The data for  $-\text{Sn}(\text{SO}_3\text{CH}_3)_3$ ,  $\text{Sn}(\text{SO}_3\text{C}_2\text{H}_5)_3$  and  $\text{Sn}(\text{SO}_3\text{H})_3$  could be formulated as  $[\text{Sn}(\text{II})\text{Sn}(\text{IV})(\text{SO}_3\text{R})_6]_x$ , or interpreted in terms of mixtures of  $\text{Sn}(\text{SO}_3\text{R})_2$  and  $\text{Sn}(\text{SO}_3\text{R})_4$ . Perhaps when Mössbauer data become available for the

$\text{Sn}(\text{SO}_3\text{R})_2$  and  $\text{Sn}(\text{SO}_3\text{R})_4$  analogues  $\text{Sn}(\text{SO}_3\text{C}_2\text{H}_5)_3$  and  $\text{Sn}(\text{SO}_3\text{CH}_3)_3$  will be shown to be mixed oxidation state tin compounds.

The  $^{119}\text{Sn}$  Mössbauer data for the solids of composition  $\text{Sn}(\text{SO}_3\text{CF}_3)_3$ ,  $\text{SnF}_3$ ,  $\text{Sn}_3\text{F}_2(\text{SO}_3\text{CF}_3)_6$  and  $\text{Sn}(\text{IV})\text{O}\cdot\text{SO}_4\text{Sn}(\text{II})(\text{SO}_3\text{F})_2$  together with the literature data for the related compounds are presented in Table 7.1. The  $^{119}\text{Sn}$  Mössbauer spectrum of  $\text{Sn}(\text{IV})\text{O}\cdot\text{SO}_4\text{Sn}(\text{II})(\text{SO}_3\text{F})_2$  is similar to those of the  $[\text{Sn}(\text{II})\text{Sn}(\text{IV})(\text{SO}_3\text{R})_6]_x$  complexes and at  $77^\circ\text{K}$  consists of absorptions at  $-0.27\text{ mm s}^{-1}$  and  $4.38\text{ mm s}^{-1}$ , clearly representative of tin(IV) and tin(II) respectively. The isomer shift of the tin(IV) site is identical to that of  $\text{Sn}(\text{SO}_3\text{F})_4$ .<sup>111</sup> However, the compound is clearly not a mixture which contains  $\text{Sn}(\text{SO}_3\text{F})_4$  since this latter species exhibits a well resolved quadrupole splitting of  $1.34\text{ mm s}^{-1}$ . The isomer shift of the Sn(II) site,  $4.38\text{ mm s}^{-1}$  is greater than that of  $\text{Sn}(\text{SO}_3\text{F})_2$ ,  $4.18\text{ mm s}^{-1}$ ,<sup>140</sup> and is close to the value for  $\text{Sn}(\text{SbF}_6)_2$ .<sup>140</sup> The solid is best formulated as  $[\text{Sn}(\text{IV})\text{O}\cdot\text{SO}_4\text{Sn}(\text{II})(\text{SO}_3\text{F})_2]_x$ .

The  $^{119}\text{Sn}$  Mössbauer spectrum of  $\text{Sn}(\text{SO}_3\text{CF}_3)_3$ , Figure 7.1, consists of two narrow resonances with isomer shifts of  $-0.2$  and  $4.39\text{ mm s}^{-1}$  which are assigned to tin(IV) and tin(II) respectively. The narrow resonances indicate a zero or near zero quadrupole splitting ( $\Delta < 0.5\text{ mm s}^{-1}$ ). These data indicate a nearly symmetrical distribution of electron density about both tin atoms in this compound. The isomer shift of the tin(IV) site,  $-0.2$ , is similar to those for  $\text{Sn}(\text{SO}_3\text{CF}_3)_4$ ,<sup>96</sup>  $\text{Sn}(\text{SO}_3\text{F})_4$ <sup>111</sup> and  $\text{K}_2\text{Sn}(\text{SO}_3\text{F})_6$ .<sup>144</sup> The isomer shift of the tin(II) site,  $4.39\text{ mm s}^{-1}$ , is larger than that for  $\text{Sn}(\text{SO}_3\text{CF}_3)_2$  ( $4.15\text{ mm s}^{-1}$ )<sup>96</sup> and similar to that for

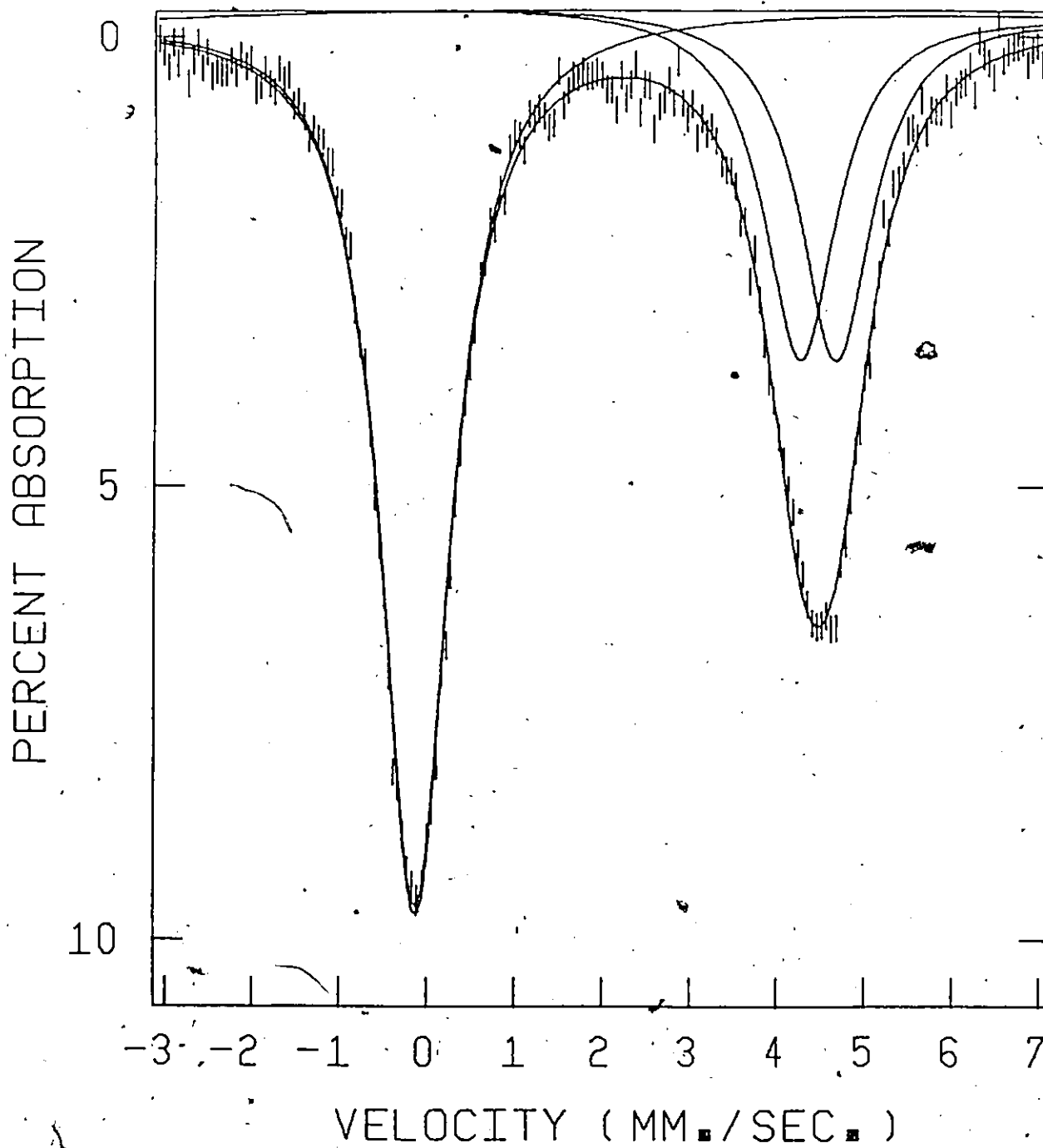


Figure 7.1.  $^{119}\text{Sn}$  Mössbauer spectrum of  $\text{Sn}(\text{SO}_3\text{CF}_3)_3$  at 77°K.

$\text{Sn}(\text{SbF}_6)_2^{140}$  ( $4.44 \text{ mm s}^{-1}$ ). The  $^{119}\text{Sn}$  Mössbauer parameters for  $\text{Sn}(\text{SO}_3\text{CF}_3)_3$  are similar to those reported previously for  $\text{Sn}(\text{SO}_3\text{CF}_3)_3$ .<sup>96</sup> The parameters are within the generally accepted experimental error with the exception of the isomer shift for the tin(II) site which was reported to be  $4.69 \text{ mm s}^{-1}$ <sup>96</sup> and measured here as  $4.39 \text{ mm s}^{-1}$ . The previously measured isomer shift of the tin(II) site for this compound is perhaps a bit high, and the isomer shift of  $4.39 \text{ mm s}^{-1}$  reported here is probably more realistic. The  $^{119}\text{Sn}$  Mössbauer spectrum of  $\text{Sn}(\text{SO}_3\text{CF}_3)_3$  was computer fitted to three lines since two lines do not give an acceptable fit to the data. This suggests a small quadrupole splitting for the tin(II) atom in  $\text{Sn}(\text{SO}_3\text{CF}_3)_3$ . This indicates that  $\text{Sn}(\text{SO}_3\text{CF}_3)_3$  is best formulated as  $[\text{Sn}(\text{II})\text{Sn}(\text{IV})(\text{SO}_3\text{CF}_3)_6]_x$  rather than  $\text{Sn}(\text{II})[\text{Sn}(\text{IV})(\text{SO}_3\text{CF}_3)_6]$  proposed by Aubke and coworkers.<sup>96</sup>

The  $^{119}\text{Sn}$  Mössbauer spectrum of  $\text{SnF}_3$  at  $77^\circ\text{K}$  consists of two unresolved quadrupole doublets with isomer shifts of  $-0.36$  and  $4.13 \text{ mm s}^{-1}$ , clearly representative of tin(IV) and tin(II) respectively. The presence of unresolved quadrupole splittings,  $\sim 0.7 \text{ mm s}^{-1}$ , is apparent since analysis as single resonances give line widths of  $\sim 1.6 \text{ mm s}^{-1}$ . These unresolved quadrupole splittings indicate a nearly symmetrical distribution of electron density about both tin atoms in this compound. The compound  $\text{SnF}_3$  or adduct  $\text{SnF}_2 \cdot \text{SnF}_4$  is clearly not a simple mixture of  $\text{SnF}_2$  and  $\text{SnF}_4$  since both of these latter species exhibit well resolved quadrupole splittings of  $1.61^{140}$  and  $1.80 \text{ mm s}^{-1}$ .<sup>112</sup> The isomer shift of the tin(IV) site,  $-0.37 \text{ mm s}^{-1}$ , is intermediate between that for

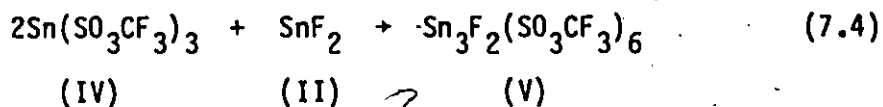
$\text{SnF}_4$  ( $-0.26 \text{ mm s}^{-1}$ ),<sup>150</sup> and that for  $\text{K}_2\text{SnF}_6$  ( $-0.43 \text{ mm s}^{-1}$ ).<sup>142</sup> Similarly, the isomer shift of the tin(II) site ( $4.13 \text{ mm s}^{-1}$ ), is intermediate between that for  $\text{SnF}_2$  ( $3.49 \text{ mm s}^{-1}$ ),<sup>140</sup> and that for  $\text{Sn}(\text{SbF}_6)_2$  ( $4.44 \text{ mm s}^{-1}$ ).<sup>140</sup> A purely ionic formulation  $\text{Sn}(\text{II})[\text{Sn}(\text{IV})\text{F}_6]$  is unlikely since it would require isomer shifts of at least  $-0.47$  and  $4.44 \text{ mm s}^{-1}$  for the tin(IV) and tin(II) sites respectively and quadrupole splittings of zero. The isomer shift of  $4.13 \text{ mm s}^{-1}$  for the tin(II) site is consistent with there being some covalent interaction in  $\text{SnF}_2 \cdot \text{SnF}_4$  presumably via Sn(II)-F-Sn(II) or Sn(II)-F-Sn(IV) bridges. The adduct  $\text{SnF}_2 \cdot \text{SnF}_4$  is perhaps best formulated as  $[\text{Sn}(\text{II})\text{Sn}(\text{IV})\text{F}_6]_x$ . The small negative isomer shift for the tin(IV) atom in  $[\text{Sn}(\text{II})\text{Sn}(\text{IV})\text{F}_6]_x$  ( $-0.26 \text{ mm s}^{-1}$ ) indicates a low s electron density at the tin(IV) atom. Octahedral  $\text{SnF}_4$  and  $[\text{SnF}_6]^{2-}$  have similar isomer shifts (Table 7.1) while matrix-isolated tetrahedral  $\text{SnF}_4$ <sup>151</sup> has a slightly larger isomer shift ( $-0.01 \text{ mm s}^{-1}$ ). The small quadrupole splitting of the tin(IV) site in  $[\text{Sn}(\text{II})\text{Sn}(\text{IV})\text{F}_6]_x$  is best interpreted in terms of a slightly distorted octahedral environment for a  $\text{Sn}(\text{IV})\text{F}_6$  unit.

The small quadrupole splitting for the tin(II) atom in  $[\text{Sn}(\text{II})\text{Sn}(\text{IV})\text{F}_6]_x$  indicates a much more cubic environment than that found for other Lewis acid-base compounds such as  $(\text{Sn}(\text{II})\text{F})_2\text{Sn}(\text{IV})\text{F}_6$  or  $(\text{SnF})_3\text{AsF}_6$  which have quadrupole splittings of  $\sim 1.5 \text{ mm s}^{-1}$ .<sup>140</sup> Such complexes have distorted tin(II) environments<sup>132,141</sup> with isomer shifts slightly smaller than observed for  $[\text{Sn}(\text{II})\text{Sn}(\text{IV})\text{F}_6]_x$ . Tin(II) compounds which are known to have isomer shifts of  $\sim 4.5 \text{ mm s}^{-1}$  and zero quadrupole splitting are  $\text{Sn}(\text{SbF}_6)_2$ ,<sup>140</sup> the tin(II) in  $\text{Sn}(\text{SO}_3\text{CF}_3)_3$  and tin(II) when

complexed with crown ether 15-crown-5.<sup>152</sup> The high isomer shift and zero quadrupole splittings are generally interpreted in terms of an ionic environment for the tin(II) in these compounds. The low isomer shift of the tin(II) in  $[\text{Sn(II)Sn(IV)F}_6]_x$ ,  $4.13 \text{ mm s}^{-1}$ , relative to the isomer shift reported for proposed ionic compounds  $\text{Sn(SbF}_6)_2$  ( $4.44 \text{ mm s}^{-1}$ ),<sup>140</sup>  $[\text{Sn(II)Sn(IV)(SO}_3\text{CF}_3)_6]_x$  ( $4.39 \text{ mm s}^{-1}$ ), suggests that the tin(II) is in an environment having a high coordination number.

A significant room temperature  $^{119}\text{Sn}$  Mössbauer absorption for both tin(II) and tin(IV) atoms in  $[\text{Sn(II)Sn(IV)F}_6]_x$  (Table 7.1) indicates that both tin atoms are strongly held in the lattice. Both ionic  $[\text{SnF}_6^{2-}]$ <sup>144</sup> and polymeric  $\text{SnF}_4$ <sup>113</sup> show a significant room temperature absorption.<sup>42</sup> Tin(II) fluoride,  $\text{SnF}_2$ , is tetrameric<sup>153</sup> and also shows a significant room temperature absorption.<sup>154</sup> The significant room temperature absorption for the tin(II) atom in  $[\text{Sn(II)Sn(IV)F}_6]_x$  compared to that in  $[\text{Sn(II)Sn(IV)(SO}_3\text{CF}_3)_6]_x$  perhaps indicates that  $[\text{Sn(II)Sn(IV)F}_6]_x$  is best regarded as a polymer.

To obtain further information about the structure of the compound with composition  $\text{Sn(SO}_3\text{CF}_3)_3$ , (IV), a redistribution reaction with  $\text{SnF}_2$  was studied. A ligand exchange reaction (equation (7.4)) between  $\text{SnF}_2$  and  $\text{Sn(SO}_3\text{CF}_3)_3$  resulted in the formation of a product of composition  $\text{Sn}_3\text{F}_2(\text{SO}_3\text{CF}_3)_6$ , (V).



Such reactions are known to occur in the formation of  $\text{SnX}(\text{OCH}_3)$  from  $\text{Sn}(\text{OCH}_3)_2$  and  $\text{SnX}_2$  ( $\text{X} = \text{Cl}, \text{I}, \text{Br}$ ),<sup>118</sup> and  $\text{SnCl}_2(\text{SO}_3\text{F})_2$  from  $\text{SnCl}_4$  and  $\text{Sn}(\text{SO}_3\text{F})_2$ .<sup>111</sup> If the complex  $\text{Sn}(\text{SO}_3\text{CF}_3)_3$  was essentially  $\text{Sn}(\text{II})[\text{Sn}(\text{IV})(\text{SO}_3\text{CF}_3)_6]$ , as formulated by Sams and coworkers,<sup>96</sup> the reaction product (V) might be expected to be  $[(\text{Sn}(\text{II})\text{F}_2)]-\text{[Sn}(\text{IV})(\text{SO}_3\text{CF}_3)_6]$ . Both vibrational and Mössbauer data of  $\text{Sn}_3\text{F}_2(\text{SO}_3\text{CF}_3)_6$  should confirm or disprove these contentions.

The  $^{119}\text{Sn}$  Mössbauer spectrum of the reaction product  $\text{Sn}_3\text{F}_2(\text{SO}_3\text{CF}_3)_6$ , is presented in Figure 7.2. The spectrum consists of a well resolved quadrupole doublet in the tin(IV) region with a relatively low isomer shift,  $-0.27 \text{ mm s}^{-1}$ , and an unresolved quadrupole doublet in the tin(II) region with a relatively high isomer shift,  $4.30 \text{ mm s}^{-1}$ . Comparison of  $^{119}\text{Sn}$  Mössbauer parameters of  $\text{Sn}_3\text{F}_2(\text{SO}_3\text{CF}_3)_6$  with those of  $\text{Sn}(\text{SO}_3\text{CF}_3)_3$  and  $\text{SnF}_2$  indicates that the data cannot be interpreted in terms of a mixture of  $\text{Sn}(\text{SO}_3\text{CF}_3)_3$  and  $\text{SnF}_2$ . The  $^{119}\text{Sn}$  Mössbauer parameters of  $\text{SnF}_2$ <sup>140</sup> are such that two lines at  $4.30$  and  $2.69 \text{ mm s}^{-1}$  would be visible in the spectrum. The  $2.69 \text{ mm s}^{-1}$  resonance is not visible in  $\text{Sn}_3\text{F}_2(\text{SO}_3\text{CF}_3)_6$  indicating that  $\text{SnF}_2$  is not present. Comparison of the  $^{119}\text{Sn}$  Mössbauer spectrum of  $\text{Sn}(\text{SO}_3\text{CF}_3)_3$ , Figure 7.1, with that of  $\text{Sn}_3\text{F}_2(\text{SO}_3\text{CF}_3)_6$ , Figure 7.2, in the tin(IV) region leads to the conclusion that the single tin(IV) resonance at  $-0.22 \text{ mm s}^{-1}$  for  $\text{Sn}(\text{SO}_3\text{CF}_3)_3$  is not present and that the compound has all been converted to  $\text{Sn}_3\text{F}_2(\text{SO}_3\text{CF}_3)_6$ .

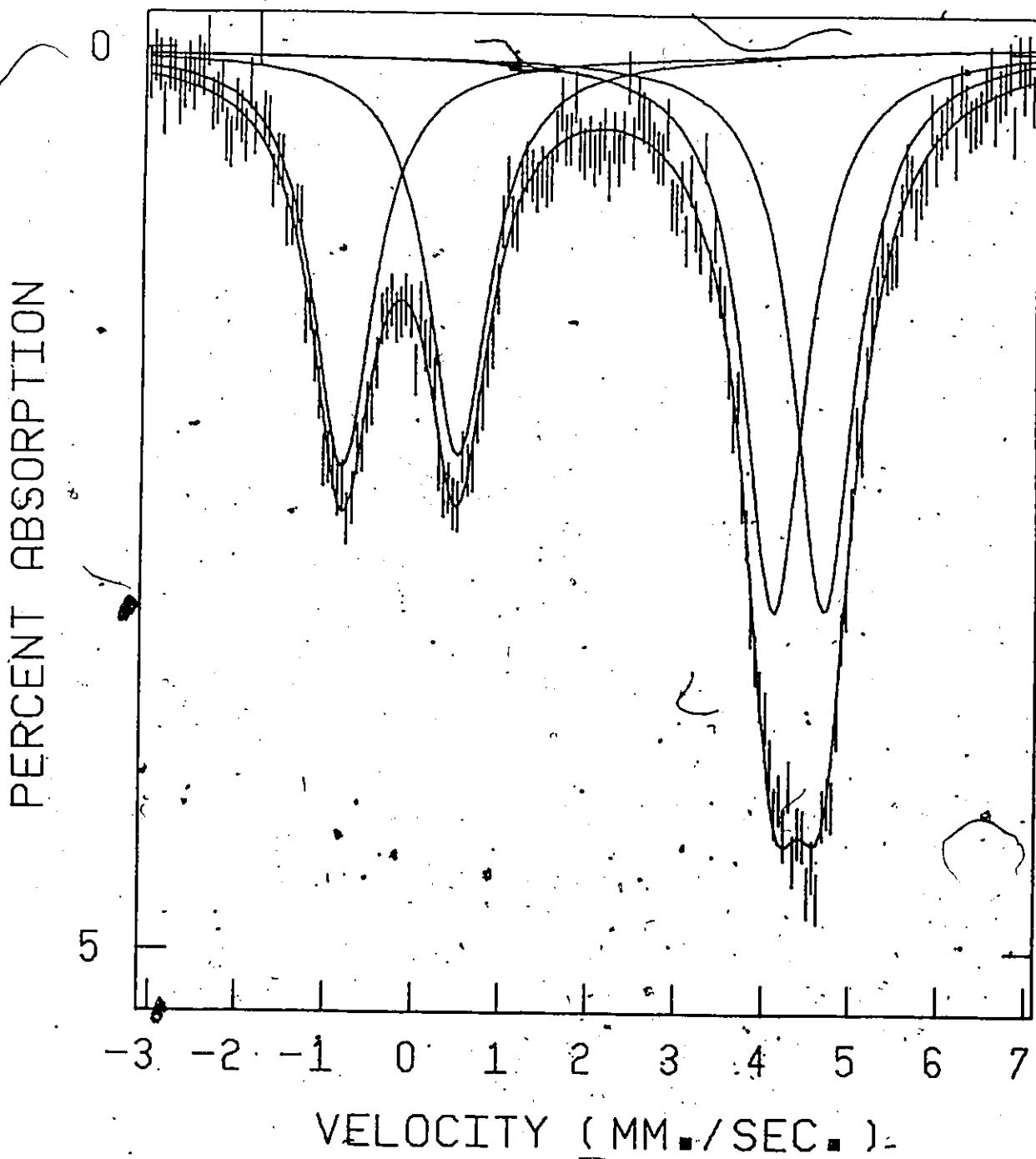


Figure 7.2.  $^{119}\text{Sn}$  Mössbauer spectrum of  $\text{Sn}_3\text{F}_2(\text{SO}_3\text{CF}_3)_6$  at  $77^\circ\text{K}$ .



Analysis of the spectrum of  $\text{Sn}_3\text{F}_2(\text{SO}_3\text{CF}_3)_6$  leads to the conclusion that this spectrum arises from tin(IV) in a very distorted environment and tin(II) in a slightly distorted environment. This is the first example of a mixed oxidation state tin compound where the tin(II) environment is nearly symmetrical while that of the tin(IV) is distorted.

The  $^{119}\text{Sn}$  Mössbauer parameters of  $\text{Sn}_3\text{F}_2(\text{SO}_3\text{CF}_3)_6$  are distinctly different from those previously reported for  $(\text{Sn}(\text{II})\text{F})_2\text{Sn}(\text{IV})\text{F}_6$ . The quadrupole splitting of the tin(II) atom in  $(\text{Sn}(\text{II})\text{F})_2\text{Sn}(\text{IV})\text{F}_6$ ,  $1.54 \text{ mm s}^{-1}$ , is significantly larger than that in  $\text{Sn}_3\text{F}_2(\text{SO}_3\text{CF}_3)_6$ . In addition, whereas the quadrupole splitting of the tin(IV) atom in  $(\text{Sn}(\text{II})\text{F})_2\text{Sn}(\text{IV})\text{F}_6$  is unresolved, that of the tin(IV) atom in  $\text{Sn}_3\text{F}_2(\text{SO}_3\text{CF}_3)_6$  is appreciable,  $1.32 \text{ mm s}^{-1}$ . These quadrupole splittings clearly indicate that the distribution of electron density in the p and/or d orbitals for the two tin atoms in  $\text{Sn}_3\text{F}_2(\text{SO}_3\text{CF}_3)_6$  is quite different to that in  $(\text{Sn}(\text{II})\text{F})_2\text{Sn}(\text{IV})\text{F}_6$ . The significantly larger isomer shift for the tin(II) site in  $\text{Sn}_3\text{F}_2(\text{SO}_3\text{CF}_3)_6$ ,  $4.30 \text{ mm s}^{-1}$ , compared to that in  $(\text{Sn}(\text{II})\text{F})_2\text{Sn}(\text{IV})\text{F}_6$ ,  $3.82 \text{ mm s}^{-1}$ , indicates a significantly larger s electron density at the tin nucleus in the former compound. The isomer shifts of the tin(IV) sites are similar as might be expected when very electronegative ligands are bonded to tin. It is clear that the tin environment in  $\text{Sn}_3\text{F}_2(\text{SO}_3\text{CF}_3)_6$  and  $(\text{Sn}(\text{II})\text{F})_2\text{Sn}(\text{IV})\text{F}_6$  are different and that the structure of  $\text{Sn}_3\text{F}_2(\text{SO}_3\text{CF}_3)_6$  is not the same as that established for  $(\text{Sn}(\text{II})\text{F})_2\text{Sn}(\text{IV})\text{F}_6$ ,<sup>132</sup> i.e., the  $\text{SnF}^+$  cation is not present. In addition, an ionic formulation such as  $[(\text{Sn}(\text{II})\text{F})_2][\text{Sn}(\text{IV})(\text{SO}_3\text{CF}_3)_6]$

would have a symmetrical tin(IV) environment as proposed for  $K_2Sn(SO_3F)_6$  and zero quadrupole splitting.

The quadrupole splitting of the tin(IV) atom in  $Sn_3F_2(SO_3CF_3)_6$ ,  $1.32 \text{ mm s}^{-1}$ , may be associated with the difference in bonding between the terminal and bridging ligands in an octahedral tin(IV) environment as has been established for  $SnF_4$ , and proposed for  $Sn(SO_3F)_4$ <sup>111</sup> and  $SnX_2(SO_3F)_2$  ( $X = F, Cl, Br$ ).<sup>41</sup> The quadrupole splitting of the tin(IV) atom in  $Sn_3F_2(SO_3CF_3)_6$  indicates that the tin(IV) is in an octahedral environment with two unidentate  $SO_3CF_3$  groups and bridging  $SO_3CF_3$  groups with fluorine bridges completing the arrangement. Such a  $Sn(IV)F_2(SO_3CF_3)_4$  unit might be expected to have a similar quadrupole splitting to  $Sn(SO_3F)_4$  since the spectra of  $SnF_4$  and  $SnF_2(SO_3F)_2$  are very similar. The quadrupole splitting of  $Sn(SO_3F)_4$  ( $1.34 \text{ mm s}^{-1}$ )<sup>111</sup> is identical to that of the tin(IV) atom in  $Sn_3F_2(SO_3CF_3)_6$  and suggests a similar octahedral structure arising from two monodentate  $SO_3CF_3$  groups and two bidentate ligands attached to the tin. The significantly larger quadrupole splitting for  $SnF_2(SO_3F)_2$ ,  $1.96 \text{ mm s}^{-1}$ , indicates that an octahedral structure arising from two terminal fluorines and two bidentate  $SO_3CF_3$  groups in  $Sn_3F_2(SO_3CF_3)_6$  is unlikely. The quadrupole splitting of the tin(II) atom in  $Sn_3F_2(SO_3CF_3)_6$  suggests that the  $Sn(IV)F_2(SO_3CF_3)_4$  unit is probably polymeric. The identical isomer shift and quadrupole splitting for the tin(II) site in  $[Sn(II)Sn(IV)(SO_3CF_3)_6]_x$  and  $Sn_3F_2(SO_3CF_3)_6$  suggests very similar tin(II) environments in both compounds. The compound  $Sn_3F_2(SO_3CF_3)_6$  is best formulated as  $[(Sn(II)SO_3CF_3)_2Sn(IV)F_2(SO_3CF_3)_4]_x$ .

## (iii) Vibrational Data

The vibrational data for the solids of composition  $\text{Sn}(\text{SO}_3\text{CF}_3)_3$ ,  $\text{Sn}_3\text{F}_2(\text{SO}_3\text{CF}_3)_6$  and  $\text{Sn}(\text{IV})\text{O}\cdot\text{SO}_4\text{Sn}(\text{II})(\text{SO}_3\text{F})_2$  together with the literature infrared data for related solids<sup>96,155</sup> are presented in Table 7.2. The assignment by Burger<sup>156</sup> for the infrared spectrum of the  $[\text{SO}_3\text{CF}_3^{-1}]$  ion is also presented in Table 7.2. The infrared spectrum of  $\text{Sn}(\text{SO}_3\text{CF}_3)_3$  given here is very similar to that of the solid  $\text{Sn}(\text{SO}_3\text{CF}_3)_3$  previously reported by Aubke and coworkers.<sup>96</sup> The Raman spectrum of solid  $\text{Sn}(\text{SO}_3\text{CF}_3)_3$  was not reported by these workers, however they did indicate that only a poorly resolved spectrum of  $\text{Sn}(\text{SO}_3\text{CF}_3)_3$  could be obtained. This problem was not encountered here and the Raman spectrum of  $\text{Sn}(\text{SO}_3\text{CF}_3)_3$  is presented in Table 7.2. A qualitative comparison of the measured intensities and frequencies in the infrared spectrum of  $\text{Sn}(\text{SO}_3\text{CF}_3)_4$ <sup>96</sup> (I), and that of  $\text{Sn}(\text{SO}_3\text{CF}_3)_2$ <sup>96</sup> (II), to those presented here for the infrared spectrum of the solid  $\text{Sn}(\text{SO}_3\text{CF}_3)_3$  (III), leads to the conclusion that the infrared spectrum of (III) is not a 1:1 mixture of (I) and (II) and confirms the Mössbauer results.

Assignment of the  $\nu\text{SO}_3$  modes is normally difficult when only infrared data are available because both  $\nu\text{CF}_3$  and  $\nu\text{SO}_3$  are typically broad bands and both are found in the same spectral range.<sup>47</sup> The ranges for the  $\nu\text{SO}_3$  and  $\nu\text{CF}_3$  modes are indicated in Table 7.2 for  $\text{Sn}(\text{SO}_3\text{CF}_3)_3$  and  $\text{Sn}_3\text{F}_2(\text{SO}_3\text{CF}_3)_6$ . The assignment made here for these compounds is based primarily on the Raman spectral data which are much better resolved than the infrared data. The  $[\text{SO}_3\text{CF}_3^-]$  ion has  $C_{3v}$  symmetry while unidentate and bidentate  $[\text{SO}_3\text{CF}_3^-]$  groups are expected to have  $C_s$  symmetry. The E

Table 7.2. Vibrational Data for  $\text{Sn}(\text{SO}_3\text{R})_3$ ,  $\text{Sn}_3\text{F}_2(\text{SO}_3\text{CF}_3)_6$ ,  $\text{Sn}(\text{IV})\text{O}\cdot\text{SO}_4\text{Sn}(\text{II})(\text{SO}_3\text{F})_2$  and Related Compounds

IR Assignment	$\text{AgSO}_3\text{CF}_3$ <sup>155</sup>		$\text{Sn}(\text{SO}_3\text{CF}_3)_4$ <sup>96</sup>		$\text{Sn}(\text{SO}_3\text{CF}_3)_2$ <sup>96</sup>		$\text{Sn}(\text{SO}_3\text{CF}_3)_3$ <sup>96</sup>		$\text{Sn}(\text{SO}_3\text{CF}_3)_3$		$\text{Sn}_3\text{F}_2(\text{SO}_3\text{CF}_3)_6$		$\text{Sn}(\text{IV})\text{O}\cdot\text{SO}_4\text{Sn}(\text{II})(\text{SO}_3\text{F})_2$		Assignment
	IR	IR	IR	IR	IR	IR	Raman	IR	Raman	IR	Raman	IR	Raman		
		1390(m,sh)													
		1360(m,s)													
1270	$\nu\text{SO}_3(\text{E})$		1280(s,sh), 1260(s,b)	1375(s) 1350(m,sh)											$\nu\text{SO}_3$
1237	$\nu\text{CF}_3(\text{A}_1)$		1220(vs,b)	1240(ms)											
1167	$\nu\text{CF}_3(\text{E})$		1210(vs,b)	1210(vs,b)											
			1170(s,sh)	1155(s)											$\nu\text{CF}_3, \nu\text{SO}_3$
			1161(s)	1150(w,sh) 1125(s,b)											
1043	$\nu\text{SO}_3(\text{A}_1)$		1049(s) 1029(ms)	1053(w)											
			980(s,b) 973(m,w)	990(w,sh) 965(s,b)											$\nu\text{SO}_3$
760	$\nu\text{S-C}(\text{A}_1)$		773(m)	773(m)											
			643(s) 622(s)	622(m,b) 600(w,sh)											
647	$\nu\text{SO}_3(\text{A}_1)$		602(m,sh)	640(m,sh) 630(s)											
582	$\nu\text{CF}_3(\text{E})$		570(w,sh)	570(w)											
579			525(w) 510(ms)	520(ms) 509(w)											
515			445(ms) 420(ms)	380(m,sh)											
351	$\nu\text{CSO}(\text{E})$		362(m)	355(w) 351(m)											
320	$\nu\text{CF}_3(\text{A}_1)$		342(ms) 320(w,sh)	345(s)											
217	$\nu\text{CF}_3(\text{E})$														

\* Infrared were recorded from 4000 to 500  $\text{cm}^{-1}$

modes of the  $[\text{SO}_3\text{CF}_3^-]$  ion are expected to be split into two components. However the complexity of the observed spectra indicates extensive splitting of the  $A_1$  modes or perhaps different types of  $\text{SO}_3\text{CF}_3$  in both  $\text{Sn}(\text{SO}_3\text{CF}_3)_3$  and  $\text{Sn}_3\text{F}_2(\text{SO}_3\text{CF}_3)_6$ . Assignment of the  $\nu\text{SO}_3$  and  $\nu\text{CF}_3$  modes in the  $\sim 1230 \text{ cm}^{-1}$  to  $\sim 1100 \text{ cm}^{-1}$  range of the vibrational spectra of these compounds is not unambiguous. The identification of a unidentate or bidentate  $[\text{SO}_3\text{CF}_3^-]$  group must be based on the frequencies of the three sulphur-oxygen stretching modes. For  $\text{Sn}(\text{SO}_3\text{F})_4$ , bands at  $\sim 1415$ ,  $\sim 1130$  and  $\sim 1080 \text{ cm}^{-1}$  indicate bridging  $[\text{SO}_3\text{F}^-]$  groups while bands at  $\sim 1430$ ,  $\sim 1230$  and  $\sim 915 \text{ cm}^{-1}$  indicate unidentate  $[\text{SO}_3\text{F}^-]$  groups based on the assignment of the vibrational data for  $\text{Sn}(\text{SO}_3\text{F})_4$ .<sup>111</sup> For  $(\text{CH}_3)_3\text{SnSO}_3\text{CF}_3$ , bands at  $1319$ ,  $1145$  and  $1045 \text{ cm}^{-1}$  have been assigned to  $\nu\text{SO}_3$  modes of a bridging  $[\text{SO}_3\text{CF}_3^-]$  group while bands at  $1226$  and  $1179 \text{ cm}^{-1}$  to  $\nu\text{CF}_3$  modes of this group.<sup>47</sup> For the  $[\text{SO}_3\text{CF}_3^-]$  ion, the bands at  $1270$  and  $1043 \text{ cm}^{-1}$  have been assigned to  $\nu\text{SO}_3$  modes while the bands at  $1237$  and  $1167 \text{ cm}^{-1}$  have been assigned to  $\nu\text{CF}_3$  modes.<sup>155</sup> However the band at  $1145 \text{ cm}^{-1}$  for  $(\text{CH}_3)_3\text{SnSO}_3\text{CF}_3$  may be one component of the  $\nu\text{CF}_3(\text{E})$  mode which is found at  $1167 \text{ cm}^{-1}$  for the  $[\text{SO}_3\text{CF}_3^-]$  ion. This suggests that it is not possible to distinguish a  $[\text{SO}_3\text{CF}_3^-]$  ion from a bridging  $[\text{SO}_3\text{CF}_3^-]$  group. For  $\text{Sn}(\text{SO}_3\text{CF}_3)_3$ <sup>96</sup> bands at  $\sim 1370$ ,  $\sim 1210$  and  $\sim 970 \text{ cm}^{-1}$  have been assigned to  $\nu\text{SO}_3$  modes of an unidentate  $[\text{SO}_3\text{CF}_3^-]$  group while bands at  $1240$  and  $1155 \text{ cm}^{-1}$  have been assigned to  $\nu\text{CF}_3$  modes of this group. However, these bands are also present in the infrared spectrum of  $\text{Sn}(\text{SO}_3\text{CF}_3)_4$  (Table 7.2) which is suggested to have only chelating  $[\text{SO}_3\text{CF}_3^-]$  groups.<sup>96</sup>

It is not possible to distinguish between unidentate and chelating  $[\text{SO}_3\text{CF}_3^-]$  groups based on the infrared data of Aubke and coworkers.<sup>47,96</sup> The bands in the spectral range  $\sim 1240$  to  $\sim 1155 \text{ cm}^{-1}$  cannot be considered characteristic of  $\nu\text{SO}_3$  modes since  $\nu\text{CF}_3$  modes are also found in this range.

For  $\text{Sn}(\text{SO}_3\text{CF}_3)_3$  and  $\text{Sn}_3\text{F}_2(\text{SO}_3\text{CF}_3)_6$  the bands at  $\sim 1370 \text{ cm}^{-1}$  are assigned to  $[\text{SO}_3\text{CF}_3^-]$  groups which are covalently bonded to tin(IV). The bands at  $\sim 1125 \text{ cm}^{-1}$  indicate bridging  $[\text{SO}_3\text{CF}_3^-]$  groups for both of these compounds. The bands at  $\sim 970 \text{ cm}^{-1}$  suggest chelating or unidentate  $[\text{SO}_3\text{CF}_3^-]$  groups. However, bands at  $\sim 1270$  and  $\sim 1040 \text{ cm}^{-1}$  are also present in the vibrational spectra of these compounds and it is possible the  $[\text{SO}_3\text{CF}_3^-]$  ion is present in both  $\text{Sn}(\text{SO}_3\text{CF}_3)_3$  and  $\text{Sn}_3\text{F}_2(\text{SO}_3\text{CF}_3)_6$  in addition to covalently bonded  $[\text{SO}_3\text{CF}_3^-]$  groups.

Trans terminal fluorines as proposed for  $\text{SnF}_2(\text{SO}_3\text{F})_2$  exhibit a strong infrared band at  $691 \text{ cm}^{-1}$  which has been assigned to the asymmetric stretch,  $\nu_{\text{as}} \text{SnF}_2$ .<sup>42</sup> Tin(IV) fluoride has trans terminal fluorine atoms and exhibits this infrared band at  $724 \text{ cm}^{-1}$ .<sup>160</sup> The absence of a strong infrared band at  $\sim 700 \text{ cm}^{-1}$  indicates that trans terminal fluorines are not present in  $\text{Sn}_3\text{F}_2(\text{SO}_3\text{CF}_3)_6$ . This suggests that the fluorines are bridging tin atoms. Unfortunately it is not possible to distinguish  $\delta\text{SO}_3$ , and  $\delta\text{CF}_3$  from the  $\nu\text{Sn-F}$  modes associated with bridging fluorines as indicated in Table 7.2. An octahedral tin(IV) geometry with unidentate  $[\text{SO}_3\text{CF}_3^-]$  groups and bridging  $[\text{SO}_3\text{CF}_3^-]$  groups and bridging fluorines is not inconsistent with the spectroscopic data

for  $\text{Sn}_3\text{F}_2(\text{SO}_3\text{CF}_3)_6$ . An octahedral tin(IV) geometry with chelating and bridging  $[\text{SO}_3\text{CF}_3^-]$  groups is not inconsistent with the spectroscopic data for  $\text{Sn}(\text{SO}_3\text{CF}_3)_3$ .

The vibrational spectra of the solid  $\text{Sn(IV)O}\cdot\text{SO}_4\text{Sn(II)(SO}_3\text{F)}_2$ , Table 7.2, shows bands in the range  $1322\text{ cm}^{-1}$  to  $905\text{ cm}^{-1}$  which are assigned to sulphur-oxygen stretching modes. The  $\nu\text{SO}_3$  modes in the range  $1300$  to  $1322\text{ cm}^{-1}$  are not characteristic of covalently bonded tin(IV) fluorosulphates which exhibit  $\nu\text{SO}_3$  modes  $> 1400\text{ cm}^{-1}$  for compounds where all the ligands are very electronegative such as  $\text{SnCl}_2(\text{SO}_3\text{F})_2$ ,<sup>111</sup>  $\text{SnF}_2(\text{SO}_3\text{F})_2$ ,<sup>42</sup>  $\text{Sn}(\text{SO}_3\text{F})_4$ ,<sup>111</sup> and  $\text{K}_2\text{Sn}(\text{SO}_3\text{F})_6$ .<sup>144</sup> The highest frequency mode found for  $\text{Sn}(\text{SO}_3\text{F})_2$  ( $1300\text{ cm}^{-1}$ <sup>140</sup>) is similar to that found here. However  $\text{Sn}(\text{SO}_3\text{F})_2$  exhibits a strong Raman band at  $1076\text{ cm}^{-1}$ <sup>140</sup> which is absent in the vibrational spectrum of  $\text{Sn(IV)O}\cdot\text{SO}_4\text{Sn(II)(SO}_3\text{F)}_2$ . The  $1322$ ,  $1213$  and  $1048\text{ cm}^{-1}$  bands observed for  $\text{Sn(IV)O}\cdot\text{SO}_4\text{Sn(II)(SO}_3\text{F)}_2$  suggest that the  $[\text{SO}_3\text{F}^-]$  groups are covalently bonded because three, rather than two, bands are observed. The remaining  $\nu\text{SO}_3$  modes in the range  $1150$  to  $905\text{ cm}^{-1}$  are assigned to the  $\text{SO}_4$  group since these are within the spectral range for the  $[\text{SO}_4^{2-}]$  group.<sup>143</sup> These modes are not observed in  $\text{Cu}(\text{SO}_3\text{F})_2$ ,<sup>156</sup>  $\text{KSO}_3\text{F}$ ,<sup>157</sup> or  $\text{Sn}(\text{SO}_3\text{F})_2$ .<sup>140</sup> The intense Raman band at  $598\text{ cm}^{-1}$  is perhaps  $\nu\text{Sn-O-Sn}$ .

The infrared spectrum of  $\text{SnF}_3$  is presented in Table 7.3 together with vibrational data for related tin fluorides from the literature. The strongest infrared band in  $\text{SnF}_4$  ( $730\text{ cm}^{-1}$ )<sup>156</sup> and the infrared active band in  $\text{SnF}_2$  ( $446\text{ cm}^{-1}$ )<sup>159</sup> are absent in  $\text{SnF}_3$ . The product  $\text{SnF}_3$ , has

Table 7.3  
 Vibrational Data for SnF<sub>3</sub> and Related Compounds

(SnF) <sub>2</sub> SnF <sub>6</sub> <sup>132</sup>	SnF <sub>2</sub> <sup>159</sup>	SnF <sub>4</sub> <sup>160</sup>	Na <sub>2</sub> SnF <sub>6</sub> <sup>161</sup>	SnF <sub>3</sub>	Assignment for SnF <sub>3</sub>
IR	IR	IR	IR Raman	IR*	
		730(s)			
		646(w)			
			599		
560(s,b)			559		
				540(s,b)	νSn-F
		472(ms)	477		
430(s)	446	436(m)			
360(s)	350			350(w)	δSn-F
			300		
		262(ms)			
		245(mw)	252	250(m)	δSn-F

\* Infrared were recorded from 4000 to 200 cm<sup>-1</sup>.



been formulated as  $[\text{Sn(II)Sn(IV)F}_6]_n$ , based on the interpretation of the  $^{119}\text{Sn}$  Mössbauer data, and the absence of the 730 and 446  $\text{cm}^{-1}$  bands in the infrared spectrum support this suggestion. Compounds with a Sn(II)-F-Sn(II) bridge have an infrared active band at  $\sim 440 \text{ cm}^{-1}$ ,  $[\text{SnF}_2, 446 \text{ cm}^{-1}; ^{159} \text{Sn}_3\text{F}_8, 430 \text{ cm}^{-1}(\text{s}); ^{132} [\text{SnF}]_3\text{AsF}_6, 444 \text{ cm}^{-1}(\text{m.b})^{140}]$  which has been assigned in  $\text{SnF}_2$  and  $[\text{SnF}]_3\text{AsF}_6$  to an asymmetric stretch of the Sn(II)-F-Sn(II) bridge.<sup>140</sup> This band is absent here and it is clear that the compound  $[\text{Sn(II)Sn(IV)F}_6]_n$  is not a polymer with strong Sn(II)-F-Sn(II) bridging. The infrared spectrum of  $[\text{Sn(II)Sn(IV)F}_6]_n$  consists of three bands (540, 350 and 250  $\text{cm}^{-1}$ ) whereas the infrared spectrum of the octahedral  $[\text{Sn(IV)F}_6^{2-}]$  ion in  $\text{Na}_2\text{SnF}_6$  has only two bands (554  $\text{cm}^{-1}$  and 300  $\text{cm}^{-1}$ ).<sup>161</sup> This indicates that if a  $[\text{Sn(IV)F}_6^{2-}]$  species is present in  $[\text{Sn(II)Sn(IV)F}_6]_n$  then the symmetry of the  $[\text{Sn(IV)F}_6^{2-}]$  ion is not that of the isolated  $[\text{Sn(IV)F}_6^{2-}]$  ion. However, it must be pointed out that the 540  $\text{cm}^{-1}$  band in the infrared spectrum of  $[\text{Sn(II)Sn(IV)F}_6]_n$  is broad and is perhaps comprised of several bands in the range 600 to 470  $\text{cm}^{-1}$ . A  $[\text{SnF}_6^{2-}]$  species with no symmetry (Cs) would be expected to exhibit at least five bands, both infrared and Raman active, of similar frequencies to those bands found in the vibrational spectra of  $\text{Na}_2\text{SnF}_6$ . The 600 to 470  $\text{cm}^{-1}$  range for  $[\text{Sn(II)Sn(IV)F}_6]_n$  may be more resolved in the Raman spectrum but unfortunately, because of fluorescence problems, the Raman spectrum of  $[\text{Sn(II)Sn(IV)F}_6]_n$  could not be obtained. A broad band at 560  $\text{cm}^{-1}$  is present in the infrared spectrum of  $(\text{Sn(II)F})_2\text{Sn(IV)F}_6$ , which has extensive Sn(II)-F-Sn(IV) bridging and a distorted octahedral  $[\text{SnF}_6^{2-}]$

species,<sup>132</sup> suggesting that perhaps a similar  $[\text{SnF}_6^{2-}]$  moiety is present in  $[\text{Sn(II)Sn(IV)F}_6]_n$ . An octahedral  $[\text{SnF}_6^{2-}]$  ion with only small distortions would be consistent with the small  $^{119}\text{Sn}$  Mössbauer quadrupole splitting for the Sn(IV) atom in  $[\text{Sn(II)Sn(IV)F}_6]_n$  as previously indicated. A six-coordinate octahedral structure arising from two monodentate and two bidentate ligands attached to tin(IV) such as has been established for  $\text{SnF}_4$ <sup>113</sup> gives a much more complex infrared spectrum than that of  $[\text{Sn(II)Sn(IV)F}_6]_n$  and such an environment cannot be present, based on the infrared data. This conclusion is consistent with the  $^{119}\text{Sn}$  Mössbauer data previously discussed. The infrared band at  $540\text{ cm}^{-1}$  is assigned to the Sn(II)-F-Sn(IV) stretch, and covalent interactions via Sn(II)-F-Sn(IV) would be consistent with the  $^{119}\text{Sn}$  Mössbauer isomer shift of the tin(II) atom in  $[\text{Sn(II)Sn(IV)F}_6]_n$  where bridging of this type has been suggested. The Sn(II)-F-Sn(IV) stretch at  $540\text{ cm}^{-1}$  is closer in frequency to the  $476\text{ cm}^{-1}$  band of  $\text{SnF}_4$ <sup>160</sup> which has been assigned to the Sn(IV)-F-Sn(IV) bridging stretch than to the  $\text{SnF}_4$   $730\text{ cm}^{-1}$  band for which was assigned to the terminal Sn-F stretch.

## CHAPTER EIGHT

### CONCLUSIONS

#### A. Summary

The acid solvolyses of hexamethylditin and hexphenylditin results in the formation of new tin compounds. The usefulness of  $^{119}\text{Sn}$  Mössbauer spectroscopy as a probe for the structural elucidation of tin compounds when combined with complimentary spectroscopic information is demonstrated.

Low temperature solvolysis of hexamethylditin in fluorosulphuric acid results in the formation of a solvated tetramethylditin dication. Reaction of hexamethylditin with halocarboxylic acids under optimum conditions results in the production of compounds with the formula  $(\text{CH}_3)_4\text{Sn}_2(\text{O}_2\text{CR})_2$ . The  $^{119}\text{Sn}$  Mössbauer data of these compounds are best interpreted in terms of two, five-coordinate, tin(IV) atoms per molecule. Infrared, Raman,  $^1\text{H}$  and  $^{13}\text{C}$  n.m.r. data are best interpreted in terms of a dimer with a symmetrically substituted planar tetramethylditin moiety bridged intramolecularly by two carboxylate groups. The spectroscopic data suggest independent molecules persist in solution, and that the average Sn-O bond length increases as the average electronegativity of the R substituent on the carboxylate ligand increases. The X-ray crystal structure of the trichloroacetato derivative together with accurate structural data for the monochloro- and trifluoroacetato derivatives supports these conclusions. Contrary to previous studies on the

structurally related trimethyltin carboxylates<sup>55,61</sup> the asymmetry in the carboxylate bridge is not related to the electronegativity of the R substituent of the carboxylate group, and is independent of the <sup>119</sup>Sn Mössbauer quadrupole splitting. The difference in the Sn-O bond lengths for the (CH<sub>3</sub>)<sub>4</sub>Sn<sub>2</sub>(O<sub>2</sub>CR)<sub>2</sub> compounds can be attributed solely to intermolecular interactions.

Compounds with the formula {[(CH<sub>3</sub>)<sub>2</sub>Sn(O<sub>2</sub>CR)]<sub>2</sub>O}<sub>2</sub> (R = CF<sub>3</sub>, CCl<sub>3</sub>) have been prepared and characterized by X-ray analysis. The crystal and molecular structure of {[(CH<sub>3</sub>)<sub>2</sub>Sn(O<sub>2</sub>CF<sub>3</sub>)]<sub>2</sub>O}<sub>2</sub> is described and compared to that of (CH<sub>3</sub>)<sub>4</sub>Sn<sub>2</sub>(O<sub>2</sub>CCF<sub>3</sub>)<sub>2</sub>.

The solvolysis of hexaphenylditin by carboxylic acids results in the formation of compounds with empirical formula Sn(O<sub>2</sub>CR)<sub>3</sub>. <sup>119</sup>Sn Mössbauer spectroscopy shows that these compounds contain both tin(II) and tin(IV), and this, together with the spectroscopic infrared and Raman data, lead to the conclusion that these compounds are best formulated as [Sn(II)Sn(IV)O(O<sub>2</sub>CR)<sub>4</sub>O(OCR)<sub>2</sub>]<sub>2</sub>.

The solvolysis of tetraphenyltin in carboxylic acids results in the formation of Sn(O<sub>2</sub>CR)<sub>4</sub> compounds. The <sup>119</sup>Sn Mössbauer data of Sn(O<sub>2</sub>CCF<sub>3</sub>)<sub>4</sub> together with the vibrational data of this compound are best interpreted in terms of the presence of both unidentate and bidentate carboxylate groups with the tin atom in an octahedral environment. <sup>119</sup>Sn Mössbauer data for Sn(O<sub>2</sub>CCCl<sub>3</sub>)<sub>4</sub> and Sn(O<sub>2</sub>CC<sub>3</sub>F<sub>7</sub>)<sub>4</sub> in the presence of excess acid are best interpreted in terms of this structure. The <sup>119</sup>Sn Mössbauer data for Sn(O<sub>2</sub>CHCl<sub>2</sub>)<sub>4</sub> and Sn(O<sub>2</sub>CCH<sub>2</sub>Cl)<sub>4</sub> in the presence of excess acid are best interpreted in terms of chelating carboxylate groups with a dodecahedral coordination.

The crystal and molecular structure of  $[\text{Sn(II)Sn(IV)O}(\text{O}_2\text{CCF}_3)_4]_2\text{C}_6\text{H}_6$ , a derivative of the  $[\text{Sn(II)Sn(IV)O}(\text{O}_2\text{CCF}_3)_4\text{O}(\text{OCCF}_3)_2]_2$  complex has been determined by single crystal X-ray diffraction. The molecular structure consists of independent centrosymmetric  $[\text{Sn(II)Sn(IV)O}(\text{O}_2\text{CCF}_3)_4]_2$  units with one benzene molecule per unit.

The solvolysis of hexaphenylditin in strong acid medium has been examined. Solid products of empirical formula  $\text{SnF}_3$  and  $\text{Sn}(\text{SO}_3\text{CF}_3)_3$  have been prepared and identified spectroscopically as  $[\text{Sn(II)Sn(IV)F}_6]_x$  and  $[\text{Sn(II)Sn(IV)}(\text{SO}_3\text{CF}_3)_6]_x$ . The  $^{119}\text{Sn}$  Mössbauer spectra of the analogous  $[\text{Sn(II)Sn(IV)}(\text{SO}_3\text{R})_6]_x$  ( $\text{R} = \text{CH}_3, \text{C}_2\text{H}_5, \text{OH}$ ) compounds in the presence of excess acid have been examined. The solid isolated from the reaction of hexaphenylditin in fluorosulphuric acid is not  $[\text{Sn(II)Sn(IV)}(\text{SO}_3\text{F})_6]_x$  and the spectroscopic and analytical data of the solid are best interpreted in terms of a compound of formulation  $[\text{Sn(IV)O}\cdot\text{SO}_4\text{Sn(II)}(\text{SO}_3\text{F})_2]_x$ . Reaction of  $[\text{Sn(II)Sn(IV)}(\text{SO}_3\text{CF}_3)_6]_x$  with  $\text{SnF}_2$  produces  $\text{Sn}_3\text{F}_2(\text{SO}_3\text{CF}_3)_6$  which is formulated as  $[(\text{Sn(II)SO}_3\text{CF}_3)_2\text{Sn(IV)F}_2(\text{SO}_3\text{CF}_3)_4]_x$ .

#### B. Suggested Topics for Future Research

Based on preparations of the tin compounds reported in this thesis, a number of new topics of interest to the tin chemist may be suggested. The successful synthesis of a series of  $(\text{CH}_3)_4\text{Sn}_2(\text{O}_2\text{CR})_2$  compounds suggests that similar compounds may be produced by the solvolysis of other hexa-alkylditin compounds in carboxylic acids. The spectroscopic study of a series of  $\text{R}_4\text{Sn}_2(\text{O}_2\text{CR}')_2$  compounds with very

bulky R groups would be of interest since these compounds would be expected to have four coordinate tin atoms. Similarly reactions of a series  $(\text{CH}_3)_n\text{Sn}-\text{M}(\text{CH}_3)_3$  ( $\text{M} = \text{Si}, \text{Ge}$ ), with carboxylic acids may produce the corresponding  $(\text{CH}_3)_4\text{SnM}(\text{O}_2\text{CR})_2$  compounds. The solvolysis of hexaphenylditin by acetic acid leads to the formation of a mixed oxidation state tin compound. The tin-containing hexaphenyl compounds,  $(\text{C}_6\text{H}_5)_3\text{SiSn}(\text{C}_6\text{H}_5)_3$  and  $(\text{C}_6\text{H}_5)_3\text{GeSn}(\text{C}_6\text{H}_5)_3$ , react with acetic acid with complete cleavage of all metal-carbon bonds, unlike the tin-free compounds,  $(\text{C}_6\text{H}_5)_3\text{GeGe}(\text{C}_6\text{H}_5)_3$ ,  $(\text{C}_6\text{H}_5)_3\text{SiGe}(\text{C}_6\text{H}_5)_3$  and  $(\text{C}_6\text{H}_5)_3\text{SiSi}(\text{C}_6\text{H}_5)_3$ , to form qualitatively compounds of composition  $\text{SnGe}(\text{O}_2\text{CCH}_3)_6$  and  $\text{SnSi}(\text{O}_2\text{CCH}_3)_6$ .<sup>162</sup> These carboxylate compounds are supposed to react with HCl to form  $\text{Cl}_3\text{Sn}-\text{GeCl}_3$  and  $\text{Cl}_3\text{Sn}-\text{SiCl}_3$ , which disproportionate at room temperature into  $\text{MCl}_4$  and  $\text{SnCl}_2$ .<sup>162</sup> A spectroscopic study of these carboxylate compounds will likely show these carboxylates to be  $[\text{Sn}(\text{II})\text{Ge}(\text{IV})\text{O}(\text{O}_2\text{CCH}_3)_4\text{O}(\text{OCCH}_3)_2]_2$  and  $[\text{Sn}(\text{II})\text{Si}(\text{IV})\text{O}(\text{O}_2\text{CCH}_3)_4\text{O}(\text{OCCH}_3)_2]_2$  respectively.

The chemical reactions of  $[\text{Sn}(\text{II})\text{Sn}(\text{IV})\text{O}(\text{O}_2\text{CR})_4\text{O}(\text{OCR})_2]_2$  compounds have not been investigated. A compound of composition  $\text{Sn}(\text{O}_2\text{CCH}_3)_3$  originally prepared by Wiberg and Behringer and identified as a ditin species was reacted with HCl to produce the proposed ditin compound  $\text{Sn}_2\text{Cl}_4(\text{O}_2\text{CCH}_3)_2$ .<sup>91</sup> Excess HCl produced  $\text{Sn}_2\text{Cl}_6$ , which disproportionates at room temperature into  $\text{SnCl}_4$  and  $\text{SnCl}_2$ .<sup>91</sup> The  $\text{Sn}_2\text{Cl}_4(\text{O}_2\text{CCH}_3)_2$  compound could have a number of possible formulations, such as  $[\text{Sn}(\text{II})\text{Sn}(\text{IV})\text{Cl}_4(\text{O}_2\text{CCH}_3)_2]_x$  or  $[\text{Sn}(\text{II})\text{Sn}(\text{IV})\text{OCl}_4\text{O}(\text{OCCH}_3)_2]_x$ . The characterization of a series of these tin carboxylates by the methods

outlined in this thesis would establish the correct formulation of these compounds. The synthesis and characterization of  $[\text{Sn(II)Sn(IV)O}(\text{O}_2\text{CC}_6\text{H}_5\text{NO}_2\text{-o})_4\text{THF}]_2$ ,<sup>105</sup>  $[\text{Sn(II)Sn(IV)O}(\text{O}_2\text{CR})_4]_2\text{C}_6\text{H}_6$ , and the series of  $[\text{Sn(II)Sn(IV)O}(\text{O}_2\text{CR})_4\text{O}(\text{OCR})_2]_2$  compounds, which are thought to contain the same  $[\text{Sn(II)Sn(IV)O}(\text{O}_2\text{CR})_4]_2$  unit, suggests that these types of compounds may be interconvertible under appropriate reaction conditions. The basic geometry of the  $[\text{Sn(II)Sn(IV)O}(\text{O}_2\text{CR})_4]_2$  unit appears to be independent of the base molecules THF and benzene, indicating an opportunity to study the effects of donor molecules on the tin(II) Mössbauer parameters without major structural changes in the  $[\text{Sn(II)Sn(IV)O}(\text{O}_2\text{CR})_4]_2$  unit. Anomalies in the tin(II) <sup>119</sup>Sn Mössbauer parameters for a series of  $[\text{Sn(II)Sn(IV)O}(\text{O}_2\text{CR})_4\text{DONOR}]_2$  compounds may be taken as an indication of structural changes in the tin(II) environment.

The characterization of "well defined" compounds with tin in both the +2 and +4 oxidation state, such as  $[(\text{Sn(II)F})_2\text{Sn(IV)F}_6]_x$ ,<sup>132</sup>  $[\text{Sn(II)Sn(IV)F}_6]_x$ ,  $[(\text{Sn(II)SO}_3\text{CF}_3)_2\text{Sn(IV)F}_2(\text{SO}_3\text{CF}_3)_4]_x$  and  $[\text{Sn(II)Sn(IV)}(\text{SO}_3\text{CF}_3)_6]_x$ , suggests the possible existence of other similar complexes in the series  $[\text{Sn(II)Sn(IV)F}_n(\text{SO}_3\text{CF}_3)_{6-n}]_x$  and  $[(\text{Sn(II)SO}_3\text{CF}_3)_2\text{Sn(IV)F}_n(\text{SO}_3\text{CF}_3)_{4-n}]_x$ . The most likely values of n are 0, 2 and 6 with the possible value of 4 implied by the proposed existence of the  $[\text{Sn(IV)F}_4(\text{SO}_3\text{CF}_3)_2]^{-2}$  anion in solution. Compounds of these types might be prepared by ligand exchange reactions of the appropriate tin compounds. For example, the compound  $[(\text{Sn(II)SO}_3\text{CF}_3)_2\text{Sn(IV)F}_6]_x$  might be prepared by the interaction of  $\text{Sn}(\text{SO}_3\text{CF}_3)_2$  with  $[\text{Sn(II)Sn(IV)F}_6]_x$

analogous to the preparation of  $[(\text{Sn}(\text{II})\text{SO}_3\text{CF}_3)_2\text{Sn}(\text{IV})\text{F}_2(\text{SO}_3\text{CF}_3)_4]_x$  from the interaction of  $\text{SnF}_2$  with  $[\text{Sn}(\text{II})\text{Sn}(\text{IV})(\text{SO}_3\text{CF}_3)_6]_x$ .

Examination of the X-ray structures of the tin(II) compounds  $\text{Sn}_2\text{F}_3\text{BF}_4$  and  $\text{Sn}_3\text{F}_5\text{BF}_4$  and spectroscopic data available for other proposed tin(II) species in solution,<sup>143</sup> such as  $\text{Sn}_4\text{F}_7\text{BF}_4$  and  $\text{Sn}_5\text{F}_9\text{BF}_4$ , suggests an even wider range of mixed oxidation state tin compounds. The fluoride,  $(\text{SnF}_2)_6\text{SnF}_4$  which is reportedly isolated from melts of  $\text{SnF}_4$  and  $\text{SnF}_2$ ,<sup>137</sup> may be an analogue of  $\text{Sn}_3\text{F}_5\text{BF}_4$ ,  $[\text{Sn}_6\text{F}_{10}\text{SnF}_6]_x$ . The structure of  $[\text{Sn}_6\text{F}_{10}\text{SnF}_6]_x$  may consist of  $\text{Sn}_6\text{F}_{10}$  tin(II) fluoride rings with octahedral  $[\text{Sn}(\text{IV})\text{F}_6]^{2-}$  anions connecting the rings. Similarly, the structure of the analogue of  $\text{Sn}_2\text{F}_3\text{BF}_4$ ,  $[\text{Sn}_4\text{F}_6\text{SnF}_6]_x$ , may consist of  $[\text{Sn}_2\text{F}_3]_n$  tin(II) fluoride polymer chains connected by octahedral  $\text{Sn}(\text{IV})\text{F}_6$  species. The successful synthesis of  $[\text{Sn}(\text{II})\text{Sn}(\text{IV})\text{F}_6]_x$  from the acid solvolysis of  $(\text{C}_6\text{H}_5)_6\text{Sn}_2$  in HF suggests that addition of the appropriate amount of  $\text{SnF}_2$  to this solvolysis reaction may result in the formation of these and other mixed oxidation state tin fluorides.



## REFERENCES

1. C. Lowig, *Ann.*, 84, 308 (1852).
2. A. K. Sawyer, "Organotin Compounds", Vol. 3, Marcel Dekker Inc., New York (1972).
3. H. Gilman, W. H. Atwell and E. K. Cartledge, *Adv. Organometal Chem.*, 4, 1 (1966).
4. N. N. Greenwood and T. C. Gibb, "Mössbauer Spectroscopy", Chapman and Hall, London (1971), p. 371 and references therein.
5. V. I. Goldanskii and R. Herber, "Chemical Applications of Mössbauer Spectroscopy", Academic Press, New York (1968).
6. G. M. Bancroft and R. H. Platt, "Mössbauer Spectra of Inorganic Compounds: Bonding and Structure", *in* *Adv. in Inorg. Chem. Radiochem.*, 15, Academic Press, New York (1972), pp. 59.
7. T. C. Gibb, "Principles of Mössbauer Spectroscopy", Chapman and Hall, London (1976).
8. H. Frauenfelder, "The Mössbauer Effect", W. A. Benjamin Inc., New York (1963).
9. J. Ballard, Ph. D. Thesis, McMaster University (1977).
10. E. V. Van den Berghe and G. P. Van der Kelen, *J. Organomet. Chem.*, 59, 175 (1973).
11. T. N. Mitchell, *J. Organomet. Chem.*, 59, 189 (1973).
12. T. N. Mitchell and G. Walter, *J. Chem. Soc. Perkin II*, 1842 (1977).

13. H. Günther, "NMR Spectroscopy", John Wiley and Sons, Toronto (1980).
14. G. H. Stout and L. H. Jensen, "X-Ray Structure Determination", MacMillan, London (1968).
15. G. Turner, Ph.D. Thesis, McMaster University (1976).
16. J. J. Zuckerman and J. A. Zubieta, "Structural Tin Chemistry", in Progress in Inorg. Chem., 24, 251, John Wiley and Sons Inc., U.S.A. (1978).
17. P. A. Flinn, "Mössbauer Isomer Shifts", G. K. Shenoy and F. E. Wagner (eds.), p. 597, North-Holland Publishing Company (1978).
18. J. K. Lees and P. A. Flinn, J. Chem. Phys., 48, 882 (1968).
19. R. V. Parish and R. H. Platt, J. Chem. Soc. A, 2145 (1969); Inorg. Chim. Acta, 4, 65 (1970).
20. B. W. Fitzsimmons, N. J. Seeley and A. W. Smith, J. Chem. Soc. A, 143 (1969).
21. M. G. Clark, A. G. Maddock and R. H. Platt, J. Chem. Soc. Dalton Trans., 281 (1972).
22. G. M. Bancroft, V. G. K. Das, F. K. Sham and M. G. Clark, J. Chem. Soc. Dalton Trans., 643 (1976).
23. V. I. Goldanskii, G. M. Gorodinskii, S. V. Kargagin and L. A. Korytho, Dokl. Akad. Nauk SSSR, 147, 127 (1961).
24. P. A. W. Dean, R. J. Gillespie and P. K. Ummat, Inorg. Synth., XV, 213 (1974).
25. G. M. Bancroft, W. K. Ong, A. G. Maddock, R. K. Prince and A. J. Stone, J. Chem. Soc. A, 1966 (1967).

26. A. R. Periera, M. Sc. Thesis, McMaster University (1973).
27. J. P. Krasznai, Ph.D. Thesis, McMaster University (1975).
28. R. Okawara and E. G. Rochow, J. Am. Chem. Soc., 82, 3285 (1960).
29. J. P. Donaldson and W. Moser, Analyst, 84, 10 (1959).
30. A. I. Vogel, "A Text-Book of Quantitative Inorganic Analysis", 3rd Ed., Longmans, London (1961).
31. A. Ladenburg, Ber., 3, 647 (1870).
32. N. S. Vyazankin, G. A. Rozuvaiv and S. P. Kornia, Zhur. Obsh. Khim, 33, 1041 (1963).
33. C. A. Kraus and W. V. Sessions, J. Am. Chem. Soc., 47, 2361 (1925).
34. G. Tagliavini and U. Belluco, Piloni Ric. Sci. Rend., 3, 889 (1963).
35. W. P. Neumann and W. P. Pedain, Tetrahedron Letters, 2461 (1964).
36. R. Sommer, B. Schneider and W. P. Neumann, Ann., 692, 12 (1964).
37. A. J. Gibbons, A. K. Sawyer and A. Ross, J. Org. Chem., 26, 2304 (1961).
38. A. J. Sawyer and H. G. Kuivila, J. Am. Chem. Soc., 85, 1010 (1963).
39. R. K. Ingham, D. S. Rosenberg and H. Gilman, Chem. Rev., 60, 478 (1960).
40. D. Seyforth, J. Am. Chem. Soc., 79, 2133 (1957).
41. P. A. Yeats, J. R. Sams and F. Aubke, Inorg. Chem., 11, 2634 (1972).
42. L. E. Levchuck, J. R. Sams and F. Aubke, Inorg. Chem., 11, 43 (1972).

43. T. H. Tan, J. R. Dalziel, P. A. Yeats, J. R. Sams, R. C. Thompson and F. Aubke, *Can. J. Chem.*, 50, 1843 (1972).
44. R. J. Gillespie, R. Kapoor and E. A. Robinson, *Can. J. Chem.*, 44, 1197 (1966).
45. T. Birchall, P. K. H. Chan and A. Periera, *J. Chem. Soc. Dalton Trans.*, 2157 (1974).
46. P. A. Yeats, B. F. E. Ford, J. R. Sams and F. Aubke, *J. Chem. Soc., Chem. Commun.*, 791 (1969).
47. P. A. Yeats, J. R. Sams and F. Aubke, *Inorg. Chem.*, 10, 1877 (1971).
48. F. A. Allen, J. Lerbscher and J. Trotter, *J. Chem. Soc. A*, 2507 (1971).
49. W. McFarlane, *J. Chem. Soc. A*, 1630 (1968).
50. A. K. Sawyer and H. G. Kuivila, *J. Org. Chem.*, 27, 837 (1962).
51. A. K. Sawyer and H. G. Kuivila, *J. Am. Chem. Soc.*, 82, 5958 (1960).
52. P. Simons and W. A. G. Graham, *J. Organomet. Chem.*, 10, 457 (1967).
53. E. V. Van den Berghe, G. P. Van der Kelen and J. Albrecht, *Inorg. Chim. Acta*, 2, 89 (1968).
54. B. F. E. Ford, B. V. Liengmé and J. R. Sams, *J. Organomet. Chem.*, 19, 53 (1969).
55. C. Poder and J. R. Sams, *J. Organomet. Chem.*, 19, 67 (1969).
56. R. E. Hester, *J. Organomet. Chem.*, 23, 127 (1970).
57. N. W. G. Debye, D. E. Fenton, S. E. Ulrich and J. J. Zuckerman, *J. Organomet. Chem.*, 28, 339 (1971).

58. T. N. Mitchell, *J. Organomet. Chem.*, 59, 189 (1973).
59. N. W. Alcock and R. E. Timms, *J. Chem. Soc. A*, 1873 (1968).
60. N. W. Alcock and R. E. Timms, *J. Chem. Soc. A*, 1876 (1968).
61. H. W. Chih and B. R. Penfold, *J. Cryst. Mol. Struct.*, 3, 285 (1973).
62. B. F. E. Ford and J. R. Sams, *J. Organomet. Chem.*, 31, 47 (1971).
63. R. E. Hester, *Indian J. of Pure and App. Phys.*, 9, 899 (1971).
64. G. Plazzogna, V. Peruzzo and G. Tagliavini, *J. Organomet. Chem.*, 24, 667 (1970).
65. M. Delmas, J. C. Maire, Y. Richard, G. Plazzogna, V. Peruzzo and G. Tagliavini, *J. Organomet. Chem.*, 30, C101 (1971).
66. W. F. Edgell and C. H. Ward, *J. Mol. Spectroscopy*, 8, 343 (1962).
67. B. Fontal and T. G. Spiro, *Inorg. Chem.*, 10, 9 (1971).
68. M. P. Brown, E. Cartmell and G. W. A. Fowles, *J. Chem. Soc.*, 506 (1960).
69. G. Bandoli and D. A. Clemante, *J. Chem. Soc., Chem. Commun.*, 311 (1971).
70. R. V. Parish and C. E. Johnson, *J. Chem. Soc. A*, 1906 (1971).
71. R. H. Herber, H. A. Stockler and W. T. Reichle, *J. Chem. Phys.*, 45, 2447 (1965).
72. C. F. Shaw and A. L. Allred, *J. Organomet. Chem.*, 28, 53 (1971).
73. B. Mathiasch, *J. Organomet. Chem.*, 141, 295 (1977).
74. B. Mathiasch, *Inorg. Nucl. Chem. Lett.*, 13, 13 (1977).
75. B. Mathiasch, *Synth. React. Inorg. Met. Org. Chem.*, 8, 103 (1978).

76. M. Kumada, M. Yamaguchi, Y. Yamamoto, J.-I, Nakajima and J. Shiina, *J. Org. Chem.*, 21, 1264 (1956).
77. K. Triplett and M. D. Curtis, *J. Organomet. Chem.*, 107, 23 (1976).
78. U. Schröder and W. P. Neumann, *Angew. Chem. Internat. Ed.*, 14, 246 (1975).
79. S. Calogero, D. A. Clemente, V. Peruzzo and G. Tagliavini, *J. Chem. Soc. Dalton Trans.*, 1173 (1979).
80. S. Calogero, P. Ganis, V. Peruzzo and G. Tagliavini, *J. Organomet. Chem.*, 191, 381 (1980).
81. A. C. Larson, *Acta Crystallogr.*, 23 644 (1967).
82. International Tables for X-Ray Crystallography, Vol. 1, Kynoch Press, Birmingham (1962).
83. R. Faggiani, J. P. Johnson, I. D. Brown and T. Birchall, *Acta Crystallogr., Sect. B*, B35, 1227 (1979).
84. R. Faggiani, J. P. Johnson, I. D. Brown and T. Birchall, *Acta Crystallogr., Sect. B*, B34, 3742 (1978).
85. L. Pauling, "Nature of the Chemical Bond", Cornell University Press, Ithaca, New York (1960), 3rd Ed.
86. D. H. Olsen and R. E. Rundle, *Inorg. Chem.*, 2, 1320 (1963).
87. H. Preut, H.-J. Haupt and F. Huber, *Z. Anorg. Allg. Chem.*, 396, 81 (1973).
88. R. Faggiani, J. P. Johnson, I. D. Brown and T. Birchall, *Acta Crystallogr., Sect. B*, B34, 3743 (1978).
89. R. Graziani, G. Bombieri, E. Forsellini, P. Furlan, V. Peruzzo and G. Tagliavini, *J. Organomet. Chem.*, 125, 43 (1977).

90. C. D. Garner, B. Hughes and T. J. King, *Inorg. Nucl. Chem. Letters*, 12, 859 (1976).
91. E. Wiber and H. Behringer, *Z. Anorg. Allg. Chem.*, 329 290 (1964).
92. P. Sartori and M. Weidenbruch, *Angew. Chem. Internat. Ed.*, 4, 1079 (1965).
93. E. N. Vasanta, G. Srivastava and R. C. Mehrotra, *Inorg. Chimi. Acta*, 26, 47 (1978).
94. D. M. Smith and W. M. D. Bryant, *J. Chem. Soc.*, 58, 2452 (1936).
95. J. D. Donaldson and A. Jelen, *J. Chem. Soc. A*, 1448 (1968).
96. R. J. Batchelor, J. N. Ruddick, J. R. Sams and F. Aubke, *Inorg. Chem.*, 16, 1414 (1977).
97. E. P. Serjeant and B. Dempsey, "Ionization Constants of Organic Acids", IUPAC Chemical Data Series -- No.23, Pergamon Press, Toronto (1979).
98. R. W. Taft, "Steric Effects in Organic Chemistry", M. S. Newman (ed.), John Wiley and Sons Inc., New York (1956).
99. P. F. R. Ewings, P. G. Harrison and D. E. Fenton, *J. Chem. Soc. Dalton Trans.*, 821 (1975).
100. P. F. R. Ewings, P. G. Harrison and T. J. King, *J. Chem. Soc. Dalton Trans.*, 1455 (1975).
101. J. D. Donaldson and B. J. Senior, *J. Inorg. Nucl. Chem.*, 31, 881 (1969).
102. J. D. Donaldson and A. Jelen, *J. Chem. Soc. A*, 2244 (1968).
103. P. G. Harrison and E. W. Thornton, *J. Chem. Soc. Dalton Trans.*, 1274 (1978).
104. J. G. Ballard and T. Birchall, *Can. J. Chem.*, 53, 3371 (1975).

105. P. F. R. Ewings, P. G. Harrison, A. Morris and T. J. King, *J. Chem. Soc. Dalton Trans.*, 1602 (1976).
106. J. D. Donaldson, E. J. Filmore and M. J. Tricker, *J. Chem. Soc. A*, 1109 (1971).
107. T. C. Gibb, B. A. Goodman and N. N. Greenwood, *J. Chem. Soc., Chem. Commun.*, 774 (1970).
108. N. W. Alcock and V. L. Tracy, *Acta Crystallogr. Sect. B*, B35, 80 (1979).
109. C. D. Garner, D. Sutton and S. C. Wallwork, *J. Chem. Soc. A*, 1949 (1967).
110. D. Potts, H. D. Sharma, A. J. Carty and A. Walker, *Inorg. Chem.*, 13, 1205 (1974).
111. P. A. Yeats, B. L. Poh, B. F. E. Ford, J. R. Sams and F. Aubke, *J. Chem. Soc. A*, 2188 (1970).
112. R. H. Herber and H. A. Stockler, "Applications of the Mössbauer Effect in Chemistry and Solid State Physics", Int. At. Energy Agency, Vienna (1966), p. 110.
113. R. Hoppe and W. Dähne, *Naturwissenschaften*, 49, 254 (1962).
114. N. W. Alcock and V. L. Tracy, *J. Chem. Soc. Dalton Trans.*, 2246 (1976).
115. R. A. Laber and A. Schmidt, *Spectrochem. Acta*, 31A, 1589 (1975).
116. E. Spinner, *J. Chem. Soc.*, 4217 (1964).
117. C. D. Garner, B. Hughes and T. J. King, *J. Chem. Soc. Dalton Trans.*, 562 (1975).



118. P. F. R. Ewings and P. G. Harrison, *J. Chem. Soc. Dalton. Trans.*, 1715 (1975).
119. A. Jelen and O. Lindquist, *Acta Chem. Scand.*, 23, 3071 (1969).
120. J. D. Donaldson, J. F. Knifton and S. D. Ross, *Spectrochimica Acta*, 21, 1043 (1965).
121. R. L. Redington and K. C. Lin, *Spectrochimica Acta*, 27A, 2445 (1971).
122. K. C. Malhotra and D. S. Katoch, *Aust. J. Chem.*, 27, 1413 (1974).
123. J. S. Ogden and M. J. Ricks, *J. Chem. Phys.*, 53, 896 (1970).
124. C. S.-C. Wang and J. M. Schreeve, *J. Organomet. Chem.*, 46, 271 (1972).
125. M. Nardelli, C. Pellizzi and G. Pellizi, *J. Organomet. Chem.*, 85, C43 (1975).
126. M. Nardelli, C. Pellizi, G. Pellizi and P. Tarasconi, *Z. Anorg. Allg. Chem.*, 431, 250 (1977).
127. H. Lüth and E. L. Anma, *J. Am. Chem. Soc.*, 91, 7515 (1969).
128. N. L. Allinger, J. A. Hirsch, M. A. Miller, I. J. Tyminski, F. A. van-Catledge, *J. Am. Chem. Soc.*, 90, 1199 (1968).
129. A. Bondi, *J. Phys. Chem.*, 68, 4111 (1964).
130. R. C. Weast, "Handbook of Chemistry and Physics", The Chemical Rubber Co., Cleveland, Ohio (1968-1969).
131. D. Mootz and H. Puhl, *Acta Crystallogr.*, 23, 471 (1967).
132. M. F. Dove and T. J. King, *J. Chem. Soc., Chem. Commun.*, 944 (1973).
133. G. Amthauer, J. Fenner, S. Hafner, W. B. Holzapfel and R. Keller, *J. Chem. Phys.*, 70, 4837 (1979).

134. K. Hassebach, G. Murken and M. Trömel, *Z. Anorg. Allg. Chem.* 397, 127 (1973).
135. A. B. Cornwell, C. A. Cornwell and P. G. Harrison, *J. Chem. Soc. Dalton Trans.*, 1612 (1976).
136. E. J. Bulten and H. A. Budding, *J. Organomet. Chem.*, 157, C3 (1978).
137. R. Sabatier, A.-M. Hebrard and J.-C. Cousseins, *C.R. Acad. Sci. Paris, Series C*, 1121 (1974).
138. Tsu Tzu Tsai and W. L. Lehn, *J. Org. Chem.*, 31, 2981 (1966).
139. R. C. Paul, J. K. Puri and K. C. Malhotra, *J. Inorg. Nucl. Chem.*, 35, 403 (1973).
140. T. Birchall, P. A. W. Dean and R. J. Gillespie, *J. Chem. Soc. A*, 1777 (1971).
141. L. Golic and J. Leban, *Acta Crystallogr. Sect. B*, B33, 232 (1977).
142. H. A. Carter, A. M. Qureshi, J. R. Sams and F. Aubke, *Can. J. Chem.*, 48, 2853 (1970).
143. C. H. Hebecker, H. G. Von Schneiring and R. Hoppe, *Naturwissenschaften*, 53, 154 (1966).
144. P. A. Yeats, J. R. Sams and F. Aubke, *Inorg. Chem.*, 12, 328 (1973).
145. A. W. Jache, "Fluorosulfuric Acid", *in Advances in Inor. Chem. and Radiochem.*, 16, 177 (1974), H. J. Emeleus and A. G. Sharpe (eds.), Academic Press, New York.
146. S. Brownstein, J. Bornais and G. Latatremouille, *Can. J. Chem.*, 56, 1419 (1978).

147. J. Bönisch and G. Bergerhoff, Universität Bonn (private communication) (1980).
148. W. Jeitschke and A. W. Sleight, Z. Naturforsch., 27b, 203 (1972).
149. J. K. Lees and P. A. Flinn, J. Chem. Phys., 48, 882 (1968).
150. R. H. Herber, H. A. Stockler and W. T. Reichle, J. Chem. Phys., 42, 2447 (1965).
151. A. Schichl, F. J. Litterst, H. Micklitz, J. P. Devort and J. M. Friedt, Chem. Phys., 20, 371 (1977).
152. R. H. Herber and G. Carroquillo, Inorg. Chem., 20, 3693 (1981).
153. G. Dénès, J. Pannetier, J. Y. Le Marouille and J. Lucas, J. Solid State Chem., 30, 335 (1979).
154. T. Birchall, G. Dénès and K. Ruebenbauer, J. Chem. Soc. Dalton Trans., 1831 (1981).
155. H. Bürger, K. Burczyk and A. Blaschette, Monatsh. Chem., 101, 102 (1970).
156. J. Goubeau and J. B. Milne, Can. J. Chem., 45, 2321 (1967).
157. M. G. Miles, G. Doyle, R. P. Cooney and R. S. Tobias, Spectrochim. Acta, Part A, 25, 1515 (1969).
158. F. A. Cotton and G. Wilkinson, "Advanced Inorganic Chemistry", p. 643, Interscience Publishers, Toronto, 3rd Ed. (1972).
159. J. D. Donaldson, R. Oteng and B. J. Senior, J. Chem. Soc., Chem. Commun., 618 (1965).
160. I. R. Beattie, N. Cheethan, T. R. Gilson, K. M. S. Livingston and D. J. Reynolds, J. Chem. Soc. A, 1910 (1971).
161. L. Kolditz and L. Preiss, Z. Anorg. Allg. Chem., 6, 2212 (1967).
162. E. Wiberg, E. Amberger and H. Cambensi, Z. Anorg. Allg. Chem., 351, 164 (1967).